



# RESEARCH & DEVELOPMENT

## *Final Report*

### **Risk Assessment of Roadside Utility Structures under Vehicular Impacts**

Prepared By

**Howie Fang, Ph.D.**

**Zheng Li**

**Oyeboade Fatoki**

**Emre Palta**

University of North Carolina at Charlotte  
Department of Mechanical Engineering & Engineering Science  
Department of Civil & Environmental Engineering  
Charlotte, NC 28223-0001

February 29, 2020

### Technical Report Documentation Page

1. Report No. <b>NCDOT 2018-24</b>	2. Government Accession No.	3. Recipient's Catalog No.	
4. Title and Subtitle <b><i>Risk Assessment of Roadside Utility Structures under Vehicular Impacts</i></b>		5. Report Date <b>February 29, 2020</b>	
		6. Performing Organization Code	
7. Author(s) <b>Howie Fang, Zheng Li, Oyeboade Fatoki, Emre Palta</b>		8. Performing Organization Report No.	
9. Performing Organization Name and Address <b>The University of North Carolina at Charlotte</b>  9201 University City Boulevard Charlotte, NC 28223-0001		10. Work Unit No. (TRAIS)	
		11. Contract or Grant No.	
12. Sponsoring Agency Name and Address <b>North Carolina Department of Transportation</b> Research and Analysis Group 1 South Wilmington Street Raleigh, North Carolina 27601		13. Type of Report and Period Covered <b>Final Report</b>  <b>August 1, 2017 – December 31, 2019</b>	
		14. Sponsoring Agency Code <b>NCDOT 2018-24</b>	
Supplementary Notes:			
16. Abstract  <p><i>Roadside structures such as bus shelters and cluster mailboxes are increasingly used in urban areas. These structures raise safety concerns due to the likelihood of being struck by errand vehicles. The main objective of this research was to evaluate a bus shelter and two types of cluster mailboxes under impacts of MASH compliant vehicles. Finite element modeling and simulations were employed as the major tool of the investigation. The simulation results showed that there was no potential occupant injury in vehicular crashes into both single- and dual-unit Type I and Type IV mailboxes under MASH TL-1 conditions. In vehicular crashes into the bus shelter under MASH TL-2 conditions, the simulation results indicated no potential occupant injury; however, there was a high likelihood of injury to adjacent pedestrians caused by the falling roof and windscreen debris. Furthermore, pedestrians inside the bus shelter were highly likely to get severe injury by the striking vehicles.</i></p>			
17. Key Words		18. Distribution Statement	
19. Security Classify. (of this report) Unclassified	20. Security classify. (of this page) Unclassified	21. No. of Pages 131	22. Price

## **Disclaimer**

The contents of this report reflect the views of the authors and not necessarily the views of the university. The authors are responsible for the facts and the accuracy of the data presented herein. The contents do not necessarily reflect the official views or policies of either the North Carolina Department of Transportation or the Federal Highway Administration. This report does not constitute a standard, specification, or regulation.

## Acknowledgments

This study was supported by the North Carolina Department of Transportation (NCDOT) under Project No. 2018-24. The authors would like to thank NCDOT personnel from the *Traffic Engineering and Safety Systems, Roadway Design Unit, Highway Division 5 – District 1, FHWA – NC Division*, and the *Research and Development Unit* for their support and cooperation during the grant period.



## **Executive Summary**

Roadside structures such as bus shelters and cluster mailboxes are increasingly used in urban areas. These structures raise safety concerns due to the likelihood of being struck by errand vehicles. The main objective of this research was to evaluate a bus shelter and two types of cluster mailboxes under impacts of MASH compliant vehicles. Finite element modeling and simulations were employed as the major tool of the investigation. The simulation results showed that there was no potential occupant injury in vehicular crashes into both single- and dual-unit Type I and Type IV mailboxes under MASH TL-1 conditions. In vehicular crashes into the bus shelter under MASH TL-2 conditions, the simulation results indicated no potential occupant injury; however, there was a high likelihood of injury to adjacent pedestrians caused by the falling roof and windscreen debris. Furthermore, pedestrians inside the bus shelter were highly likely to get severe injury by the striking vehicles.

# Table of Contents

Technical Report Documentation Page .....	ii
Disclaimer .....	iii
Acknowledgments.....	iv
Executive Summary .....	v
Table of Contents.....	vi
List of Tables .....	viii
List of Figures.....	ix
1. Introduction.....	1
1.1 Background .....	1
1.2 Research Objectives and Tasks.....	2
2. Literature Review.....	5
2.1 Safety Evaluation Standards and Procedures.....	5
2.2 Cluster Mailbox Configurations and Specifications .....	6
2.3 Performance Evaluation of Mailbox Units .....	7
2.4 Bus Shelter Configurations and Specifications.....	10
2.5 Performance Evaluation of Bus Shelters .....	12
2.6 Occupant Safety Assessment in Vehicular Crash Events .....	12
3. Finite Element Modeling of Vehicles, Occupant, Cluster Mailboxes and the Bus Shelter	18
3.1 FE Models of Two Test Vehicles .....	18
3.2 FE Model of the Hybrid III Crash Test Dummy.....	19
3.3 FE Models of Cluster Mailboxes .....	20
3.4 FE Model of the Bus Shelter.....	22
3.5 FE Models of Road Surfaces .....	24
3.6 Simulation Setup for Cluster Mailboxes.....	24
3.7 Simulation Setup for the Bus Shelter.....	30
4. Simulation Results and Analysis of Cluster Mailboxes.....	32
4.1 Simulations Results of Category 1 .....	32
4.2 Simulations Results of Category 2.....	48
4.3 Simulations Results of Category 3.....	64
4.4 Simulations Results of Category 4.....	80
5. Simulation Results and Analysis of the Bus Shelter.....	97

5.1 Case 1: The bus shelter impacted by a 2010 Toyota Yaris at 0° .....	97
5.2 Case 2: The bus shelter impacted by a 2010 Toyota Yaris at 25° .....	100
5.3 Case 3: The bus shelter impacted by a 2006 Ford F250 at 0°.....	104
5.4 Case 4: The bus shelter impacted by a 2006 Ford F250 at 25°.....	107
6. Findings and Conclusions .....	111
7. References .....	113

## List of Tables

Table 2.1 Specifications of current regular cluster mailboxes.

Table 3.1 Simulation matrix for Category 1: Type I mailboxes impacted by a 2010 Toyota Yaris.

Table 3.2 Simulation matrix for Category 2: Type I mailboxes impacted by a 2006 Ford F250.

Table 3.3 Simulation matrix for Category 3: Type IV mailboxes impacted by a 2010 Toyota Yaris.

Table 3.4 Simulation matrix for Category 4: Type IV mailboxes impacted by a 2006 Ford F250.

Table 3.5 Simulation matrix for the bus shelter.

Table 4.1 Vehicular responses, OIVs, and ORAs for Category 1 – Case 1.

Table 4.2 Dummy responses and injury parameters for Category 1 – Case 1.

Table 4.3 Vehicular responses, OIVs, and ORAs for Category 1 – Case 2.

Table 4.4 Dummy responses and injury parameters for Category 1 – Case 2.

Table 4.5 Vehicular responses, OIVs, and ORAs for Category 1 – Case 3.

Table 4.6 Dummy responses and injury parameters for Category 1 – Case 3.

Table 4.7 Vehicular responses, OIVs, and ORAs for Category 1 – Case 4.

Table 4.8 Dummy responses and injury parameters for Category 1 – Case 4.

Table 4.9 Vehicular responses, OIVs, and ORAs for Category 1 – Case 5.

Table 4.10 Dummy responses and injury parameters for Category 1 – Case 5.

Table 4.11 Vehicular responses, OIVs, and ORAs for Category 1 – Case 6.

Table 4.12 Dummy responses and injury parameters for Category 1 – Case 6.

Table 4.13 Vehicular responses, OIVs, and ORAs for Category 1 – Case 7.

Table 4.14 Dummy responses and injury parameters for Category 1 – Case 7.

Table 4.15 Vehicular responses, OIVs, and ORAs for Category 1 – Case 8.

Table 4.16 Dummy responses and injury parameters for Category 1 – Case 8.

Table 4.17 Vehicular responses, OIVs, and ORAs for Category 2 – Case 1.

Table 4.18 Vehicle trajectory during impact for Category 2 – Case 1.

Table 4.19 Vehicular responses, OIVs, and ORAs for Category 2 – Case 2.

Table 4.20 Dummy responses and injury parameters for Category 2 – Case 2.

Table 4.21 Vehicular responses, OIVs, and ORAs for Category 2 – Case 3.

Table 4.22 Dummy responses and injury parameters for Category 2 – Case 3.

Table 4.23 Vehicular responses, OIVs, and ORAs for Category 2 – Case 4.

Table 4.24 Dummy responses and injury parameters for Category 2 – Case 4.

Table 4.25 Vehicular responses, OIVs, and ORAs for Category 2 – Case 5.

Table 4.26 Dummy responses and injury parameters for Category 2 – Case 5.

Table 4.27 Vehicular responses, OIVs, and ORAs for Category 2 – Case 6.

Table 4.28 Dummy responses and injury parameters for Category 2 – Case 6.

Table 4.29 Vehicular responses, OIVs, and ORAs for Category 2 – Case 7.

Table 4.30 Dummy responses and injury parameters for Category 2 – Case 7.

Table 4.31 Vehicular responses, OIVs, and ORAs for Category 2 – Case 8.

Table 4.32 Dummy responses and injury parameters for Category 2 – Case 8.

Table 4.33 Vehicular responses, OIVs, and ORAs for Category 3 – Case 1.

Table 4.34 Dummy responses and injury parameters for Category 3 – Case 1.

Table 4.35 Vehicular responses, OIVs, and ORAs for Category 3 – Case 2.

Table 4.36 Dummy responses and injury parameters for Category 3 – Case 2.

Table 4.37 Vehicular responses, OIVs, and ORAs for Category 3 – Case 3.

Table 4.38 Dummy responses and injury parameters for Category 3 – Case 3.

Table 4.39 Vehicular responses, OIVs, and ORAs for Category 3 – Case 4.

Table 4.40 Dummy responses and injury parameters for Category 3 – Case 4.

Table 4.41 Vehicular responses, OIVs, and ORAs for Category 3 – Case 5.

Table 4.42 Dummy responses and injury parameters for Category 3 – Case 5.

Table 4.43 Vehicular responses, OIVs, and ORAs for Category 3 – Case 6.

Table 4.44 Dummy responses and injury parameters for Category 3 – Case 6.

Table 4.45 Vehicular responses, OIVs, and ORAs for Category 3 – Case 7.

Table 4.46 Dummy responses and injury parameters for Category 3 – Case 7.

Table 4.47 Vehicular responses, OIVs, and ORAs for Category 3 – Case 8.

Table 4.48 Dummy responses and injury parameters for Category 3 – Case 8.

Table 4.49 Vehicular responses, OIVs, and ORAs for Category 4 – Case 1.

Table 4.50 Dummy responses and injury parameters for Category 4 – Case 1.

Table 4.51 Vehicular responses, OIVs, and ORAs for Category 4 – Case 2.

Table 4.52 Dummy responses and injury parameters for Category 4 – Case 2.

Table 4.53 Vehicular responses, OIVs, and ORAs for Category 4 – Case 3.

Table 4.54 Dummy responses and injury parameters for Category 4 – Case 3.

Table 4.55 Vehicular responses, OIVs, and ORAs for Category 4 – Case 4.

Table 4.56 Dummy responses and injury parameters for Category 4 – Case 4.

Table 4.57 Vehicular responses, OIVs, and ORAs for Category 4 – Case 5.

Table 4.58 Dummy responses and injury parameters for Category 4 – Case 5.

Table 4.59 Vehicular responses, OIVs, and ORAs for Category 4 – Case 6.

Table 4.60 Dummy responses and injury parameters for Category 4 – Case 6.

Table 4.61 Vehicular responses, OIVs, and ORAs for Category 4 – Case 7.

Table 4.62 Dummy responses and injury parameters for Category 4 – Case 7.

Table 4.63 Vehicular responses, OIVs, and ORAs for Category 4 – Case 8.

Table 4.64 Dummy responses and injury parameters for Category 4 – Case 8.

Table 5.1 Vehicular response, OIVs, and ORAs for Case 1.

Table 5.2 Dummy responses and injury parameters for Case 1.

Table 5.3 Vehicular responses, OIVs, and ORAs for Case 2.

Table 5.4 Dummy responses and injury parameters for Case 2.

Table 5.5 Vehicular responses, OIVs, and ORAs for Case 3.

Table 5.6 Dummy responses and injury parameters for Case 3.

Table 5.7 Vehicular responses, OIVs, and ORAs for Case 4.

Table 5.8 Dummy responses and injury parameters for Case 4.

## **List of Figures**

Figure 1.1 A typical bus shelter (a) and a bus shelter crash incident (b).

Figure 1.2 Cluster mailboxes (a) and crash incident on a cluster mailbox (b).

Figure 1.3 Finite element models of a crash test dummy and MASH compliant vehicles.

Figure 1.4 Finite element models of cluster mailboxes and the bus shelter.

Figure 2.1 Neighborhood mailboxes.

Figure 2.2 Configurations of the six types of cluster mailboxes.

Figure 2.3 Commonly used bus shelter designs in North Carolina.

Figure 3.1 FE models of the two MASH compliant vehicles used in crash simulations.

Figure 3.2 The FE model of a Hybrid III 50th percentile crash test dummy.

Figure 3.3 FE model of the Type I cluster mailbox.

Figure 3.4 FE model of the Type IV cluster mailbox.

Figure 3.5 FE model of a bolt-and-nut connection.

Figure 3.6 Dual-unit cluster mailbox configuration (a) Type I (b) Type IV.

Figure 3.7 FE model of the typical bus shelter with clip joints details.

Figure 3. 8 The dimensions of the Brasco Slimline SL-510-OF bus shelter.

Figure 3.9 FE models of two road surfaces for crash simulations.

Figure 3.10 Two impact locations for crash simulations with double cluster mailboxes (a) Corner (b) Mid-point.

Figure 3.11 Full simulation models for the eight simulation cases of Category 1.

Figure 3.12 Full simulation models for the eight simulation cases of Category 2.

Figure 3.13 Full simulation models for the eight simulation cases of Category 3.

Figure 3.14 Full simulation models for the eight simulation cases of Category 4.

Figure 3.15 Full models for the four simulation cases of the bus shelter.

Figure 4.1 The full simulation model (a) and deformed vehicle model after impact (b) for Category 1 – Case 1.

Figure 4.2 Vehicle trajectory during impact for Category 1 – Case 1.

Figure 4.3 The full simulation model (a) and deformed vehicle model after impact (b) for Category 1 – Case 2.

Figure 4.4 Vehicle trajectory during impact for Category 1 – Case 2.

Figure 4.5 The full simulation model (a) and deformed vehicle model after impact (b) for Category 1 –

Case 3.

Figure 4.6 Vehicle trajectory during impact for Category 1 – Case 3.

Figure 4.7 The full simulation model (a) and deformed vehicle model after impact (b) for Category 1 –

Case 4.

Figure 4.8 Vehicle trajectory during impact for Category 1 – Case 4.

Figure 4.9 The full simulation model (a) and deformed vehicle model after impact (b) for Category 1 –

Case 5.

Figure 4.10 Vehicle trajectory during impact for Category 1 – Case 5.

Figure 4.11 The full simulation model (a) and deformed vehicle model after impact (b) for Category 1 –

Case 6.

Figure 4.12 Vehicle trajectory during impact for Category 1 – Case 6.

Figure 4.13 The full simulation model (a) and deformed vehicle model after impact (b) for Category 1 –

Case 7.

Figure 4.14 Vehicle trajectory during impact for Category 1 – Case 7.

Figure 4.15 The full simulation model (a) and deformed vehicle model after impact (b) for Category 1 –

Case 8.

Figure 4.16 Vehicle trajectory during impact for Category 1 – Case 8.

Figure 4.17 The full simulation model (a) and deformed vehicle model after impact (b) for Category 2 –

Case 1

Figure 4.18 Vehicle trajectory during impact for Category 2 – Case 1.

Figure 4.19 The full simulation model (a) and deformed vehicle model after impact (b) for Category 2 –

Case 2.

Figure 4.20 Vehicle trajectory during impact for Category 2 – Case 2.

Figure 4.21 The full simulation model (a) and deformed vehicle model after impact (b) for Category 2 –

Case 3.

Figure 4.22 Vehicle trajectory during impact for Category 2 – Case 3.

Figure 4.23 The full simulation model (a) and deformed vehicle model after impact (b) for Category 2 –

Case 4.

Figure 4.24 Vehicle trajectory during impact for Category 2 – Case 4.

Figure 4.25 The full simulation model (a) and deformed vehicle model after impact (b) for Category 2 –

Case 5.

Figure 4.26 Vehicle trajectory during impact for Category 2 – Case 5.

Figure 4.27 The full simulation model (a) and deformed vehicle model after impact (b) for Category 2 –

Case 6.



Figure 4.28 Vehicle trajectory during impact for Category 2 – Case 6.

Figure 4.29 The full simulation model (a) and deformed vehicle model after impact (b) for Category 2 – Case 7.

Figure 4.30 Vehicle trajectory during impact for Category 2 – Case 7.

Figure 4.31 The full simulation model (a) and deformed vehicle model after impact (b) for Category 2 – Case 8.

Figure 4.32 Vehicle trajectory during impact for Category 2 – Case 8.

Figure 4.33 The full simulation model (a) and deformed vehicle model after impact (b) for Category 3 – Case 1.

Figure 4.34 Vehicle trajectory during impact for Category 3 – Case 1.

Figure 4.35 The full simulation model (a) and deformed vehicle model after impact (b) for Category 3 – Case 2.

Figure 4.36 Vehicle trajectory during impact for Category 3 – Case 2.

Figure 4.37 The full simulation model (a) and deformed vehicle model after impact (b) for Category 3 – Case 3.

Figure 4.38 Vehicle trajectory during impact for Category 3 – Case 3.

Figure 4.39 The full simulation model (a) and deformed vehicle model after impact (b) for Category 3 – Case 4.

Figure 4.40 Vehicle trajectory during impact for Category 3 – Case 4.

Figure 4.41 The full simulation model (a) and deformed vehicle model after impact (b) for Category 3 – Case 5.

Figure 4.42 Vehicle trajectory during impact for Category 3 – Case 5.

Figure 4.43 The full simulation model (a) and deformed vehicle model after impact (b) for Category 3 – Case 6.

Figure 4.44 Vehicle trajectory during impact for Category 3 – Case 6.

Figure 4.45 The full simulation model (a) and deformed vehicle model after impact (b) for Category 3 – Case 7.

Figure 4.46 Vehicle trajectory during impact for Category 3 – Case 7.

Figure 4.47 The full simulation model (a) and deformed vehicle model after impact (b) for Category 3 – Case 8.

Figure 4.48 Vehicle trajectory during impact for Category 3 – Case 8.

Figure 4.49 The full simulation model (a) and deformed vehicle model after impact (b) for Category 4 – Case 1.

Figure 4.50 Vehicle trajectory during impact for Category 4 – Case 1.

Figure 4.51 The full simulation model (a) and deformed vehicle model after impact (b) for Category 4 – Case 2.

Figure 4.52 Vehicle trajectory during impact for Category 4 – Case 2.

Figure 4.53 The full simulation model (a) and deformed vehicle model after impact (b) for Category 4 – Case 3.

Figure 4.54 Vehicle trajectory during impact for Category 4 – Case 3.

Figure 4.55 The full simulation model (a) and deformed vehicle model after impact (b) for Category 4 – Case 4.

Figure 4.56 Vehicle trajectory during impact for Category 4 – Case 4.

Figure 4.57 The full simulation model (a) and deformed vehicle model after impact (b) for Category 4 – Case 5.

Figure 4.58 Vehicle trajectory during impact for Category 4 – Case 5.

Figure 4.59 The full simulation model (a) and deformed vehicle model after impact (b) for Category 4 – Case 6.

Figure 4.60 Vehicle trajectory during impact for Category 4 – Case 6.

Figure 4.61 The full simulation model (a) and deformed vehicle model after impact (b) for Category 4 – Case 7.

Figure 4.62 Vehicle trajectory during impact for Category 4 – Case 7.

Figure 4.63 The full simulation model (a) and deformed vehicle model after impact (b) for Category 4 – Case 8.

Figure 4.64 Vehicle trajectory during impact for Category 4 – Case 8.

Figure 5.1 The full simulation model (a) and deformed vehicle model after impact (b) for Case 1.

Figure 5.2 Vehicle trajectory during impact for Case 1.

Figure 5.3 Crash simulation details for Case 1.

Figure 5.4 Crash test dummy response for Case 1.

Figure 5.5 The maximum debris trajectory distance for Case 1.

Figure 5.6 The full simulation model (a) and deformed vehicle model after impact (b) for Case 2.

Figure 5.7 Vehicle trajectory during impact for Case 2.

Figure 5.8 Crash simulation details for Case 2.

Figure 5.9 Crash test dummy response for Case 2

Figure 5.10 The maximum debris trajectory distance for Case 2.

Figure 5. 11 The full simulation model (a) and deformed vehicle model after impact (b) for Case 3.

Figure 5.12 Vehicle trajectory during impact for Case 3.

Figure 5.13 Crash simulation details for Case 3.

Figure 5.14 Crash test dummy response for Case 3.

Figure 5.15 The maximum debris trajectory distance for Case 3.

Figure 5.16 The full simulation model (a) and deformed vehicle model after impact (b) for Case 4.

Figure 5.17 Vehicle trajectory during impact for Case 4.

Figure 5.18 Crash simulation details for Case 4.

Figure 5.19 Crash test dummy response for Case 4.

Figure 5.20 The maximum debris trajectory distance for Case 4.

# 1. Introduction

With the rapid economic development and population growth in urban areas, medium-sized and large cities have been experiencing fast expansions that stimulate the improvement of urban infrastructures such as public transportation and community utilities. Public transportation, e.g., buses, serves as an efficient means to reduce the traffic volume while saving energy. Bus stops or bus shelters are typically installed at bus stations along the routes. In newly developed communities, the traditional single-family mailboxes are replaced by cluster box units (CBUs) (also called cluster mailboxes) so as to make mail delivery more efficient and cost effective. The increasing number of roadside utilities such as bus shelters and cluster mailboxes increases the potential of vehicular crashes, which raises safety concern for passengers and/or pedestrians involved in these crashes. To this end, analysis of vehicular crashes and safety evaluation of these roadside utilities are needed to determine the potential risks for occupants and/or pedestrians.

## 1.1 Background

Figure 1.1(a) shows a typical bus shelter installed on the side of the road along the bus route. The bus shelter is composed of metal frames and polycarbonate coverings. When crashed by the errand vehicles, bus shelters may cause fatality or severe injuries to the occupants as well as pedestrians. Figure 1.1(b) shows a small passenger car crashing into a bus shelter, resulting in the death of the driver due to the relatively high rigidity of the bus shelter. On the other side, a severely damaged bus shelter may also cause severe injuries to the occupants due to intrusions into the occupant compartment. Furthermore, the debris of the shattered polycarbonate glasses imposes safety risks for pedestrians in the proximity of the crash location.



Figure 1.1 A typical bus shelter (a) and a bus shelter crash incident (b).

Similar to bus shelters, cluster mailboxes also raise safety concerns. Commonly used cluster mailboxes are made of aluminum and come with various sizes. In most communities with cluster mailboxes, several units are installed together and aligned to form a mailbox hub, as shown in Figure 1.2(a). Although cluster mailboxes are typically placed in communities with relatively low speed limits, they could still cause severe injuries or fatality when hit by passenger cars as the case shown in Figure 1.2(b).

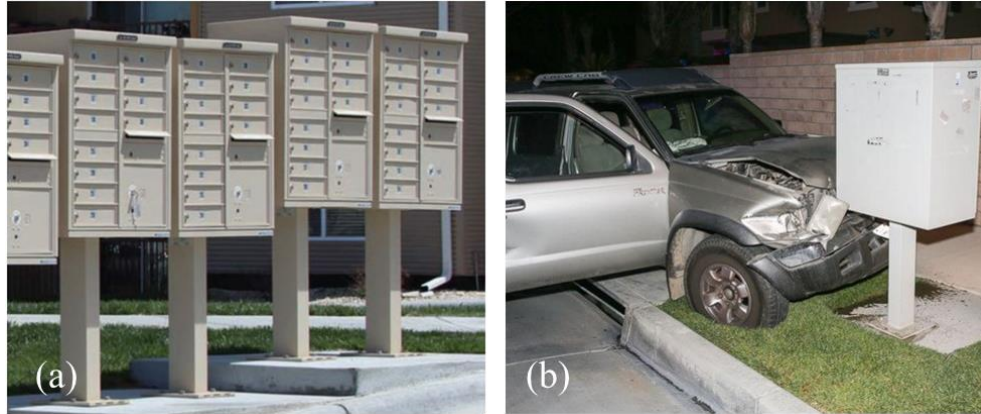


Figure 1.2 Cluster mailboxes (a) and crash incident on a cluster mailbox (b).

Roadside safety features are required to be tested to satisfy the safety requirements specified by Manual for Assessing Safety Hardware (MASH). Currently, there are no specific requirements in MASH for safety evaluations of bus shelters and cluster mailboxes. To assess such roadside utilities for the potential risks of occupants inside the striking vehicles and/or pedestrians near the crash events, the MASH evaluation criteria for supportive structures can be adopted. Following the MASH standards, cluster mailboxes are required to comply with MASH Test Level 1 (TL-1) conditions and bus shelters should comply with MASH Test Level 2 (TL-2) conditions. At MASH TL-1 conditions, the structure is impacted by a small passenger car (1100C) and a pickup truck (2270P) at an impact speed of 31 mph (50 km/h) and impact angles of 0° and 25°. At MASH TL-2 conditions, the structure is impacted by the 1100C and 2270P vehicles at an impact speed of 44 mph (70 km/h) and impact angles of 0° and 25°.

## 1.2 Research Objectives and Tasks

The main objective of this study was to evaluate the risks of occupants and pedestrians due to vehicular crashes into cluster mailboxes and a bus shelter under MASH TL-1 and TL-2 conditions, respectively. Full-scale finite element (FE) modeling and simulations were employed in this research using two MASH compliant vehicles, a 2010 Toyota Yaris (1100C) and a 2006 Ford F250 (2270P). A 50<sup>th</sup> percentile Hybrid III crash test dummy was incorporated into both vehicle models for assessing occupant risk. The damages and structural integrity of the bus shelter and cluster mailboxes were also evaluated. The research project had five major tasks as stated below.

### Task 1: Literature Review and Data Collection

In this task, literature on vehicular crash testing and modeling related to roadside utility structures was reviewed to assist with model development and validation for crash simulations of this project. Literature on the design and installation of bus shelters and cluster mailboxes were also collected.

### Task 2: FE Model Development and Validation

In this task, the FE models of a Hybrid III crash test dummy, a small passenger car, and a pickup truck were obtained from the previous research projects (see Figure 1.3) and modified suit the needs of this project. The small passenger car (i.e., a 2010 Toyota Yaris) had a mass of 2,425 lbs. (1,100 kg) and the pickup truck (i.e., a 2006 Ford F250) had a mass of 5,004 lbs. (2,270 kg). Both vehicle models met the MASH requirements and therefore were MASH compliant vehicles.

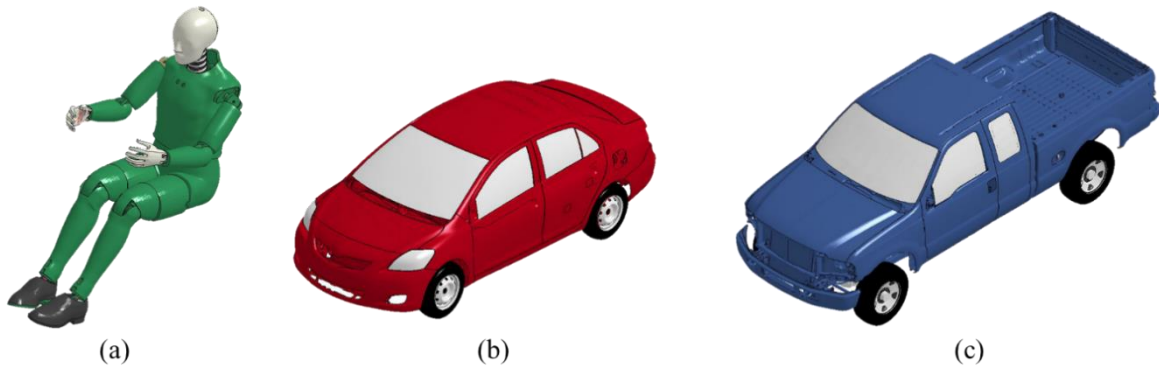


Figure 1.3 Finite element models of a crash test dummy and MASH compliant vehicles.  
(a) A Hybrid III crash test dummy; (b) A 2010 Toyota Yaris; and (c) A 2006 Ford F250.

The FE model of the crash test dummy was validated using a sled test before it was integrated into the vehicle models. The integrated vehicle models (i.e., with the dummy, seatbelt, and airbag, etc.) were validated using standard vehicle crashworthiness tests. The FE models of a bus shelter and two types of cluster mailboxes, as shown in Figure 1.4, were created based on design specifications and NCDOT requirements. The cluster mailboxes were evaluated under two site conditions: 1) placed on a flat terrain without curb, and 2) placed on a flat terrain behind a curb (with an 8-ft distance from the curb face).

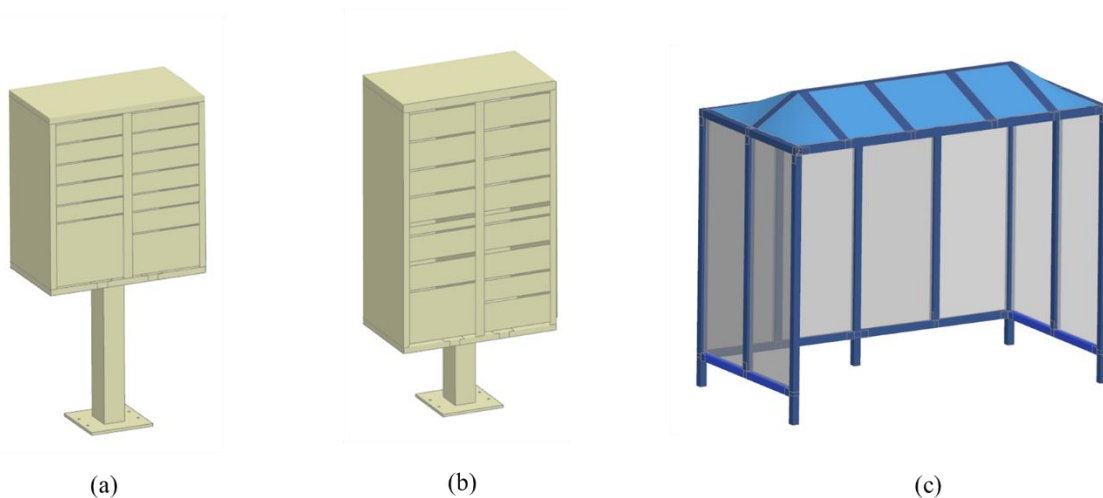


Figure 1.4 Finite element models of cluster mailboxes and the bus shelter.  
(a) A Type I mailbox; (b) a Type IV mailbox; and (c) a bus shelter.

### Task 3: Evaluation of Two Typical Cluster Mailboxes under Vehicular Impacts

In this task, the cluster mailboxes were evaluated under impacts of the MASH 1100C and 2270P vehicles at an impact speed of 31 mph (50 km/h) and impact angles of 0° and 25°. Two initial impact locations on the cluster mailboxes, nearest corner and midpoint, were chosen in the simulations of 25° impacts on the dual-unit mailboxes to identify the worst-case scenario. The cluster mailboxes were evaluated at two site conditions: on a flat terrain with and without a curb.

In addition to the damage to the vehicular structure such as intrusions and deformations, the responses of the crash test dummy were evaluated using head, chest and pelvis accelerations. The head injury criterion (HIC<sub>15</sub>) was adopted to assess the severity of occupant injury. In addition, mailbox displacements and debris trajectories were analyzed to assess the potential risk caused to adjacent objects including the occupant in the impacting vehicle.

#### Task 4: Evaluation of a Bus Shelter under Vehicular Impacts

In this task, the bus shelter was evaluated under impacts of the MASH 1100C and 2270P vehicles at an impact speed of 44 mph (70 km/h) and impact angles of 0° and 25°. Several impact locations on the bus shelter were chosen for the simulations to identify the worst-case scenario. In addition to the damage to the vehicular structure such as intrusions and deformations, the responses of the crash test dummy were evaluated using head, chest and pelvis accelerations. The HIC<sub>15</sub> criterion was adopted to evaluate the severity of occupant injury. In addition to these responses, the structural integrity of the bus shelter was determined along with shelter dislocation, deformation, and debris trajectories, which could cause potential injuries to nearby pedestrians as well as the vehicular occupant.

Given the wide variety of bus shelters, it was infeasible to examine all different designs of bus shelters. Since most bus shelters are made of frames with similar structures members and overall rigidity, a bus shelter commonly used in North Carolina was used in the vehicular crash simulations of this project. The effects structural rigidity of bus shelter on vehicular responses and bus shelter failure mechanism were studied to determine the appropriate level of rigidity of the bus shelter.

#### Task 5: Final Report

This final report provides a comprehensive summary of research activities, findings, and outcomes for this project. It synthesizes the literature review, FE modeling efforts, simulation results, and research findings on the evaluation of a bus shelter and two types of cluster mailbox. The final report also provides risk assessment of the bus shelter and cluster mailboxes at MASH TL-2 and TL-1 conditions, respectively.

## **2. Literature Review**

### **2.1 Safety Evaluation Standards and Procedures**

The first recommended procedures for full-scale vehicular crash testing were published as Highway Research Correlation Service Circular 482. This one-page document specified the overall requirements for the testing vehicle in terms of vehicle mass, impact speed, and impact angle. Circular 482 was considered the prototype of all subsequent testing standards, even though it only provided a limited scope of barriers testing and left a number of questions open to discussions (Ross et al. 1993).

In 1973, researchers at the Southwest Research Institute conducted research sponsored by the National Cooperative Highway Research Program (NCHRP) under Project 22-2 with the main objective of addressing some of the questions that were not resolved in Circular 482. The results were published in NCHRP Report 153 to provide a “Recommended Procedures for Vehicle Crash Testing of Highway Appurtenances.” The NCHRP Report 153 collected data from more than 70 individuals and agencies and was widely accepted in the field of crash testing of roadside safety features. In 1978, after modifying some particular area treatment, the TRB Committee on Roadside Safety Features (A2A04) published a revised version of the standard as Transportation Research Circular 191.

In 1980, researchers at the Southwest Research Institute conducted another research under NCHRP Project 22-2(4) to expand the scope of Circular 191 by introducing new procedures and updating the evaluation criteria. The research results were published in NCHRP Report 230, which was widely accepted as the primary reference for performance evaluation of highway safety features.

In 1993, the American Association of State Highway and Transportation Officials (AASHTO) updated the old standards, NCHRP Report 230, with NCHRP Report 350, which provided a comprehensive procedure for safety performance evaluations. The main updates from NCHRP Report 230 to Report 350 were summarized as follows.

1. The range of testing highway features was expanded to more types of safety features including barriers, terminals, crash cushions, breakaway support structures, utility poles, truck-mounted attenuators and work zone traffic control devices.
2. More test vehicles were included to meet the needs of different levels of performance requirements: a 700-kg compact passenger car, an 8000-kg single-unit cargo truck, and a 36000-kg tractor-trailer.
3. Six basic test levels were defined for various classes of roadside safety features and a number of optional tests were offered.
4. A guideline was included for selecting the critical impact point in crash tests on redirection-type of safety hardware.
5. Enhanced measurement techniques for assessing occupant risk as well as guidelines for the device installation and test instrumentation were provided.
6. The preferred and maximum levels of occupant impact velocities and ride-down accelerations were introduced for the first time. The limits of lateral occupant impact velocity were set to be the same as those in the longitudinal direction. The redirection criteria were updated with a limit of 12 m/s for the longitudinal velocity change.
7. Computer simulations and state-of-art methods were reviewed.



8. The units in testing procedures were all converted to metric system.

For over a decade, the NCHRP Report 350 had been the widely adopted standards for roadside safety features. In an effort to improve NCHRP Report 350 and address issues found in practice, the NCHRP Project 22-14(02) was initiated in 2008. This project, “Improvement of Procedures for the Safety Performance Evaluation of Roadside Features,” resulted in a new roadside safety standard, the Manual for Assessing Safety Hardware (MASH) (AASHTO 2009), which was developed to supersede NCHRP Report 350. Note that MASH only addresses the crash testing of roadside safety features; it does not replace any of the guidelines given by the AASHTO Roadside Design Guide. The following gives the major updates in MASH on test vehicles, test conditions, and evaluation criteria from NCHRP Report 350.

#### Test Vehicles and Test Conditions

1. The mass of the small passenger car was changed from 1,809 lb (820 kg) to 2,420 lb (1,100 kg).
2. The mass of the pickup truck was changed from 4,409 lb (2000 kg) to 5,000 lb (2,270kg).
3. The mass of single-unit truck was changed from 17,636 lb (8,000 kg) to 22,000 lb (10,000 kg).
4. The pickup truck test vehicle must have a minimum height of center of gravity of 28 inches.
5. The impact speed for the single-unit truck was increased from 49.7 mph (80 km/h) to 55.9 mph (90 km/h).
6. For length-of-need testing of the terminals and crash cushions, the impact angle was increased from 20° to 25°.
7. For oblique end impacts of gating terminals and crash cushions, the impact angle was reduced from 15° to 5°.
8. The option for using passenger car test vehicles older than six years was removed.

#### Evaluation Criteria

1. The qualitative evaluation criteria of windshield and occupant compartment damage were replaced by quantitative criteria.
2. The marginal pass option was removed. Only a pass/fail criterion will be used.
3. The maximum roll and pitch angles were set to 75°.

In 2016, AASHTO published the second edition of MASH (AASHTO 2016), which included significant updates such as a new matrix for cable barrier testing on slopes, modifications to several test vehicle dimensions, and updated test documentation requirements.

## **2.2 Cluster Mailbox Configurations and Specifications**

The earliest prototype of cluster mailboxes, which could be dated several decades ago, was composed of a mount support attached with two or more boxes. In the early 1980’s, a new type of combined mailboxes called neighborhood mailboxes, as shown in Figure 2.1, were installed in some communities in the United States (Campise et al. 1984). In 2005, the new "F" specification for cluster box units (CBUs) was developed and approved by USPS for all mailbox manufacturers. Both the outdated Neighborhood Delivery Collection Box Units (NDCBUs) and the "E" series

CBUs should now be replaced by the new cluster mailboxes (Florence Corporation 2017).

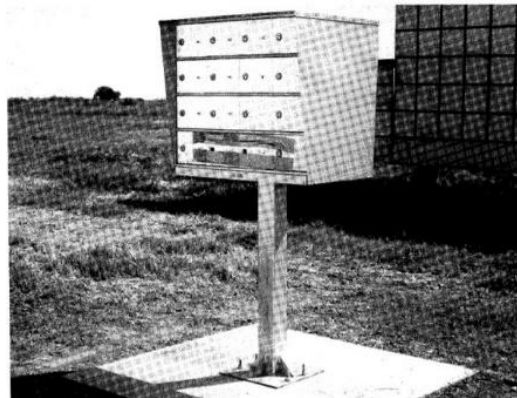


Figure 2.1 Neighborhood mailboxes.

Most of today's CBUs are made by Florence Manufacturing. Table 2.1 gives the detailed specifications of the six types of current models of cluster mailboxes, as shown in Figure 2.2.

Table 2.1 Specifications of current regular cluster mailboxes.

Models #	CBU Type	Installed Height	Installed Width	Installed Depth	Pedestal Height	Weight (lbs)	Standard Tenant Compartment Dimensions	Mailbox Compartments
1570-8XX	Type I	62"	30-½"	18"	28-½"	144	3"H×12"W×15"D	8
1570-12XX	Type II	62"	30-½"	18"	28-½"	144	3"H×12"W×15"D	12
1570-16XX	Type III	62"	30-½"	18"	14-½"	175	3"H×12"W×15"D	16
1570-13XX	Type IV	62"	30-½"	18"	14-½"	167	4-¾"H×12"W×15"D	13
1570-4T5XX	Type V	62"	30-½"	18"	28-½"	145	6-½"H×12"W×15"D	4
1570-8T6XX	Type VI	62"	30-½"	18"	14-½"	176	3"H×12"W×15"D	8



Figure 2.2 Configurations of the six types of cluster mailboxes.

### 2.3 Performance Evaluation of Mailbox Units

Started in 1978, Ross et al. conducted five full-scale crash tests to evaluate the impact responses of rural mailbox installations (Ross et al. 1980). In these tests, the 1972 Chevrolet Vegas with a weight of 2,250 lb (1,022 kg) was used to impact the mailboxes at an impact speed of 60 mph (96.6 km/h). The mailbox installations used in the crash tests ranged from single box installation to four-box installation with wood post support or standard steel pipe support. The crash test results showed that the test vehicles had severe damages impacting the multi-box units mounted on flat boards, since the boards could easily penetrate the windshield. The study recommended that the

attachment between the boxes and the post should be given careful attention to reduce the possibility of intrusion into the windshield or the occupant compartment when separated during an impact.

Subsequently, Rose et al. (1980) conducted another series of full-scale crash tests on five different designs of mailbox supports with a variety of support configurations, embedment depth and embedment methods. The test vehicle and impact conditions were the same as those in their previous study. The effect of initial impact points was also considered in this study by offsetting the posts relative to the centerline of the vehicle's bumper cover as well as the vehicle's travel direction. For single-box support design, no penetration into the occupant compartment was observed in the tests as the windshield remained unbroken and the vehicle had only minor damage.

Campise et al. (1984) conducted a research on the performance evaluation of "neighborhood" mailboxes in collaboration with the Texas State Department of Highways and Public Transportation. In their research, twelve to sixteen boxes were housed together in a metal framework and supported by a single upright post that was attached to a concrete foundation. Based on the results of some previous crash tests showing the hazard of certain mailbox installations along roadway shoulders, a vehicle crash test was conducted using a 1978 Honda Civic impacting a typical neighborhood mailbox at 62.3 mph (100.2 km/h). The test results showed that the vehicle exhibited violent rollovers, which did not meet the recommended performance criteria by NCHRP Report 230. It was proposed that this type of mailbox or similar installation should not be placed within the clear zone of high-speed roadways.

Faller et al. (1988) conducted a series of full-scale crash tests of a mailbox support system developed by the Nebraska Department of Roads that was used to accommodate a wide range of mailbox sizes. Four crash tests were conducted with a 1,840-lb (835-kg) 1979 Volkswagen Rabbit for two types of mailbox mounting systems (i.e. the one embedded in the weak soil foundation and the one in strong soil foundation) at the impact speed of 20 mph (32.2 km/h) and 60 mph (96.6 km/h) respectively. The different configurations of the boxes mounted on the post were also considered. One was a single box and the other was two-separate-box. It was observed from the crash tests that the mailbox support system functioned as expected, keeping the mailbox units attached to the post without any detached fragments to penetrate into the occupant compartment. The test results on impact severity were within the acceptable limits specified by NCHRP Report 230. The test vehicle was shown to remain stable and upright during and after the impacts, with no sign of potential ramping or rollover.

In a research project by Ross et al. (1993) at Texas Transportation Institute (TTI), eleven full-scale crash tests were conducted to study mailbox brackets in accordance with NCHRP Report 230. The adequacy of bracket, which was developed by the Texas Department of Transportation (TxDOT) and used as an attachment between the mailbox and support post, was verified through the crash tests. The crash tests demonstrated acceptable impact performance of most mailboxes mounted on a 2 lb/ft steel winged channel support, a 2-in O.D. thin-walled steel tube support, or a standard Foresight Tubular support. The modified Foresight Tubular support with a replacement footing, had a relatively smaller insertion depth to the ground socket than the original design and also met the impact performance expectation. It was observed in the study that another vandal-proof mailbox, which was made of 1/4-inch steel plates and mounted on a 2 lb/ft steel winged channel

post, penetrated the occupant compartment at a relatively high speed.

In the work of Paulsen et al. (1996) at the Midwest Roadside Safety Facility (MwRSF), they designed a new breakaway base for CBUs and NDCBUs to improve the safety performance under vehicular impacts. A 2.2-kN horizontal static pull test and a 500-hour salt spray test were conducted to determine the durability of the new design. Finite element modeling and simulation with LS-DYNA were employed to evaluate the safety performance under impact conditions. The simulation results showed that the CBUs could meet the evaluation criteria by NCHRP Report 350. However, it was unable to determine the risk level of occupant compartment intrusions due to the CBU projectile at the current study level. The results of the static and corrosion tests demonstrated the abilities of the CBUs to withstand daily-use load conditions and extreme corrosion conditions. Based on the static test, they also performed static calculations to determine the optimal material of the anchor bolt that would fracture in a brittle manner.

In a research project sponsored by the Midwest State's Regional Pooled Fund Research Program, Vogel et al. (1998) studied the breakaway supports for small signs and mailbox installations. Based on the study, they suggested that round pipes, square tubing or U-channels could be used as the support systems for mailboxes to maintain crashworthiness following the evaluation criteria of NCHRP Report 350.

Bligh et al. (2001) conducted three full-scale crash tests on a 4×4 wood, 2 lb/ft U-channel, and 3-inch diameter pipe, respectively, to investigate the impact performance of these three support posts for molded plastic mailboxes. In each of the crash tests with an 820C test vehicle, the upper molded mailbox was separated from the lower base unit, leading to a secondary contact between the mailbox and the vehicle's hood and windshield. Despite the cracking and tearing of the windshield in the tests of wood and steel pipe posts, there was no potential risk for occupant compartment intrusions. The vehicle remained upright and stable during and after the impacts. All molded plastic mailboxes with the three support posts met the safety requirements specified in NCHRP Report 350, even though the impact responses of the different types of support posts varied. The 4×4 timber support post was recommended for use with molded plastic mailboxes to achieve good impact performance.

In the study of Tahan et al. (2005), finite element modeling and simulation coupled with full-scale crash testing for 24 selected impact scenarios were employed to evaluate the safety performance of the secure mailboxes, which were heavier and larger than traditional standard mailboxes. The detailed models of four types of secure mailboxes were developed and validated with pendulum crash tests. The research team conducted a parametric study with numerical simulations on mailbox sizes, heights, mounting configurations and post sizes to investigate the effects of mailbox geometries on the impact responses under impacts of a Geo Metro (820C) test vehicle at 62 mph (100 km/h). A critical impact case, in which the mailbox components hit the lower portion of the vehicle windshield, was selected from FE simulation and validated by conducting an actual full-scale crash test, which confirmed the prediction of FE simulation results.

Sheikh et al. (2006) performed two full-scale crash tests on a multiple-mailbox mounting system developed by Shur-Tite to evaluate its safety performance before sending it to manufacturing. The crash tests were conducted in association with NCHRP Report 350 with a 1995 Geo Metro (1,808

lb) test vehicle at an impact speed of 22.1 mph (35.6 km/h). During the crash tests, the mailbox mount was pulled out of the ground and carried along by the impacting vehicle. The mailboxes were found deformed but remained attached. The test vehicle was found to have minimal damage in the forms of hood indentations and front bumper indentions due to contact with the mailbox support post. No occupant compartment deformation was observed during the crash tests and the occupant impact velocities and occupant ride-down accelerations were found to be within the recommended limits.

In a research project sponsored by TxDOT, Bligh et al. (2009) evaluated the safety performance of a dual- and a multi-unit mailbox system using two full-scale crash tests at TL-3 conditions specified by NCHRP Report 350. Both the dual-unit and multi-unit mailboxes failed at the mount systems that were yielded to the test vehicle and pulled out of the anchor sleeves. For dual-unit mailbox, no occupant compartment deformation occurred. For the multi-unit mailbox, one of the mailbox units scratched and shattered the windshield over an area of  $26.8 \times 9.8$  inches with a maximum depth of 1.1 inches. However, occupant risk assessment parameters (i.e., occupant impact velocities and occupant ride-down accelerations) were still within the recommended limits.

It was reported in the study by Dobrovolny et al. (2013) that the frequency of crash incidents involving mailboxes ranged from 0.11% to 0.66% in United States. The ratio of fatal crashes in all mailbox related crashes was below 0.2% from the data provided by the Departments of Transportation of 15 states. Following the assessment of risks presented by the mailboxes, they provided crashworthiness enhancement and placement guidance to prioritize safety initiatives, in an effort to contribute to reducing crash severity.

In a research project sponsored by TxDOT, Dobrovolny et al. (2019) conducted impact testing and crashworthiness evaluation of multiple mailbox supports for use with locking architectural mailboxes. Based on the MASH evaluation criteria, the larger and heavier locking mailboxes on multiple-mount support posts did not meet the requirements due to vehicle windshield deformation and intrusions. Based on the crash testing results, they proposed two new designs for multiple mailbox supports for use with a combination of lockable and standard mailboxes. The new designs were evaluated through full-scale crash testing and were found to satisfy the required evaluation criteria for low-speed and high-speed impacts by a passenger car. Upon impacts, both systems yielded to the vehicle and were pulled out of the foundation sockets without causing severe occupant compartment deformations.

## **2.4 Bus Shelter Configurations and Specifications**

There are a wide variety of bus shelters, from the traditional 5×10 ft brown box to the modern bus rapid transit station. In North Carolina, bus shelters are considered roadside utilities that should be examined and approved by NCDOT before installations. A number of approved bus shelters are available in the market, which are mainly manufactured by Asheville Design Center, Brasco International, Columbia Equipment, Duo-Gard Industries, Jericho Palm, LNI Custom Manufacturing and Tolar Manufacturing Company.

A bus shelter is typically composed of structural components (supporting columns, cross beams, shelter roof, and walls), functional components (seating bench, bicycle parking rack, and schedule or map display), and accessories (trash receptacle, advertisement display, security lighting, and art

decorations). Bus shelter frames are typically made of metals such as aluminum, which is often used in bus shelter roofs. For bus shelter walls, glass and polycarbonate are the two most popular materials. Tempered or laminate safety glass performs well in shattering resistance, which could lower the risk of pedestrian injuries from flying glass debris in a vehicular crash event into the bus shelter. In comparison, bus shelter walls made of thin-wall or multi-wall polycarbonate could offer a higher strength and better capability to withstand impacts while having a lower weight than glass walls.

Among the bus shelters approved by NCDOT, there are still variations in structural configurations, which might lead to different performance in vehicle crash event. Figure 2.3 shows six popular bus shelters used in North Carolina.



Figure 2.3 Commonly used bus shelter designs in North Carolina.

(a) The Eclipse bus shelter; (b) The Arcade bus shelter; (c) The Dome Slimline bus shelter; (d) The Shade bus shelter; (e) The Interlude bus shelter; and (f) The Techline bus shelter.

The Eclipse shelter, as seen in Figure 2.3(a), is manufactured by Brasco International and has a dimension of 5×10 ft. The columns are 4.5-inch round tubes, supporting three different type of roof: arc, slope or curved. Three sides of the bus shelter are installed with glass walls as wind screens. The Eclipse bus shelter is typically used in locations with a maximum wind speed of 130 mph (209 km/h) (Brasco 2015).

The Arcade bus shelter called, shown in Figure 2.3(b), was descended from the Eclipse bus shelter with a similar structural configuration and equipped with an integrated gutter system and a strong triangular header support.

The Dome Slimline, as shown in Figure 2.3(c), is the most economical bus shelter also

manufactured by Brasco International. This bus shelter has a ¼-inch thick white or bronze acrylic dome roof supported by a 5×10 ft aluminum frame.

The Shade bus shelter (Figure 2.3(d)) distinguishes itself from the other bus shelters with its canopy roof and a single line of three 6-inch round aluminum columns, which significantly improve its structural durability. The Shade bus shelter provides an aluminum windscreen that could withstand winds up to 175 mph (282 km/h).

Figure 2.3(e) shows the Interlude bus shelter that features a cantilever roof with turnbuckle details and is designed to withstand hurricane rated winds up to 175 mph (282 km/h). This bus shelter provides up to 7-ft canopy roof for shade and can be sided with multiple modules to provide a long-span coverage for pedestrians.

Similar to the Interlude bus shelter, the Techline bus shelter as shown in Figure 2.3 (f), features a smooth, curved roof supported by interconnected square aluminum columns. This bus shelter has a dimension ranging from 5×10 ft to 5×15 ft and is designed to withstand winds at a maximum of 100 mph (161 km/h).

## **2.5 Performance Evaluation of Bus Shelters**

There is few literature on the impact performance of bus shelters. According to the bus shelter and bus stop guidelines developed by NCDOT (2017), the posted speed limit of roadways adjacent to bus shelters should be no more than 45 mph (72 km/h) to reduce the safety risk in the event of a vehicular crash.

According to the NCDOT Product Evaluation Program (NCDOT 2013), structural adequacy evaluation is required before the installation of bus shelters. Bus shelters should be placed within right-of-way and meet the following requirements:

1. The bus shelter should be designed to be able to withstand local winds with the maximum speeds ranging from 90 mph (145 km/h) to 130 mph (209 km/h) from the west side to the east coast of North Carolina.
2. The bus shelter should be correctly designed to resist all applicable loads in accordance with ASCE/SEI 7: Minimum Design Loads for Buildings and Other Structures.
3. The main wind force resisting system for the bus shelter should be correctly designed in accordance with the AASHTO Standard Specifications for Structural Support for Highway Signs, Luminaires and Traffic Signals.

The placement of bus shelters should satisfy safe and efficient operations of vehicular or pedestrian traffic and manifest the connectivity with sidewalk system. Bus shelters may employ materials such as transparent glass walls as covering to improve solar lighting for the safety of riders and pedestrians.

## **2.6 Occupant Safety Assessment in Vehicular Crash Events**

Occupant safety in vehicular crash events is commonly evaluated through the use of crash test dummies in standardized crash tests. Since the occurrence of the first Hybrid III dummy in 1976, Hybrid III crash test dummies have become a family of different sized dummies, including adult



male, adult female, and children of different ages. Based on a Hybrid III dummy, Pearlman et al. (1996) developed and tested the first pregnant crash test dummy by fitting a pregnancy insert which was composed of an elasticized vinyl uterine shell, simulated silicon amniotic fluid, and a 28-week simulated fetus. Accelerometers were instrumented in the head and thorax of the simulated fetus to predict the safety risk of both the fetal and maternal compartments. A series of thirty-nine crash tests were conducted with impact speeds ranging from 10 to 25 mph (0 to 40 km/h) under six different restraint conditions. The test results showed that at all tested speeds, there were three- to four-time increases in the forces transmitted to the abdomen area with the placement of a lap belt. The study recommended that the three-point restraint system should be employed to reduce the likelihood of injuries.

In 1997, Marzougui et al. (1997) conducted crash simulation of a New Car Assessment Program (NCAP) test and validated the finite element (FE) model of a 1993 Ford Taurus, which impacted a rigid wall at 30 mph (48 km/h) in both the crash test and simulation. In their study, a Hybrid III dummy and the driver side airbag were incorporated into the vehicle model and used in the numerical simulation. The FE simulation results had relatively good agreement with the actual crash test on the overall crash profile, HIC value, head and chest accelerations in the dummy, and the timing of airbag deployment. However, the numerical model developed in the study was limited by the computing power at the time and thus lacked sufficient details to fully assess the occupant injury. Marzougui et al. suggested that seat surface orientation, contact adjustment between the dummy and seat, detailed parts, and material models for certain components should be considered for model improvement.

Spinelli et al. (1999) conducted a study on occupant safety analysis using FE modeling and simulation of vehicular crashes. A series of crash simulations were performed to study the airbag “must-fire” and “no-fire” conditions as well as the occupant kinematics with cab-over-engine type of trucks. The crash simulations for no-fire condition consisted of a low-speed crash at 9.3 mph (15 km/h) against a rigid barrier and a high-speed crash at 31.1 mph (50 km/h) against a traffic-light pole. The crash simulations for the must-fire condition included a 21.7 mph (35 km/h) crash against a rigid barrier, a 18.6 mph (30 km/h) full frontal crash against a 20-ton parked trailer, and a 18.6 mph (30 km/h) 50% offset crash against the same parked trailer. In the study, the vehicle deceleration histories were used to evaluate occupant kinematics, which was well predicted in comparison with the actual crash tests.

Noureddine et al. (2002) developed a detailed Hybrid III dummy model that was used in the simulation of a full-scale crash test. The major components of the dummy model, such as head, chest, and neck, were validated using test data of the physical dummy, i.e., the acceleration histories and displacement profiles. They suggested that the dummy model could be employed as a reasonably accurate tool to investigate occupant safety in crashworthiness simulations when combined with other vehicle and restraint system models.

In the study conducted by Kirkpatrick et al. (2003), they developed an occupant FE model in LS-DYNA by combining anthropomorphic test device (ATD) deformable segments, joints, and additional flexible components. The FE model was validated using the time histories of head and chest accelerations for a 50<sup>th</sup> percentile Hybrid III dummy used in a sled test. They concluded that the occupant model could be computationally efficient for crash analysis of roadside safety



features and provide evaluation of the inertia effects of the occupants on the vehicle crash response.

Manoogian et al. (2007) used computational method to study the risk assessment of pregnant occupants under vehicular impacts. A validated MADYMO model of a 30-week pregnant occupant was employed to study the occupant response in an NCAP frontal crash. The FE models of nine compliant test vehicles, ranging within 10 model years and three different weight classes, were used in the crash simulations. These FE models were all equipped with three-point seatbelt restrain systems and airbags. Based on simulation results, they suggested that the uterine strain should be taken as the parameter to predict fetal injury or fetal-loss risk caused by placental abruption. The simulation results also showed that the average risk of adverse fetal outcome was 85% and a case with a change of equivalent velocity of 35 mph (56 km/h) or more was considered highly risky.

In the study of Teng et al. (2008), the multibody dynamics method was utilized to analyze the dynamic response of human body in a crash event and to assess the injuries on the occupant's head, chest, and pelvis. The occupant responses predicted by the multibody dynamics method using a 15-segment occupant dynamic model were found to have a good agreement with both test data of the actual frontal crash tests and the FE simulation results using a detailed Hybrid III 50<sup>th</sup> percentile dummy. The study provided a potential approach for evaluating vehicle safety with the cost-efficient multibody dynamic method.

In the study by Ueda et al. (2012), they combined multibody and FE modeling techniques to model human body responses and evaluate occupant safety. It was concluded that the evaluation technique based on multi-body modeling using MADYMO offered a simple, easy, flexible, and cost-efficient numerical analysis.

In the research project by Austin (2012) on lower extremity injuries and intrusions in frontal crashes, they found that intrusion induced occupant injuries were usually more severe than non-intrusion induced injuries. The study explored some potential causal factors associated with lower extremity injuries and found a strong correlation between floor pan intrusions and lower leg injuries, while no clear relationship was found between intrusions of the instrument panel and knee bolster and upper leg injuries. A regression model was also employed in the study to estimate the independent effect of intrusions on the probability of lower extremity injuries.

Deng et al. (2013) conducted a parametric study to analyze the effects of side curtain airbag deployment on the head of a 50<sup>th</sup> percentile Hybrid III dummy in a side impact. Full-scale FE simulations were performed using a 1996 Dodge Neon model to investigate various factors on their contributions to occupant responses, i.e., the HIC36 value and the peak head acceleration. The Taguchi method was adopted in the design of experiment and the analysis of variance was performed to predict the contributions of two main factors, the impact velocity and initial airbag inlet temperature, to the HIC36 value, which were found to be 43.2% and 10.5%, respectively. Similarly, the contributions to the peak head acceleration were found to be 30.8%, 12.9%, and 3.8% from the impact velocity, initial airbag inlet temperature, and airbag trigger time, respectively. The study also provided a practical guidance to help mitigate the occupant injury risk using design optimization.

In the work of Untaroiu et al. (2013), they assessed and validated the THOR-NT dummy model

by comparing the numerical simulation results with the kinetic and kinematic data from sled tests at an impact speed of 24.9 mph (40 km/h). The time histories of the displacements of certain key components of the dummy body, as well as the interaction forces between the dummy and seatbelt, were shown to have a relatively good agreement between test data and simulation results. An objective rating technique was introduced in the assessment of the THOR dummy model and showed an average rating "fair-to-acceptable" for the THOR dummy model.

Reichert et al. (2014) conducted research on occupant safety evaluation using FE simulations. A detailed 2010 Toyota Yaris model, which was combined with an airbag and three dummy models, i.e., the Hybrid III, THOR, and THUMS models, was employed in the investigation. The FE models were validated using crash test data of the NCAP frontal impact, IIHS 40-percent offset impact, and NHTSA oblique frontal impact. A sensitivity analysis was also conducted in the study on impact parameters, occupant seating positions, and restraint system variations. It was concluded that the integrated model could be used to simulate and analyze the effects beyond the validated configurations.

Shi et al. (2015) investigated the effect of obesity on occupant responses in frontal crashes with the whole-body human FE models. A parametric analysis based on the Taguchi orthogonal array was conducted to evaluate occupant injuries in relation to body mass indices (BMIs), a parameter indicating the relative level of obesity. It was observed from the study that occupants with high obesity carried significantly higher risk of injuries to the thorax and lower extremities than those with low obesity.

In the study by Keon et al. (2016), they performed occupant risk assessment using multiple crash test dummies in frontal crash tests at an impact speed of 35 mph (56 km/h). A THOR 50<sup>th</sup> male (THOR-50M) dummy was positioned in the driver seat and two Hybrid III 5<sup>th</sup> percentile adult female (AF05) dummies were positioned in the front passenger seat and the rear right passenger seat, following the seating procedures of the NCAP and FMVSS No. 214 Side Impact Compliance Test Procedures. Compared with data from previous NCAP crash test using a 50<sup>th</sup> percentile Hybrid III dummy (AM50), Keon et al. found that the THOR-50M dummy predicted a higher risk of chest and femur injury than the AM50 dummy, and that the AF05 dummy in the front passenger seat showed a lower femur compression due to the larger distance from the dash board. In all the crash tests, the AF05 dummy in the rear right passenger seat predicted a substantially higher risk of head, neck, and chest injury than the dummy in the front passenger seat, with 3.8 to 6.2 times greater joint probability of injury.

Wang et al. (2018) performed numerical analysis of occupant head injuries caused by impacting the dump truck panel during a crash event. A detailed human head model and a dump truck cockpit model were employed in the FE simulations of the study. Specifically, they investigated the contributions of panel parameters such as panel type, elastic modulus of the filling, elastic modulus of the frame, and the distance between panel connection joints under different impact conditions. Based on the numerical analysis, they suggested that a soft panel with both lower elastic moduli for the filling and the frame as well as a longer fixing distance could be more helpful to prevent occupant head injury. A sensitivity analysis was subsequently performed in the study, which showed that the fixing distance and elastic modulus of the frame could significantly affect the peak head acceleration and the maximum skull stress.

Recently, Xu et al. (2018) reviewed literature on the development and validation of dummies and human models used in crash tests and suggested that there existed some limitations in the existing crash test dummies studies. They acknowledged that existing FE models of crash test dummies played an important role in studying occupant injuries and provided practical guidance for vehicle safety enhancement. However, since the current commercial crash test dummies were typically developed based on the human characteristics of Europeans and Americans, these models might not represent well the human characteristics of people from other countries or regions. Furthermore, the elderly, obese and dwarf males or females were more vulnerable to fatality or severe injuries in a crash event; therefore, these factors should be taken into consideration in future research on occupant safety.

Using validated FE models, Asadinia et al. (2018) conducted a sensitivity analysis and optimization for occupant safety in a vehicular frontal crash based on ECE R94 regulations. In the study, the peak head accelerations and head injury criteria (HIC36) were taken as the two objective functions in the sensitivity analysis and optimization while the distance between the airbag and dummy, trigger time, initial inflator gas temperature, and tank pressure were selected as the design variables. The optimal design setting, which meant the best for occupant safety, was found to be 35 cm of airbag-dummy distance, 15 ms for the trigger time, 900 K of initial gas temperature, and 200 KPa of the tank pressure. They also indicated that the sensitivity indices of the four design variables to occupant safety (i.e., the peak head acceleration and HIC36) ranked from the highest to lowest in the order of airbag-dummy distance, trigger time, initial gas temperature, and tank pressure.

In the study of Zhao et al. (2018), they combined a baseline virtual testing model with a detailed human model of an average male that was developed by the Global Human Body Models Consortium. The combined model was used to study occupant safety and protection in a versatile seating environment in autonomous vehicles. Finite element simulations were performed for frontal crashes at 25 mph (40 km/h) with 12 different occupant facing directions and equipped with three-point seatbelts. The simulation results showed that there were large variations in occupant responses due to the change of directions of impact pulses as well as the changes of interactions between occupant and seatbelts for different seating positions. It was identified in the study as the two worst cases when rear facing and side rear facing respectively due to neck hyperextension and hitting the seat side structure.

In the review by Linder et al. (2019) on occupant safety assessment under vehicular crashes, they indicated that developing occupant models for the female population was necessary due to the lower protection level for females in crash events than that for males. Crash test dummies and human body models representing the average females, or new dedicated occupant models, have been gradually employed in some recent studies of occupant safety assessment. The results of these studies could be useful in providing practical guidance to automobile manufacturers to enhance the robustness of the current occupant protection systems.

Ressi et al. (2019) conducted a preliminary study on occupant injury risk assessment for Highly Automated Vehicles (HAVs) with respect to seat configurations and crash load directions. Given the popularity of HAVs, there is an increased demand of flexibility in seat adjustment and

positioning compared to traditional vehicles. This also increases the uncertainty of occupant responses with new seat positions in vehicular crashes. To this end, Ressi et al. developed a new, efficient method by using the restraining potential as a numerical analysis tool before depth analysis (i.e., detailed FE simulation) to evaluate the occupant response for any given interior configuration.

### 3. Finite Element Modeling of Vehicles, Occupant, Cluster Mailboxes and the Bus Shelter

The numerical simulation work of this study involved FE models of two vehicles equipped with airbags and seatbelts, a Hybrid III 50<sup>th</sup> percentile crash test dummy, two types of cluster mailboxes, and a Brasco 5 x 10 ft Slimline Bus Shelter. The two vehicle models were a 2010 Toyota Yaris (1100C) and a 2006 Ford F250 (2270P), which were both MASH compliant vehicles. The two types cluster mailboxes were a Type I and a Type IV cluster mailbox that were both evaluated as a single unit and as dual units. The crash simulations for safety assessment of the cluster mailboxes were conducted at MASH TL-1 conditions, i.e., impacted by both the 1100C and 2270P vehicles at a speed of 31 mph (50 km/h) and impact angles of 0° or 25°. The crash simulations for the bus shelter were conducted at MASH TL-2 conditions, i.e., impacted by both the 1100C and 2270P vehicles at a speed of 44 mph (71 km/h) and impact angles of 0° or 25°. In all the simulation cases, the vehicles departed from the travel lane at the prescribed impact speeds and angles before hitting the cluster mailboxes or the bus shelter. The impact speed was defined in the vehicle's travel direction, and the impact angle was defined as the angle between the vehicle's travel direction and the horizontal direction of the cluster mailbox's or the bus shelter's front face.

#### 3.1 FE Models of Two Test Vehicles

Figure 3.1 shows the FE models of the two test vehicles used in this project, a 2010 Toyota Yaris passenger car (MASH 1100C) and a 2006 Ford F250 pickup truck (MASH 2270P).



Figure 3.1 FE models of the two MASH compliant vehicles used in crash simulations.  
(a) A 2010 Toyota Yaris passenger car; and (b) a 2006 Ford F250 pickup truck.

The FE model of the 2010 Toyota Yaris had a total of 926 components that were meshed into 602,106 nodes and 582,690 elements (15,165 solid, 562,821 shell, 4,685 beam, and 19 discrete elements). Eleven different material models were used, including

- The piecewise linear plasticity model defined for most steel components;
- The rigid model for mounting hardware;
- The elastic model for the tires and other rubber components;
- The Blatz-Ko rubber model for nearly incompressible rubber cushions;
- The viscous damping model for the shock absorbers;

- The low-density foam model for the radiator core;
- The spot-weld model for sheet metal connections;
- The null material model defined for contact purposes;
- The linear elastic and nonlinear spring models for the spring-damper suspensions; and
- The fabric model for airbag system components.

Hourglass control was used on components that could potentially experience large deformations. The Wang-Nefske Model with a reference geometry method was used in this vehicle model to simulate airbag deployment during a crash event. The FE model of the 2010 Toyota Yaris was developed at the Center for Collision Safety and Analysis, and validated using test data of full frontal, offset frontal, and side impact tests (NCAC 2011, NCAC 2012).

The FE model of the 2006 Ford F250 was composed of 746 components that were meshed into 737,986 nodes and 735,895 elements (25,905 solid, 2,305 beam, 707,656 shell, and 29 discrete elements). Eleven different constitutive models were used, including

- The piecewise linear plasticity model defined for most steel components;
- The rigid model for mounting hardware;
- The elastic model for the tires and other rubber components;
- The linear and nonlinear elastic spring model for the suspension springs;
- The viscous damping model for the shock absorbers;
- The low-density foam model for the radiator core;
- The spot-weld model for sheet metal connections;
- The viscoelastic model for radiator support mounts;
- The Blatz-Ko rubber model for nearly incompressible rubber cushions;
- The null material model for contact purposes; and
- The Simple Airbag Model the airbag.

Hourglass control was used on various components that could potentially experience large deformations. The FE model of the 2006 Ford F250 was originally developed at the National Crash Analysis Center and validated with NHTSA's NCAP frontal impact test (NCAC 2008).

In crash simulations of vehicles impacting roadside utilities such as cluster mailboxes or bus shelters, both the vehicles and roadside utilities could undergo large nonlinear deformations and a large number of components would interact with each other during the crash event. To correctly simulate the vehicular and structural responses, appropriate contact algorithms should be chosen with careful attention to accurately capture the interactions among different parts. Such contact handling was critical to the numerical stability of the simulations as well as to the realistic responses of the vehicles or roadside utilities. In the FE models of the two test vehicles, the contact algorithms were chosen iteratively through trial-and-error to obtain the appropriate contact definitions for the crash simulations of this project.

### **3.2 FE Model of the Hybrid III Crash Test Dummy**

Figure 3.2 shows the FE model a detailed Hybrid III 50<sup>th</sup> percentile crash test dummy ( $\alpha$  version), which was developed by the Livermore Software Technology Corporation and used in this project. The FE model of the Hybrid III 50<sup>th</sup> percentile crash test dummy had a total of 349 components that were meshed into 228,706 nodes and 338,506 elements (186,808 solid, 151,455 shell, one

discrete, and 242 beam elements) with an overall weight of 176 lb (79.86 kg). Nine material models were used in this dummy model including the elastic model for bones and skull, viscoelastic model for skins, low-density viscous foam model for chest pad, low-density foam model for molded foam, Blatz-Ko rubber model and elastic spring model for some joint connections or supports, and null material model for contact analysis only (i.e., no actual physical properties). Rigid model and viscous foam model were also used in the crash test dummy model.



Figure 3.2 The FE model of a Hybrid III 50th percentile crash test dummy.

Accelerometers were defined in the FE model of the Hybrid III 50<sup>th</sup> percentile crash test dummy in the head, chest, spine, belly, pelvis, both knees, and both ankles. These accelerometers were defined using Seatbelt Accelerometer Elements, which could record the time histories of accelerations at locations of potential injury and help to evaluate occupant safety.

The dummy model was positioned into the FE models of the 2010 Toyota Yaris and 2006 Ford F250 based on NHTSA's positioning guidelines for crash testing. The dummy occupant was restrained by a three-point seatbelt system. In the initial crash simulations, it was observed that the edge of the tensioned seatbelt penetrated into the dummy's shoulder joint. After carefully selecting the contact algorithms, these unrealistic penetrations were eliminated.

### 3.3 FE Models of Cluster Mailboxes

The two types of cluster mailboxes used in this study were the Type I and Type IV cluster mailboxes manufactured by Florence Manufacturing Company. Both types of the cluster mailboxes had a width of 30 ½ inches (0.77 m), a depth of 18 inches (0.46 m), and an overall height of 62 inches (1.57 m) above the ground. The major differences between these two types of cluster mailboxes were the size of the box units or the number of boxes, and the height of the pedestal. The Type I cluster mailbox, as shown in Figure 3.3, had a 28 ½-in (0.72 m) pedestal, while the Type IV had a 14 ½-in (0.37 m) pedestal as shown in Figure 3.4.

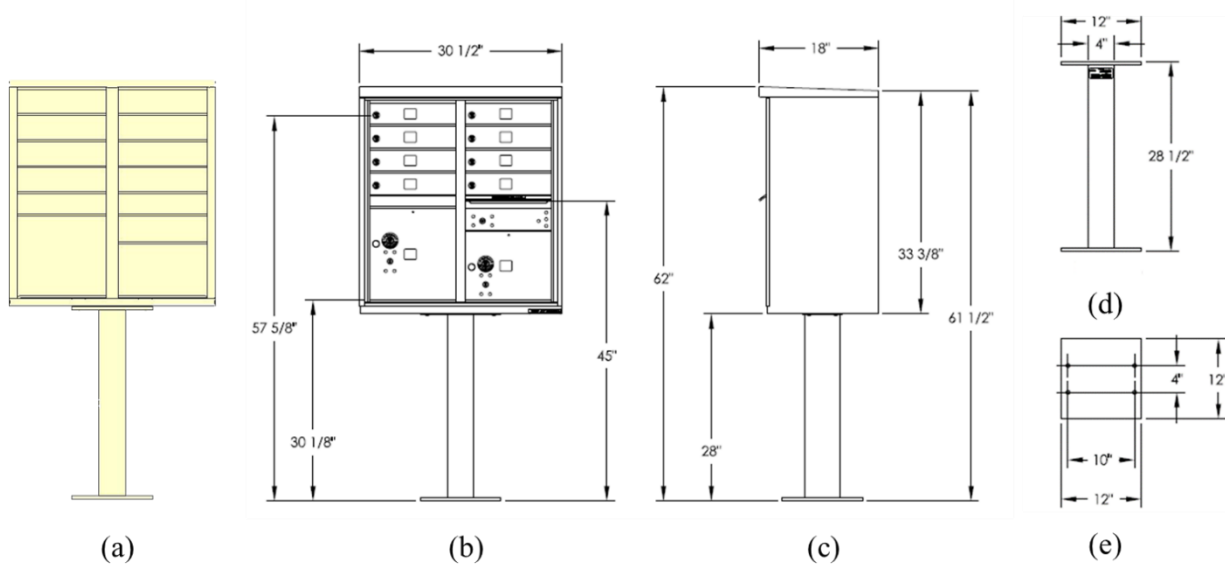


Figure 3.3 FE model of the Type I cluster mailbox.  
(a) FE model; (b) Front view; (c) Side view; (d) Pedestal; and (e) Pedestal base.

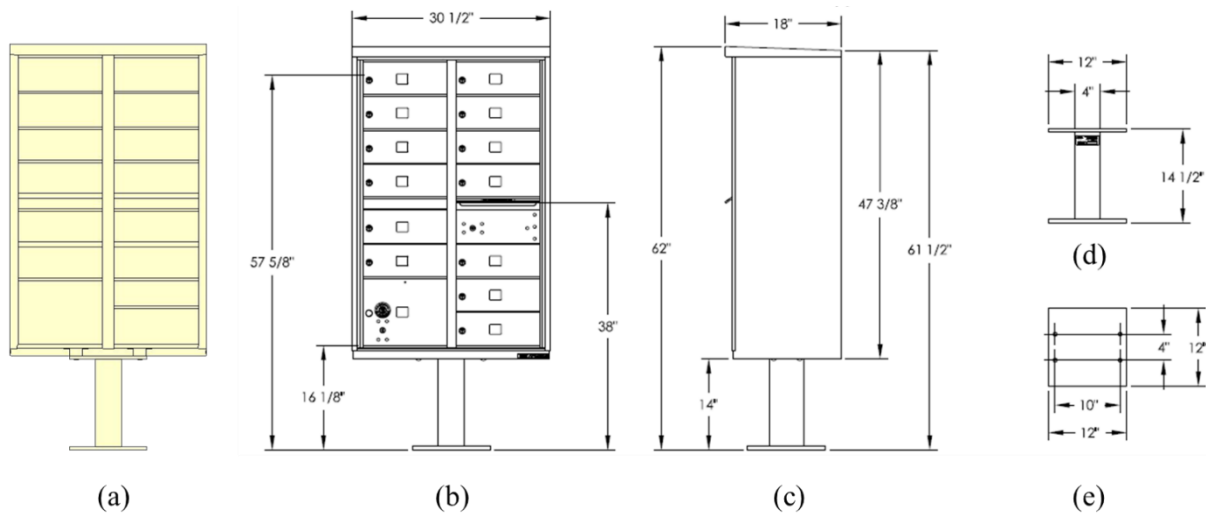


Figure 3.4 FE model of the Type IV cluster mailbox.  
(a) FE model; (b) Front view; (c) Side view; (d) Pedestal; and (e) Pedestal base.

The FE model of the Type I cluster mailbox had a total of 22 parts that were meshed into 387,349 nodes and 322,147 elements (241,760 solid, 80,383 shell, and 4 discrete elements). This cluster mailbox was mainly composed of inner slots and doors, top cover sheet, bottom cover sheet, outer box, front face frame, pedestal, pedestal base plate, pedestal top plate, horizontal supporting beams, and four pairs of bolts and nuts. Three different material models were used in the Type I mailbox model: the kinematic plasticity model for most metal parts such as doors, cover sheets, and pedestal, the rigid material model and nonlinear spring model for bolt-and-nut connections. The FE model of the Type IV cluster mailbox had 314,502 nodes and 262,531 elements (188,896 solid, 73,631 shell, and 4 discrete elements); it had the same material models as those used in the



FE model of the Type I cluster mailbox.

The bolt-and-nut connections were used between the pedestal top plate and the horizontal beams. Figure 3.5 illustrates the modeling scheme on how the clamping force is provided by the bolt-and-nut connection in the FE model. A discrete element was embedded inside the bolt, with its two ends sharing nodes with bolt head and the nut, respectively. A sliding contact definition was specified between the bolt and nut to allow small, translational movement. The clamping force was triggered by a prescribed elongation of the discrete element. The pedestal base plate was fixed to the ground as boundary conditions.

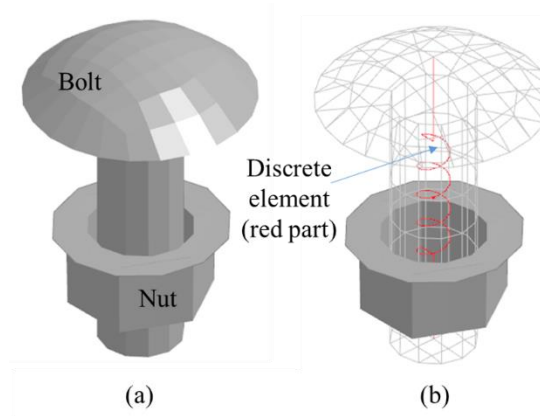


Figure 3.5 FE model of a bolt-and-nut connection.

(a) FE model of a bolt and nut; (b) Discrete element utilized in the bolt-and-nut model.

In the crash simulations of this project, both the single- and dual-unit cluster mailboxes were evaluated. Figure 3.6 shows the FE models of a dual-unit Type I and a dual-unit Type IV cluster mailboxes. The two units were placed side by side with a 3-inch gap between the two units.

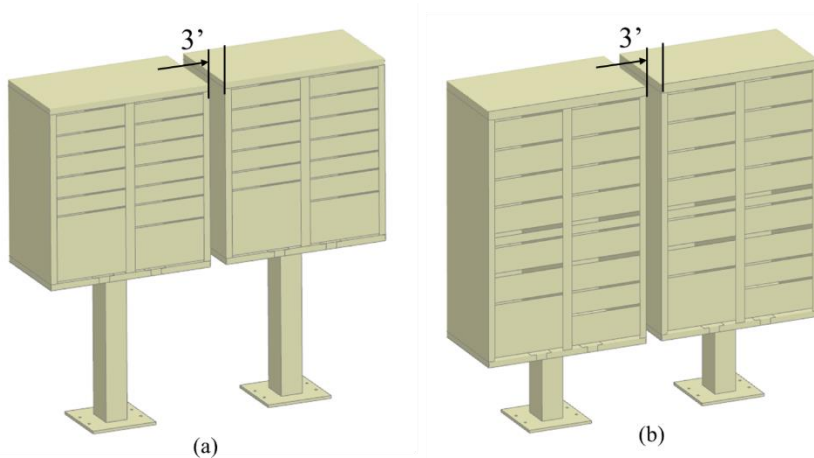


Figure 3.6 Dual-unit cluster mailbox configuration (a) Type I (b) Type IV.

### 3.4 FE Model of the Bus Shelter

The FE model of the bus shelter was developed based on a “typical” bus shelter chosen in this study, the Brasco Slimline SL-510-OF bus shelter. The bus shelter model consisted of 124 parts

including roof covering, roof frame, polycarbonate windscreen, structural columns, bolts and nuts, and cubic clip joints. These components were meshed into 151,378 nodes and 151,251 elements (151,216 shell and 35 discrete elements). The roof frames and structural columns were connected via seven cubical clip joints. The polycarbonate windscreen was constrained to the frames and columns by sharing nodes along the edges of these parts. Figure 3.7 shows the overall bus shelter model and the cubical clip joints.

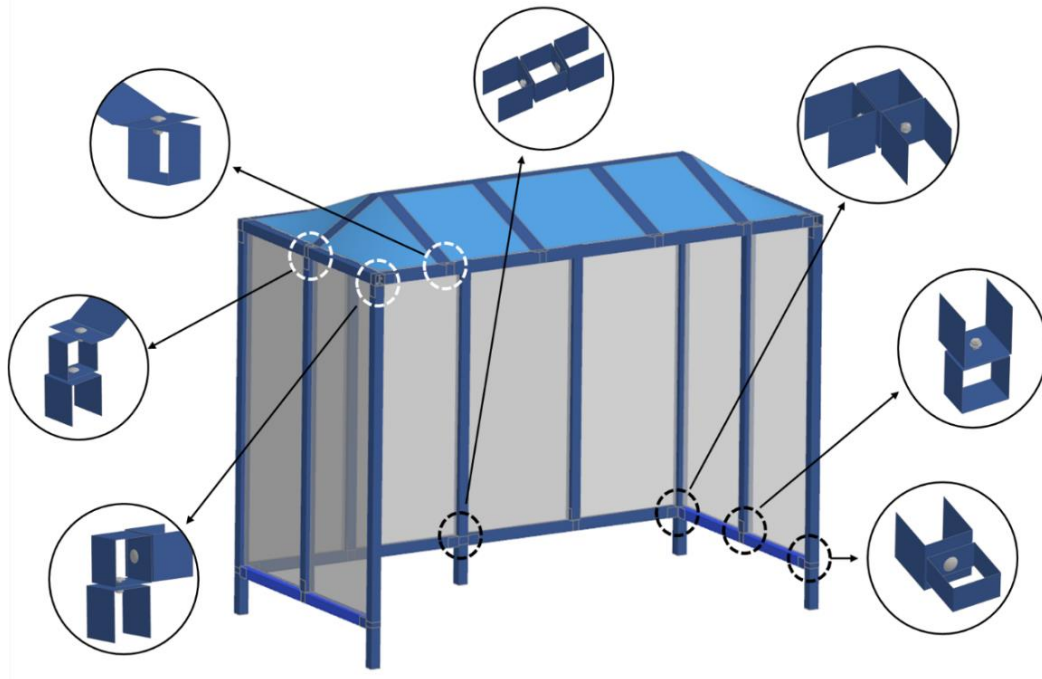


Figure 3.7 FE model of the typical bus shelter with clip joints details.

Figure 3.8 shows the bus shelter's overall dimensions; it is 111 ½ inches (2.83 m) long, 57 inches (1.45 m) wide, and 84 ⅛ inches (2.14 m) tall excluding the cone shaped roof.

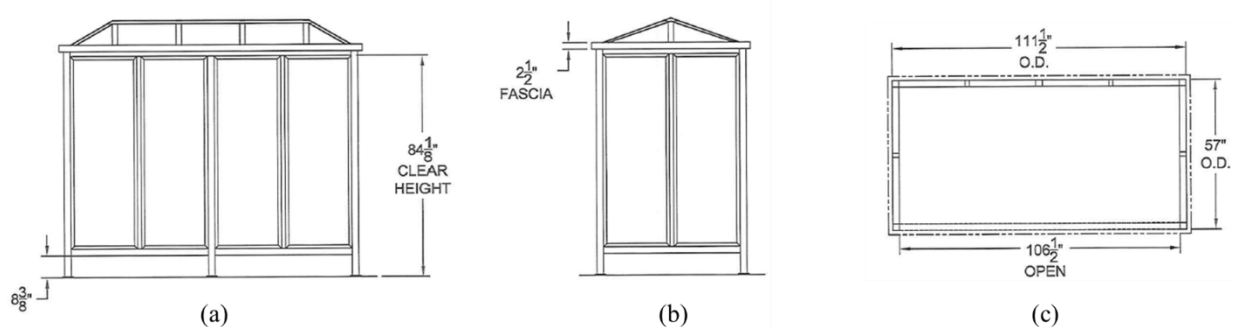


Figure 3. 8 The dimensions of the Brasco Slimline SL-510-OF bus shelter.  
(a) Front view; (b) Side View; and (c) Plane view.

Four different material models were used in the bus shelter model: the elastic model with an eroding option based on the principal stress for the polycarbonate windscreen, the kinematic

plasticity model for all the metal parts including the columns, roof frames, and cubical clips, and the rigid model with a nonlinear spring model for the bolt-and-nut pair with an initial offset to trigger the clamping force. The lower ends of the five columns of the bus shelter were fixed to the ground surface as boundary conditions.

### 3.5 FE Models of Road Surfaces

In this study, the crash simulations for the cluster mailboxes were conducted under two road conditions: on a flat road and on a road with a curb. The FE model of the flat road was simply a 4-node shell element, while the FE model of the road with a curb was composed of two flat surfaces connected by a 5-inch high curb. For both road surface models, the rigid material model was used. Figure 3.9 shows the FE models of the two types of road surfaces used in the crash simulation. The FE model of the road with a curb was only used in the crash simulations of cluster mailboxes in which the cluster mailboxes were placed at 8 ft (2.44 m) behind the curb.

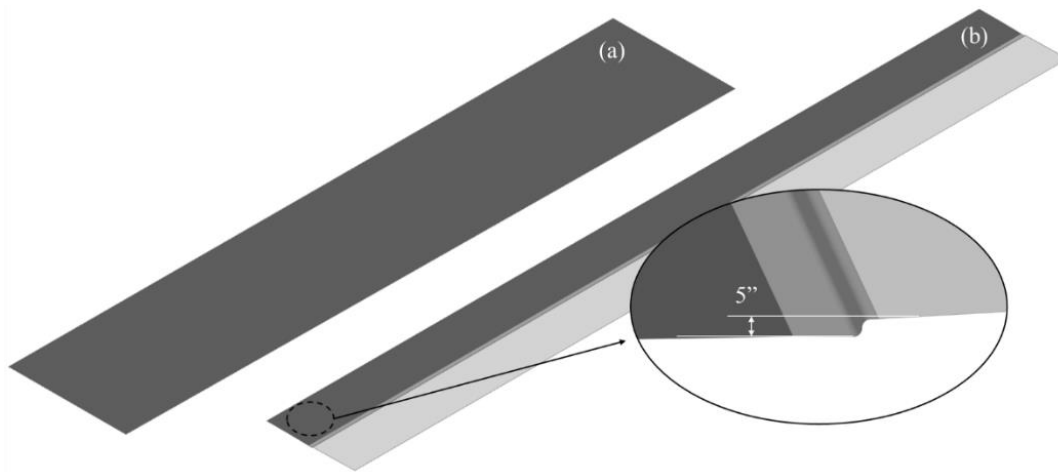


Figure 3.9 FE models of two road surfaces for crash simulations.  
(a) A flat road surface; and (b) a road with a curb.

### 3.6 Simulation Setup for Cluster Mailboxes

The crash simulations for cluster mailboxes involved two types of mailboxes (Type I and Type IV), two configurations (single- and dual-unit), two test vehicles (a 2010 Toyota Yaris and 2006 Ford F250), two impact angles ( $0^\circ$  and  $25^\circ$ ), and two types of road surfaces (a flat road and road with a curb). For the  $0^\circ$  impacts, the vehicle impacted the mailbox from the side with the vehicle's centerline aligned with mailbox's centerline. For the  $25^\circ$  impacts, there were no specific requirements in MASH for the impact location in the cases of the dual-unit cluster mailboxes. In this project, two impact locations were selected: at a corner and at the mid-point of the dual-unit cluster mailboxes, as shown in Figure 3.10. For crash simulations on the road with a curb, only the  $25^\circ$  impact angle was used (the cases of  $0^\circ$  impacts on the road with a curb would be the same as those on the flat road).

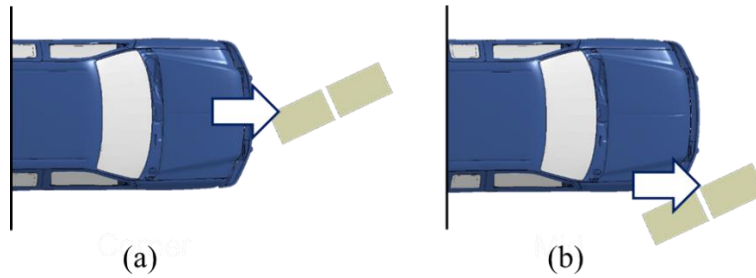


Figure 3.10 Two impact locations for crash simulations with double cluster mailboxes (a) Corner (b) Mid-point.

With all the aforementioned conditions, a total of 32 crash simulations were required for cluster mailboxes and these simulations were divided into four categories as follows.

- Category 1: Type I cluster mailboxes impacted by a 2010 Toyota Yaris (1100C);
- Category 2: Type I cluster mailboxes impacted by a 2006 Ford F250 (2270P);
- Category 3: Type IV cluster mailboxes impacted by a 2010 Toyota Yaris (1100C); and
- Category 4: Type IV cluster mailboxes impacted by a 2006 Ford F250 (2270P).

There were a total of eight simulations in Category 1, all of which were conducted using the 1100C test vehicle with an impact speed of 31 mph (50 km/h). The eight simulation cases were: (1) a single-unit Type I cluster mailbox with 0° impact angle; (2) a single-unit Type I cluster mailbox on a flat road with 25° impact angle; (3) a dual-unit Type I cluster mailbox with 0° impact angle; (4) a dual-unit Type I cluster mailbox on a flat road with 25° impact angle and impacted at the corner; (5) a dual-unit Type I cluster mailbox on a flat road with 25° impact angle and impacted at the mid-point; (6) a single-unit Type I cluster mailbox behind a curb with 25° impact angle; (7) a dual-unit Type I cluster mailbox behind a curb with 25° impact angle and impacted at the corner; and (8) a dual-unit Type I cluster mailbox behind a curb with 25° impact angle and impacted at the mid-point. Table 3.1 gives a summary of the eight simulation cases of Category 1, which are also illustrated by the full simulation models in Figure 3.11.

In Category 2, there were a total of eight simulations, all of which were conducted using the 2270P test vehicle with an impact speed of 31 mph (50 km/h). The eight simulation cases were exactly the same as the respective ones in Category 1 except for the test vehicle. Table 3.2 gives a summary of the eight simulation cases of Category 2, which are also illustrated by the full simulation models in Figure 3.12.

Category 3 had a total of eight simulations, all of which were conducted on the Type IV mailboxes using the 1100C test vehicle with an impact speed of 31 mph (50 km/h). The eight simulation cases were exactly the same as the respective ones in Category 1 except for type of the mailboxes. Table 3.3 gives a summary of the eight simulation cases of Category 3, which are also illustrated by the full simulation models in Figure 3.13.

Category 4 had a total of eight simulations, all of which were conducted using the 2270P test vehicle with an impact speed of 31 mph (50 km/h). The eight simulation cases were exactly the same as the respective ones in Category 3 except for the test vehicle. Table 3.4 gives a summary of the eight simulation cases of Category 4, which are also illustrated by the full simulation models in Figure 3.14.

Table 3.1 Simulation matrix for Category 1: Type I mailboxes impacted by a 2010 Toyota Yaris.

Impact speed	Impact angle	On a flat road			Behind a Curb		
		Single-unit	Dual-unit		Single-unit	Dual-unit	
31 mph (50 km/h)	0°	(1)	(3)		/	/	
	25°	(2)	(4) Corner	(5) Mid-point	(6)	(7) Corner	(8) Mid-point

Table 3.2 Simulation matrix for Category 2: Type I mailboxes impacted by a 2006 Ford F250.

Impact speed	Impact angle	Flat road			Behind the Curb		
		Single-unit	Dual-unit		Single-unit	Dual-unit	
31 mph (50 km/h)	0°	(1)	(3)		/	/	
	25°	(2)	(4) Corner	(5) Mid-point	(6)	(7) Corner	(8) Mid-point

Table 3.3 Simulation matrix for Category 3: Type IV mailboxes impacted by a 2010 Toyota Yaris.

Impact speed	Impact angle	Flat road			Behind the Curb		
		Single-unit	Dual-unit		Single-unit	Double-unit	
31 mph (50 km/h)	0°	(1)	(3)		/	/	
	25°	(2)	(4) Corner	(5) Mid-point	(6)	(7) Corner	(8) Mid-point

Table 3.4 Simulation matrix for Category 4: Type IV mailboxes impacted by a 2006 Ford F250.

Impact speed	Impact angle	Flat road			Behind the Curb		
		Single-unit	Dual-unit		Single-unit	Dual-unit	
31 mph (50 km/h)	0°	(1)	(3)		/	/	
	25°	(2)	(4) Corner	(5) Mid-point	(6)	(7) Corner	(8) Mid-point

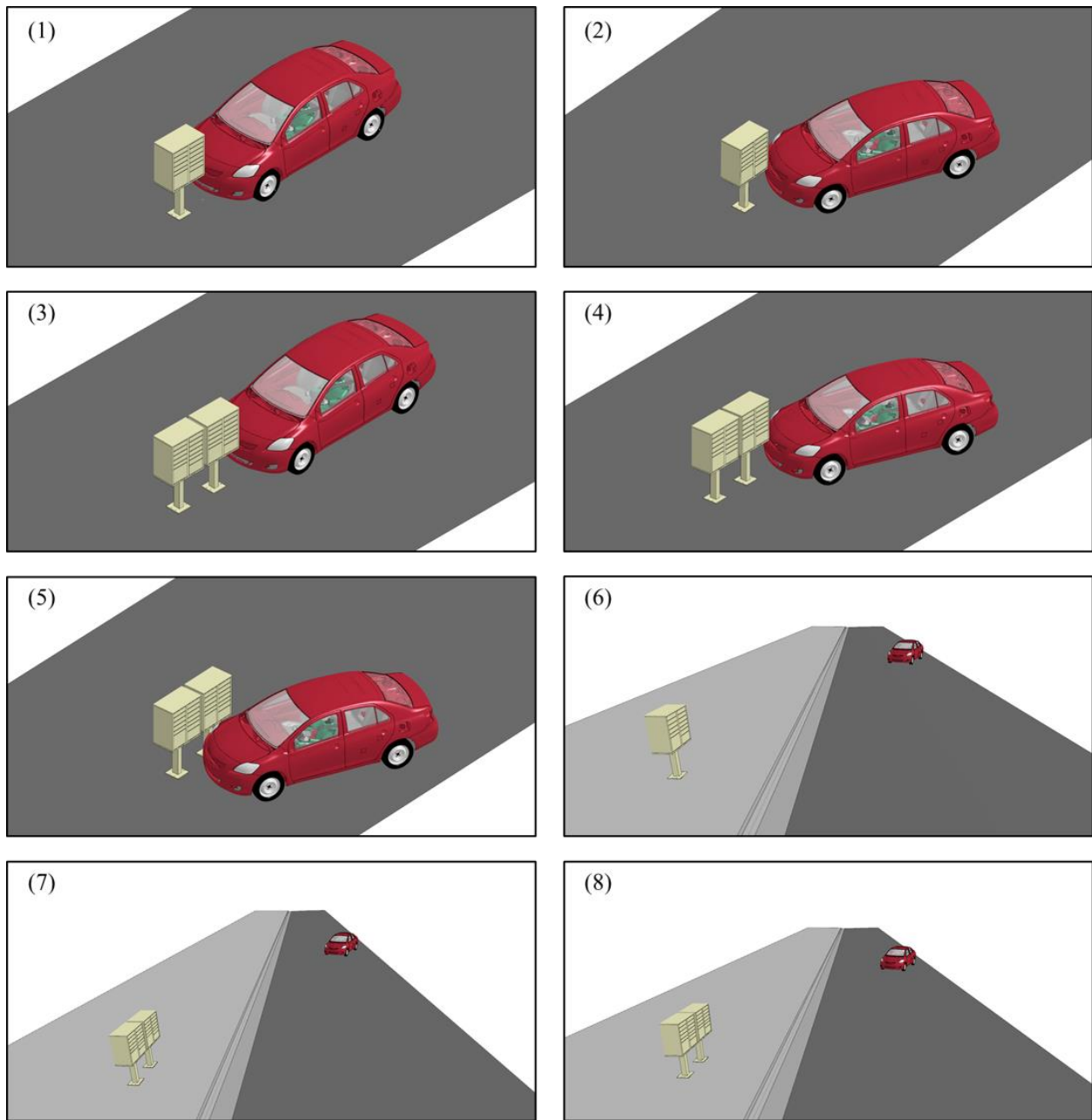


Figure 3.11 Full simulation models for the eight simulation cases of Category 1.

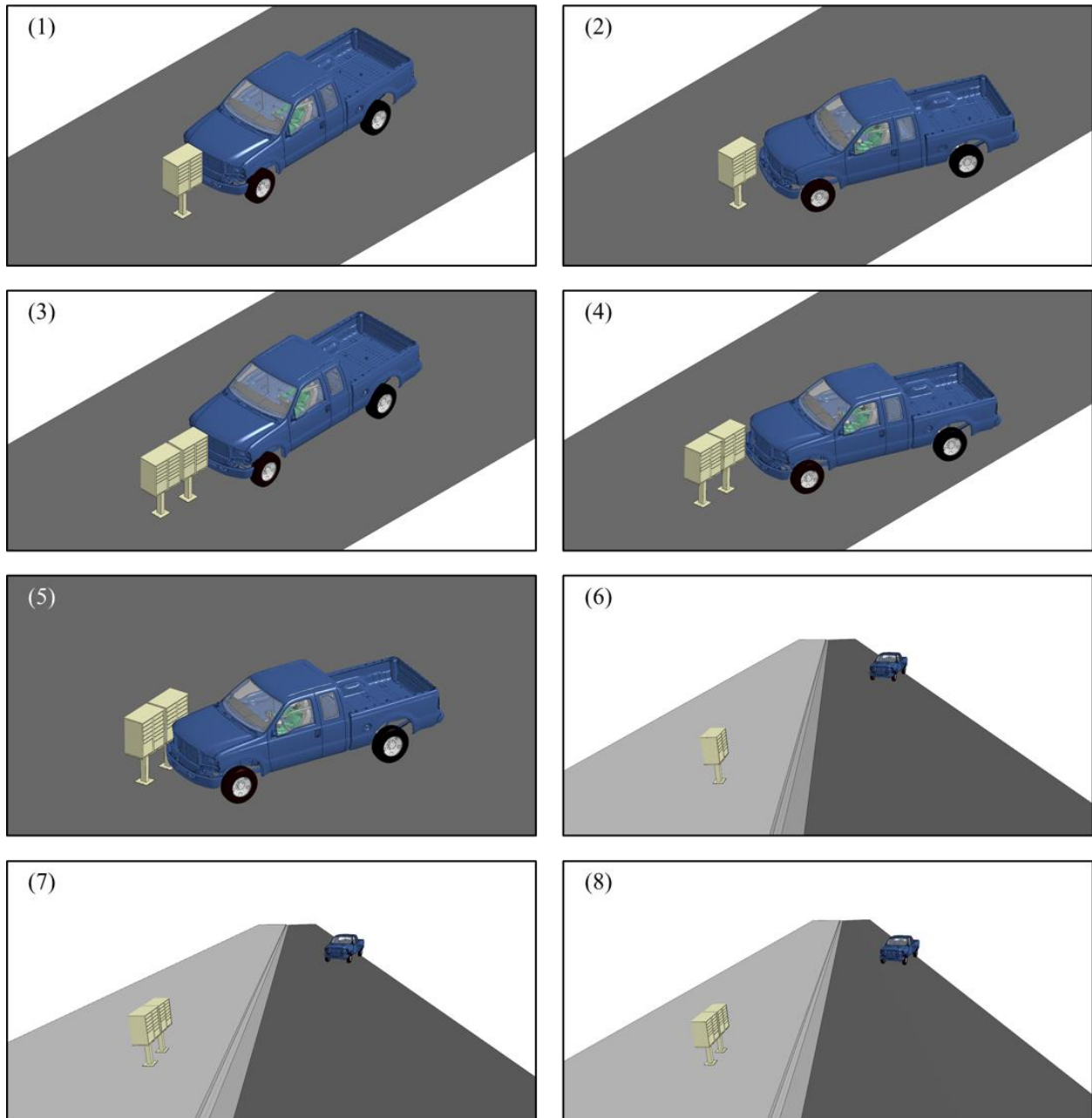


Figure 3.12 Full simulation models for the eight simulation cases of Category 2.

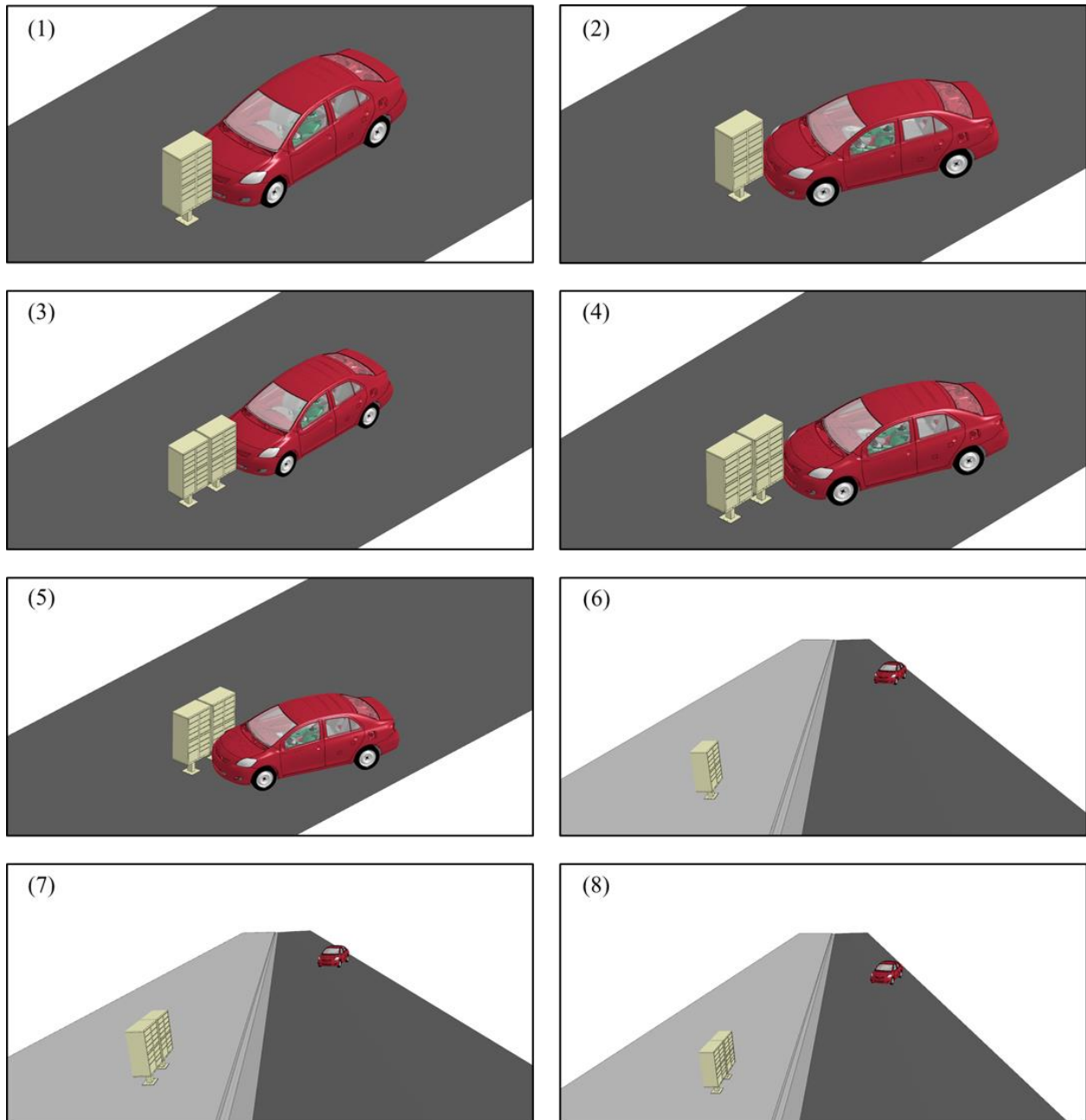


Figure 3.13 Full simulation models for the eight simulation cases of Category 3.



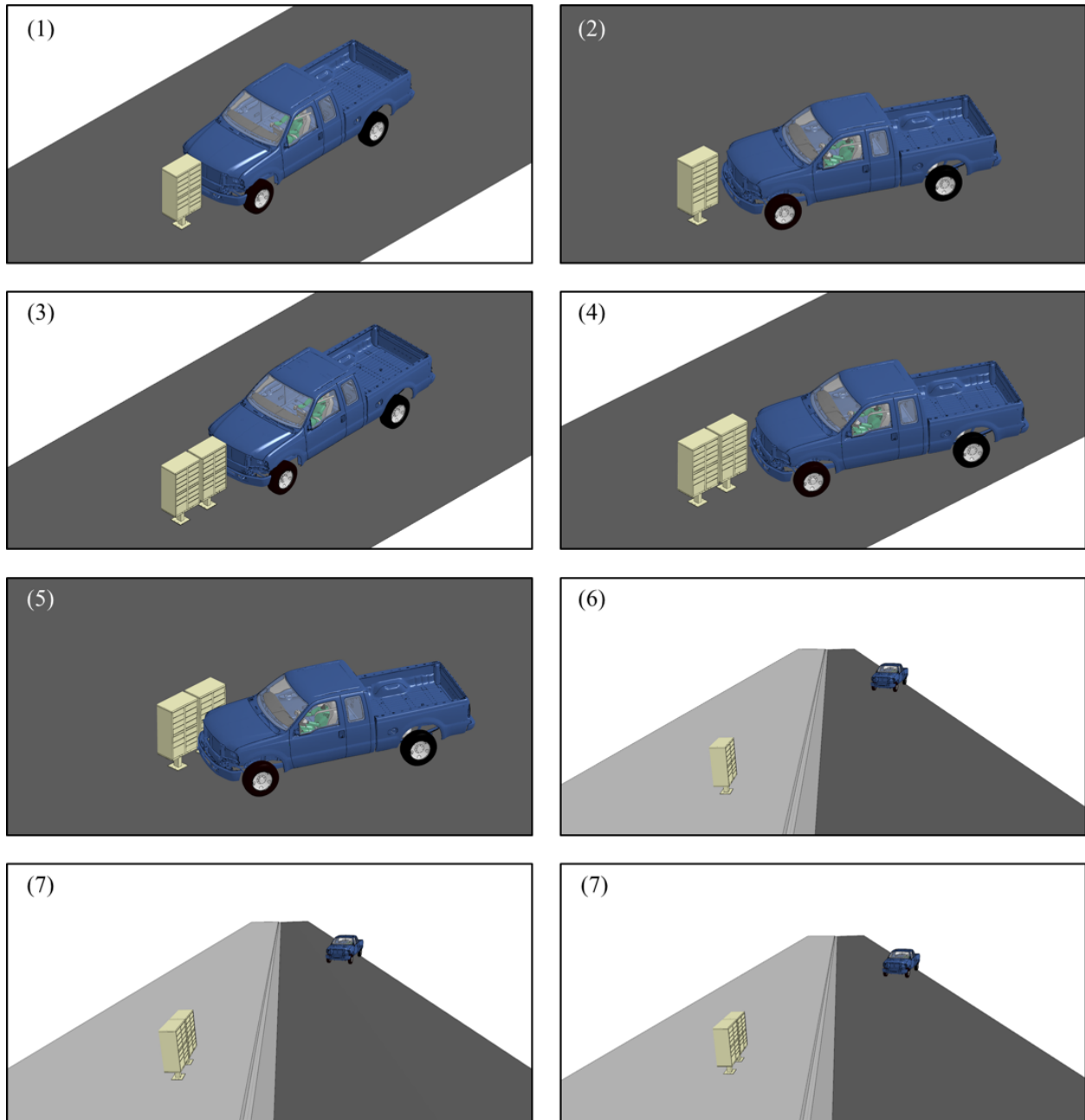


Figure 3.14 Full simulation models for the eight simulation cases of Category 4.

### 3.7 Simulation Setup for the Bus Shelter

For the bus shelter under vehicular impacts, occupant safety was evaluated under MASH TL-2 conditions (i.e., at an impact speed of 44 mph (71 km/h)) for the following four impact cases: (1) the bus shelter was impacted by a 2010 Toyota Yaris at 0° impact angle; (2) the bus shelter was impacted by a 2010 Toyota Yaris at 25° impact angle; (3) the bus shelter was impacted by a 2006 Ford F250 at 0° impact angle; and (4) the bus shelter was impacted by a 2006 Ford F250 at 25° impact angle. All the above mentioned crash simulations were conducted on a flat road. For the cases with a 25° impact angle, the impact location was chosen as the vertical column of the bus

shelter that was the closest to the test vehicle. Table 3.15 gives the simulation matrix for the bus shelter and Figure 3.15 shows the full simulation models for the four cases.

Table 3.5 Simulation matrix for the bus shelter.

<b>Crash Simulations for the Bus Shelter</b>					
Test utility	Impact speed	Road type	Test vehicle	Impact angle (No. of simulation cases)	
The typical bus shelter	44 mph (71 km/h)	Flat road	2010 Toyota Yaris	0° (1)	25° (2)
			2006 Ford F250	0° (3)	25° (4)

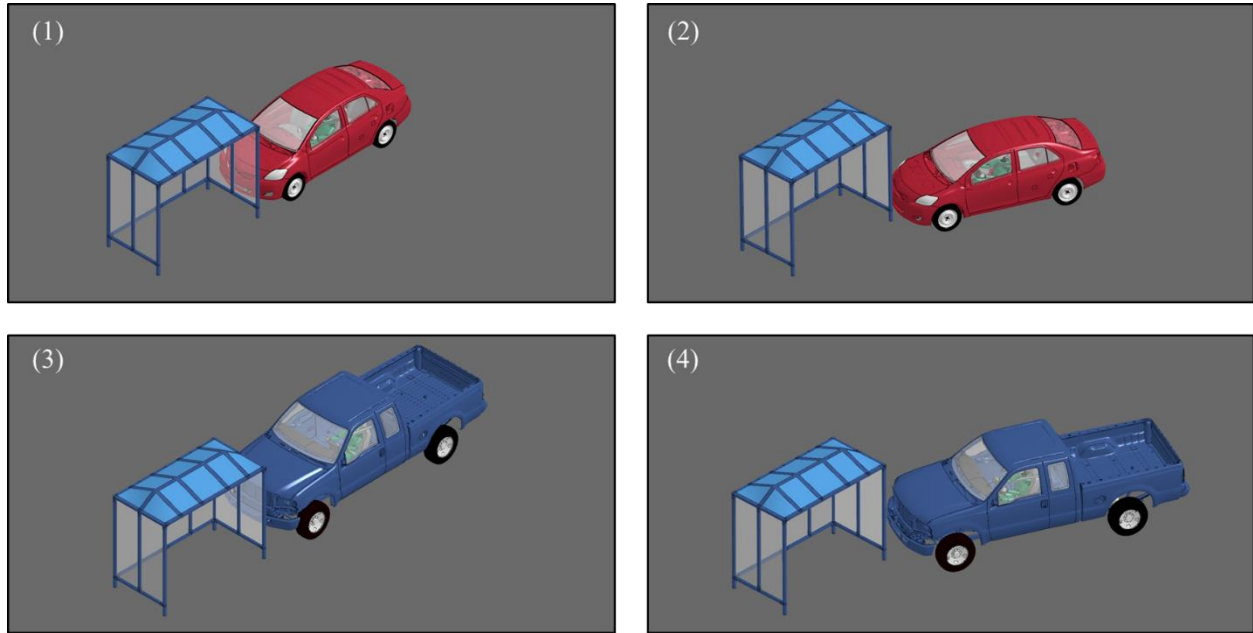


Figure 3.15 Full models for the four simulation cases of the bus shelter.

## 4. Simulation Results and Analysis of Cluster Mailboxes

The 32 crash simulations for cluster mailboxes in the four categories were performed at MASH TL-1 conditions and the simulation results were analyzed to evaluate occupant responses and potential injuries. The occupant risk was evaluated using MASH criteria on occupant impact velocities (OIVs), occupant ride-down accelerations (ORA), and roll and pitch angles of the test vehicles. The time histories of accelerations measured on the crash dummy (i.e., on head, chest, and pelvis) were also examined. The probability of skull injury was assessed based on the head injury criteria (HIC<sub>15</sub>). Vehicle trajectories during crash events were obtained and presented in overlapping contour plots to provide a comprehensive understanding of the impact responses.

The OIVs are the “occupant velocities” upon impacting the interior surface of the vehicle compartment; they are calculated in the longitudinal or lateral directions independently. The ORAs are also calculated independently in the longitudinal and lateral directions; they are the highest values of vehicular accelerations averaged over any 10-ms interval after the occupant impacting the interior surface of the vehicle compartment. According to MASH, the longitudinal or lateral OIV should not exceed 12.2 m/s and the longitudinal or lateral ORA should not exceed 20.49 G. The maximum allowed roll and pitch angles are 75°.

The HICs are calculated using the time history of head accelerations as follows.

$$HIC = \text{Max} \left\{ (t_2 - t_1) \left[ \frac{\int_{t_1}^{t_2} a(t) dt}{t_2 - t_1} \right]^{2.5} \right\}$$

where  $a(t)$  is the resultant head accelerations of the crash test dummy with a unit of gravitational acceleration (G), and  $t_1$  and  $t_2$  are two time instants defining an interval of  $(t_2$  and  $t_1)$ . By definition, the time interval  $t_2 - t_1$  for HIC<sub>15</sub> should be no more than 15 ms. The probability of skull fracture injury was defined by Hertz (1993) as

$$p(HIC) = \frac{1}{\sqrt{2\pi}} \int_{-\infty}^{\frac{\ln(HIC) - 6.96352}{0.84664}} e^{-\frac{t^2}{2}} dt$$

The threshold of HIC<sub>15</sub> for adults is 700, which gives a probability of 31% of skull fracture injury based on Hertz (1993).

### 4.1 Simulations Results of Category 1

In Category 1, the occupant risk was evaluated under vehicular crashes of a 1100C small passenger car (i.e., a 2010 Toyota Yaris) into Type I cluster mailboxes at an impact speed of 31 mph (50 km/h). The eight simulation cases in Category 1 are summarized as follows.

- Case 1: A single-unit Type I cluster mailbox with 0° impact angle;
- Case 2: A single-unit Type I cluster mailbox on a flat road with 25° impact angle;
- Case 3: A dual-unit Type I cluster mailbox with 0° impact angle;

- Case 4: A dual-unit Type I cluster mailbox on a flat road with 25° impact angle and impacted at the corner;
- Case 5: A dual-unit Type I cluster mailbox on a flat road with 25° impact angle and impacted at the mid-point;
- Case 6: A single-unit Type I cluster mailbox behind a curb with 25° impact angle;
- Case 7: A dual-unit Type I cluster mailbox behind a curb with 25° impact angle and impacted at the corner; and
- Case 8: A dual-unit Type I cluster mailbox behind a curb with 25° impact angle and impacted at the mid-point.

#### 4.1.1 Category 1 – Case 1

In this case, a 2010 Toyota Yaris crashed into a single-unit Type I cluster mailbox on a flat road at 31 mph (50 km/h) and with 0° impact angle. Figure 4.1 shows the full simulation model before impact and the deformed vehicle model after impact. Figure 4.2 shows the overlapping contour plot of vehicle trajectory for this case. The vehicle's roll and pitch angles, OIVs, and ORAs were calculated and summarized in Table 4.1. Table 4.2 gives the acceleration histories of the crash test dummy on the head, chest, and pelvis. The HIC<sub>15</sub> and the probability of skull injury were also calculated for this case, as given in Table 4.2.

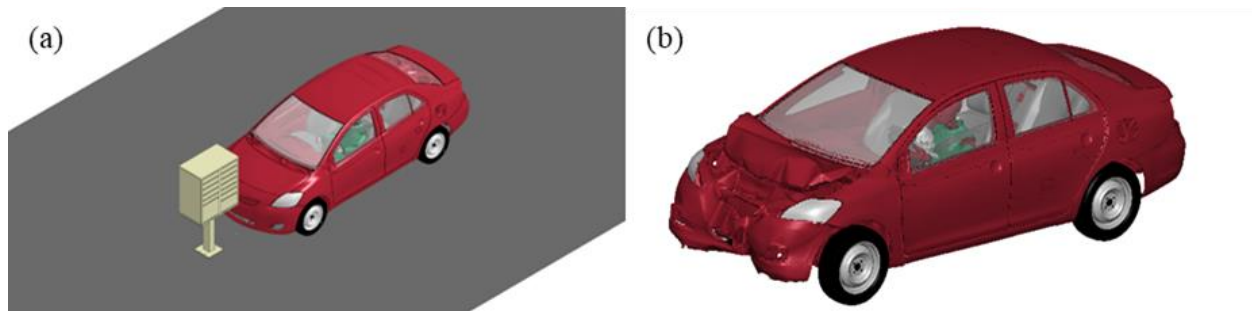


Figure 4.1 The full simulation model (a) and deformed vehicle model after impact (b) for Category 1 – Case 1.

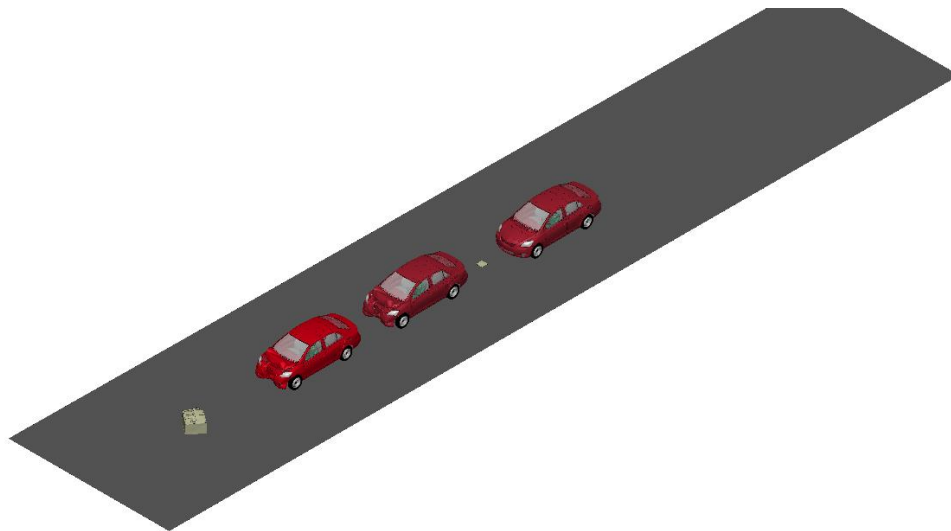
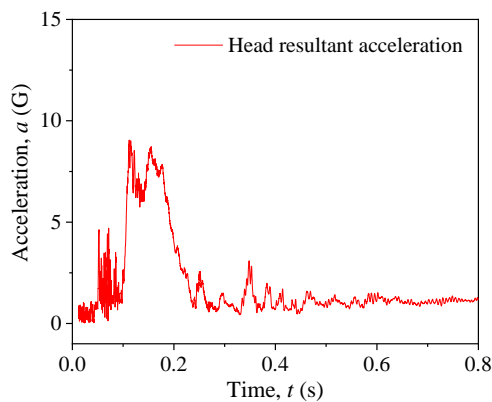
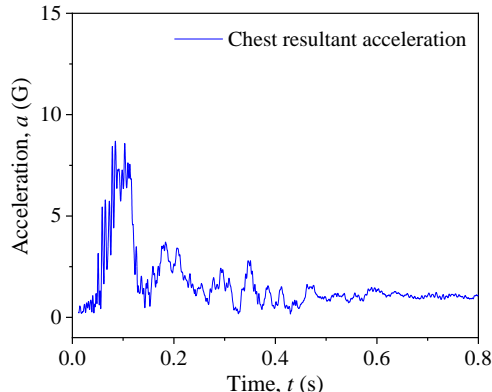
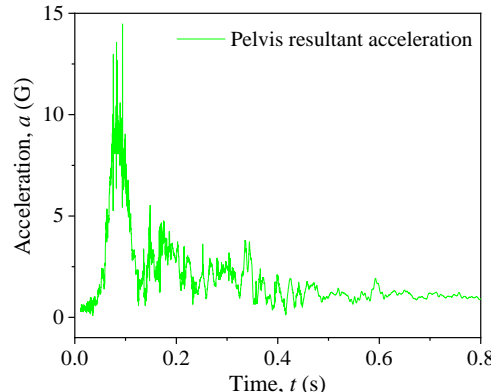


Figure 4.2 Vehicle trajectory during impact for Category 1 – Case 1.

Table 4.1 Vehicular responses, OIVs, and ORAs for Category 1 – Case 1.

Parameter	OIV (m/s)		ORA (G)		Vehicular Response	
	Longitudinal	Lateral	Longitudinal	Lateral	Roll angle	Pitch angle
Simulation Result	3.45	0.02	3.53	4.06	0.57°	0.60°
MASH Limit	12.2	12.2	20.49	20.49	75°	75°
Pass/Fail	Pass	Pass	Pass	Pass	Pass	Pass

Table 4.2 Dummy responses and injury parameters for Category 1 – Case 1.

Dummy head acceleration		Head impact criteria			
	Head injury parameter	Value	Threshold	Pass/Fail	
	HIC <sub>15</sub>	2.90	700	Pass	
	$p(\text{HIC}_{15})$	0 %	31%	Pass	
Dummy chest acceleration		Dummy pelvis acceleration			
					

The simulation results of Category 1 – Case 1 showed that the connection joints between the upper mailbox body and the pedestal failed immediately upon impact by the Yaris, triggering the separation and forward ejection of the mailbox upper body. Due to the low clearance of the Yaris, the pedestal was pushed and dragged forward by the vehicle, and eventually failed at the connection with the ground base due to the shear forces from dragging. It was observed that the main structure of upper mailbox body mostly remained intact except for some warping of the slot doors. For occupant response, the dummy's head moved forward and slightly lowered due to the impact pulse, but it did not touch the deployed airbag. The maximum head acceleration was approximately 9 G and the HIC<sub>15</sub> value was calculated to be 2.90, far below the threshold value of 700 and indicating no possibility of skull injury. The trajectory of the mailbox indicated no possibility of hitting the windshield of vehicle, eliminating the possibility of compartment

intrusions. The vehicle's roll and pitch angles, as well as the OIVs and ORAs in both longitudinal and lateral directions, were all within the MASH allowed limits. The above analysis indicated that there was no potential occupant injury for this impact case.

#### 4.1.2 Category 1 – Case 2

In this case, a 2010 Toyota Yaris crashed into a single-unit Type I cluster mailbox on a flat road at 31 mph (50 km/h) and with 25° impact angle. Figure 4.3 shows the full simulation model before impact and the deformed vehicle model after impact. Figure 4.4 shows the overlapping contour plot of vehicle trajectory for this case. The vehicle's roll and pitch angles, OIVs, and ORAs were calculated and summarized in Table 4.3. Table 4.4 gives the acceleration histories of the crash test dummy on the head, chest, and pelvis. The HIC<sub>15</sub> and the probability of skull injury were also calculated for this case, as given in Table 4.4.

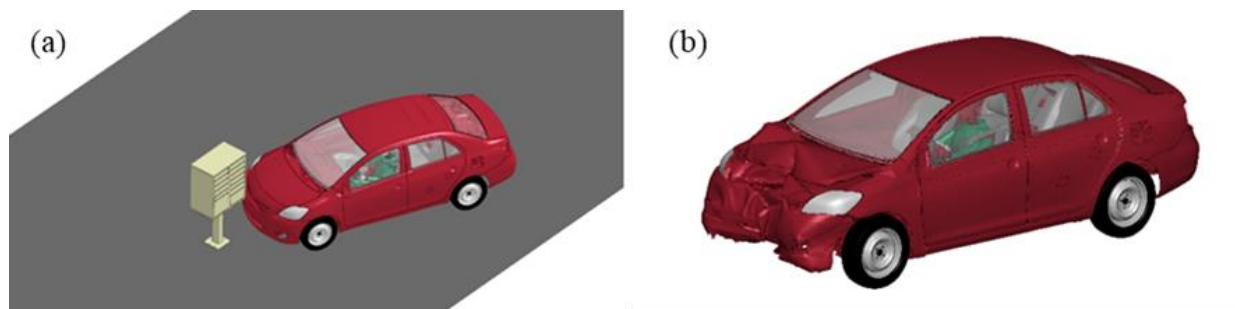


Figure 4.3 The full simulation model (a) and deformed vehicle model after impact (b) for Category 1 – Case 2.

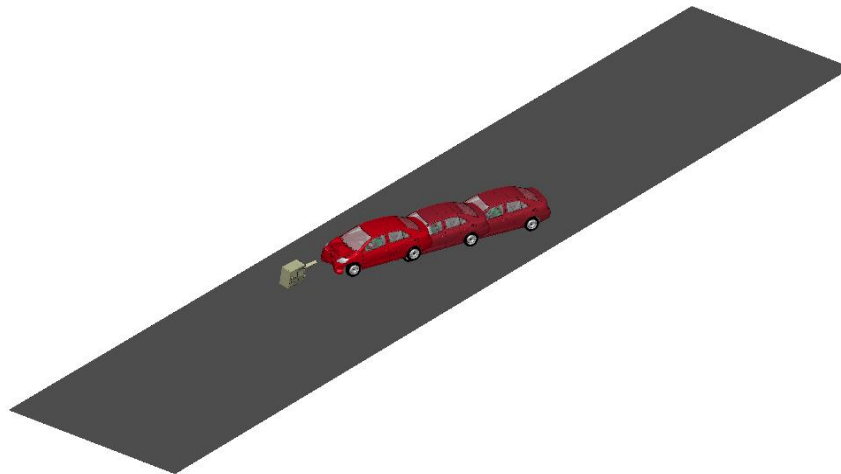
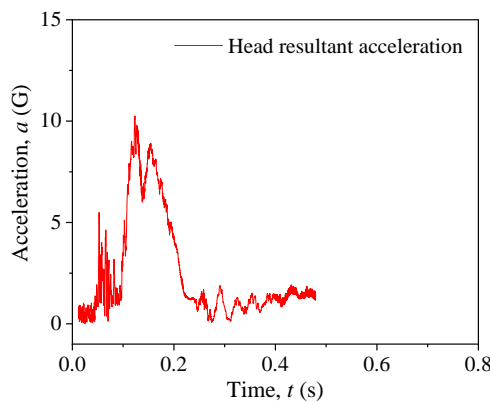
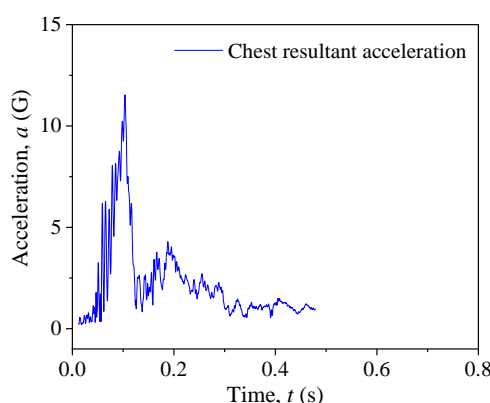
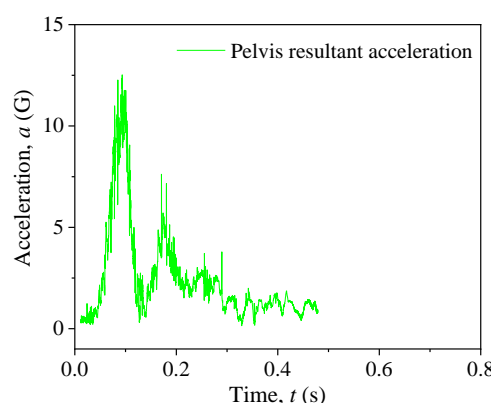


Figure 4.4 Vehicle trajectory during impact for Category 1 – Case 2.

Table 4.3 Vehicular responses, OIVs, and ORAs for Category 1 – Case 2.

Parameter	OIV (m/s)		ORA (G)		Vehicular Response	
	Longitudinal	Lateral	Longitudinal	Lateral	Roll angle	Pitch angle
Simulation Result	3.45	0.08	0.81	1.03	0.68°	1.47°
MASH Limit	12.2	12.2	20.49	20.49	75°	75°
Pass/Fail	Pass	Pass	Pass	Pass	Pass	Pass

Table 4.4 Dummy responses and injury parameters for Category 1 – Case 2.

Dummy head acceleration		Head impact criteria			
	Head injury parameter	Value	Threshold	Pass/Fail	
	HIC <sub>15</sub>	3.72	700	Pass	
	$p(\text{HIC}_{15})$	0 %	31%	Pass	
Dummy chest acceleration		Dummy pelvis acceleration			
					

The simulation results of Category 1 – Case 2 showed that the vehicular and occupant responses were similar to those for Category 1 – Case 1. In case 2, however, the mailbox upper body and the pedestal remained connected and were pushed forward by the test vehicle. The trajectory of the mailbox showed that it would not hit the windshield of vehicle and there was no possibility of compartment intrusions. The vehicle's roll and pitch angles, as well as the OIVs and ORAs in both longitudinal and lateral directions, were all within the MASH allowed limits. The maximum head acceleration of the crash test dummy was approximately 10 G and the HIC<sub>15</sub> value was calculated to be 3.72, far below the threshold value of 700 and indicating no possibility of skull injury. The above analysis indicated that there was no potential occupant injury for this impact case.

#### 4.1.3 Category 1 – Case 3

In this case, a 2010 Toyota Yaris crashed into a dual-unit Type I cluster mailbox on a flat road at 31 mph (50 km/h) and with 0° impact angle. Figure 4.5 shows the full simulation model before impact and the deformed vehicle model after impact. Figure 4.6 shows the overlapping contour plot of vehicle trajectory for this case. The vehicle's roll and pitch angles, OIVs, and ORAs were calculated and summarized in Table 4.5. Table 4.6 gives the acceleration histories of the crash test dummy on the head, chest, and pelvis. The HIC<sub>15</sub> and the probability of skull injury were also calculated for this case, as given in Table 4.6.

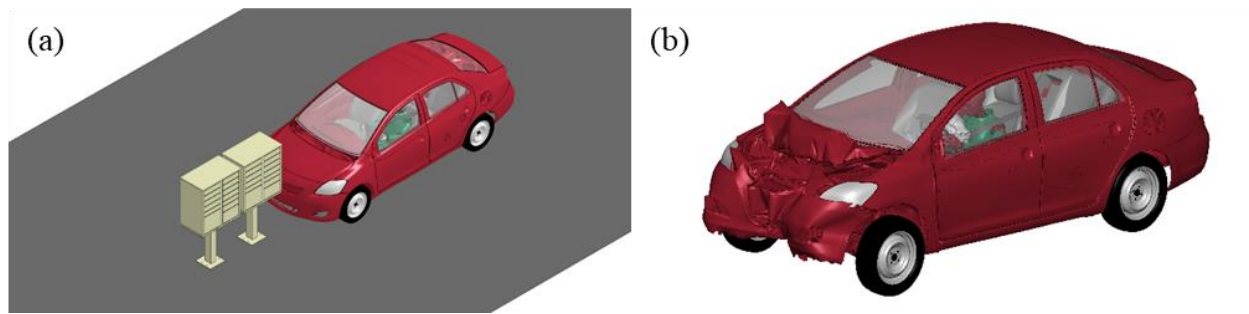


Figure 4.5 The full simulation model (a) and deformed vehicle model after impact (b) for Category 1 – Case 3.

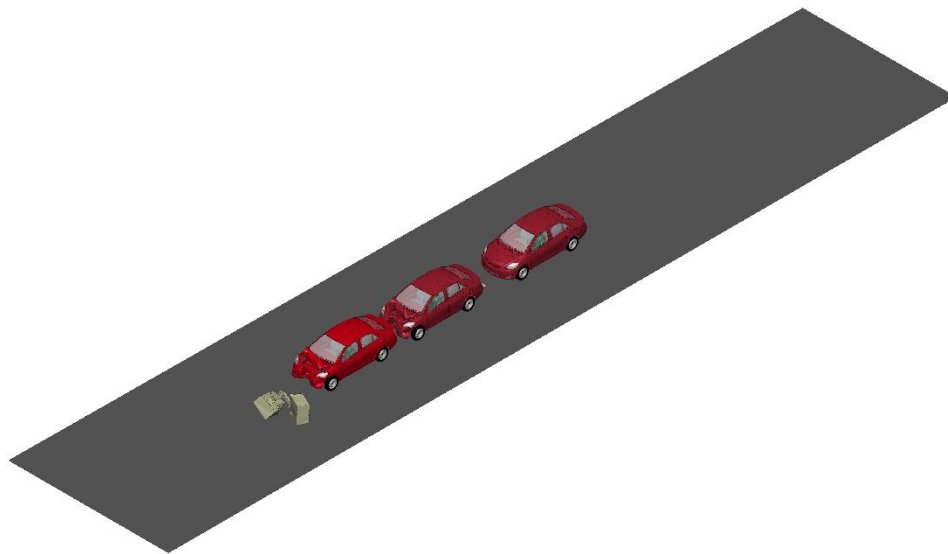


Figure 4.6 Vehicle trajectory during impact for Category 1 – Case 3.

Table 4.5 Vehicular responses, OIVs, and ORAs for Category 1 – Case 3.

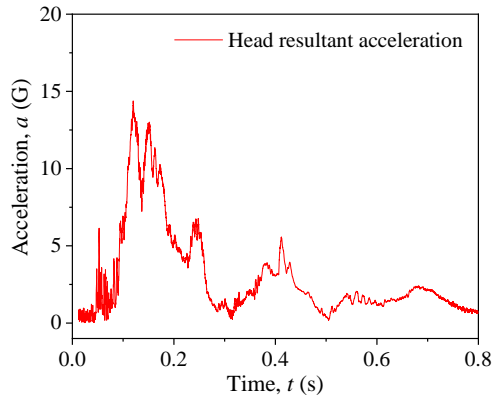
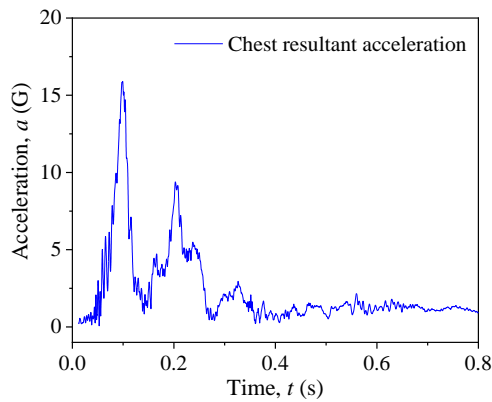
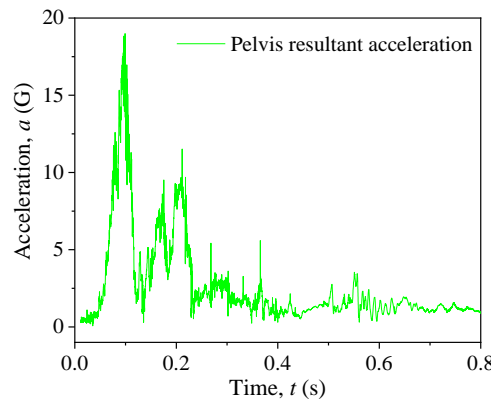
Parameter	OIV (m/s)		ORA (G)		Vehicular Response	
	Longitudinal	Lateral	Longitudinal	Lateral	Roll angle	Pitch angle
Simulation Result	5.14	0.07	1.70	4.17	0.69°	1.91°
MASH Limit	12.2	12.2	20.49	20.49	75°	75°
Pass/Fail	Pass	Pass	Pass	Pass	Pass	Pass

The simulation results of Category 1 – Case 3 showed that the connection between the pedestal and upper body of the unit being impacted first did not fail completely due to support from the other mailbox unit. Subsequently, the pedestals of the two mailbox units stuck between the front wheels and the two units were pushed forward, causing severe warpage and wrinkling on the vehicle's hood. Compared to the single-unit mailbox, the dual-unit mailbox caused larger deformation on the impacting vehicle. Nevertheless, the trajectory of the mailbox indicated no possibility of hitting the windshield of vehicle, eliminating the possibility of compartment intrusions. The vehicle's roll and pitch angles, as well as the OIVs and ORAs in both longitudinal and lateral directions, were all within the MASH allowed limits. For occupant response, the maximum head acceleration was approximately 14 G and the HIC<sub>15</sub> value was calculated to be



9.02, far below the threshold value of 700 and indicating no possibility of skull injury. The above analysis indicated that there was no potential occupant injury for this impact case.

Table 4.6 Dummy responses and injury parameters for Category 1 – Case 3.

Dummy head acceleration	Head impact criteria			
	Head injury parameter	Value	Threshold	Pass/Fail
	HIC <sub>15</sub>	9.02	700	Pass
	$p(\text{HIC}_{15})$	0 %	31%	Pass
Dummy chest acceleration	Dummy pelvis acceleration			
				

#### 4.1.4 Category 1 – Case 4

In this case, a 2010 Toyota Yaris crashed into a dual-unit Type I cluster mailbox on a flat road at 31 mph (50 km/h) and with 25° impact angle at the corner. Figure 4.7 shows the full simulation model before impact and the deformed vehicle model after impact. Figure 4.8 shows the overlapping contour plot of vehicle trajectory for this case. The vehicle's roll and pitch angles, OIVs, and ORAs were calculated and summarized in Table 4.7. Table 4.8 gives the acceleration histories of the crash test dummy on the head, chest, and pelvis. The HIC<sub>15</sub> and the probability of skull injury were also calculated for this case, as given in Table 4.8.

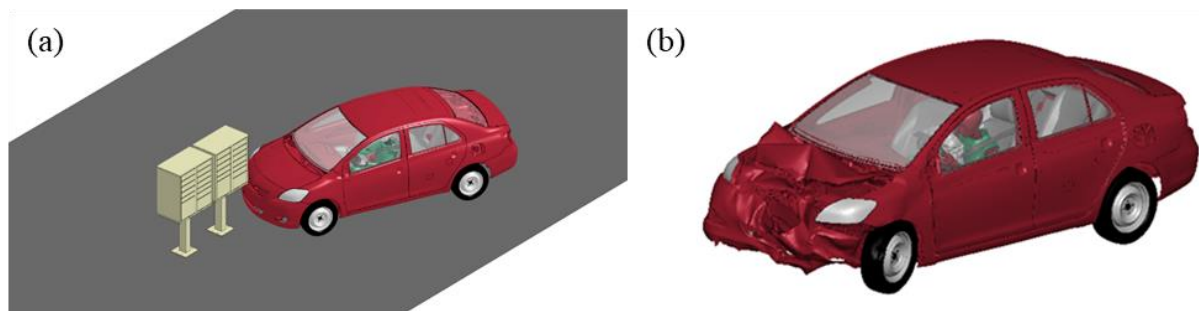


Figure 4.7 The full simulation model (a) and deformed vehicle model after impact (b) for Category 1 – Case 4.

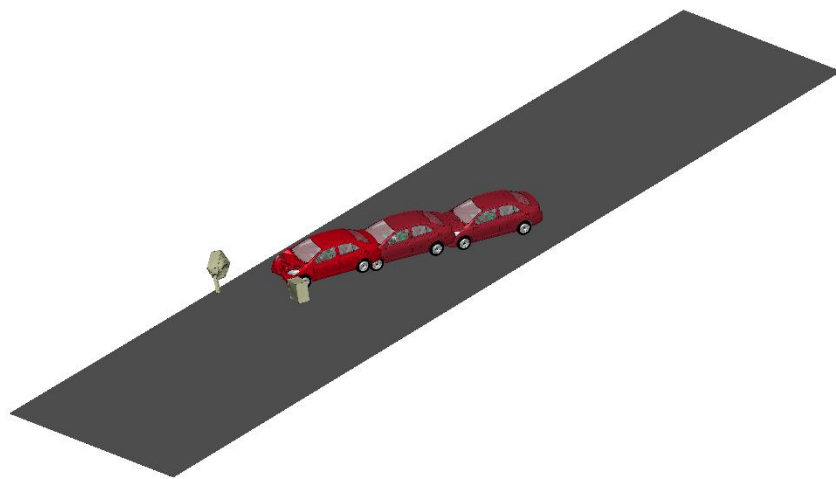
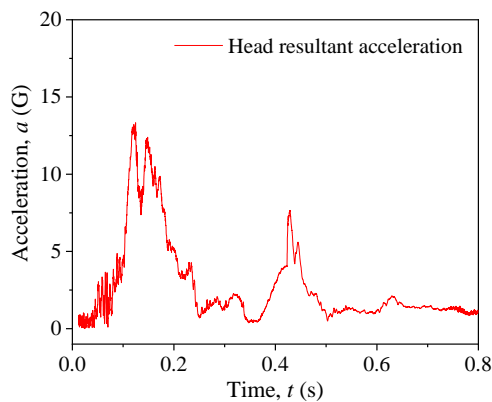
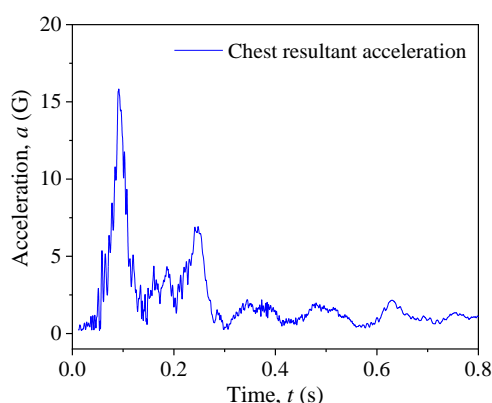
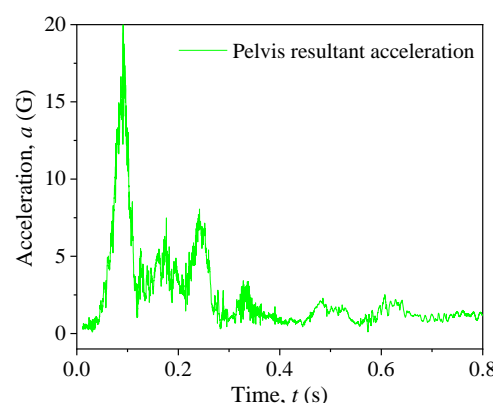


Figure 4.8 Vehicle trajectory during impact for Category 1 – Case 4.

Table 4.7 Vehicular responses, OIVs, and ORAs for Category 1 – Case 4.

Parameter	OIV (m/s)		ORA (G)		Vehicular Response	
	Longitudinal	Lateral	Longitudinal	Lateral	Roll angle	Pitch angle
Simulation Result	5.11	0.37	3.04	1.82	1.57°	0.58°
MASH Limit	12.2	12.2	20.49	20.49	75°	75°
Pass/Fail	Pass	Pass	Pass	Pass	Pass	Pass

Table 4.8 Dummy responses and injury parameters for Category 1 – Case 4.

Dummy head acceleration		Head impact criteria			
	Head injury parameter	Value	Threshold	Pass/Fail	
	HIC <sub>15</sub>	7.64	700	Pass	
	$p(\text{HIC}_{15})$	0 %	31%	Pass	
Dummy chest acceleration		Dummy pelvis acceleration			
					

The simulation results of Category 1 – Case 4 showed that both units were knocked off the ground and the connection between the pedestal and upper body of the unit being impacted first failed while the pedestal and upper body of the second unit stay connected. Due to the 25° impact angle and interactions between the two units, the first unit was pushed to the driver side of the vehicle while the second unit was pushed forward. The trajectory of the mailbox indicated no possibility of hitting the windshield of vehicle, eliminating the possibility of compartment intrusions. The vehicle's roll and pitch angles, as well as the OIVs and ORAs in both longitudinal and lateral directions, were all within the MASH allowed limits. For occupant responses, the dummy's head moved forward and touched the deployed airbag. The maximum head acceleration was approximately 13 G and the HIC<sub>15</sub> value was calculated to be 7.64, far below the threshold value of 700 and indicating no possibility of skull injury. The above analysis indicated that there was no potential occupant injury for this impact case.

#### 4.1.5 Category 1 – Case 5

In this case, a 2010 Toyota Yaris crashed into a dual-unit Type I cluster mailbox on a flat road at 31 mph (50 km/h) and with 25° impact angle at the mid-point. Figure 4.9 shows the full simulation model before impact and the deformed vehicle model after impact. Figure 4.10 shows the overlapping contour plot of vehicle trajectory for this case. The vehicle's roll and pitch angles, OIVs, and ORAs were calculated and summarized in Table 4.9. Table 4.10 gives the acceleration histories of the crash test dummy on the head, chest, and pelvis. The HIC<sub>15</sub> and the probability of skull injury were also calculated for this case, as given in Table 4.10.

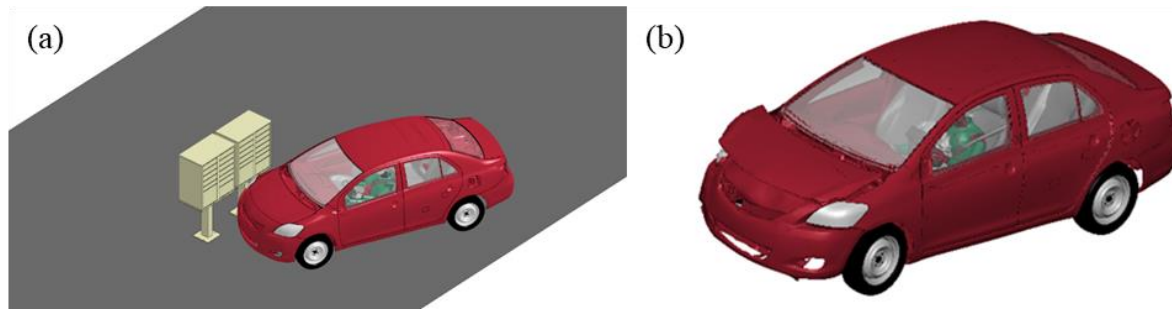


Figure 4.9 The full simulation model (a) and deformed vehicle model after impact (b) for Category 1 – Case 5.

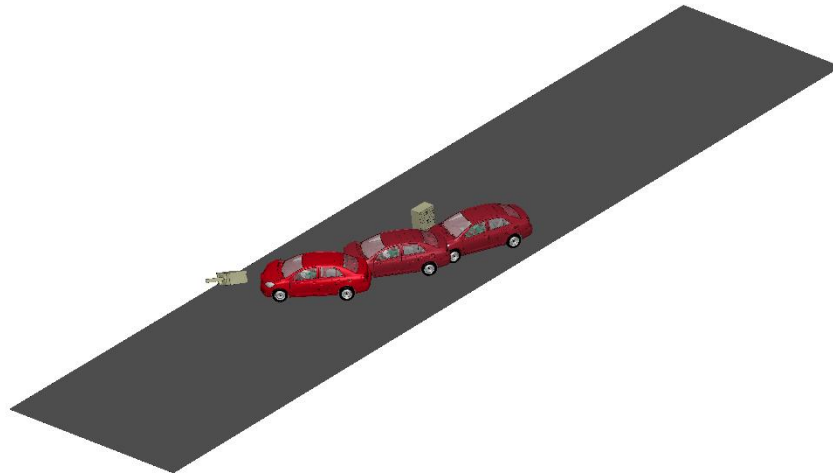
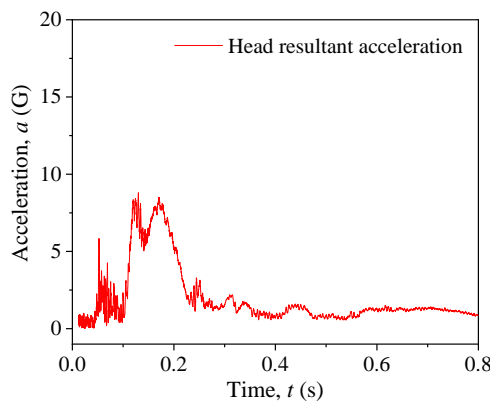
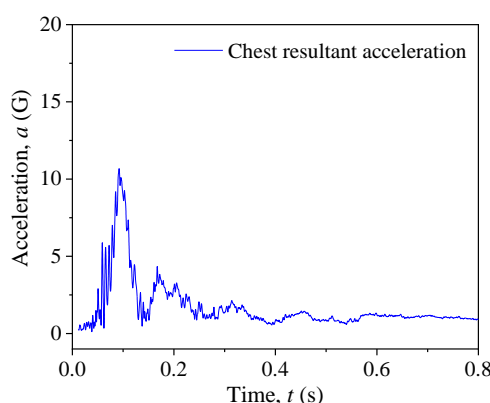
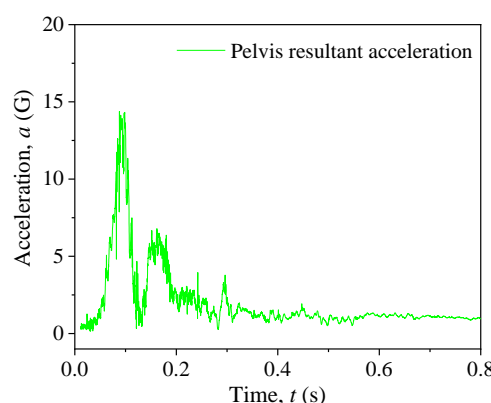


Figure 4.10 Vehicle trajectory during impact for Category 1 – Case 5.

Table 4.9 Vehicular responses, OIVs, and ORAs for Category 1 – Case 5.

Parameter	OIV (m/s)		ORA (G)		Vehicular Response	
	Longitudinal	Lateral	Longitudinal	Lateral	Roll angle	Pitch angle
Simulation Result	3.53	0.10	0.99	1.05	0.46°	0.85°
MASH Limit	12.2	12.2	20.49	20.49	75°	75°
Pass/Fail	Pass	Pass	Pass	Pass	Pass	Pass

Table 4.10 Dummy responses and injury parameters for Category 1 – Case 5.

Dummy head acceleration	Head impact criteria			
	Head injury parameter	Value	Threshold	Pass/Fail
	HIC <sub>15</sub>	2.65	700	Pass
	<i>p</i> (HIC <sub>15</sub> )	0 %	31%	Pass
Dummy chest acceleration	Dummy pelvis acceleration			
				

The simulation results of Category 1 – Case 5 showed that the vehicle had only minor scratches on the hood upon impacting the first mailbox unit, and the hood was popped open upon impacting the second unit. There was no severe damage for the test vehicle after the impact. The first mailbox unit remained in place while the second unit was detached from the ground and pushed forward by the striking vehicle. The trajectory of the mailbox showed that there was no possibility of hitting the windshield of vehicle, eliminating the possibility of compartment intrusions. The vehicle's roll and pitch angles, as well as the OIVs and ORAs in both longitudinal and lateral directions, were all within the MASH allowed limits. During the impact, the dummy's head moved forward and slightly touched the deployed airbag. The maximum head acceleration was approximately 8 G and the  $HIC_{15}$  value was calculated to be 2.65, far below the threshold value of 700 and indicating no possibility of skull injury. The above analysis indicated that there was no potential occupant injury for this impact case. The OIV, ORA and  $HIC_{15}$  were all similar to those of the single-unit Type I mailbox impacted by the Toyota Yaris at 25° impact angle. It was also observed that the impact severity of Category 1 – Case 5, i.e., the dual-unit Type I mailbox impacted at the mid-point, was slightly less severe than Category 1 – Case 4, i.e., the same mailbox impacted at the corner.

#### 4.1.6 Category 1 – Case 6

In this case, a 2010 Toyota Yaris crashed into a single-unit Type I cluster mailbox behind a curb at 31 mph (50 km/h) and with 25° impact angle. Figure 4.11 shows the full simulation model before impact and the deformed vehicle model after impact. Figure 4.12 shows the overlapping contour plot of vehicle trajectory for this case. The vehicle's roll and pitch angles, OIVs, and ORAs were calculated and summarized in Table 4.11. Table 4.12 gives the acceleration histories of the crash test dummy on the head, chest, and pelvis. The HIC<sub>15</sub> and the probability of skull injury were also calculated for this case, as given in Table 4.12.

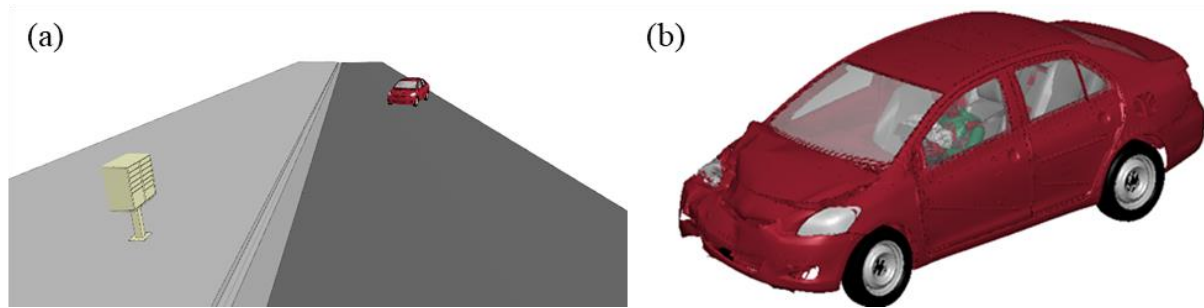


Figure 4.11 The full simulation model (a) and deformed vehicle model after impact (b) for Category 1 – Case 6.

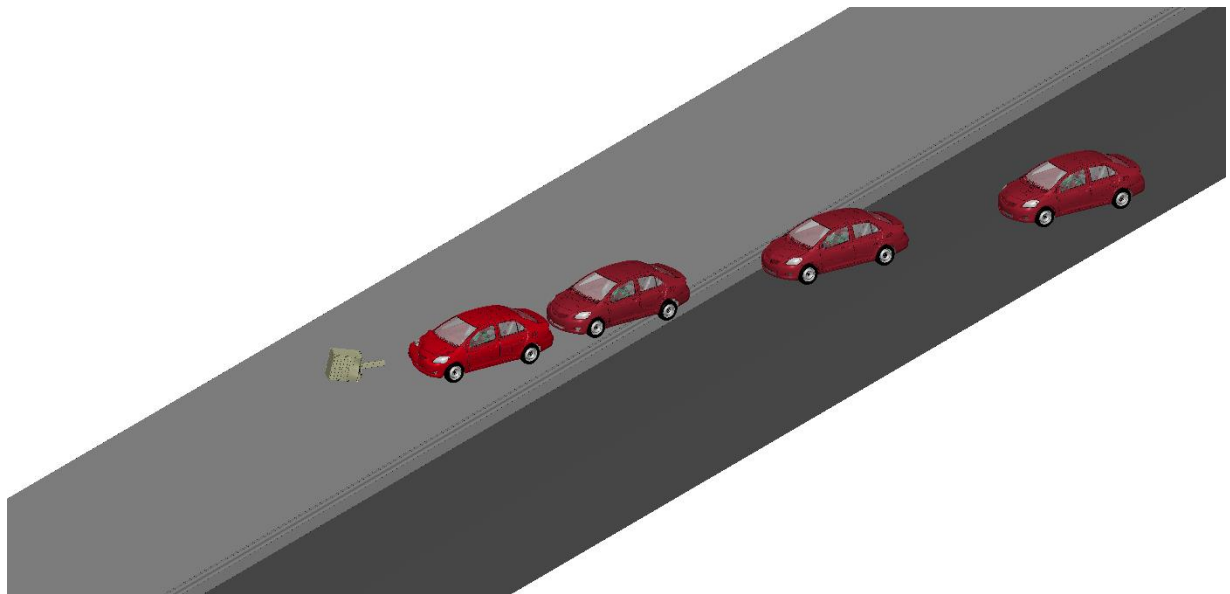
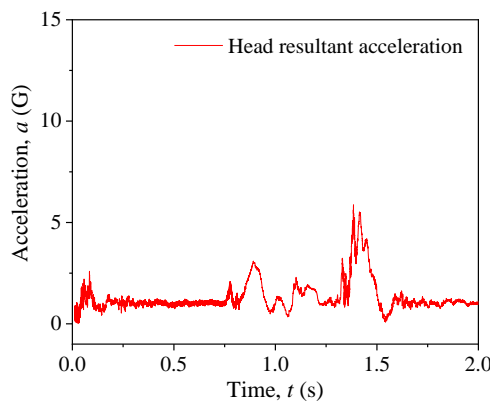
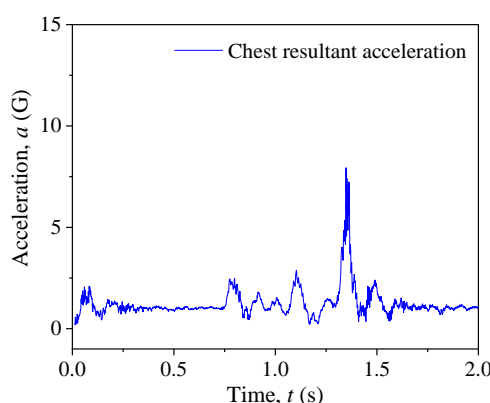
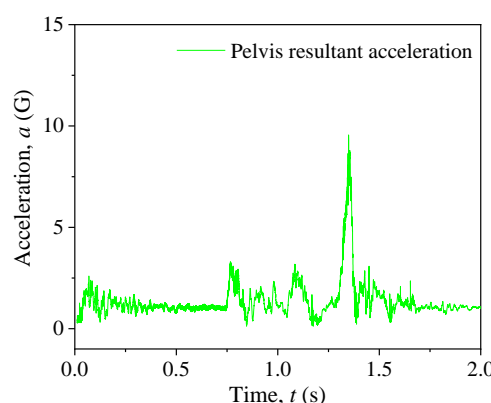


Figure 4.12 Vehicle trajectory during impact for Category 1 – Case 6.

Table 4.11 Vehicular responses, OIVs, and ORAs for Category 1 – Case 6.

Parameter	OIV (m/s)		ORA (G)		Vehicular Response	
	Longitudinal	Lateral	Longitudinal	Lateral	Roll angle	Pitch angle
Simulation Result	1.69	0.47	5.09	3.11	4.24°	1.81°
MASH Limit	12.2	12.2	20.49	20.49	75°	75°
Pass/Fail	Pass	Pass	Pass	Pass	Pass	Pass

Table 4.12 Dummy responses and injury parameters for Category 1 – Case 6.

Dummy head acceleration		Head impact criteria			
		Head injury parameter	Value	Threshold	Pass/Fail
		HIC <sub>15</sub>	0.91	700	Pass
		$p(\text{HIC}_{15})$	0 %	31%	Pass
Dummy chest acceleration		Dummy pelvis acceleration			
					

The simulation results of Category 1 – Case 6 were similar to those of Category 1 – Case 2 in which the same mailbox was placed on a flat road without curb. The connection between the pedestal and the upper body did not fail and the mailbox was pushed forward by the test vehicle. The test vehicle had only minor damages around the front passenger-side light. The trajectory of the mailbox showed that there was no possibility of hitting the windshield of vehicle, eliminating the possibility of compartment intrusions. The vehicle's roll and pitch angles, as well as the OIVs and ORAs in both longitudinal and lateral directions, were all within the MASH allowed limits. It was observed that the dummy swung laterally when the vehicle passed the curb with four wheels contacting the curb at different time. This can be seen from the several peaks in the head, chest, and pelvis accelerations. During impact, the dummy's head moved forward and slightly lowered due to the impact pulse, but it did not touch the deployed airbag. The maximum head acceleration was approximately 6 G and the HIC<sub>15</sub> value was calculated to be 0.91, far below the threshold value of 700 and indicating no possibility of skull injury. The above analysis indicated that there was no potential occupant injury for this impact case.

#### 4.1.7 Category 1 – Case 7

In this case, a 2010 Toyota Yaris crashed into a dual-unit Type I cluster mailbox behind a curb at 31 mph (50 km/h) and with 25° impact angle at the corner. Figure 4.13 shows the full simulation

model before impact and the deformed vehicle model after impact. Figure 4.14 shows the overlapping contour plot of vehicle trajectory for this case. The vehicle's roll and pitch angles, OIVs, and ORAs were calculated and summarized in Table 4.13. Table 4.14 gives the acceleration histories of the crash test dummy on the head, chest, and pelvis. The HIC<sub>15</sub> and the probability of skull injury were also calculated for this case, as given in Table 4.14.

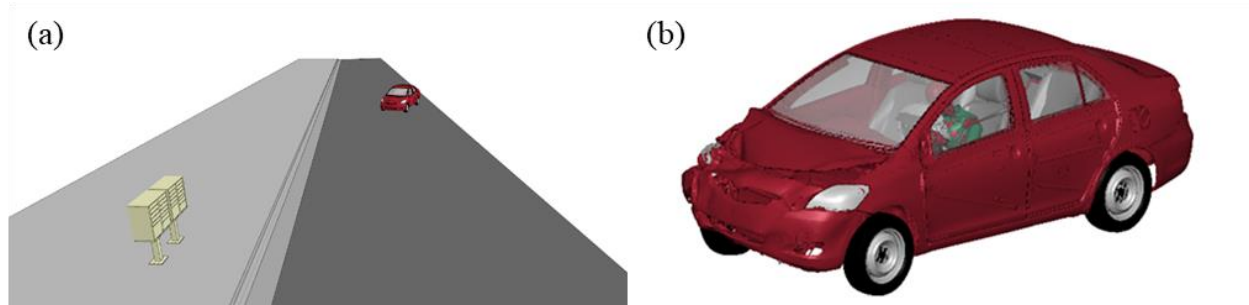


Figure 4.13 The full simulation model (a) and deformed vehicle model after impact (b) for Category 1 – Case 7.

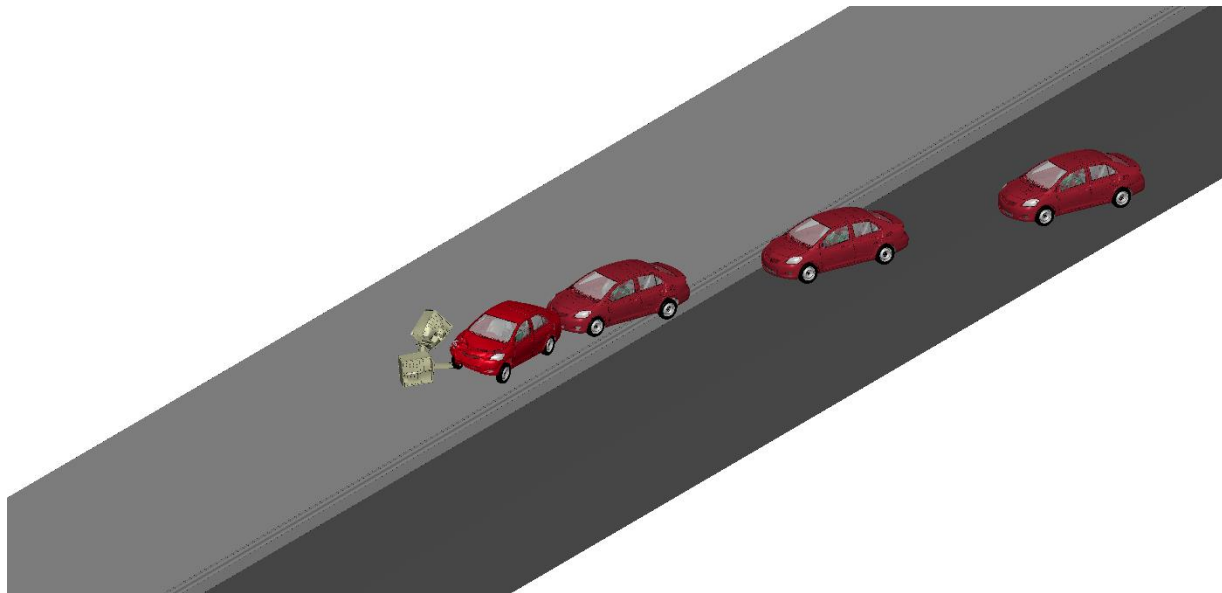


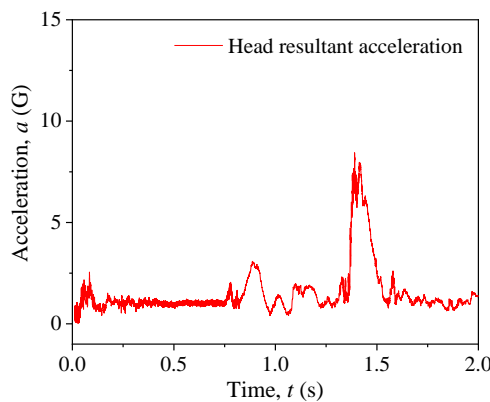
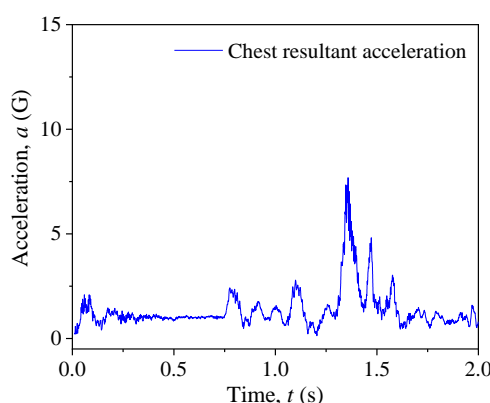
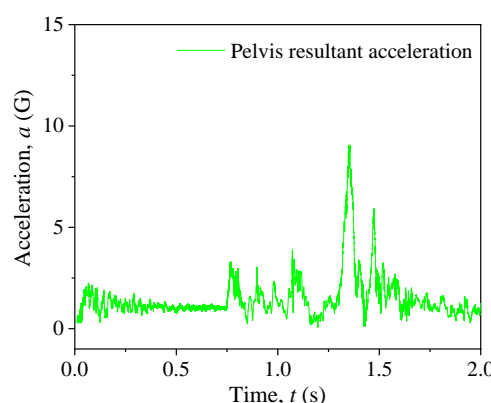
Figure 4.14 Vehicle trajectory during impact for Category 1 – Case 7.

Table 4.13 Vehicular responses, OIVs, and ORAs for Category 1 – Case 7.

Parameter	OIV (m/s)		ORA (G)		Vehicular Response	
	Longitudinal	Lateral	Longitudinal	Lateral	Roll angle	Pitch angle
Simulation Result	1.86	0.43	6.56	2.82	4.35°	5.18°
MASH Limit	12.2	12.2	20.49	20.49	75°	75°
Pass/Fail	Pass	Pass	Pass	Pass	Pass	Pass



Table 4.14 Dummy responses and injury parameters for Category 1 – Case 7.

Dummy head acceleration	Head impact criteria			
	Head injury parameter	Value	Threshold	Pass/Fail
	HIC <sub>15</sub>	2.37	700	Pass
	$p(\text{HIC}_{15})$	0 %	31%	Pass
Dummy chest acceleration	Dummy pelvis acceleration			
				

The simulation results of Category 1 – Case 7 showed that the two mailbox units were pushed forward together by the striking vehicle. The pedestals and upper bodies remained connected, reducing the chance of the pedestals intruding into the occupant compartment from underneath. The vehicles damage was mainly on the hood. The trajectory of the mailbox showed no possibility of hitting the windshield of vehicle, eliminating the possibility of compartment intrusions. The vehicle's roll and pitch angles were larger than those of the previous case but were well below the MASH limits. The OIVs and ORAs in both longitudinal and lateral directions were all within the MASH allowed limits. For occupant response, the dummy's head moved forward and slightly lowered due to the impact pulse, but it did not touch the deployed airbag. The maximum head acceleration was approximately 7.5 G and the HIC<sub>15</sub> value was calculated to be 2.37, far below the threshold value of 700 and indicating no possibility of skull injury. The above analysis indicated that there was no potential occupant injury for this impact case.

#### 4.1.8 Category 1 – Case 8

In this case, a 2010 Toyota Yaris crashed into a dual-unit Type I cluster mailbox behind a curb at 31 mph (50 km/h) and with 25° impact angle at the mid-point. Figure 4.15 shows the full simulation model before impact and the deformed vehicle model after impact. Figure 4.16 shows the overlapping contour plot of vehicle trajectory for this case. The vehicle's roll and pitch angles,

OIVs, and ORAs were calculated and summarized in Table 4.15. Table 4.16 gives the acceleration histories of the crash test dummy on the head, chest, and pelvis. The HIC<sub>15</sub> and the probability of skull injury were also calculated for this case, as given in Table 4.16.

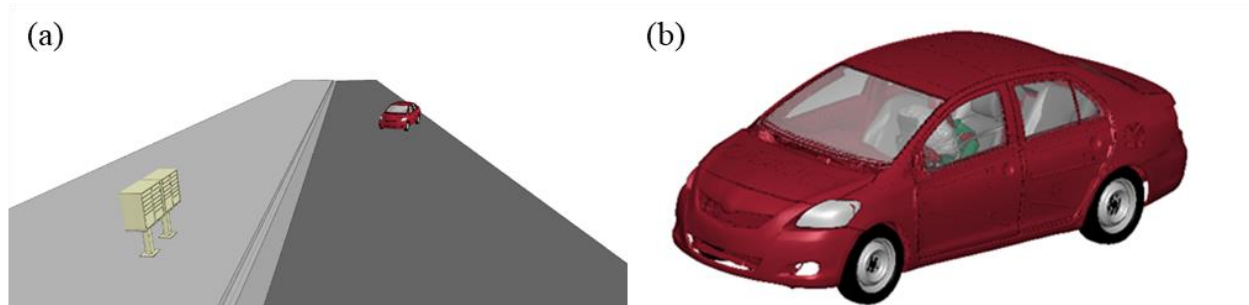


Figure 4.15 The full simulation model (a) and deformed vehicle model after impact (b) for Category 1 – Case 8.

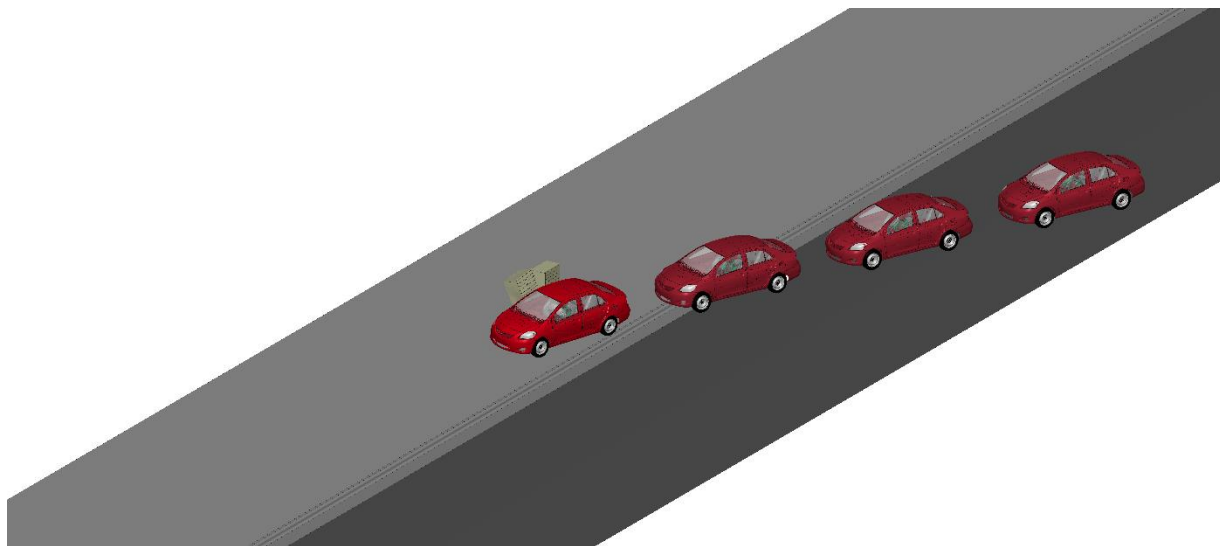


Figure 4.16 Vehicle trajectory during impact for Category 1 – Case 8.

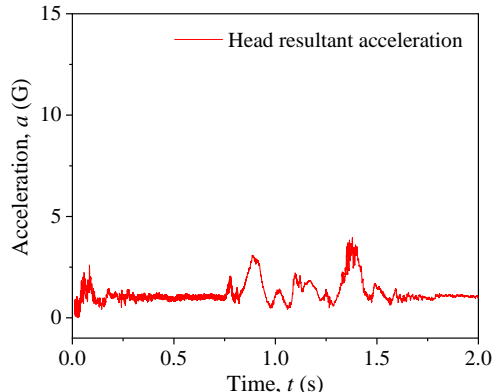
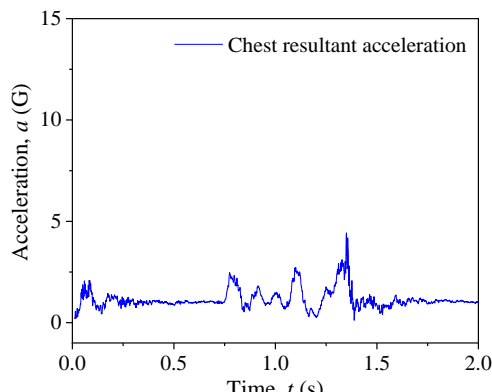
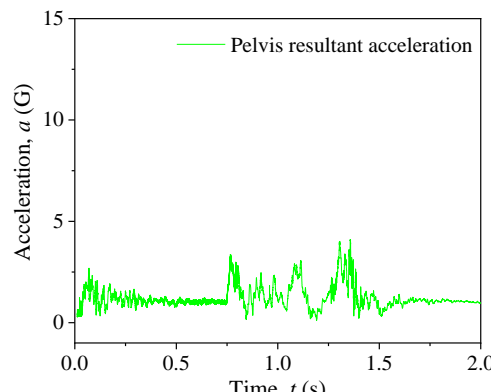
Table 4.15 Vehicular responses, OIVs, and ORAs for Category 1 – Case 8.

Parameter	OIV (m/s)		ORA (G)		Vehicular Response	
	Longitudinal	Lateral	Longitudinal	Lateral	Roll angle	Pitch angle
Simulation Result	1.65	0.86	2.59	2.77	4.35°	1.82°
MASH Limit	12.2	12.2	20.49	20.49	75°	75°
Pass/Fail	Pass	Pass	Pass	Pass	Pass	Pass

The simulation results of Category 1 – Case 8 showed that when the vehicle impacted the mailbox at the mid-point after passing the curb, it barely touched the first unit and pushed the second unit to bend backwards. The two mailbox units were not detached from the ground after the impact. In this case, the mailbox will not cause any compartment intrusions. The vehicle's roll and pitch angles, as well as the OIVs and ORAs in both longitudinal and lateral directions, were all within the MASH allowed limits. For occupant response, the dummy's head did not have significant

movement and thus did not touch the deployed airbag. The maximum head acceleration was approximately 3.5 G and the  $HIC_{15}$  value was calculated to be 0.30, far below the threshold value of 700 and indicating no possibility of skull injury. The above analysis indicated that there was no potential occupant injury for this impact case.

Table 4.16 Dummy responses and injury parameters for Category 1 – Case 8.

Dummy head acceleration		Head impact criteria			
	Head injury parameter	Value	Threshold	Pass/Fail	
	HIC <sub>15</sub>	0.30	700	Pass	
	<i>p</i> (HIC <sub>15</sub> )	0 %	31%	Pass	
Dummy chest acceleration		Dummy pelvis acceleration			
					

## 4.2 Simulations Results of Category 2

In Category 2, the occupant risk was evaluated under vehicular crashes of a 2270P pickup truck (i.e., a 2006 Ford F250) into Type I cluster mailboxes at an impact speed of 31 mph (50 km/h). The eight simulation cases in Category 2 are summarized as follows.

- Case 1: A single-unit Type I cluster mailbox with 0° impact angle;
- Case 2: A single-unit Type I cluster mailbox on a flat road with 25° impact angle;
- Case 3: A dual-unit Type I cluster mailbox with 0° impact angle;
- Case 4: A dual-unit Type I cluster mailbox on a flat road with 25° impact angle and impacted at the corner;
- Case 5: A dual-unit Type I cluster mailbox on a flat road with 25° impact angle and impacted at the mid-point;
- Case 6: A single-unit Type I cluster mailbox behind a curb with 25° impact angle;
- Case 7: A dual-unit Type I cluster mailbox behind a curb with 25° impact angle and

impacted at the corner; and  
Case 8: A dual-unit Type I cluster mailbox behind a curb with 25° impact angle and impacted at the mid-point.

#### 4.2.1 Category 2 – Case 1

In this case, a 2006 Ford F250 crashed into a single-unit Type I cluster mailbox on a flat road at 31 mph (50 km/h) and with 0° impact angle. Figure 4.17 shows the full simulation model before impact and the deformed vehicle model after impact. Figure 4.18 shows the overlapping contour plot of vehicle trajectory for this case. The vehicle's roll and pitch angles, OIVs, and ORAs were calculated and summarized in Table 4.17. Table 4.18 gives the acceleration histories of the crash test dummy on the head, chest, and pelvis. The HIC<sub>15</sub> and the probability of skull injury were also calculated for this case, as given in Table 4.18.

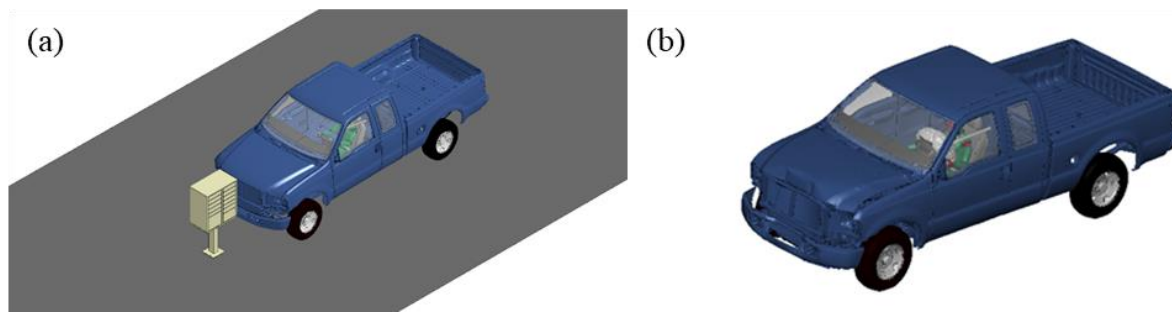


Figure 4.17 The full simulation model (a) and deformed vehicle model after impact (b) for Category 2 – Case 1

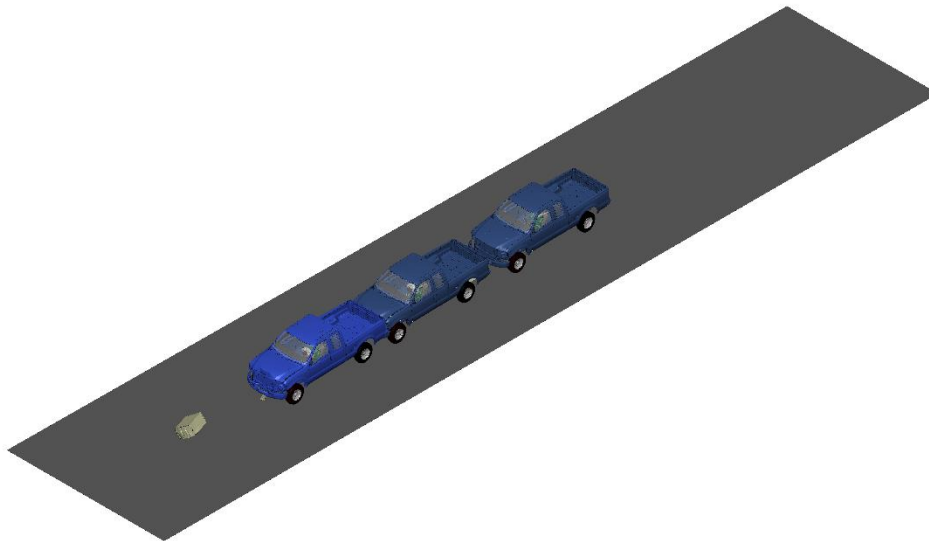
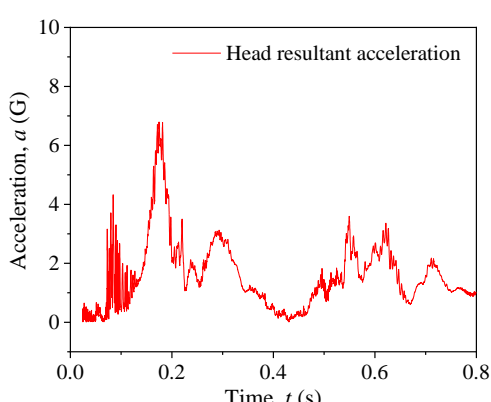
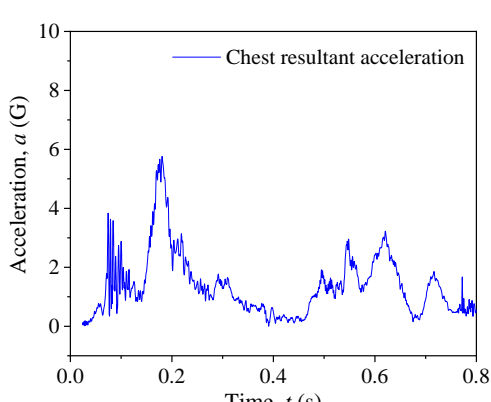
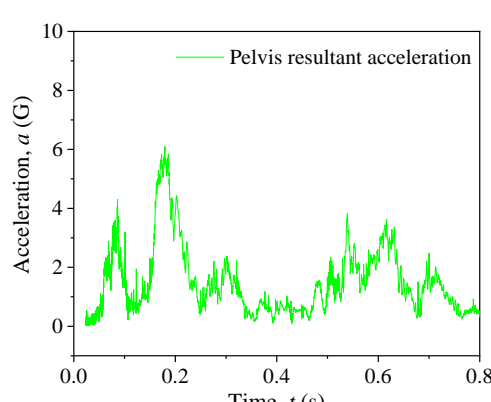


Figure 4.18 Vehicle trajectory during impact for Category 2 – Case 1.

Table 4.17 Vehicular responses, OIVs, and ORAs for Category 2 – Case 1.

Parameter	OIV (m/s)		ORA (G)		Vehicular Response	
	Longitudinal	Lateral	Longitudinal	Lateral	Roll angle	Pitch angle
Simulation Result	1.45	0.20	1.88	0.90	1.03°	0.72°
MASH Limit	12.2	12.2	20.49	20.49	75°	75°
Pass/Fail	Pass	Pass	Pass	Pass	Pass	Pass

Table 4.18 Vehicle trajectory during impact for Category 2 – Case 1.

Dummy head acceleration		Head impact criteria			
		Head injury parameter	Value	Threshold	Pass/Fail
		HIC <sub>15</sub>	1.38	700	Pass
		<i>p</i> (HIC <sub>15</sub> )	0 %	31%	Pass
Dummy chest acceleration		Dummy pelvis acceleration			
					

The simulation results of Category 2 – Case 1 showed that the connection between pedestal and upper body failed when impacted by the Ford F250. The pedestal stuck under the vehicle's chassis and the upper unit was pushed forward by the vehicle. The trajectory of the mailbox showed that there was no possibility hitting the windshield of vehicle, eliminating the possibility of compartment intrusions. The damage to the test vehicle was minimal with only a shallow dent on the hood. The vehicle's roll and pitch angles, as well as the OIVs and ORAs in both longitudinal and lateral directions, were all within the MASH allowed limits. For occupant response, the dummy's head did not have significant movement and thus did not touch the deployed airbag. The maximum head acceleration was approximately 7 G, 2 G lower than the same impact condition with a Toyota Yaris. The HIC<sub>15</sub> value was calculated to be 1.38, far below the threshold value of 700 and indicating no possibility of skull injury. The above analysis indicated that there was no potential occupant injury for this impact case.

#### 4.2.2 Category 2 – Case 2

In this case, a 2006 Ford F250 crashed into a single-unit Type I cluster mailbox on a flat road at 31 mph (50 km/h) and with 25° impact angle. Figure 4.19 shows the full simulation model before impact and the deformed vehicle model after impact. Figure 4.20 shows the overlapping contour plot of vehicle trajectory for this case. The vehicle's roll and pitch angles, OIVs, and ORAs were calculated and summarized in Table 4.19. Table 4.20 gives the acceleration histories of the crash test dummy on the head, chest, and pelvis. The HIC<sub>15</sub> and the probability of skull injury were also calculated for this case, as given in Table 4.20.

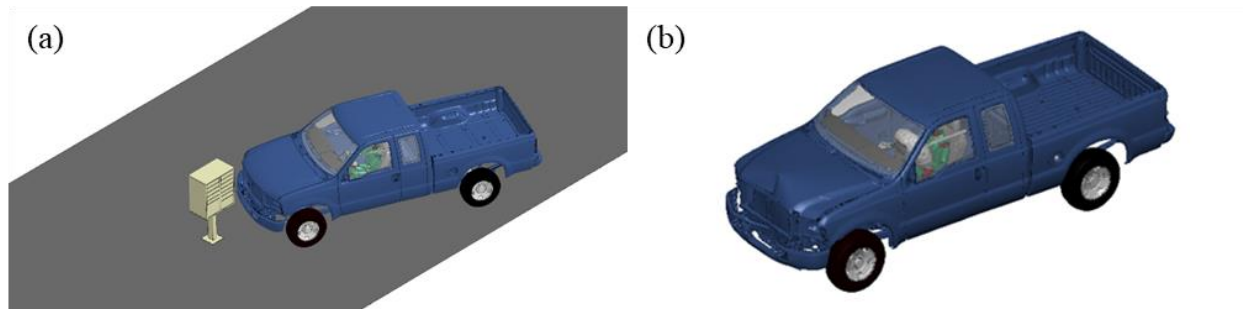


Figure 4.19 The full simulation model (a) and deformed vehicle model after impact (b) for Category 2 – Case 2.

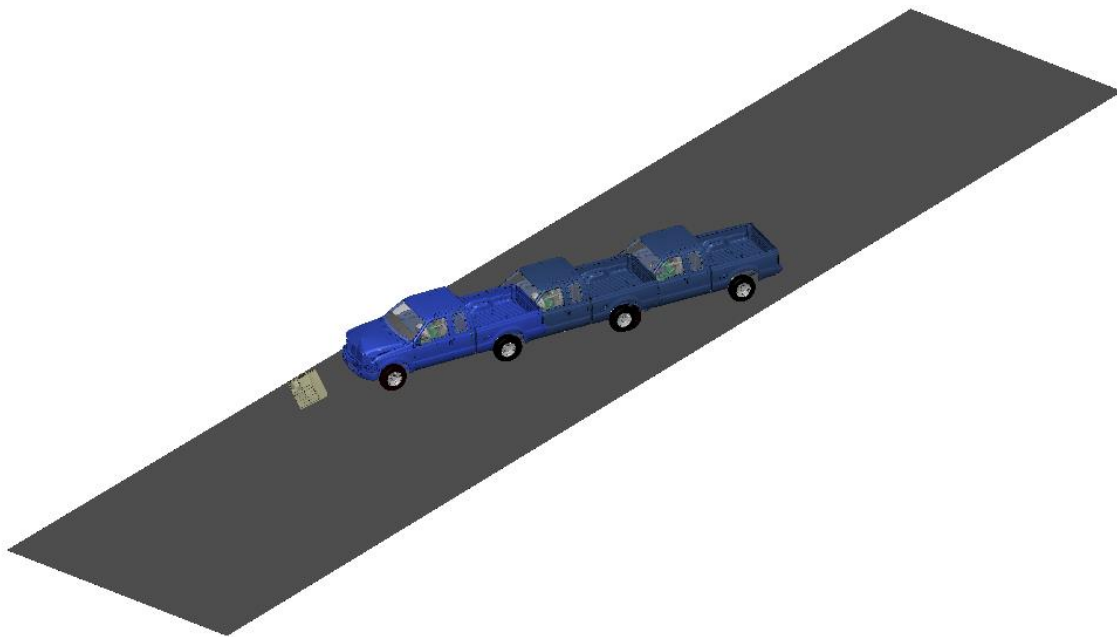
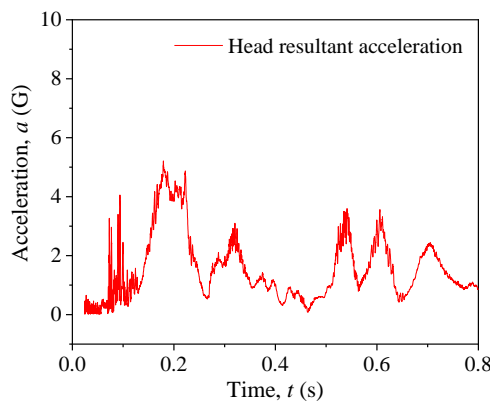
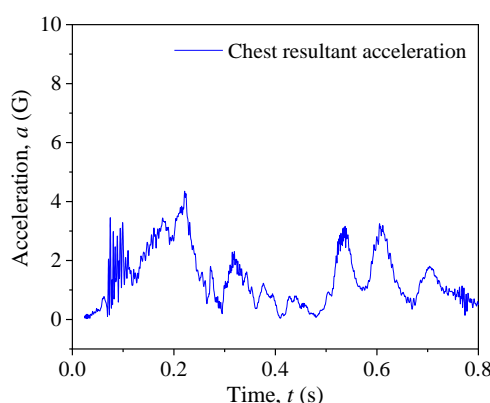
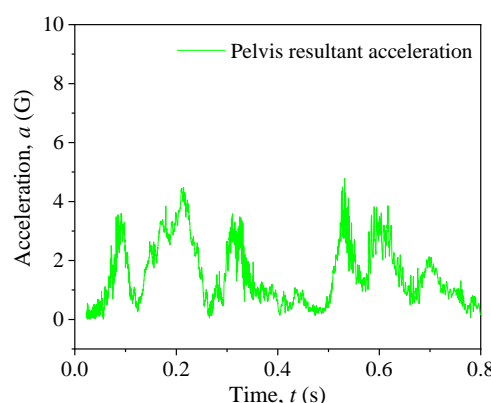


Figure 4.20 Vehicle trajectory during impact for Category 2 – Case 2.

Table 4.19 Vehicular responses, OIVs, and ORAs for Category 2 – Case 2.

Parameter	OIV (m/s)		ORA (G)		Vehicular Response	
	Longitudinal	Lateral	Longitudinal	Lateral	Roll angle	Pitch angle
Simulation Result	1.60	0.17	1.02	0.96	2.87°	0.92°
MASH Limit	12.2	12.2	20.49	20.49	75°	75°
Pass/Fail	Pass	Pass	Pass	Pass	Pass	Pass

Table 4.20 Dummy responses and injury parameters for Category 2 – Case 2.

Dummy head acceleration	Head impact criteria			
	Head injury parameter	Value	Threshold	Pass/Fail
	HIC <sub>15</sub>	0.73	700	Pass
	$p(\text{HIC}_{15})$	0 %	31%	Pass
Dummy chest acceleration	Dummy pelvis acceleration			
				

The simulation results of Category 2 – Case 2 were similar to those of the previous case with 0° impact angle. The mailbox upper body was separated from the pedestal upon impact and pushed forward by the vehicle. The damage on the vehicle was a V-shape dent on the hood due to impacting the corner mailbox. The trajectory of the mailbox showed that there was no possibility hitting the windshield of vehicle, eliminating the possibility of compartment intrusions. The vehicle's roll and pitch angles, as well as the OIVs and ORAs in both longitudinal and lateral directions, were all within the MASH allowed limits. During impact, the dummy's head moved forward but did not touch the deployed airbag. The maximum head acceleration was approximately 5 G and the HIC<sub>15</sub> value was calculated to be 0.73, far below the threshold value of 700 and indicating no possibility of skull injury. The above analysis indicated that there was no potential occupant injury for this impact case.

#### 4.2.3 Category 2 – Case 3

In this case, a 2006 Ford F250 crashed into a dual-unit Type I cluster mailbox on a flat road at 31 mph (50 km/h) and with 0° impact angle. Figure 4.21 shows the full simulation model before impact and the deformed vehicle model after impact. Figure 4.22 shows the overlapping contour plot of vehicle trajectory for this case. The vehicle's roll and pitch angles, OIVs, and ORAs were calculated and summarized in Table 4.21. Table 4.22 gives the acceleration histories of the crash

test dummy on the head, chest, and pelvis. The  $HIC_{15}$  and the probability of skull injury were also calculated for this case, as given in Table 4.22.

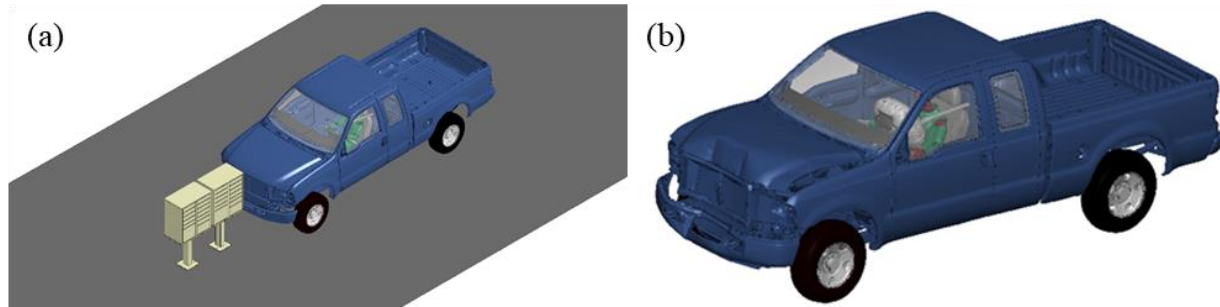


Figure 4.21 The full simulation model (a) and deformed vehicle model after impact (b) for Category 2 – Case 3.

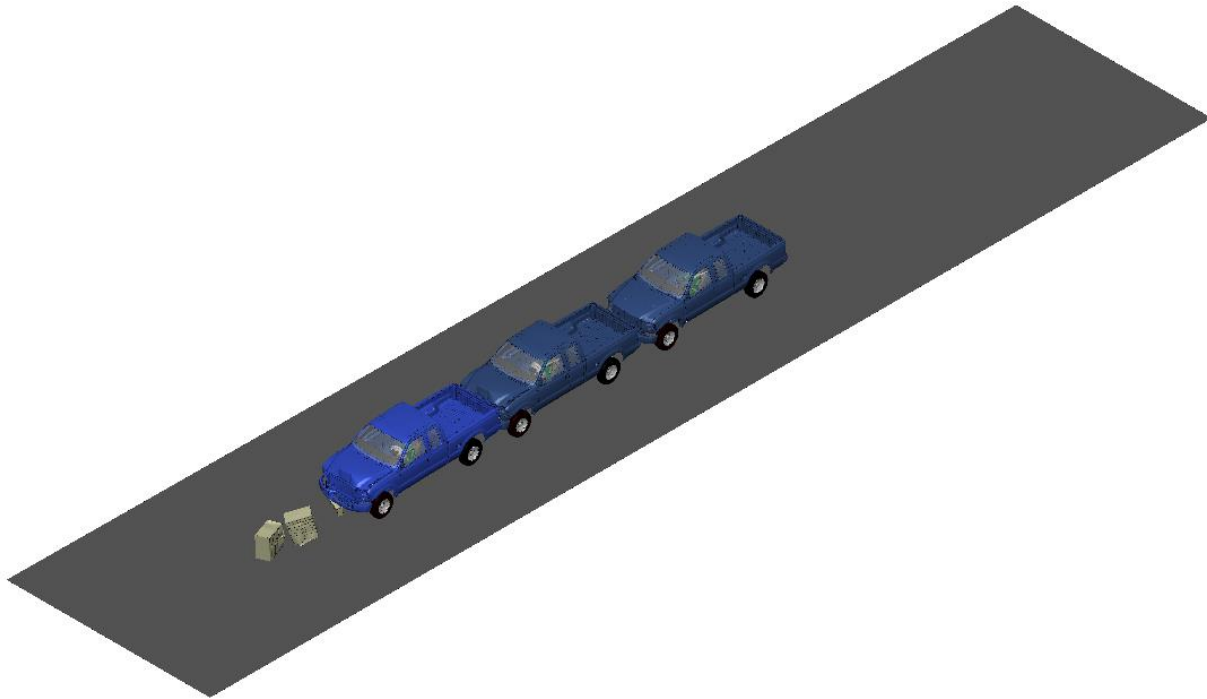


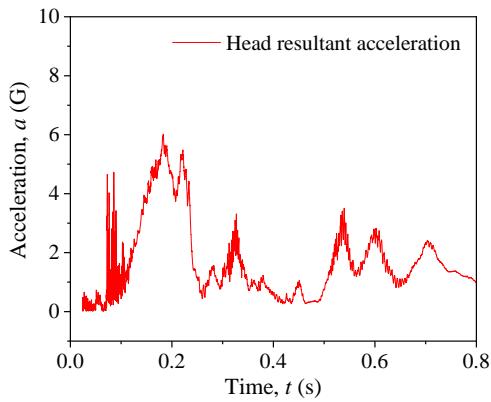
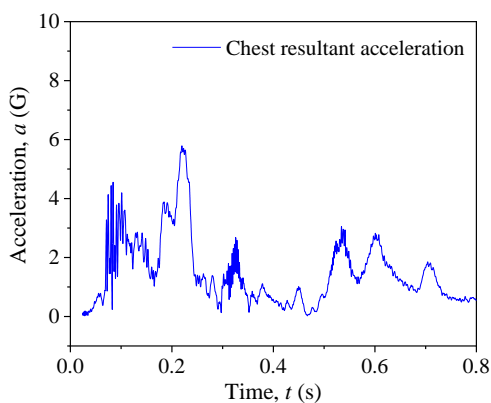
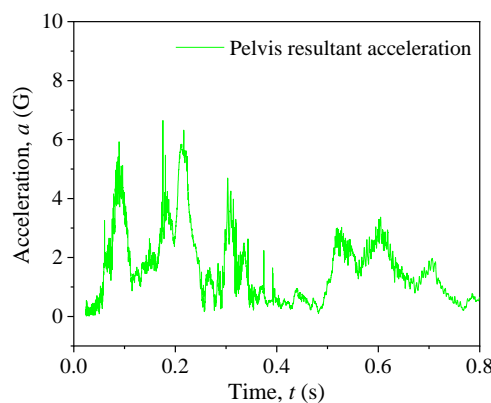
Figure 4.22 Vehicle trajectory during impact for Category 2 – Case 3.

Table 4.21 Vehicular responses, OIVs, and ORAs for Category 2 – Case 3.

Parameter	OIV (m/s)		ORA (G)		Vehicular Response	
	Longitudinal	Lateral	Longitudinal	Lateral	Roll angle	Pitch angle
Simulation Result	2.20	0.22	1.51	0.85	1.19°	0.81°
MASH Limit	12.2	12.2	20.49	20.49	75°	75°
Pass/Fail	Pass	Pass	Pass	Pass	Pass	Pass



Table 4.22 Dummy responses and injury parameters for Category 2 – Case 3.

Dummy head acceleration		Head impact criteria			
		Head injury parameter	Value	Threshold	Pass/Fail
		HIC <sub>15</sub>	1.08	700	Pass
		$p(\text{HIC}_{15})$	0 %	31%	Pass
Dummy chest acceleration		Dummy pelvis acceleration			
					

The simulation results of Category 2 – Case 3 showed that the upper bodies of both mailbox units were separated from the pedestals and pushed forward by the vehicle. The damage on the vehicle was only a large, flat dent on the hood with the hood partially popped up. The trajectory of the mailbox showed that there was no possibility for it to hit the windshield of vehicle, eliminating the possibility of compartment intrusions. The vehicle's roll and pitch angles, as well as the OIVs and ORAs in both longitudinal and lateral directions, were all within the MASH allowed limits. During impact, the dummy's head moved forward but did not touch the deployed airbag. The maximum head acceleration was approximately 6 G and the HIC<sub>15</sub> value was calculated to be 1.08, far below the threshold value of 700 and indicating no possibility of skull injury. The above analysis indicated that there was no potential occupant injury for this impact case.

#### 4.2.4 Category 2 – Case 4

In this case, a 2006 Ford F250 crashed into a dual-unit Type I cluster mailbox on a flat road at 31 mph (50 km/h) and with 25° impact angle at the corner. Figure 4.23 shows the full simulation model before impact and the deformed vehicle model after impact. Figure 4.24 shows the overlapping contour plot of vehicle trajectory for this case. The vehicle's roll and pitch angles, OIVs, and ORAs were calculated and summarized in Table 4.23. Table 4.24 gives the acceleration

histories of the crash test dummy on the head, chest, and pelvis. The  $HIC_{15}$  and the probability of skull injury were also calculated for this case, as given in Table 4.24.

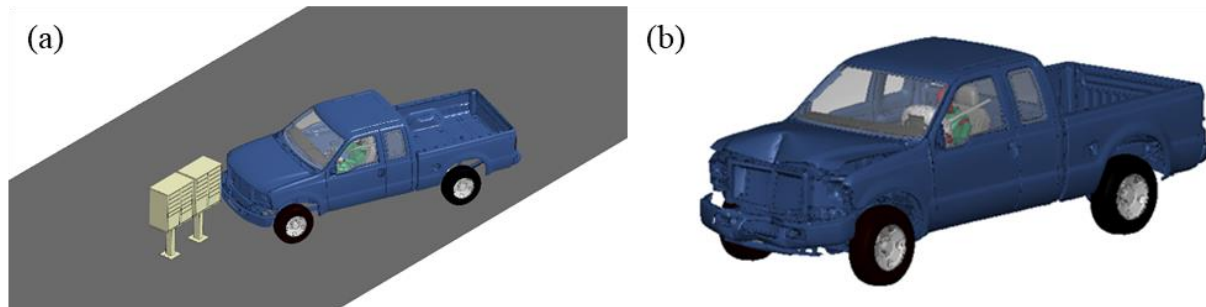


Figure 4.23 The full simulation model (a) and deformed vehicle model after impact (b) for Category 2 – Case 4.

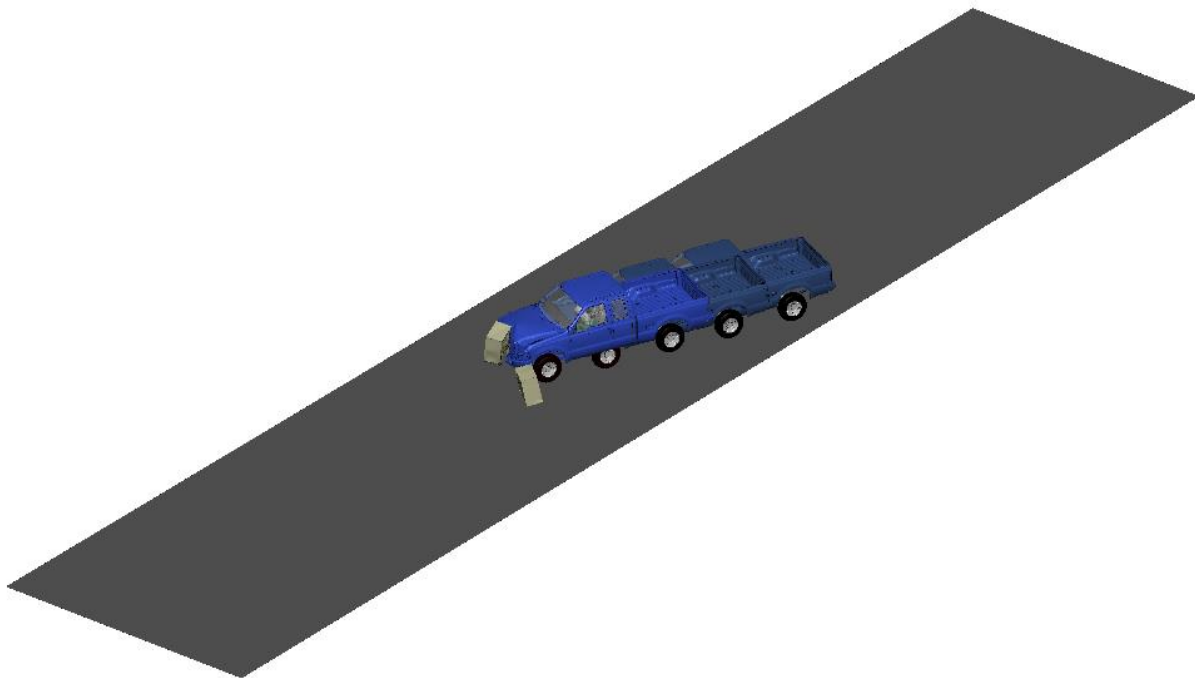
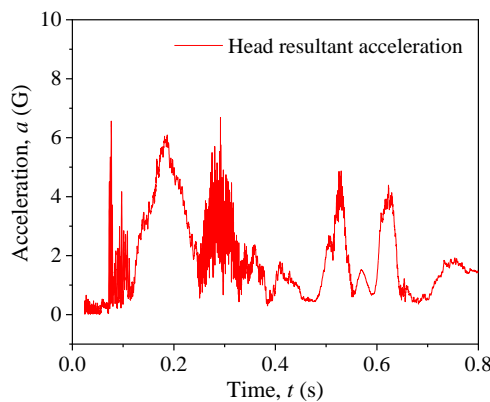
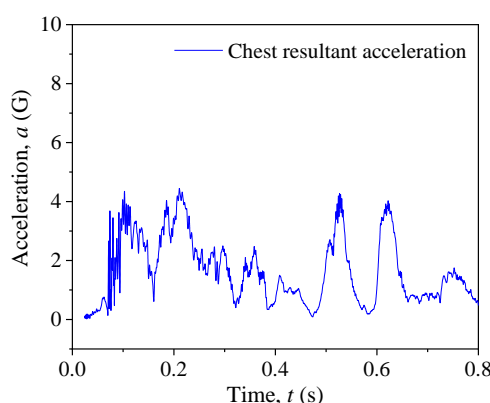
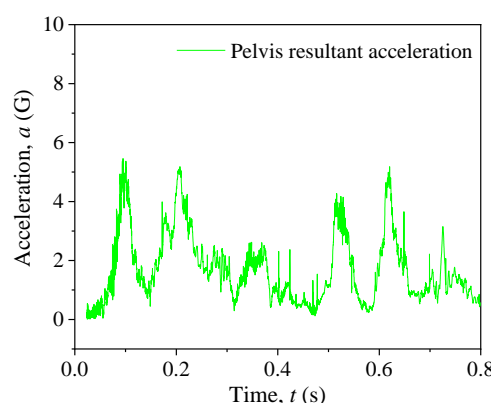


Figure 4.24 Vehicle trajectory during impact for Category 2 – Case 4.

Table 4.23 Vehicular responses, OIVs, and ORAs for Category 2 – Case 4.

Parameter	OIV (m/s)		ORA (G)		Vehicular Response	
	Longitudinal	Lateral	Longitudinal	Lateral	Roll angle	Pitch angle
Simulation Result	2.64	0.13	1.63	1.13	1.27°	0.95°
MASH Limit	12.2	12.2	20.49	20.49	75°	75°
Pass/Fail	Pass	Pass	Pass	Pass	Pass	Pass

Table 4.24 Dummy responses and injury parameters for Category 2 – Case 4.

Dummy head acceleration	Head impact criteria			
	Head injury parameter	Value	Threshold	Pass/Fail
	HIC <sub>15</sub>	1.20	700	Pass
	$p(\text{HIC}_{15})$	0 %	31%	Pass
Dummy chest acceleration	Dummy pelvis acceleration			
				

The simulation results of Category 2 – Case 4 showed that the connection between the pedestal and upper body of the unit being impacted first failed immediately, leaving the upper unit stuck between the vehicle’s front and the second unit, which was pushed down to the ground. The wheel rolled over the pedestal of second mailbox while the upper body being pushed by the vehicle, resulting the failure of the connection. At the end of the crash, both mailbox units were pushed forward by the test vehicle. The damage on the vehicle was a sharp V-shape dent on the hood. The trajectory of the mailbox showed that there was no possibility of hitting the windshield of vehicle, eliminating the possibility of compartment intrusions. The vehicle’s roll and pitch angles, as well as the OIVs and ORAs in both longitudinal and lateral directions, were all within the MASH allowed limits. For occupant response, the dummy’s head moved forward for a long distance due to impact pulses, but it did not touch the deployed airbag. The maximum head acceleration was approximately 6 G and the HIC<sub>15</sub> value was calculated to be 1.20, far below the threshold value of 700 and indicating no possibility of skull injury. The above analysis indicated that there was no potential occupant injury for this impact case.

#### 4.2.5 Category 2 – Case 5

In this case, a 2006 Ford F250 crashed into a dual-unit Type I cluster mailbox on a flat road at 31 mph (50 km/h) and with 25° impact angle at the mid-point. Figure 4.25 shows the full simulation

model before impact and the deformed vehicle model after impact. Figure 4.26 shows the overlapping contour plot of vehicle trajectory for this case. The vehicle's roll and pitch angles, OIVs, and ORAs were calculated and summarized in Table 4.25. Table 4.26 gives the acceleration histories of the crash test dummy on the head, chest, and pelvis. The HIC<sub>15</sub> and the probability of skull injury were also calculated for this case, as given in Table 4.26.

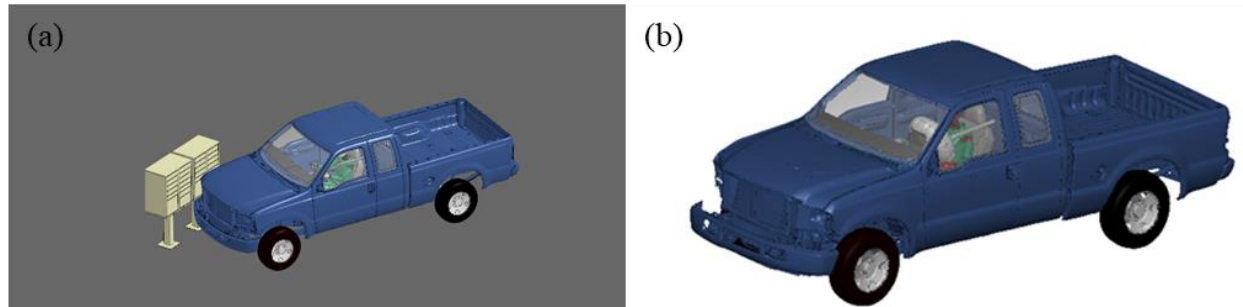


Figure 4.25 The full simulation model (a) and deformed vehicle model after impact (b) for Category 2 – Case 5.

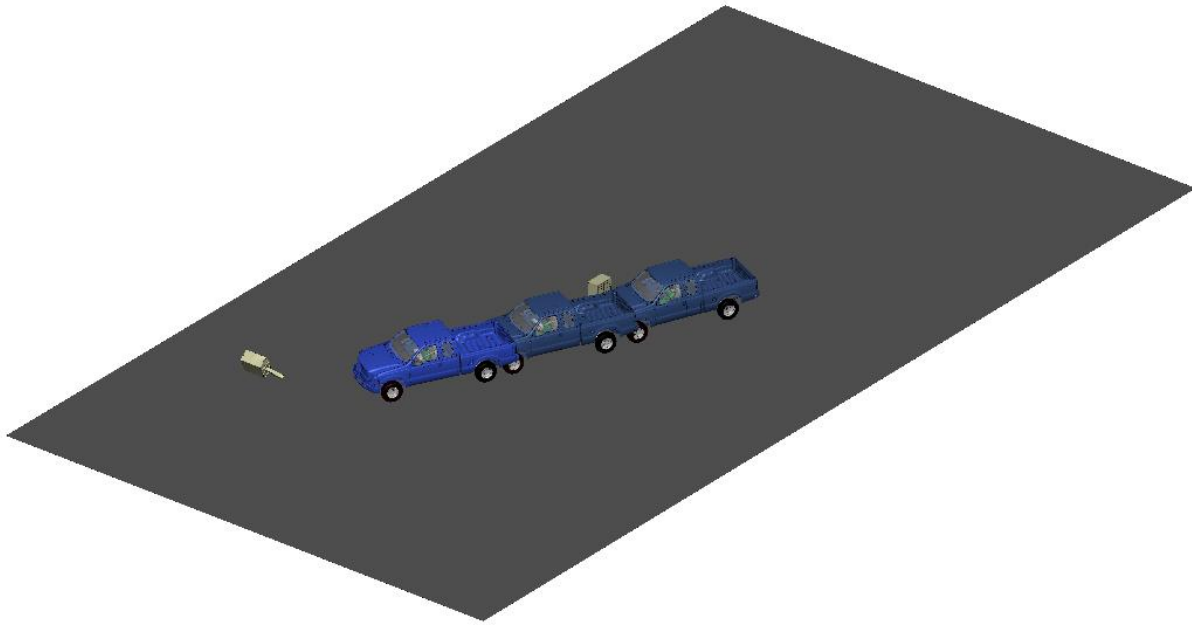
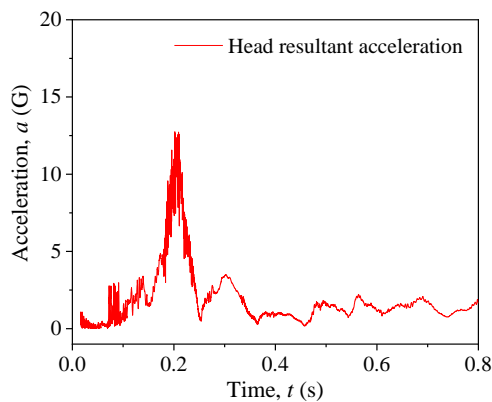
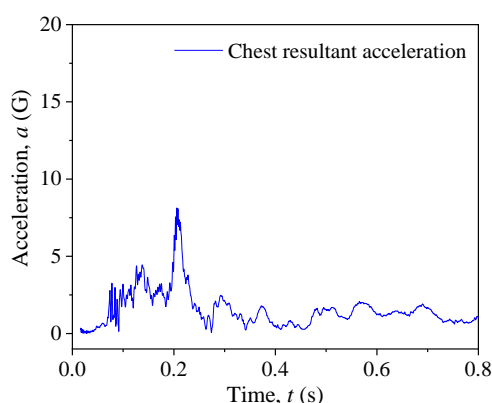
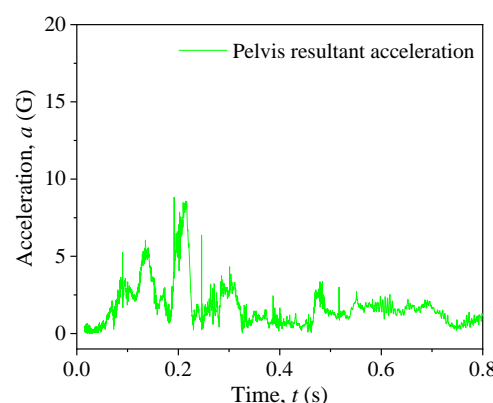


Figure 4.26 Vehicle trajectory during impact for Category 2 – Case 5.

Table 4.25 Vehicular responses, OIVs, and ORAs for Category 2 – Case 5.

Parameter	OIV (m/s)		ORA (G)		Vehicular Response	
	Longitudinal	Lateral	Longitudinal	Lateral	Roll angle	Pitch angle
Simulation Result	1.98	0.42	1.38	1.68	3.55°	0.80°
MASH Limit	12.2	12.2	20.49	20.49	75°	75°
Pass/Fail	Pass	Pass	Pass	Pass	Pass	Pass

Table 4.26 Dummy responses and injury parameters for Category 2 – Case 5.

Dummy head acceleration	Head impact criteria			
	Head injury parameter	Value	Threshold	Pass/Fail
	HIC <sub>15</sub>	5.16	700	Pass
	$p(\text{HIC}_{15})$	0 %	31%	Pass
Dummy chest acceleration	Dummy pelvis acceleration			
				

The simulation results of Category 2 – Case 5 showed that mailbox unit impacted first by the vehicle remained attached to the ground while the second unit was separated from the ground and pushed forward along the vehicle’s travel direction. The damage on the vehicle was a dent around the front right corner of the hood. The trajectory of the mailbox showed that there was no possibility of hitting the windshield of vehicle, eliminating the possibility of compartment intrusions. The vehicle’s roll and pitch angles, as well as the OIVs and ORAs in both longitudinal and lateral directions, were all within the MASH allowed limits. For occupant response, the dummy’s head did not touch the deployed airbag and the maximum head acceleration was approximately 12.5 G. The HIC<sub>15</sub> value was calculated to be 5.16, which was far below the threshold value of 700 and indicating no possibility of skull injury. The above analysis indicated that there was no potential occupant injury for this impact case.

#### 4.2.6 Category 2 – Case 6

In this case, a 2006 Ford F250 crashed into a single-unit Type I cluster mailbox behind a curb at 31 mph (50 km/h) and with 25° impact angle. Figure 4.27 shows the full simulation model before impact and the deformed vehicle model after impact. Figure 4.28 shows the overlapping contour plot of vehicle trajectory for this case. The vehicle's roll and pitch angles, OIVs, and ORAs were calculated and summarized in Table 4.27. Table 4.28 gives the acceleration histories of the crash test dummy on the head, chest, and pelvis. The HIC<sub>15</sub> and the probability of skull injury were also calculated for this case, as given in Table 4.28.

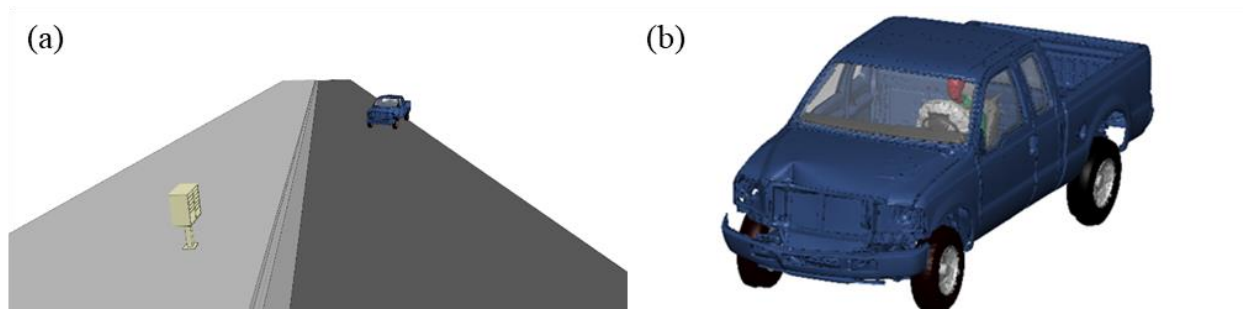


Figure 4.27 The full simulation model (a) and deformed vehicle model after impact (b) for Category 2 – Case 6.

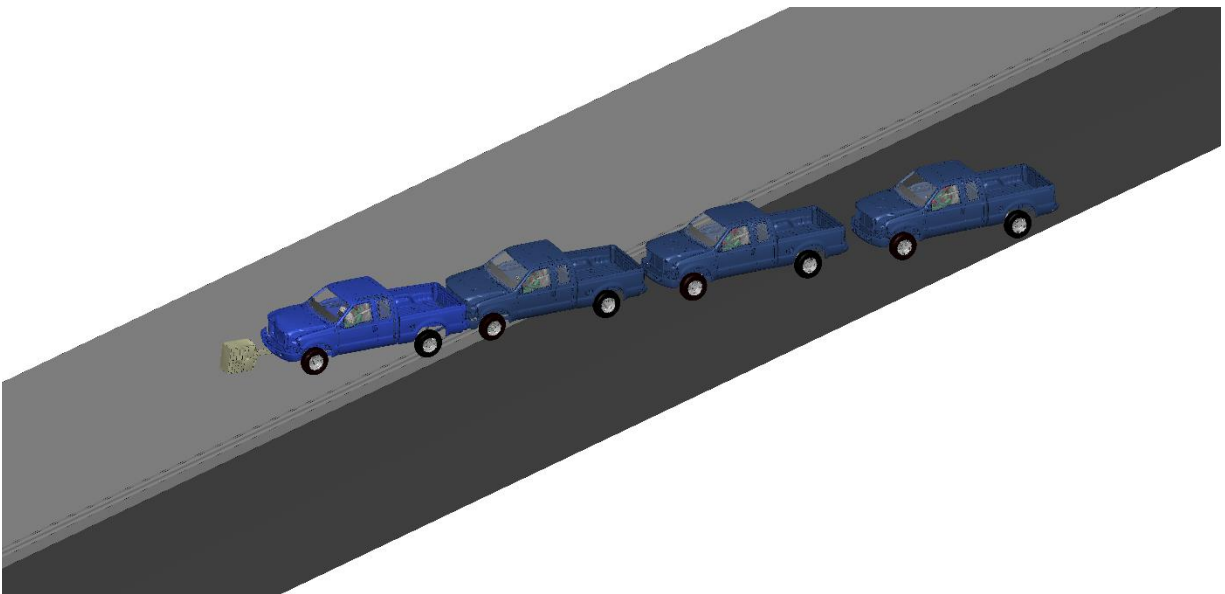
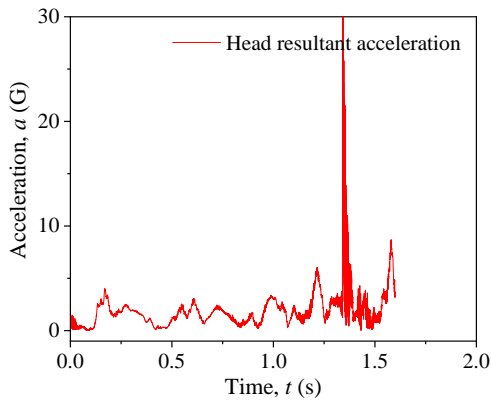
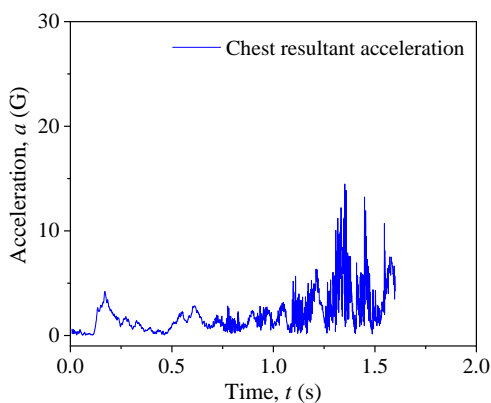
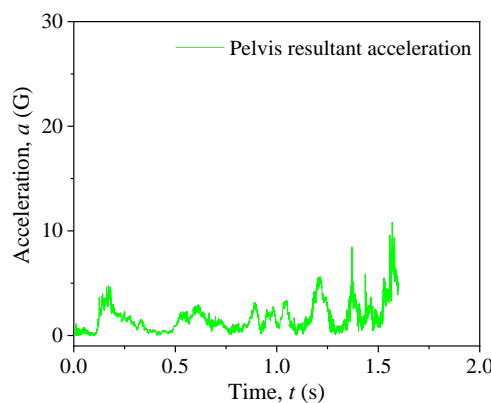


Figure 4.28 Vehicle trajectory during impact for Category 2 – Case 6.

Table 4.27 Vehicular responses, OIVs, and ORAs for Category 2 – Case 6.

Parameter	OIV (m/s)		ORA (G)		Vehicular Response	
	Longitudinal	Lateral	Longitudinal	Lateral	Roll angle	Pitch angle
Simulation Result	1.09	0.27	4.03	3.00	5.96°	1.73°
MASH Limit	12.2	12.2	20.49	20.49	75°	75°
Pass/Fail	Pass	Pass	Pass	Pass	Pass	Pass

Table 4.28 Dummy responses and injury parameters for Category 2 – Case 6.

Dummy head acceleration		Head impact criteria			
		Head injury parameter	Value	Threshold	Pass/Fail
		HIC <sub>15</sub>	8.98	700	Pass
		$p(\text{HIC}_{15})$	0 %	31%	Pass
Dummy chest acceleration		Dummy pelvis acceleration			
					

The simulation results of Category 2 – Case 6 showed that the connection of the mailbox to the ground failed quickly upon impact and the mailbox was pushed forward with the pedestal still connected with the upper body. The damage on the vehicle was limit to the front, with a deep V-shape dent on hood. The trajectory of the mailbox showed that there was no possibility of hitting the windshield of vehicle, eliminating the possibility of compartment intrusions. The vehicle's roll and pitch angles, as well as the OIVs and ORAs in both longitudinal and lateral directions, were all within the MASH allowed limits. During impact, the dummy's head moved forward but did not touch the deployed airbag. It should be noted that there was a large peak acceleration at approximately 1.3 second on the dummy head. Upon analysis of the dummy's responses and accelerations at the chest and pelvis, the peak head acceleration was deemed to be a numerical noise and should not be considered as a safety issue. The HIC<sub>15</sub> value was calculated to be 8.98, far below the threshold value of 700 and indicating no possibility of skull injury. The above analysis indicated that there was no potential occupant injury for this impact case.

#### 4.2.7 Category 2 – Case 7

In this case, a 2006 Ford F250 crashed into a dual-unit Type I cluster mailbox on a road behind the curb at 31 mph (50 km/h) and with 25° impact angle at the corner. Figure 4.29 shows the full simulation model before impact and the deformed vehicle model after impact. Figure 4.30 shows

the overlapping contour plot of vehicle trajectory for this case. The vehicle's roll and pitch angles, OIVs, and ORAs were calculated and summarized in Table 4.29. Table 4.30 gives the acceleration histories of the crash test dummy on the head, chest, and pelvis. The HIC<sub>15</sub> and the probability of skull injury were also calculated for this case, as given in Table 4.30.

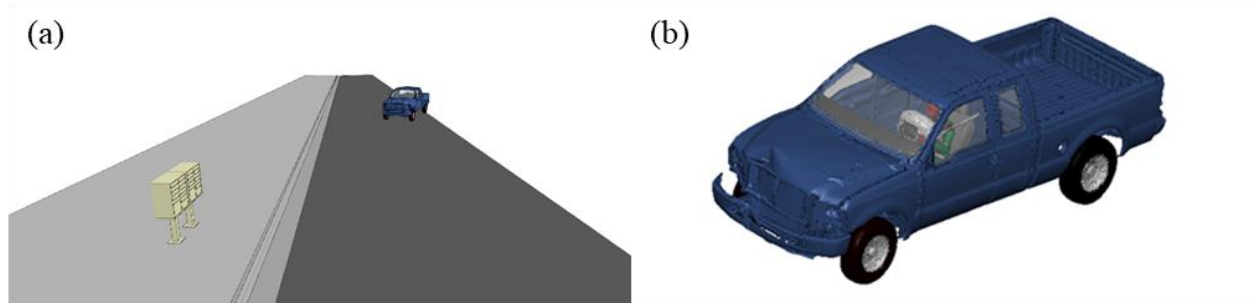


Figure 4.29 The full simulation model (a) and deformed vehicle model after impact (b) for Category 2 – Case 7.

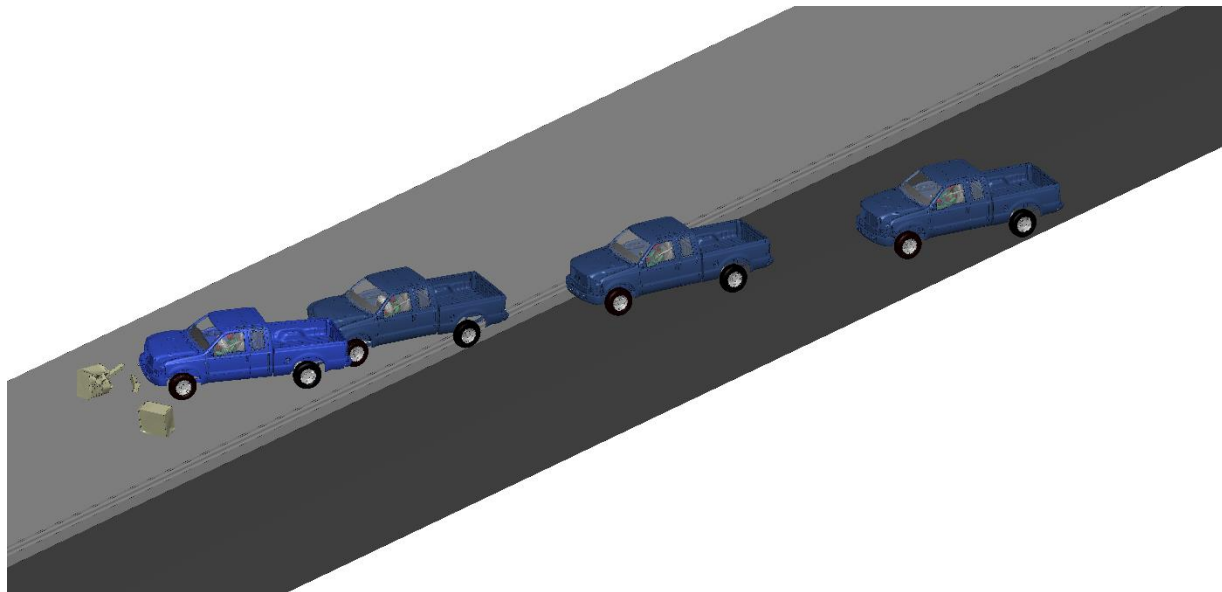


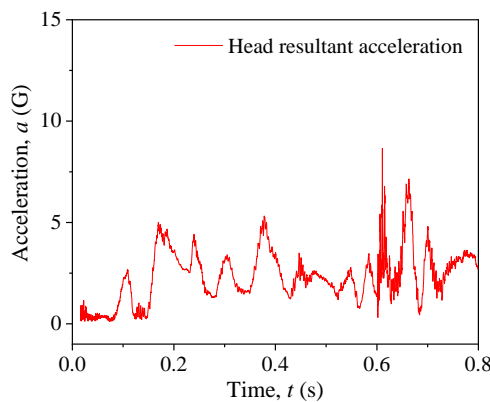
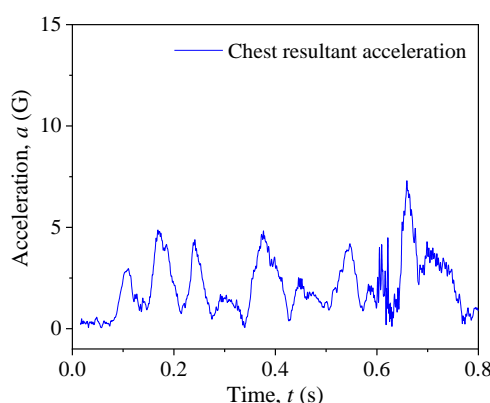
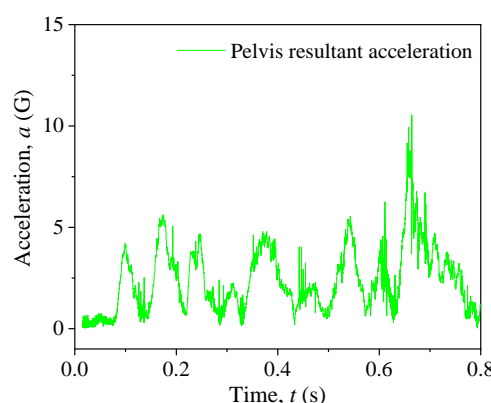
Figure 4.30 Vehicle trajectory during impact for Category 2 – Case 7.

Table 4.29 Vehicular responses, OIVs, and ORAs for Category 2 – Case 7.

Parameter	OIV (m/s)		ORA (G)		Vehicular Response	
	Longitudinal	Lateral	Longitudinal	Lateral	Roll angle	Pitch angle
Simulation Result	2.31	0.49	3.08	1.75	6.36°	1.44°
MASH Limit	12.2	12.2	20.49	20.49	75°	75°
Pass/Fail	Pass	Pass	Pass	Pass	Pass	Pass



Table 4.30 Dummy responses and injury parameters for Category 2 – Case 7.

Dummy head acceleration	Head impact criteria			
	Head injury parameter	Value	Threshold	Pass/Fail
	HIC <sub>15</sub>	1.36	700	Pass
	$p(\text{HIC}_{15})$	0 %	31%	Pass
Dummy chest acceleration	Dummy pelvis acceleration			
				

The simulation results of Category 2 – Case 7 showed that the mailbox unit being impacted first was quickly detached from the ground, with its upper body stuck between the vehicle and the second mailbox unit. The second mailbox unit was subsequently pushed down to the ground and the upper body was separated from the pedestal due to dragging and ripping effects. There were severe warpages and wrinkles on the front of the first mailbox unit. The damage on the vehicle was a V-shape dent on hood, which was slightly popped open. The trajectory of the mailbox showed that there was no possibility for it to hit the windshield of vehicle, eliminating the possibility of compartment intrusions. The vehicle's roll and pitch angles, as well as the OIVs and ORAs in both longitudinal and lateral directions, were all within the MASH allowed limits. For occupant response, the dummy's head moved forward but did not touch the deployed airbag. The HIC<sub>15</sub> value was calculated to be 1.36, far below the threshold value of 700 and indicating no possibility of skull injury. The above analysis indicated that there was no potential occupant injury for this impact case.

#### 4.2.8 Category 2 – Case 8

In this case, a 2006 Ford F250 crashed into a dual-unit Type I cluster mailbox on a road behind the curb at 31 mph (50 km/h) and with 25° impact angle at the mid-point. Figure 4.31 shows the full simulation model before impact and the deformed vehicle model after impact. Figure 4.32

shows the overlapping contour plot of vehicle trajectory for this case. The vehicle's roll and pitch angles, OIVs, and ORAs were calculated and summarized in Table 4.31. Table 4.32 gives the acceleration histories of the crash test dummy on the head, chest, and pelvis. The HIC<sub>15</sub> and the probability of skull injury were also calculated for this case, as given in Table 4.32.

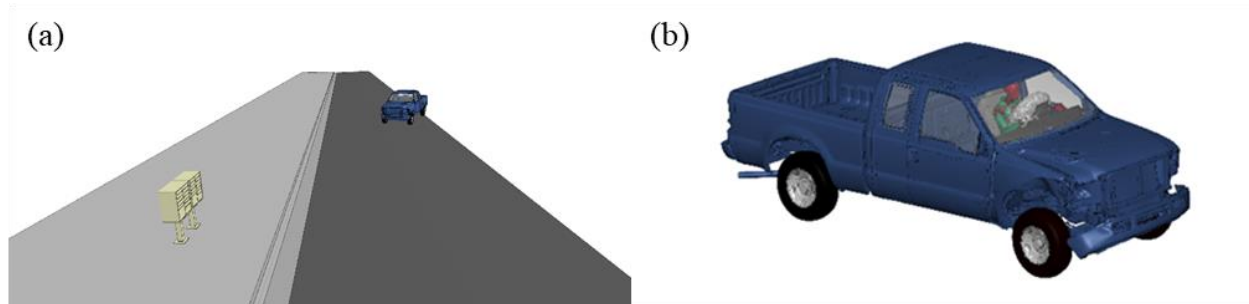


Figure 4.31 The full simulation model (a) and deformed vehicle model after impact (b) for Category 2 – Case 8.

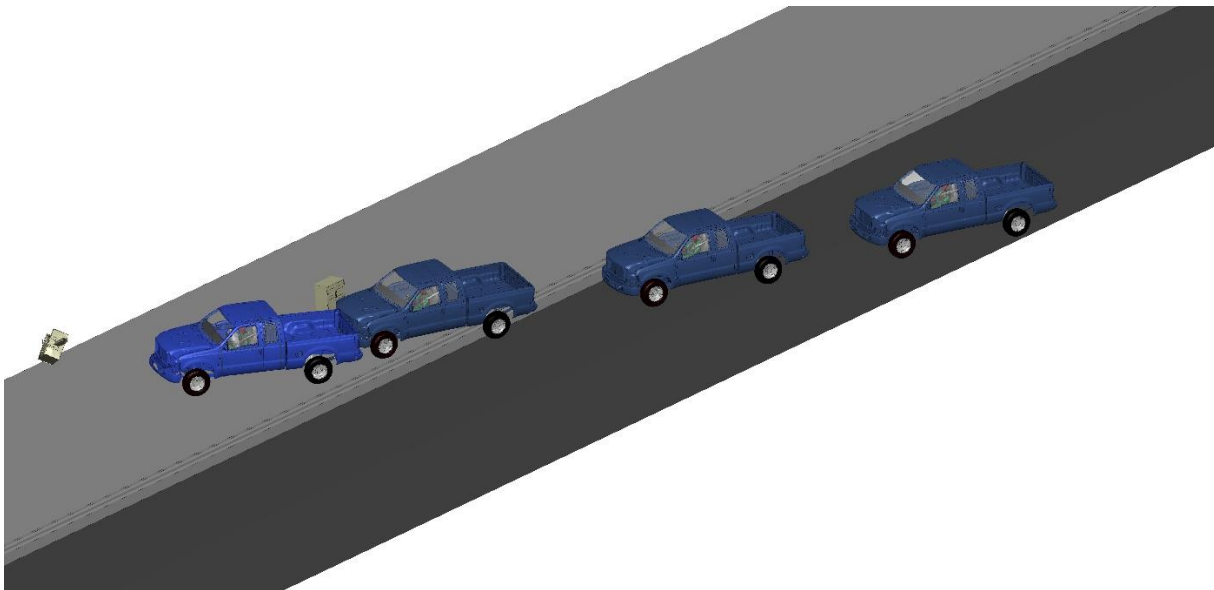


Figure 4.32 Vehicle trajectory during impact for Category 2 – Case 8.

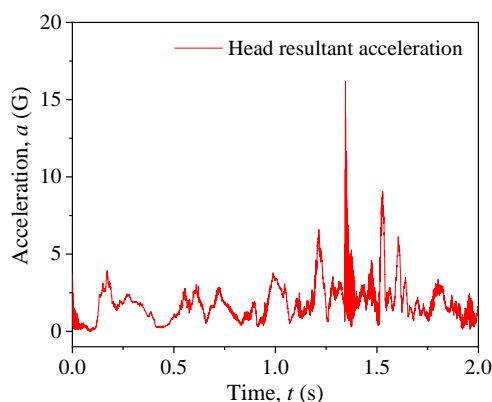
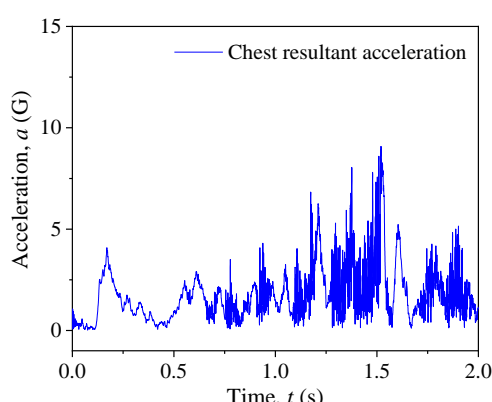
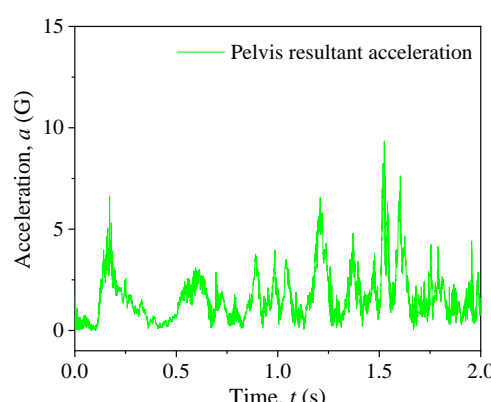
Table 4.31 Vehicular responses, OIVs, and ORAs for Category 2 – Case 8.

Parameter	OIV (m/s)		ORA (G)		Vehicular Response	
	Longitudinal	Lateral	Longitudinal	Lateral	Roll angle	Pitch angle
Simulation Result	1.11	0.29	5.03	3.27	6.36°	2.19°
MASH Limit	12.2	12.2	20.49	20.49	75°	75°
Pass/Fail	Pass	Pass	Pass	Pass	Pass	Pass

The simulation results of Category 2 – Case 8 showed that mailbox unit impacted first by the vehicle remained attached to the ground while the second unit was separated from the ground and pushed forward along the vehicle's travel direction. The damage on the vehicle was localized to the front right corner of the vehicle. The trajectory of the mailbox showed that there was no possibility of hitting the windshield of vehicle, eliminating the possibility of compartment

intrusions. The vehicle's roll and pitch angles, as well as the OIVs and ORAs in both longitudinal and lateral directions, were all within the MASH allowed limits. During impact, the dummy's head moved forward and slightly touched the deployed airbag. The HIC15 value was calculated to be 2.55, far below the threshold value of 700 and indicating no possibility of skull injury. The above analysis indicated that there was no potential occupant injury for this impact case.

Table 4.32 Dummy responses and injury parameters for Category 2 – Case 8.

Dummy head acceleration		Head impact criteria			
	Head injury parameter	Value	Threshold	Pass/Fail	
	HIC <sub>15</sub>	2.55	700	Pass	
	$p(\text{HIC}_{15})$	0 %	31%	Pass	
Dummy chest acceleration		Dummy pelvis acceleration			
					

### 4.3 Simulations Results of Category 3

In Category 3, the occupant risk was evaluated under vehicular crashes of a 1100C small passenger car (i.e., a 2010 Toyota Yaris) into Type IV cluster mailboxes at an impact speed of 31 mph (50 km/h). The eight simulation cases in Category 3 are summarized as follows.

- Case 1: A single-unit Type IV cluster mailbox with 0° impact angle;
- Case 2: A single-unit Type IV cluster mailbox on a flat road with 25° impact angle;
- Case 3: A dual-unit Type IV cluster mailbox with 0° impact angle;
- Case 4: A dual-unit Type IV cluster mailbox on a flat road with 25° impact angle and impacted at the corner;
- Case 5: A dual-unit Type IV cluster mailbox on a flat road with 25° impact angle and impacted at the mid-point;
- Case 6: A single-unit Type IV cluster mailbox behind a curb with 25° impact angle;

- Case 7: A dual-unit Type IV cluster mailbox behind a curb with 25° impact angle and impacted at the corner; and
- Case 8: A dual-unit Type IV cluster mailbox behind a curb with 25° impact angle and impacted at the mid-point.

#### 4.3.1 Category 3 – Case 1

In this case, a 2010 Toyota Yaris crashed into a single-unit Type IV cluster mailbox on a flat road at 31 mph (50 km/h) and with 0° impact angle. Figure 4.33 shows the full simulation model before impact and the deformed vehicle model after impact. Figure 4.34 shows the overlapping contour plot of vehicle trajectory for this case. The vehicle's roll and pitch angles, OIVs, and ORAs were calculated and summarized in Table 4.33. Table 4.34 gives the acceleration histories of the crash test dummy on the head, chest, and pelvis. The  $HIC_{15}$  and the probability of skull injury were also calculated for this case, as given in Table 4.34.

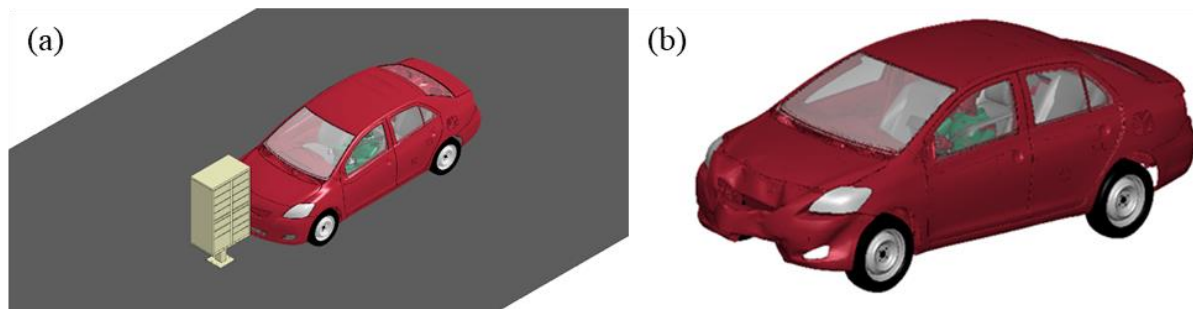


Figure 4.33 The full simulation model (a) and deformed vehicle model after impact (b) for Category 3 – Case 1.

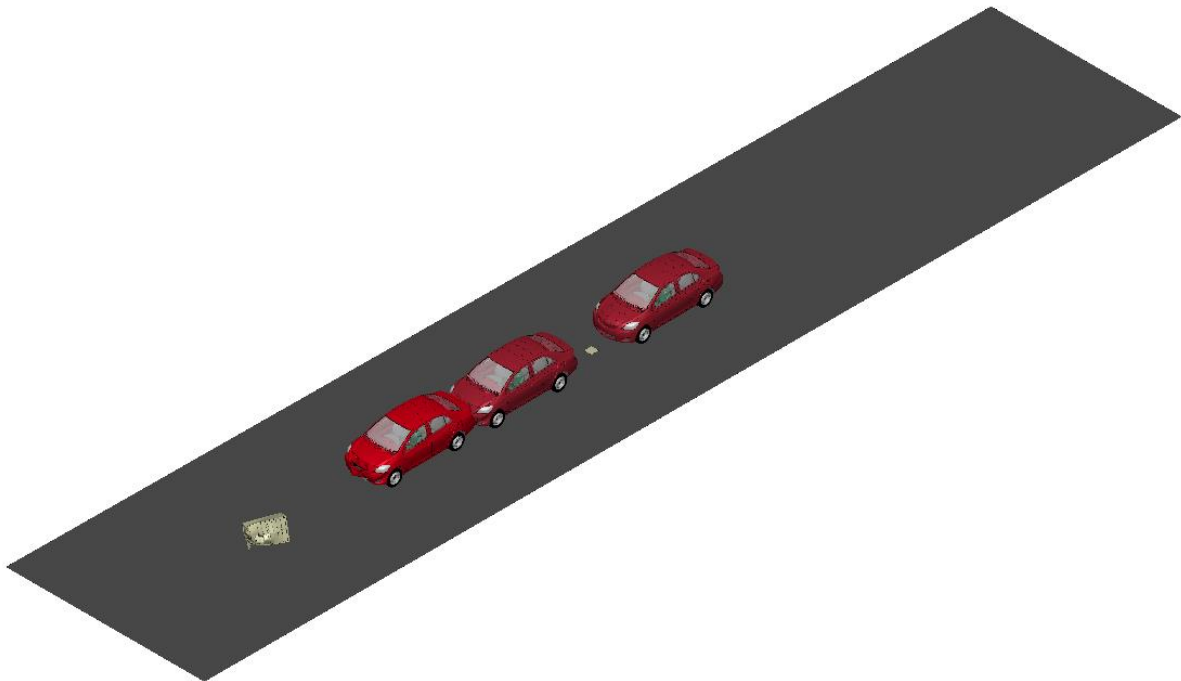
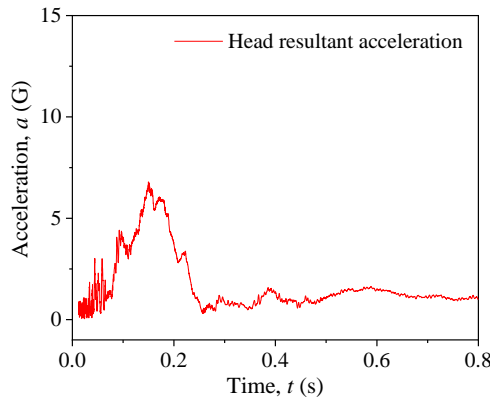
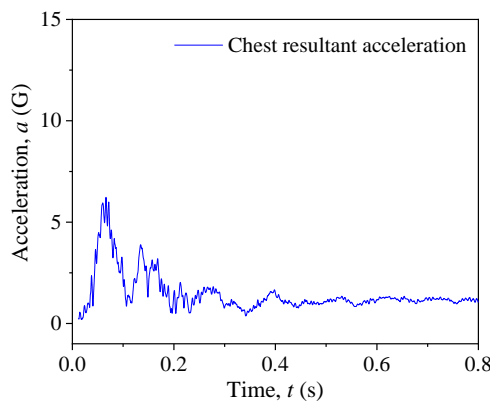
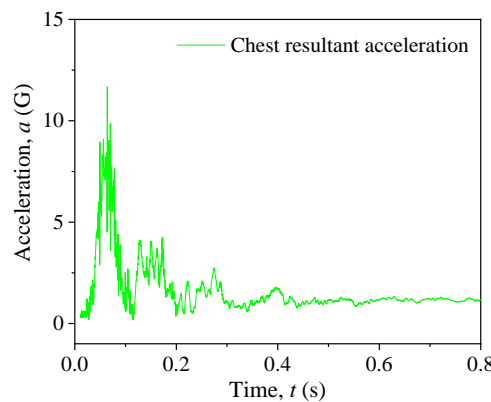


Figure 4.34 Vehicle trajectory during impact for Category 3 – Case 1.

Table 4.33 Vehicular responses, OIVs, and ORAs for Category 3 – Case 1.

Parameter	OIV (m/s)		ORA (G)		Vehicular Response	
	Longitudinal	Lateral	Longitudinal	Lateral	Roll angle	Pitch angle
Simulation Result	3.52	0.08	1.05	1.84	0.57°	1.05°
MASH Limit	12.2	12.2	20.49	20.49	75°	75°
Pass/Fail	Pass	Pass	Pass	Pass	Pass	Pass

Table 4.34 Dummy responses and injury parameters for Category 3 – Case 1.

Dummy head acceleration		Head impact criteria			
	Head injury parameter	Value	Threshold	Pass/Fail	
	HIC <sub>15</sub>	1.52	700	Pass	
	$p(\text{HIC}_{15})$	0 %	31%	Pass	
Dummy chest acceleration		Dummy pelvis acceleration			
	Chest resultant acceleration				

The simulation results of Category 3 – Case 1 showed that the pedestal was separated from the upper body upon impact and stuck under the chassis of the Yaris. The upper body was pushed forward by the vehicle and caused minor damage to the front bumper and hood of the vehicle. The trajectory of the mailbox showed that there was no possibility of hitting the windshield of vehicle, eliminating the possibility of compartment intrusions. The vehicle's roll and pitch angles, as well as the OIVs and ORAs in both longitudinal and lateral directions, were all within the MASH allowed limits. The dummy's head moved forward and barely touched the deployed airbag. The HIC<sub>15</sub> value was calculated to be 1.52, far below the threshold value of 700 and indicating no possibility of skull injury. The above analysis indicated that there was no potential occupant injury for this impact case.

#### 4.3.2 Category 3 – Case 2

In this case, a 2010 Toyota Yaris crashed into a single-unit Type IV cluster mailbox on a flat road at 31 mph (50 km/h) and with 25° impact angle. Figure 4.35 shows the full simulation model before impact and the deformed vehicle model after impact. Figure 4.36 shows the overlapping contour plot of vehicle trajectory for this case. The vehicle's roll and pitch angles, OIVs, and ORAs were calculated and summarized in Table 4.35. Table 4.36 gives the acceleration histories of the crash test dummy on the head, chest, and pelvis. The HIC<sub>15</sub> and the probability of skull injury were also calculated for this case, as given in Table 4.36.

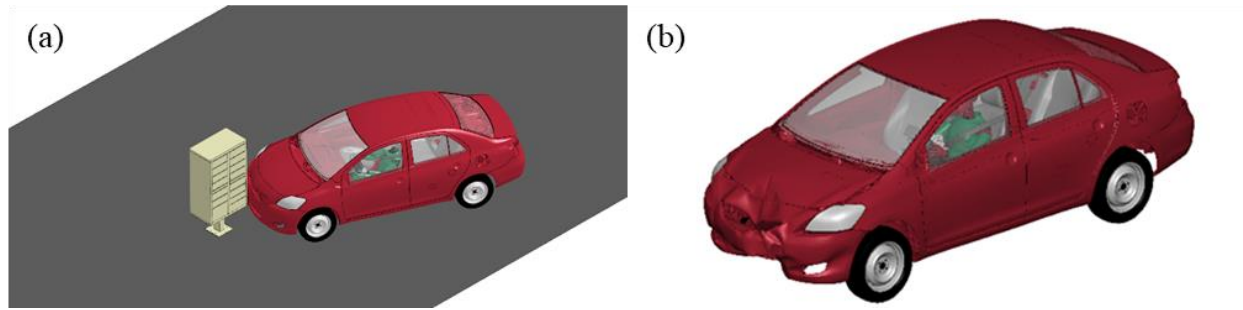


Figure 4.35 The full simulation model (a) and deformed vehicle model after impact (b) for Category 3 – Case 2.

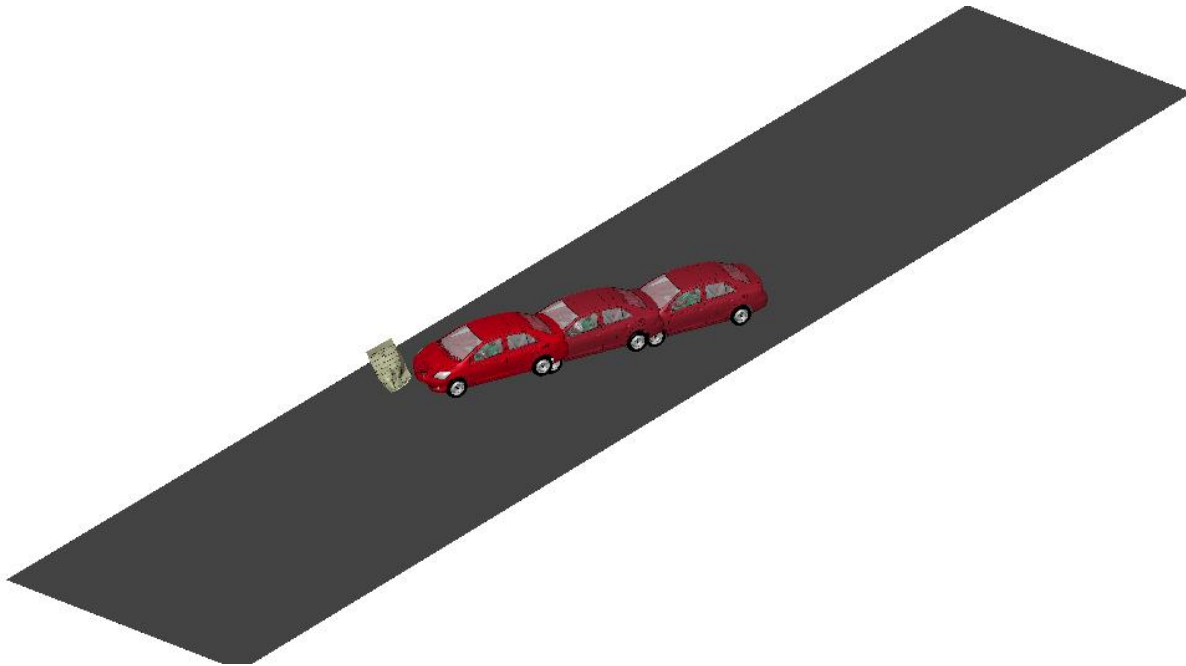
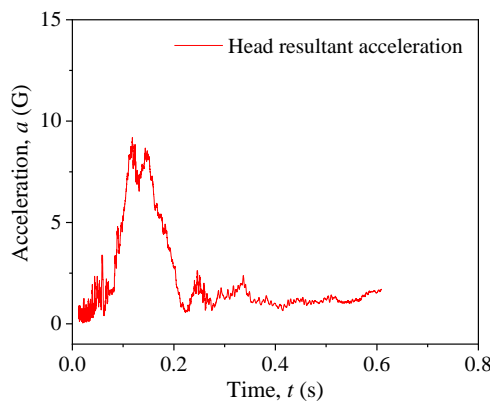
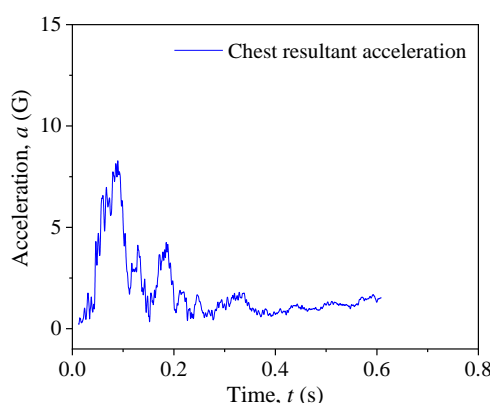
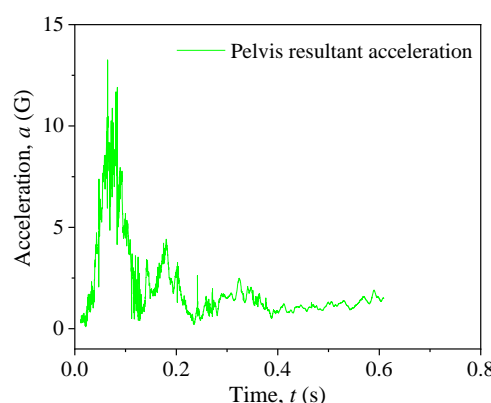


Figure 4.36 Vehicle trajectory during impact for Category 3 – Case 2.

Table 4.35 Vehicular responses, OIVs, and ORAs for Category 3 – Case 2.

Parameter	OIV (m/s)		ORA (G)		Vehicular Response	
	Longitudinal	Lateral	Longitudinal	Lateral	Roll angle	Pitch angle
Simulation Result	3.69	0.24	1.09	1.41	0.51°	0.75°
MASH Limit	12.2	12.2	20.49	20.49	75°	75°
Pass/Fail	Pass	Pass	Pass	Pass	Pass	Pass

Table 4.36 Dummy responses and injury parameters for Category 3 – Case 2.

Dummy head acceleration	Head impact criteria			
	Head injury parameter	Value	Threshold	Pass/Fail
	HIC <sub>15</sub>	2.99	700	Pass
	$p(\text{HIC}_{15})$	0 %	31%	Pass
Dummy chest acceleration	Dummy pelvis acceleration			
				

The simulation results of Category 3 – Case 2 was similar to the results of Category 3 – Case 1 in terms of mailbox failure and trajectory as well as vehicle damages. The vehicle's roll and pitch angles, as well as the OIVs and ORAs in both longitudinal and lateral directions, were all within the MASH allowed limits. similar as the last case. During impact, the dummy's head moved forward and slightly touched the deployed airbag. The maximum head acceleration was approximately 9 G and the HIC<sub>15</sub> value was calculated to be 2.99, far below the threshold value of 700 and indicating no possibility of skull injury. The above analysis indicated that there was no potential occupant injury for this impact case.

#### 4.3.3 Category 3 – Case 3

In this case, a 2010 Toyota Yaris crashed into a dual-unit Type IV cluster mailbox on a flat road at 31 mph (50 km/h) and with 0° impact angle. Figure 4.37 shows the full simulation model before impact and the deformed vehicle model after impact. Figure 4.38 shows the overlapping contour plot of vehicle trajectory for this case. The vehicle's roll and pitch angles, OIVs, and ORAs were calculated and summarized in Table 4.37. Table 4.38 gives the acceleration histories of the crash test dummy on the head, chest, and pelvis. The HIC<sub>15</sub> and the probability of skull injury were also calculated for this case, as given in Table 4.38.

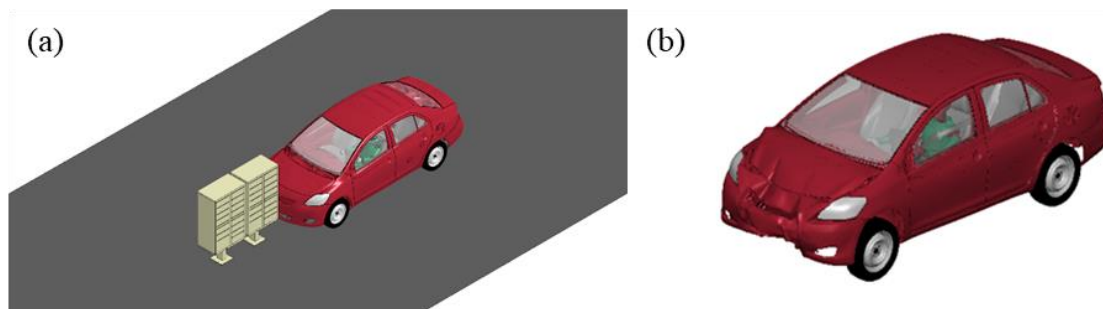


Figure 4.37 The full simulation model (a) and deformed vehicle model after impact (b) for Category 3 – Case 3.

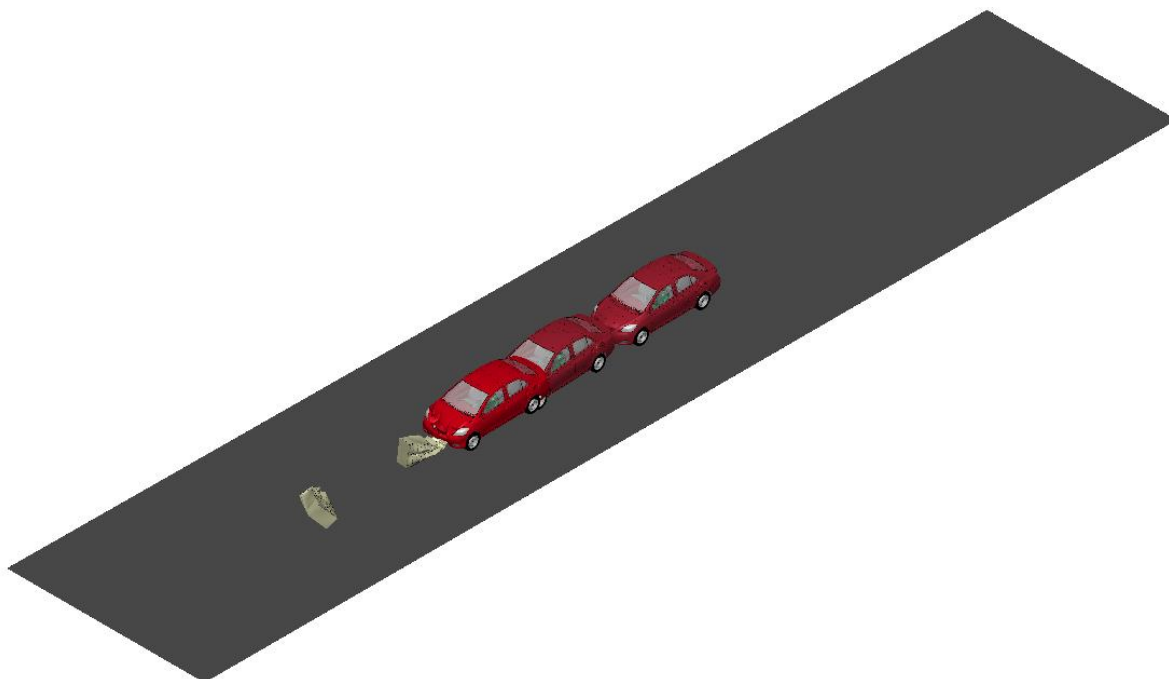


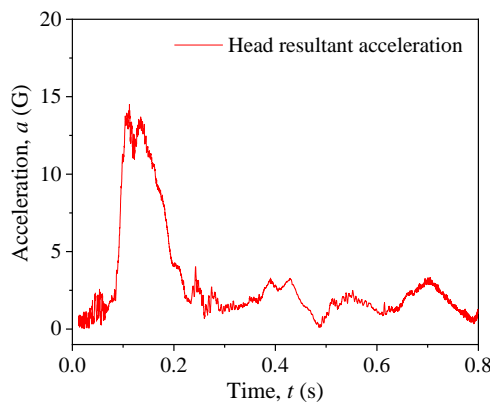
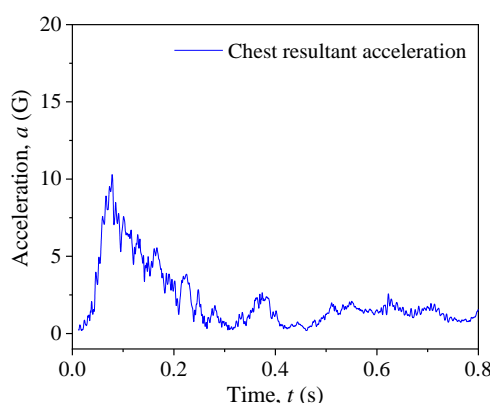
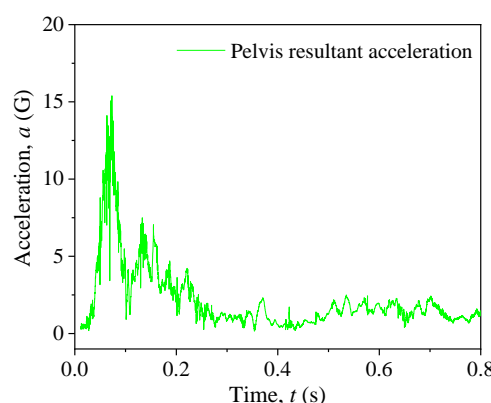
Figure 4.38 Vehicle trajectory during impact for Category 3 – Case 3.

Table 4.37 Vehicular responses, OIVs, and ORAs for Category 3 – Case 3.

Parameter	OIV (m/s)		ORA (G)		Vehicular Response	
	Longitudinal	Lateral	Longitudinal	Lateral	Roll angle	Pitch angle
Simulation Result	6.36	0.18	3.59	3.22	0.89°	3.13°
MASH Limit	12.2	12.2	20.49	20.49	75°	75°
Pass/Fail	Pass	Pass	Pass	Pass	Pass	Pass



Table 4.38 Dummy responses and injury parameters for Category 3 – Case 3.

Dummy head acceleration		Head impact criteria			
		Head injury parameter	Value	Threshold	Pass/Fail
		HIC <sub>15</sub>	9.70	700	Pass
		$p(\text{HIC}_{15})$	0 %	31%	Pass
Dummy chest acceleration		Dummy pelvis acceleration			
					

The simulation results of Category 3 – Case 3 showed that the pedestals of both units were separated from the upper bodies upon impacts of the vehicle. Both upper units were pushed forward by the vehicle, with the unit impacted first severely damaged. The larger mass of the Type IV mailbox caused larger damage on the vehicle's front than that for the Type I mailbox. The trajectory of the mailbox showed that there was no possibility of hitting the windshield of vehicle, eliminating the possibility of compartment intrusions. The vehicle's roll and pitch angles, as well as the OIVs and ORAs in both longitudinal and lateral directions, were all within the MASH allowed limits. During impact, the dummy's head moved forward and hit the deployed airbag. The maximum head acceleration was approximately 14 G and the HIC<sub>15</sub> value was calculated to be 9.70, far below the threshold value of 700 and indicating no possibility of skull injury. The above analysis indicated that there was no potential occupant injury for this impact case.

#### 4.3.4 Category 3 – Case 4

In this case, a 2010 Toyota Yaris crashed into a dual-unit Type IV cluster mailbox on a flat road at 31 mph (50 km/h) and with 25° impact angle at the corner. Figure 4.39 shows the full simulation model before impact and the deformed vehicle model after impact. Figure 4.40 shows the overlapping contour plot of vehicle trajectory for this case. The vehicle's roll and pitch angles, OIVs, and ORAs were calculated and summarized in Table 4.39. Table 4.40 gives the acceleration

histories of the crash test dummy on the head, chest, and pelvis. The  $HIC_{15}$  and the probability of skull injury were also calculated for this case, as given in Table 4.40.

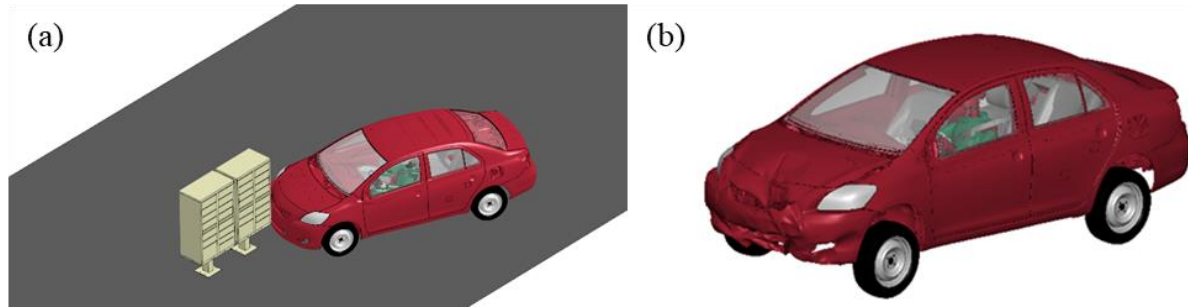


Figure 4.39 The full simulation model (a) and deformed vehicle model after impact (b) for Category 3 – Case 4.

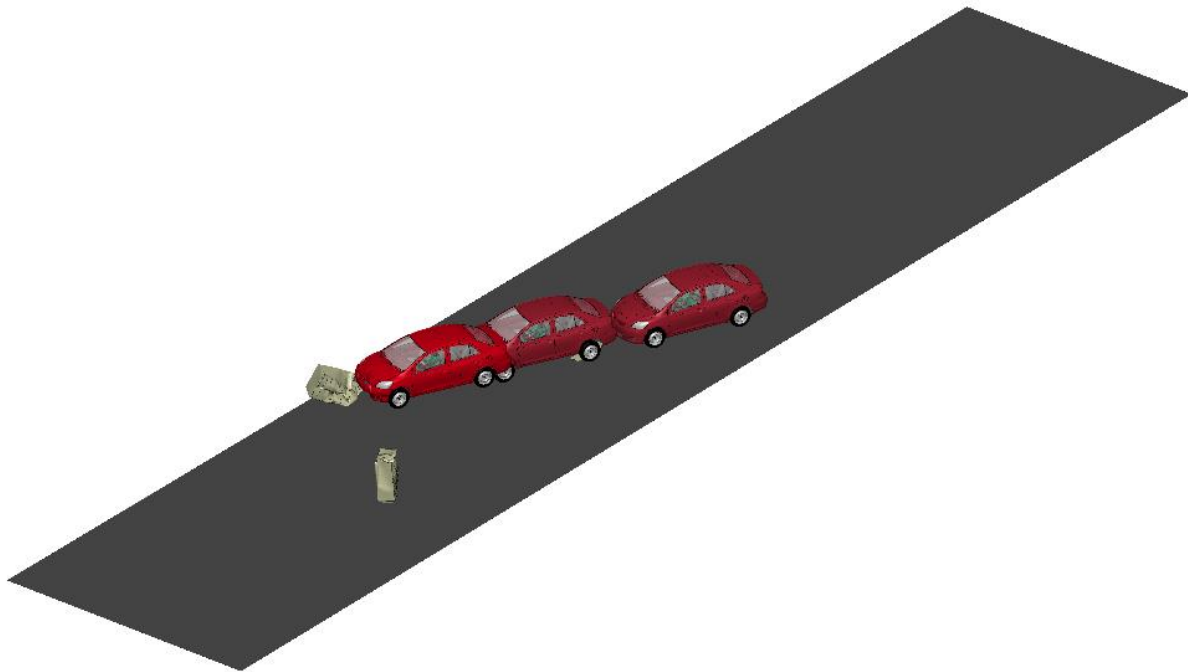
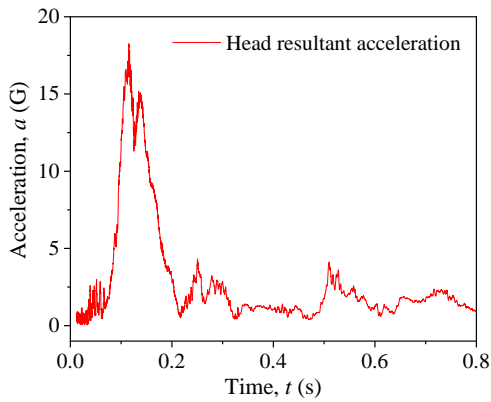
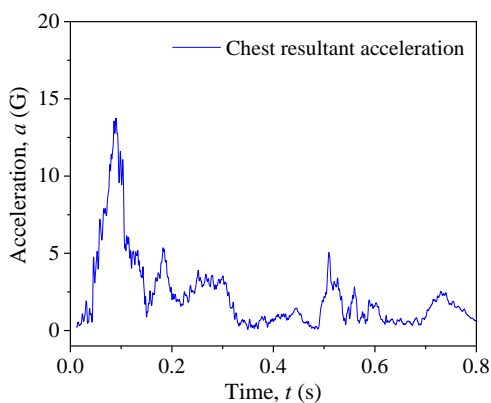
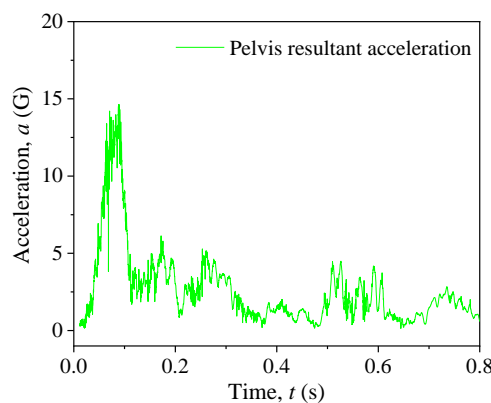


Figure 4.40 Vehicle trajectory during impact for Category 3 – Case 4.

Table 4.39 Vehicular responses, OIVs, and ORAs for Category 3 – Case 4.

Parameter	OIV (m/s)		ORA (G)		Vehicular Response	
	Longitudinal	Lateral	Longitudinal	Lateral	Roll angle	Pitch angle
Simulation Result	5.99	0.45	6.09	4.96	3.24°	2.38°
MASH Limit	12.2	12.2	20.49	20.49	75°	75°
Pass/Fail	Pass	Pass	Pass	Pass	Pass	Pass

Table 4.40 Dummy responses and injury parameters for Category 3 – Case 4.

Dummy head acceleration		Head impact criteria			
		Head injury parameter	Value	Threshold	Pass/Fail
		HIC <sub>15</sub>	15.89	700	Pass
		$p(\text{HIC}_{15})$	0 %	31%	Pass
Dummy chest acceleration		Dummy pelvis acceleration			
					

The simulation results of Category 3 – Case 4 were similar to those of Case 3 in terms of mailbox failures and vehicle damage. The two upper units were pushed forward by the vehicle and the trajectory of the mailbox indicated no possibility of hitting the windshield of vehicle, eliminating the possibility of compartment intrusions. The vehicle's roll and pitch angles, as well as the OIVs and ORAs in both longitudinal and lateral directions, were all within the MASH allowed limits. In this case, the dummy's head moved forward and hit the deployed airbag. The maximum head acceleration was approximately 18 G and the HIC<sub>15</sub> value was calculated to be 15.89, far below the threshold value of 700 and indicating no possibility of skull injury. The above analysis indicated that there was no potential occupant injury for this impact case.

#### 4.3.5 Category 3 – Case 5

In this case, a 2010 Toyota Yaris crashed into a dual-unit Type IV cluster mailbox on a flat road at 31 mph (50 km/h) and with 25° impact angle at the mid-point. Figure 4.41 shows the full simulation model before impact and the deformed vehicle model after impact. Figure 4.42 shows the overlapping contour plot of vehicle trajectory for this case. The vehicle's roll and pitch angles, OIVs, and ORAs were calculated and summarized in Table 4.41. Table 4.42 gives the acceleration histories of the crash test dummy on the head, chest, and pelvis. The HIC<sub>15</sub> and the probability of skull injury were also calculated for this case, as given in Table 4.42.

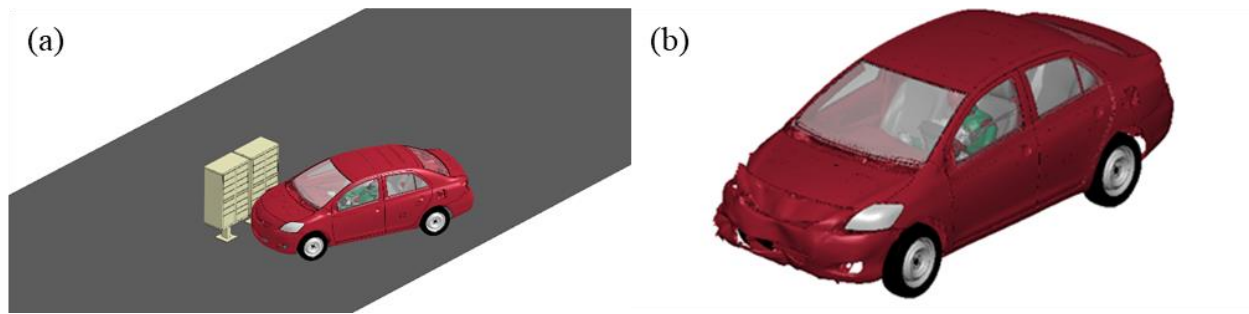


Figure 4.41 The full simulation model (a) and deformed vehicle model after impact (b) for Category 3 – Case 5.

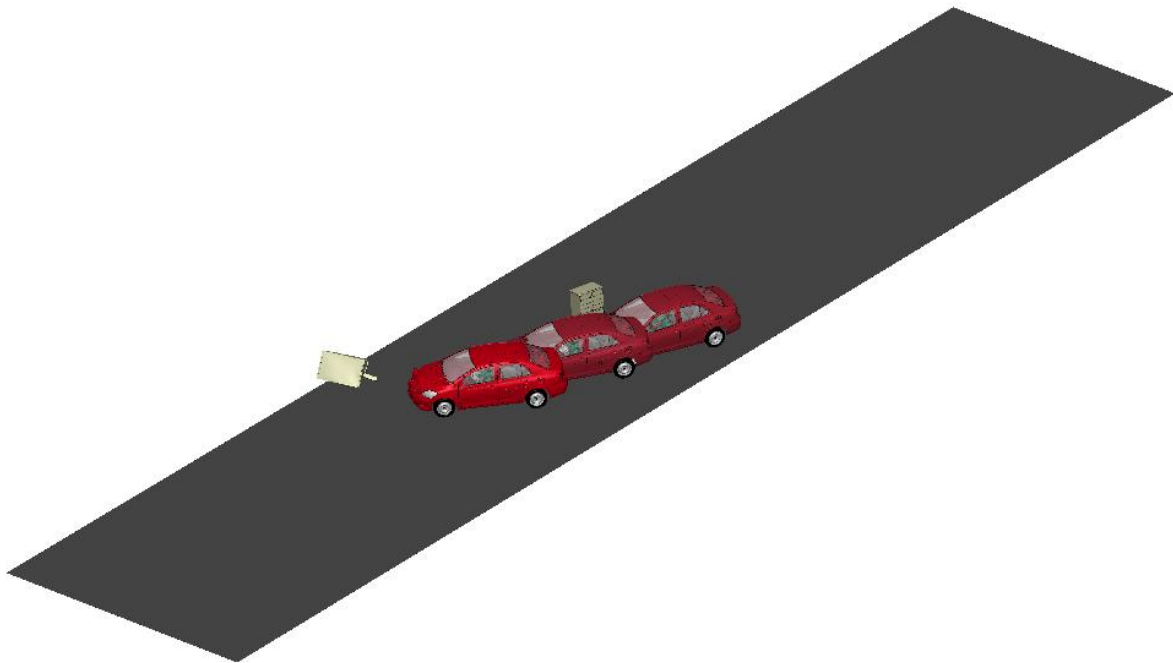


Figure 4.42 Vehicle trajectory during impact for Category 3 – Case 5.

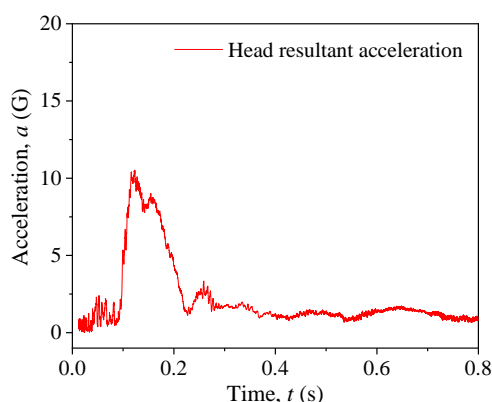
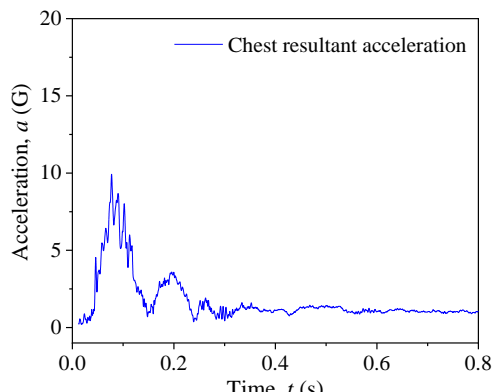
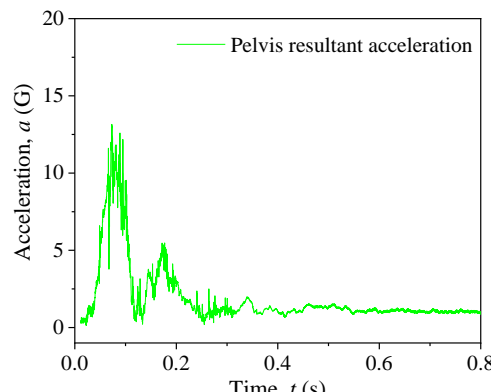
Table 4.41 Vehicular responses, OIVs, and ORAs for Category 3 – Case 5.

Parameter	OIV (m/s)		ORA (G)		Vehicular Response	
	Longitudinal	Lateral	Longitudinal	Lateral	Roll angle	Pitch angle
Simulation Result	3.75	0.63	1.39	2.44	2.87°	0.89°
MASH Limit	12.2	12.2	20.49	20.49	75°	75°
Pass/Fail	Pass	Pass	Pass	Pass	Pass	Pass

The simulation results of Category 3 – Case 5 showed that the mailbox unit impacted first by the vehicle remained attached to the ground. The second mailbox unit was pushed down to the ground with the pedestal attached to the upper body. The damage of the vehicle was on the front bumper and hood. The trajectory of the mailbox showed that there was no possibility of hitting the windshield of vehicle, eliminating the possibility of compartment intrusions. The vehicle's roll and pitch angles, as well as the OIVs and ORAs in both longitudinal and lateral directions, were all within the MASH allowed limits. During impact, the dummy's head moved forward and hit

deployed airbag. The maximum head acceleration was approximately 10 G, lower than that of Case 4 in which the vehicle impacted the corner of the mailbox. The  $HIC_{15}$  value was calculated to be 4.63, far below the threshold value of 700 and indicating no possibility of skull injury. The above analysis indicated that there was no potential occupant injury for this impact case.

Table 4.42 Dummy responses and injury parameters for Category 3 – Case 5.

Dummy head acceleration	Head impact criteria			
	Head injury parameter	Value	Threshold	Pass/Fail
	$HIC_{15}$	4.63	700	Pass
	$p(HIC_{15})$	0 %	31%	Pass
Dummy chest acceleration	Dummy pelvis acceleration			
				

#### 4.3.6 Category 3 – Case 6

In this case, a 2010 Toyota Yaris crashed into a single-unit Type IV cluster mailbox on a road behind the curb at 31 mph (50 km/h) and with 25° impact angle. Figure 4.43 shows the full simulation model before impact and the deformed vehicle model after impact. Figure 4.44 shows the overlapping contour plot of vehicle trajectory for this case. The vehicle's roll and pitch angles, OIVs, and ORAs were calculated and summarized in Table 4.43. Table 4.44 gives the acceleration histories of the crash test dummy on the head, chest, and pelvis. The  $HIC_{15}$  and the probability of skull injury were also calculated for this case, as given in Table 4.44.

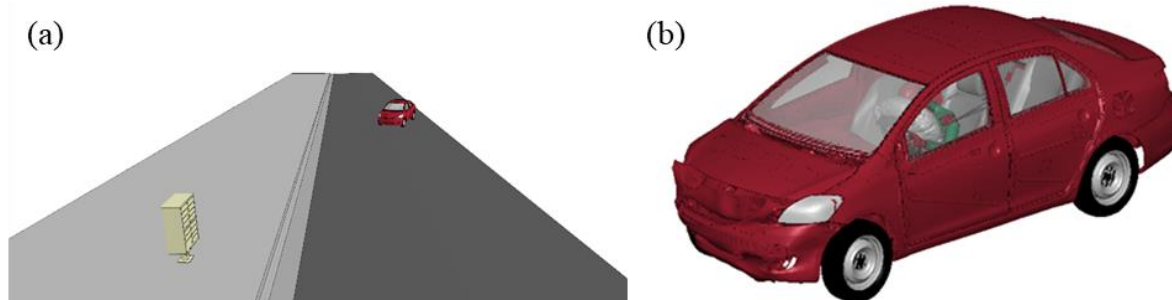


Figure 4.43 The full simulation model (a) and deformed vehicle model after impact (b) for Category 3 – Case 6.

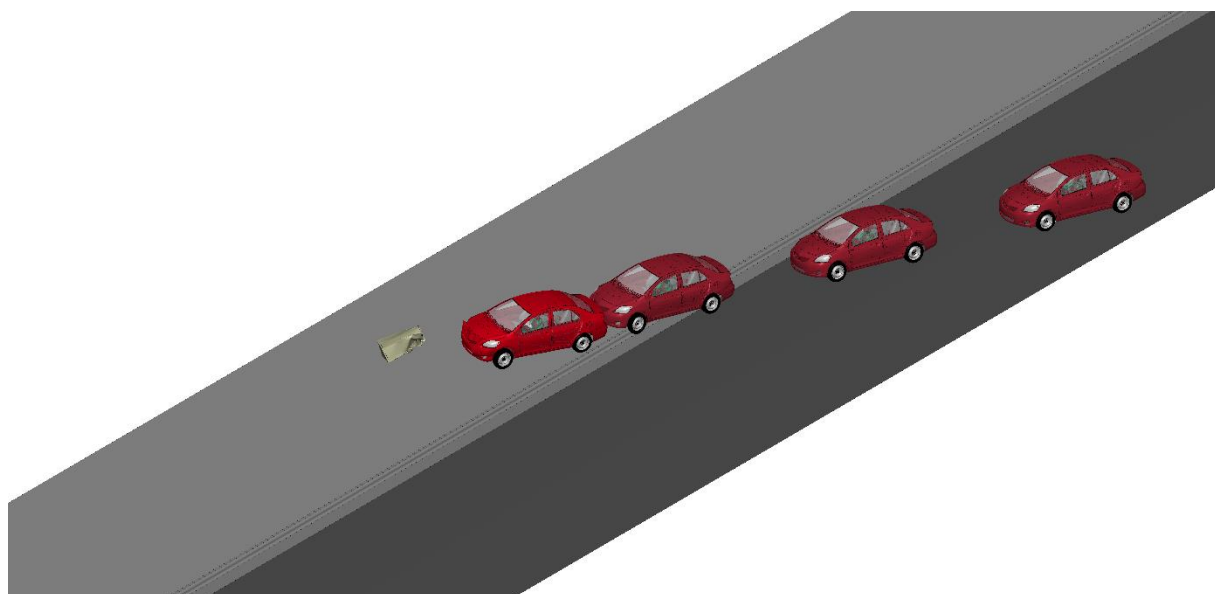


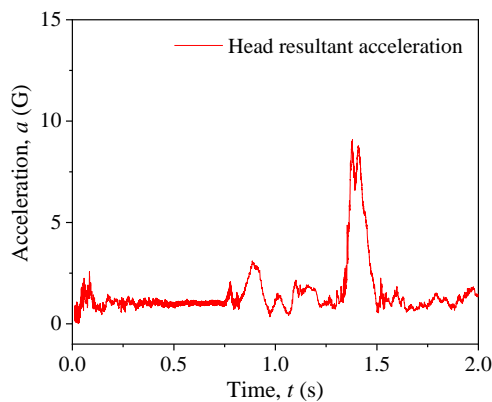
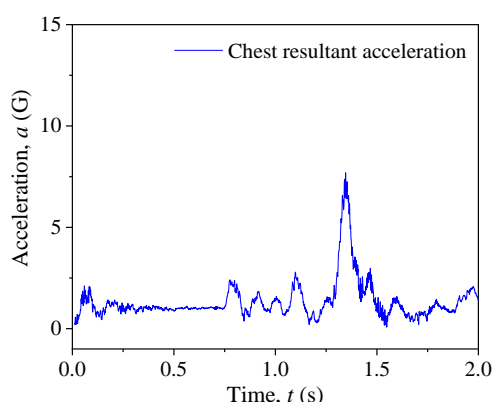
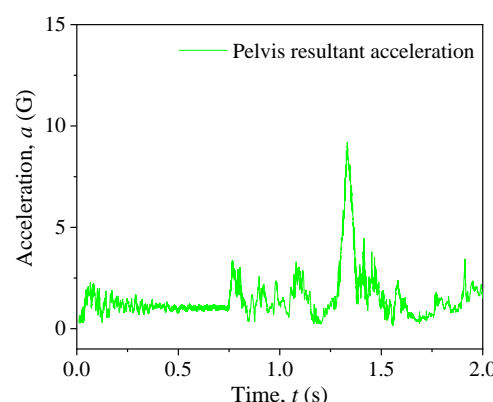
Figure 4.44 Vehicle trajectory during impact for Category 3 – Case 6.

Table 4.43 Vehicular responses, OIVs, and ORAs for Category 3 – Case 6.

Parameter	OIV (m/s)		ORA (G)		Vehicular Response	
	Longitudinal	Lateral	Longitudinal	Lateral	Roll angle	Pitch angle
Simulation Result	1.87	0.52	5.52	3.78	7.74°	7.34°
MASH Limit	12.2	12.2	20.49	20.49	75°	75°
Pass/Fail	Pass	Pass	Pass	Pass	Pass	Pass

The simulation results of Category 3 – Case 6 showed that the upper unit was detached from the pedestal upon impact and was severely damaged on the front. The upper body was pushed by the vehicle and the damage on the vehicle was minimal. The trajectory of the mailbox showed that there was no possibility for it to hit the windshield of vehicle, eliminating the possibility of compartment intrusions. The vehicle's roll and pitch angles, as well as the OIVs and ORAs in both longitudinal and lateral directions, were all within the MASH allowed limits. During impact, the dummy's head moved forward hit the deployed airbag. The maximum head acceleration was approximately 9 G and the HIC<sub>15</sub> value was calculated to be 3.09, far below the threshold value of 700 and indicating no possibility of skull injury. The above analysis indicated that there was no potential occupant injury for this impact case.

Table 4.44 Dummy responses and injury parameters for Category 3 – Case 6.

Dummy head acceleration	Head impact criteria			
	Head injury parameter	Value	Threshold	Pass/Fail
	HIC <sub>15</sub>	3.09	700	Pass
	$p(\text{HIC}_{15})$	0 %	31%	Pass
Dummy chest acceleration	Dummy pelvis acceleration			
				

#### 4.3.7 Category 3 – Case 7

In this case, a 2010 Toyota Yaris crashed into a dual-unit Type IV cluster mailbox on a road behind the curb at 31 mph (50 km/h) and with 25° impact angle at the corner. Figure 4.45 shows the full simulation model before impact and the deformed vehicle model after impact. Figure 4.46 shows the overlapping contour plot of vehicle trajectory for this case. The vehicle's roll and pitch angles, OIVs, and ORAs were calculated and summarized in Table 4.45. Table 4.46 gives the acceleration histories of the crash test dummy on the head, chest, and pelvis. The HIC<sub>15</sub> and the probability of skull injury were also calculated for this case, as given in Table 4.46.

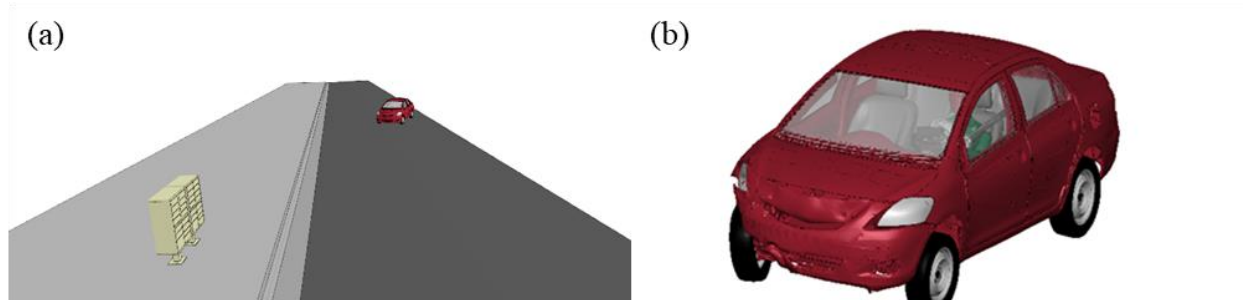


Figure 4.45 The full simulation model (a) and deformed vehicle model after impact (b) for Category 3 – Case 7.

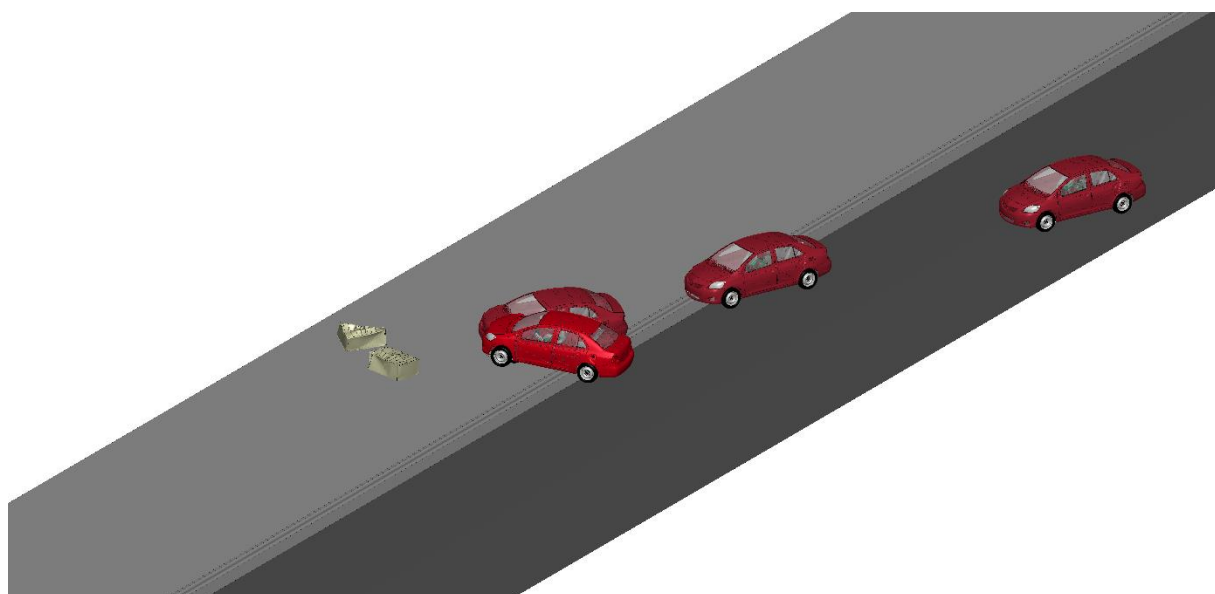


Figure 4.46 Vehicle trajectory during impact for Category 3 – Case 7.

Table 4.45 Vehicular responses, OIVs, and ORAs for Category 3 – Case 7.

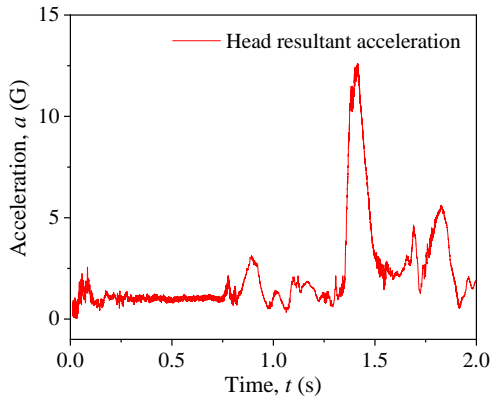
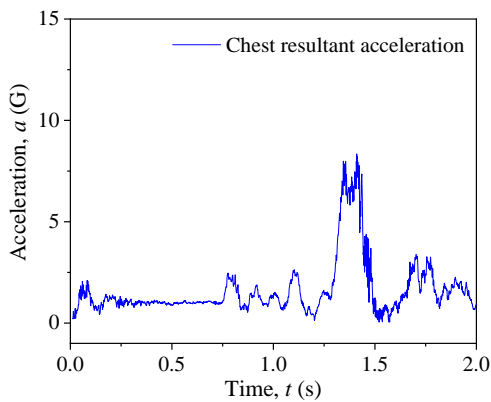
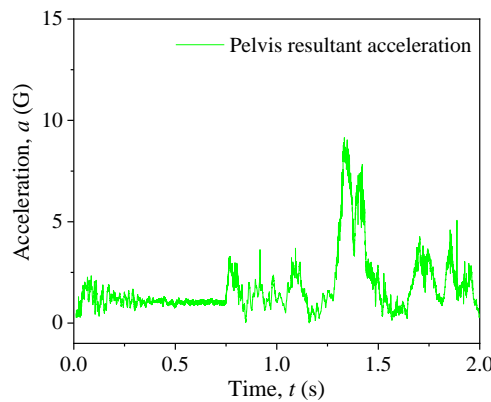
Parameter	OIV (m/s)		ORA (G)		Vehicular Response	
	Longitudinal	Lateral	Longitudinal	Lateral	Roll angle	Pitch angle
Simulation Result	1.81	0.85	7.74	5.20	6.19°	7.57°
MASH Limit	12.2	12.2	20.49	20.49	75°	75°
Pass/Fail	Pass	Pass	Pass	Pass	Pass	Pass

The simulation results of Category 3 – Case 7 showed that the upper body of the unit impacted first was separated from the pedestal instantly upon impact, followed by the detachment of the upper body of the second unit from the pedestal. The pedestal of the second mailbox unit, which was still fastened tightly to the ground, stuck on the chassis of the vehicle and caused the vehicle to spin. Consequently, the mailbox units were not pushed further and there was no possibility of penetrating the occupant compartment. The vehicle's roll and pitch angles, as well as the OIVs and ORAs in both longitudinal and lateral directions, were all within the MASH allowed limits. During impact, the dummy's head moved forward and hit the deployed airbag. The maximum head acceleration was approximately 12.5 G and the HIC<sub>15</sub> value was calculated to be 7.88, far below



the threshold value of 700 and indicating no possibility of skull injury. The above analysis indicated that there was no potential occupant injury for this impact case.

Table 4.46 Dummy responses and injury parameters for Category 3 – Case 7.

Dummy head acceleration		Head impact criteria		
	Head injury parameter	Value	Threshold	Pass/Fail
	$HIC_{15}$	7.88	700	Pass
	$p(HIC_{15})$	0 %	31%	Pass
Dummy chest acceleration		Dummy pelvis acceleration		
				

#### 4.3.8 Category 3 – Case 8

In this case, a 2010 Toyota Yaris crashed into a dual-unit Type IV cluster mailbox on a road behind the curb at 31 mph (50 km/h) and with 25° impact angle at the mid-point. Figure 4.47 shows the full simulation model before impact and the deformed vehicle model after impact. Figure 4.48 shows the overlapping contour plot of vehicle trajectory for this case. The vehicle's roll and pitch angles, OIVs, and ORAs were calculated and summarized in Table 4.47. Table 4.48 gives the acceleration histories of the crash test dummy on the head, chest, and pelvis. The  $HIC_{15}$  and the probability of skull injury were also calculated for this case, as given in Table 4.48.

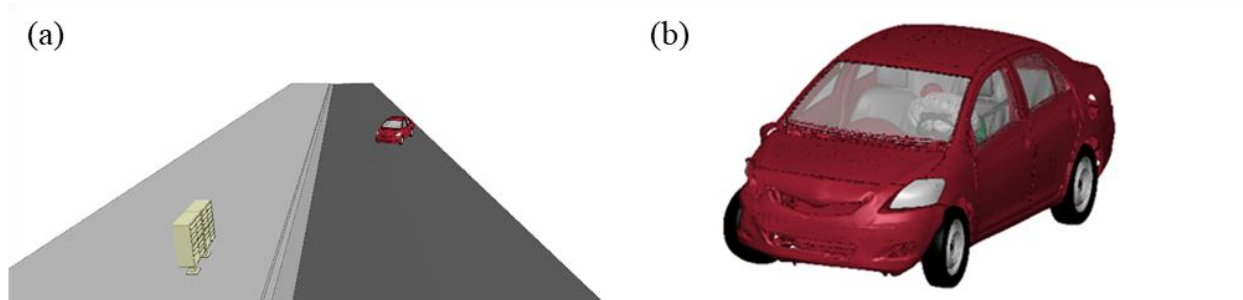


Figure 4.47 The full simulation model (a) and deformed vehicle model after impact (b) for Category 3 – Case 8.

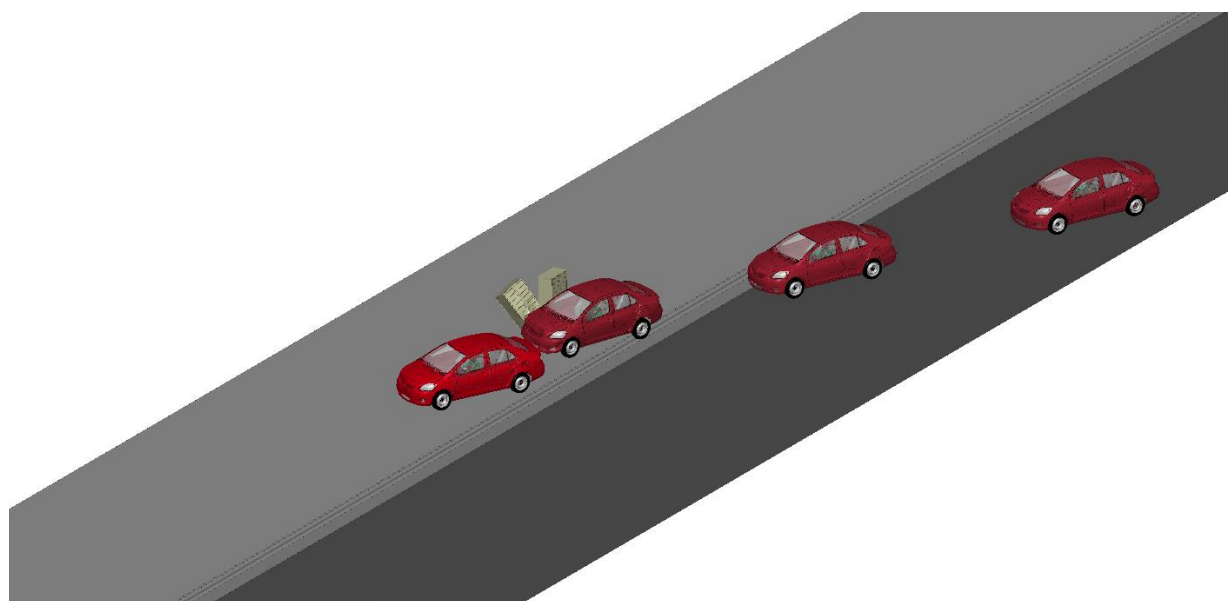


Figure 4.48 Vehicle trajectory during impact for Category 3 – Case 8.

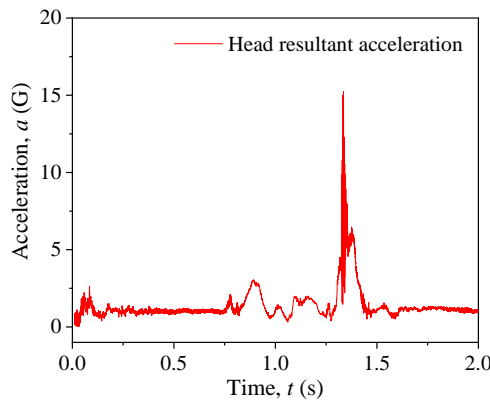
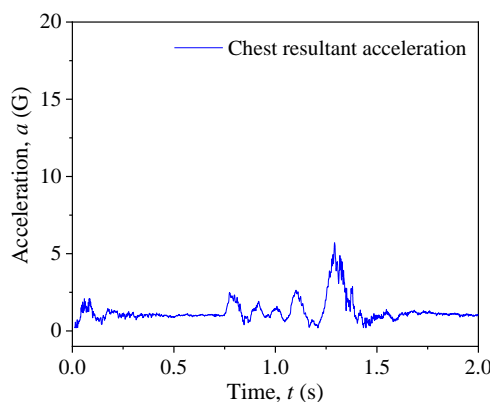
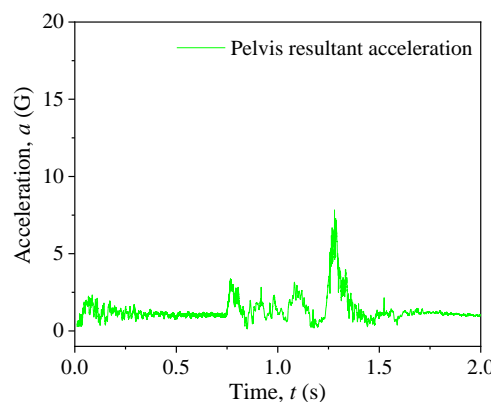
Table 4.47 Vehicular responses, OIVs, and ORAs for Category 3 – Case 8.

Parameter	OIV (m/s)		ORA (G)		Vehicular Response	
	Longitudinal	Lateral	Longitudinal	Lateral	Roll angle	Pitch angle
Simulation Result	1.68	0.86	4.41	2.28	4.41°	1.80°
MASH Limit	12.2	12.2	20.49	20.49	75°	75°
Pass/Fail	Pass	Pass	Pass	Pass	Pass	Pass

The simulation results of Category 3 – Case 8 showed that the mailbox unit being impacted first was mostly intact, while the second mailbox unit was pushed leaning backwards with no failure on the connections with the pedestal and to the ground. The damage on the vehicle was minimal and localized on the front right corner. The trajectory of the mailbox showed no possibility of hit the windshield of vehicle and thus no possibility of penetrating the occupant compartment. The vehicle's roll and pitch angles, as well as the OIVs and ORAs in both longitudinal and lateral directions, were all within the MASH allowed limits. For occupant response, the dummy's head moved forward and hit the deployed airbag. The maximum head acceleration was approximately 15 G and the HIC<sub>15</sub> value was calculated to be 2.68, far below the threshold value of 700 and indicating no possibility of skull injury. The above analysis indicated that there was no potential

occupant injury for this impact case. The above analysis indicated that there was no potential occupant injury for this impact case.

Table 4.48 Dummy responses and injury parameters for Category 3 – Case 8.

Dummy head acceleration		Head impact criteria			
	Head injury parameter	Value	Threshold	Pass/Fail	
	HIC <sub>15</sub>	2.68	700	Pass	
	$p(\text{HIC}_{15})$	0 %	31%	Pass	
Dummy chest acceleration		Dummy pelvis acceleration			
					

#### 4.4 Simulations Results of Category 4

In Category 4, the occupant risk was evaluated under vehicular crashes of a 2270P pickup truck (i.e., a 2006 Ford F250) into Type IV cluster mailboxes at an impact speed of 31 mph (50 km/h). The eight simulation cases in Category 4 are summarized as follows.

- Case 1: A single-unit Type IV cluster mailbox with 0° impact angle;
- Case 2: A single-unit Type IV cluster mailbox on a flat road with 25° impact angle;
- Case 3: A dual-unit Type IV cluster mailbox with 0° impact angle;
- Case 4: A dual-unit Type IV cluster mailbox on a flat road with 25° impact angle and impacted at the corner;
- Case 5: A dual-unit Type IV cluster mailbox on a flat road with 25° impact angle and impacted at the mid-point;
- Case 6: A single-unit Type IV cluster mailbox behind a curb with 25° impact angle;
- Case 7: A dual-unit Type IV cluster mailbox behind a curb with 25° impact angle and impacted at the corner; and
- Case 8: A dual-unit Type IV cluster mailbox behind a curb with 25° impact angle and

impacted at the mid-point.

#### 4.4.1 Category 4 – Case 1

In this case, a 2006 Ford F250 crashed into a single-unit Type IV cluster mailbox on a flat road at 31 mph (50 km/h) and with 0° impact angle. Figure 4.49 shows the full simulation model before impact and the deformed vehicle model after impact. Figure 4.50 shows the overlapping contour plot of vehicle trajectory for this case. The vehicle's roll and pitch angles, OIVs, and ORAs were calculated and summarized in Table 4.49. Table 4.50 gives the acceleration histories of the crash test dummy on the head, chest, and pelvis. The  $HIC_{15}$  and the probability of skull injury were also calculated for this case, as given in Table 4.50.

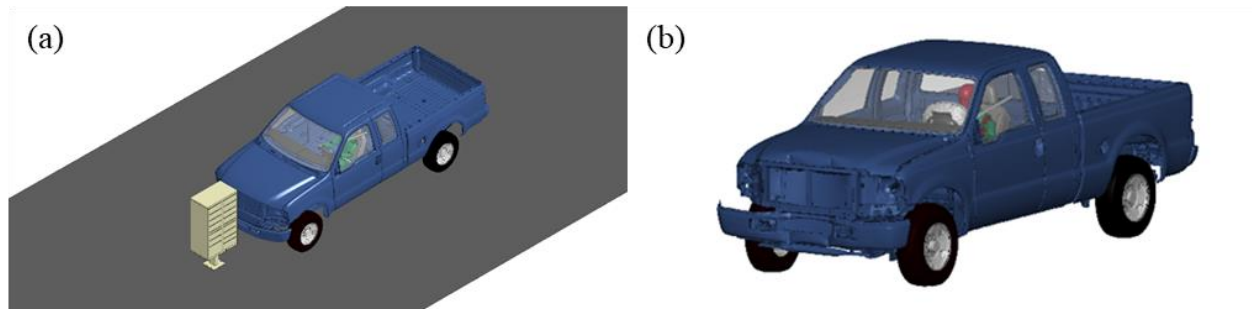


Figure 4.49 The full simulation model (a) and deformed vehicle model after impact (b) for Category 4 – Case 1.

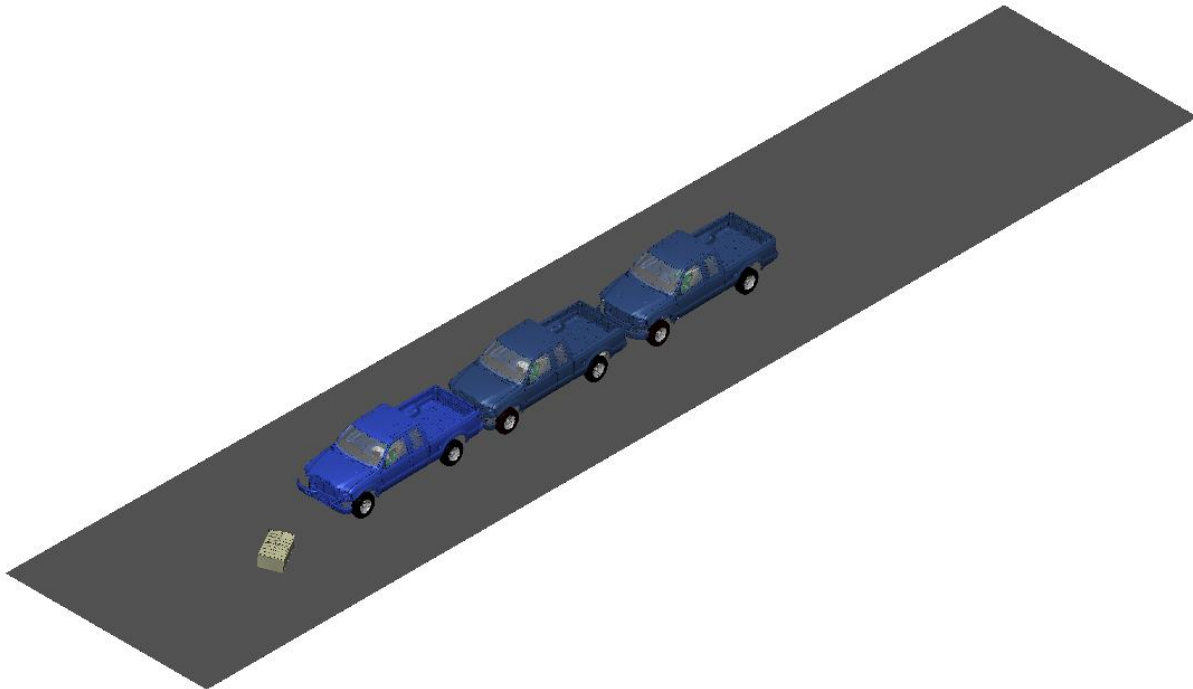
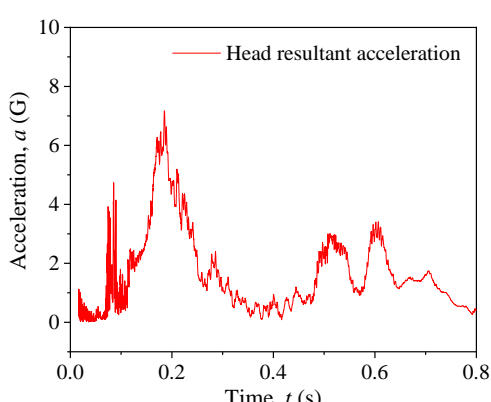
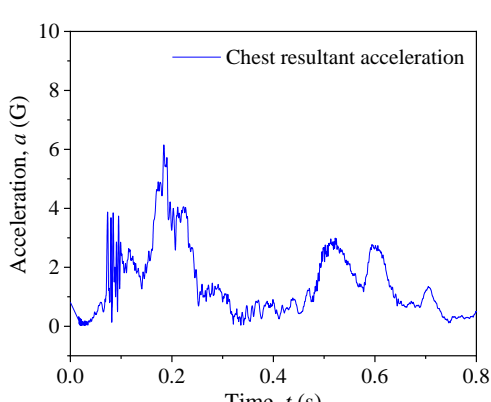
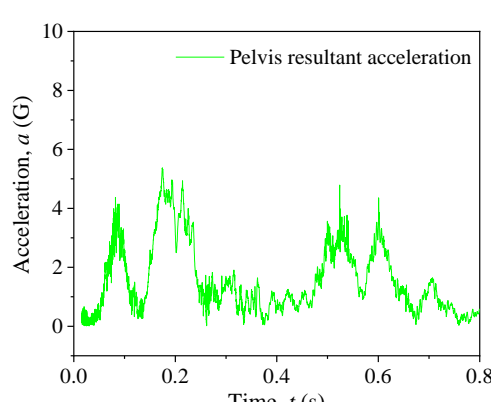


Figure 4.50 Vehicle trajectory during impact for Category 4 – Case 1.

Table 4.49 Vehicular responses, OIVs, and ORAs for Category 4 – Case 1.

Parameter	OIV (m/s)		ORA (G)		Vehicular Response	
	Longitudinal	Lateral	Longitudinal	Lateral	Roll angle	Pitch angle
Simulation Result	1.63	0.04	2.46	0.69	1.16°	0.52°
MASH Limit	12.2	12.2	20.49	20.49	75°	75°
Pass/Fail	Pass	Pass	Pass	Pass	Pass	Pass

Table 4.50 Dummy responses and injury parameters for Category 4 – Case 1.

Dummy head acceleration		Head impact criteria			
		Head injury parameter	Value	Threshold	Pass/Fail
		HIC <sub>15</sub>	1.44	700	Pass
		<i>p</i> (HIC <sub>15</sub> )	0 %	31%	Pass
Dummy chest acceleration		Dummy pelvis acceleration			
					

The simulation results of Category 4 – Case 1 showed that the upper unit of the mailbox was detached from the pedestal instantly upon impact and pushed forward by the vehicle in its travel direction. The damage on the vehicle was minimal, a shallow flat dent on the front. The trajectory of the mailbox showed no possibility of hitting the windshield of vehicle and thus no possibility of penetrating the occupant compartment. The vehicle's roll and pitch angles, as well as the OIVs and ORAs in both longitudinal and lateral directions, were all within the MASH allowed limits. During impact, the dummy's head moved forward but did not hit the deployed airbag. The maximum head acceleration was approximately 7 G and the HIC<sub>15</sub> value was calculated to be 1.44, far below the threshold value of 700 and indicating no possibility of skull injury. The above analysis indicated that there was no potential occupant injury for this impact case.

#### 4.4.2 Category 4 – Case 2

In this case, a 2006 Ford F250 crashed into a single-unit Type IV cluster mailbox on a flat road at 31 mph (50 km/h) and with 25° impact angle. Figure 4.51 shows the full simulation model before impact and the deformed vehicle model after impact. Figure 4.52 shows the overlapping contour plot of vehicle trajectory for this case. The vehicle's roll and pitch angles, OIVs, and ORAs were calculated and summarized in Table 4.51. Table 4.52 gives the acceleration histories of the crash test dummy on the head, chest, and pelvis. The HIC<sub>15</sub> and the probability of skull injury were also calculated for this case, as given in Table 4.52.

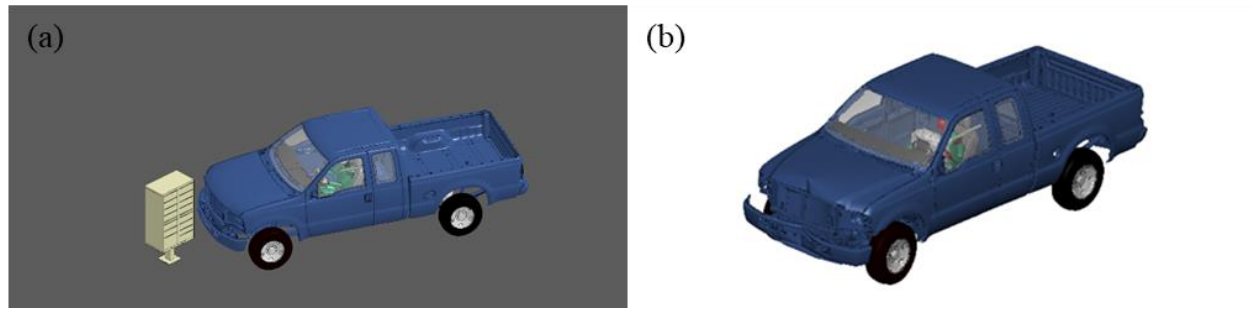


Figure 4.51 The full simulation model (a) and deformed vehicle model after impact (b) for Category 4 – Case 2.

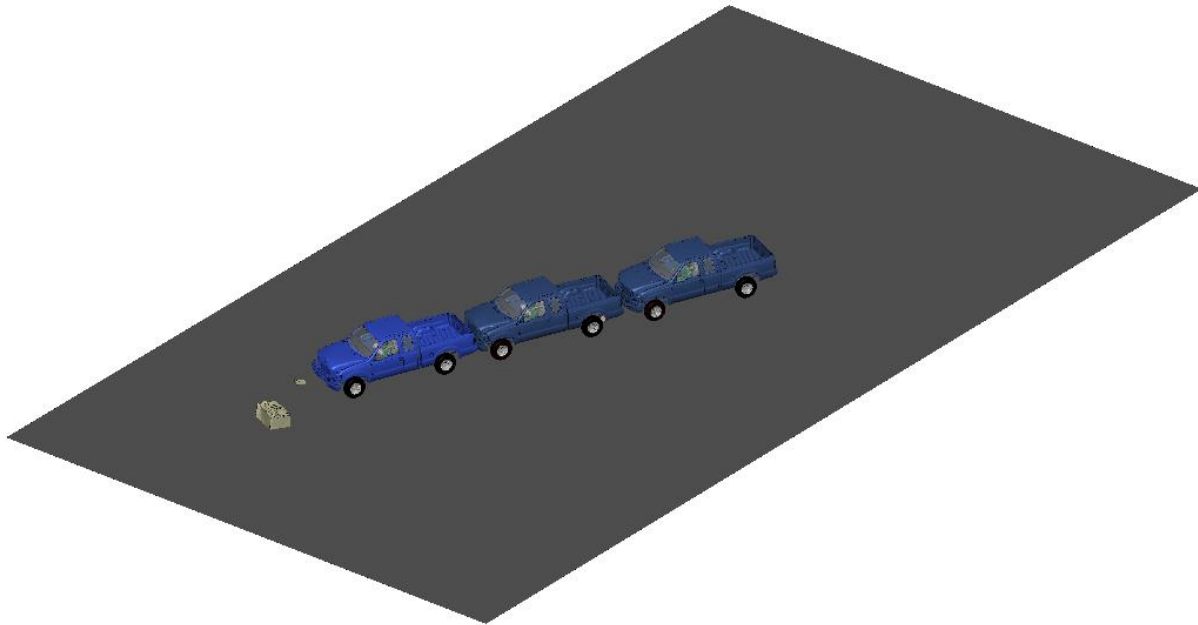
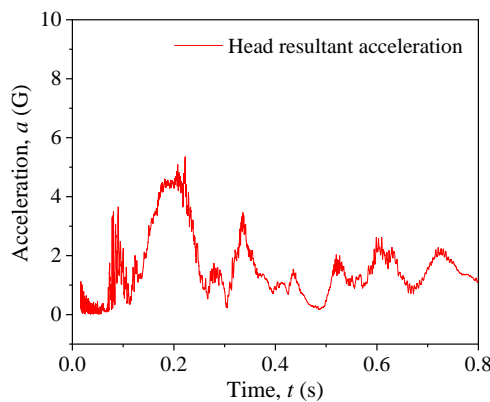
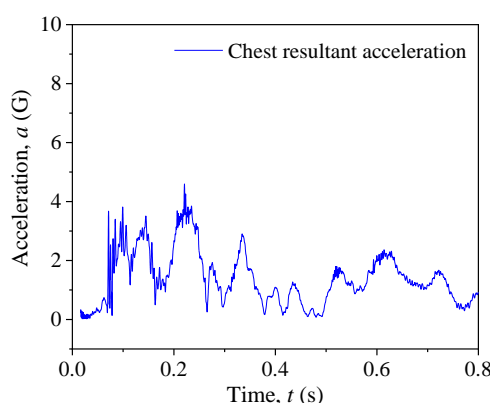
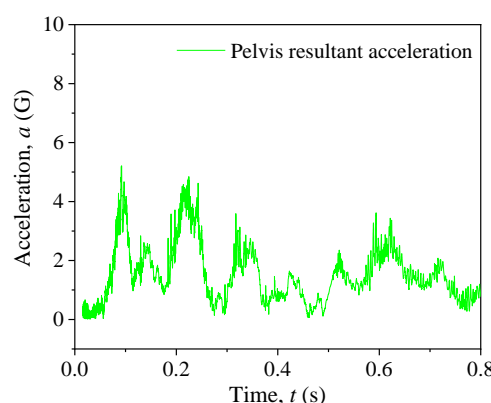


Figure 4.52 Vehicle trajectory during impact for Category 4 – Case 2.

Table 4.51 Vehicular responses, OIVs, and ORAs for Category 4 – Case 2.

Parameter	OIV (m/s)		ORA (G)		Vehicular Response	
	Longitudinal	Lateral	Longitudinal	Lateral	Roll angle	Pitch angle
Simulation Result	1.83	0.26	0.93	1.00	0.71°	0.64°
MASH Limit	12.2	12.2	20.49	20.49	75°	75°
Pass/Fail	Pass	Pass	Pass	Pass	Pass	Pass

Table 4.52 Dummy responses and injury parameters for Category 4 – Case 2.

Dummy head acceleration	Head impact criteria			
	Head injury parameter	Value	Threshold	Pass/Fail
	HIC <sub>15</sub>	0.66	700	Pass
	$p(\text{HIC}_{15})$	0 %	31%	Pass
Dummy chest acceleration	Dummy pelvis acceleration			
				

The simulation results of Category 4 – Case 2 showed that the upper body of the mailbox was detached from the pedestal upon impacts and pushed and forward in the vehicle’s travel direction. The mailbox was severely damage but the damage to the vehicle was minimal. The trajectory of the mailbox showed no possibility of hitting the windshield of vehicle and thus no possibility of penetrating the occupant compartment. The vehicle’s roll and pitch angles, as well as the OIVs and ORAs in both longitudinal and lateral directions, were all within the MASH allowed limits. During impact, the dummy’s head moved forward and but did not touch the deployed airbag. The maximum head acceleration was approximately 5 G and the HIC<sub>15</sub> value was calculated to be 0.66, far below the threshold value of 700 and indicating no possibility of skull injury. The above analysis indicated that there was no potential occupant injury for this impact case.

#### 4.4.3 Category 4 – Case 3

In this case, a 2006 Ford F250 crashed into a dual-unit Type IV cluster mailbox on a flat road at 31 mph (50 km/h) and with 0° impact angle. Figure 4.53 shows the full simulation model before impact and the deformed vehicle model after impact. Figure 4.54 shows the overlapping contour plot of vehicle trajectory for this case. The vehicle’s roll and pitch angles, OIVs, and ORAs were calculated and summarized in Table 4.53. Table 4.54 gives the acceleration histories of the crash

test dummy on the head, chest, and pelvis. The  $HIC_{15}$  and the probability of skull injury were also calculated for this case, as given in Table 4.54.

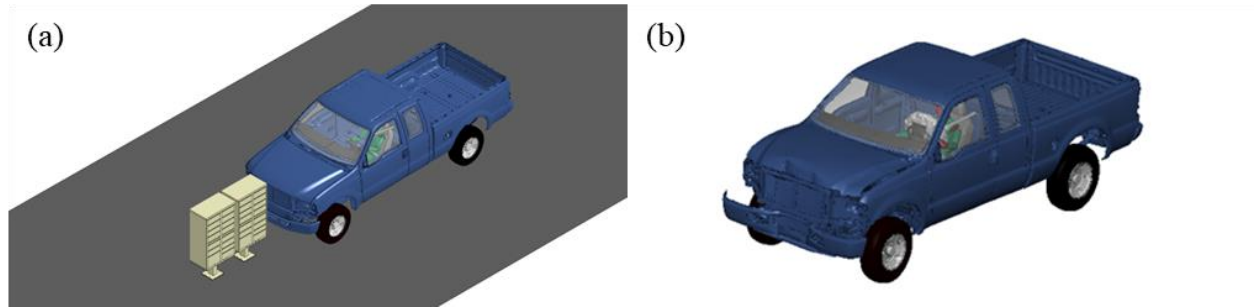


Figure 4.53 The full simulation model (a) and deformed vehicle model after impact (b) for Category 4 – Case 3.

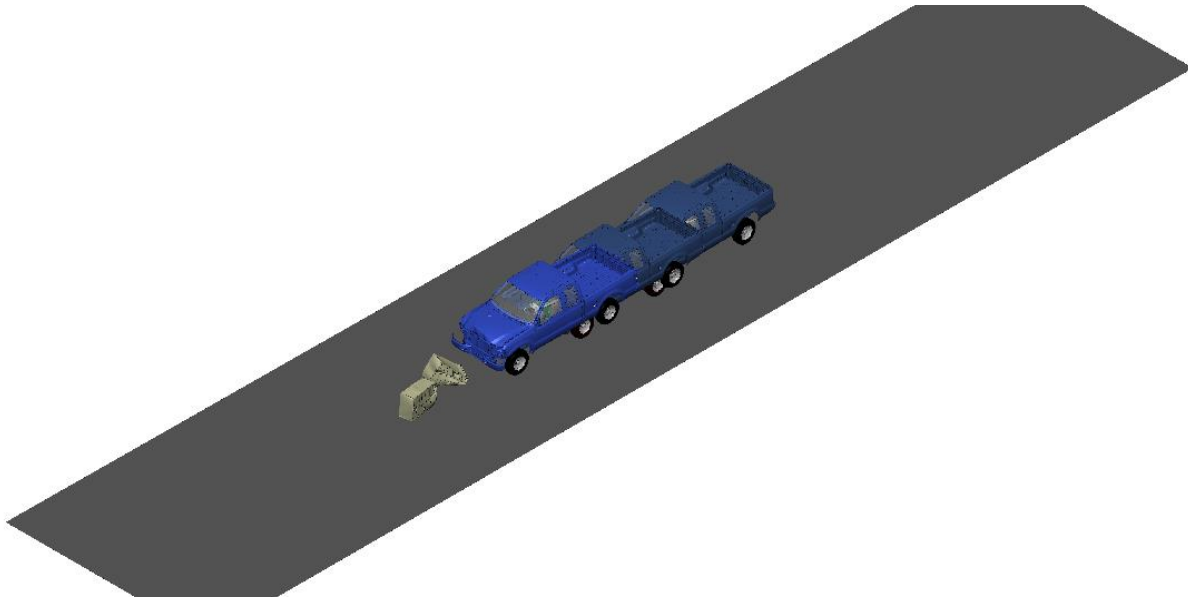


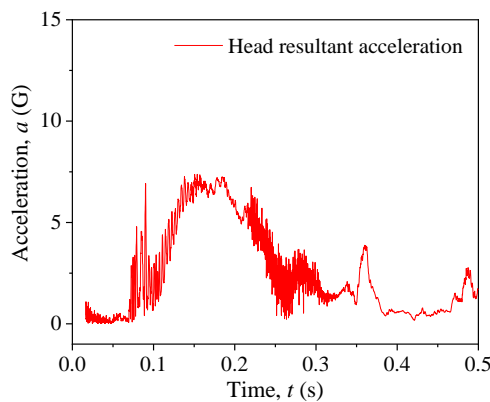
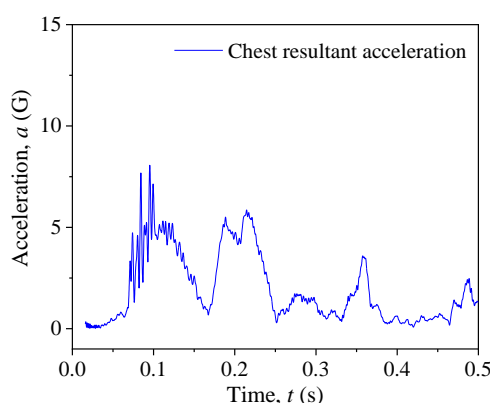
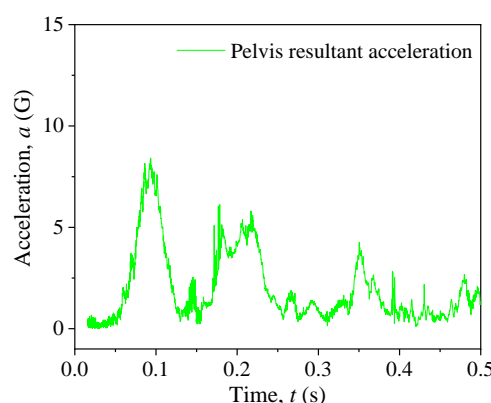
Figure 4.54 Vehicle trajectory during impact for Category 4 – Case 3.

Table 4.53 Vehicular responses, OIVs, and ORAs for Category 4 – Case 3.

Parameter	OIV (m/s)		ORA (G)		Vehicular Response	
	Longitudinal	Lateral	Longitudinal	Lateral	Roll angle	Pitch angle
Simulation Result	3.12	0.02	2.28	2.04	1.01°	0.73°
MASH Limit	12.2	12.2	20.49	20.49	75°	75°
Pass/Fail	Pass	Pass	Pass	Pass	Pass	Pass



Table 4.54 Dummy responses and injury parameters for Category 4 – Case 3.

Dummy head acceleration		Head impact criteria			
	Head injury parameter	Value	Threshold	Pass/Fail	
	HIC <sub>15</sub>	1.95	700	Pass	
	$p(\text{HIC}_{15})$	0 %	31%	Pass	
Dummy chest acceleration		Dummy pelvis acceleration			
					

The simulation results of Category 4 – Case 3 showed that both pedestals were detached from the upper bodies upon impact and were pushed forward in the vehicle’s travel direction, with the unit impacted first having larger damage than the second unit. The damage on the vehicle was shown as a shallow dent on the front. The trajectory of the mailbox showed no possibility of hitting the windshield of vehicle and thus no possibility of penetrating the occupant compartment. The vehicle’s roll and pitch angles, as well as the OIVs and ORAs in both longitudinal and lateral directions, were all within the MASH allowed limits. During impact, the dummy’s head moved forward and hit the deployed airbag. The maximum head acceleration was approximately 7 G and the HIC<sub>15</sub> value was calculated to be 1.95, far below the threshold value of 700 and indicating no possibility of skull injury. The above analysis indicated that there was no potential occupant injury for this impact case.

#### 4.4.4 Category 4 – Case 4

In this case, a 2006 Ford F250 crashed into a dual-unit Type IV cluster mailbox on a flat road at 31 mph (50 km/h) and with 25° impact angle at the corner. Figure 4.55 shows the full simulation model before impact and the deformed vehicle model after impact. Figure 4.56 shows the overlapping contour plot of vehicle trajectory for this case. The vehicle’s roll and pitch angles, OIVs, and ORAs were calculated and summarized in Table 4.55. Table 4.56 gives the acceleration

histories of the crash test dummy on the head, chest, and pelvis. The  $HIC_{15}$  and the probability of skull injury were also calculated for this case, as given in Table 4.56.

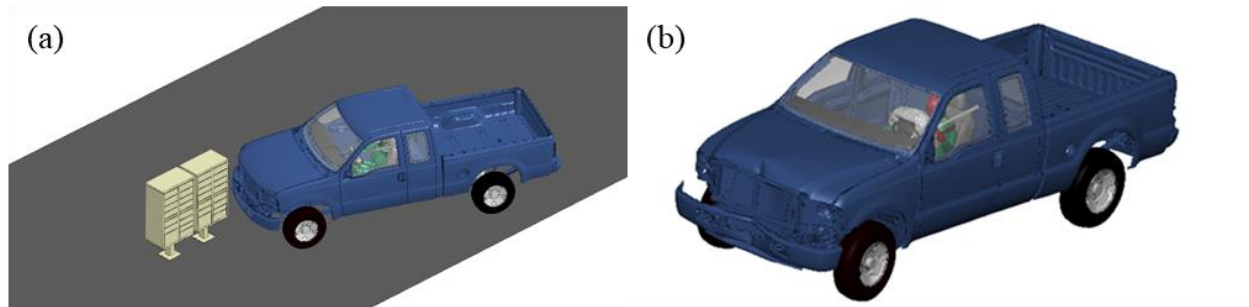


Figure 4.55 The full simulation model (a) and deformed vehicle model after impact (b) for Category 4 – Case 4.

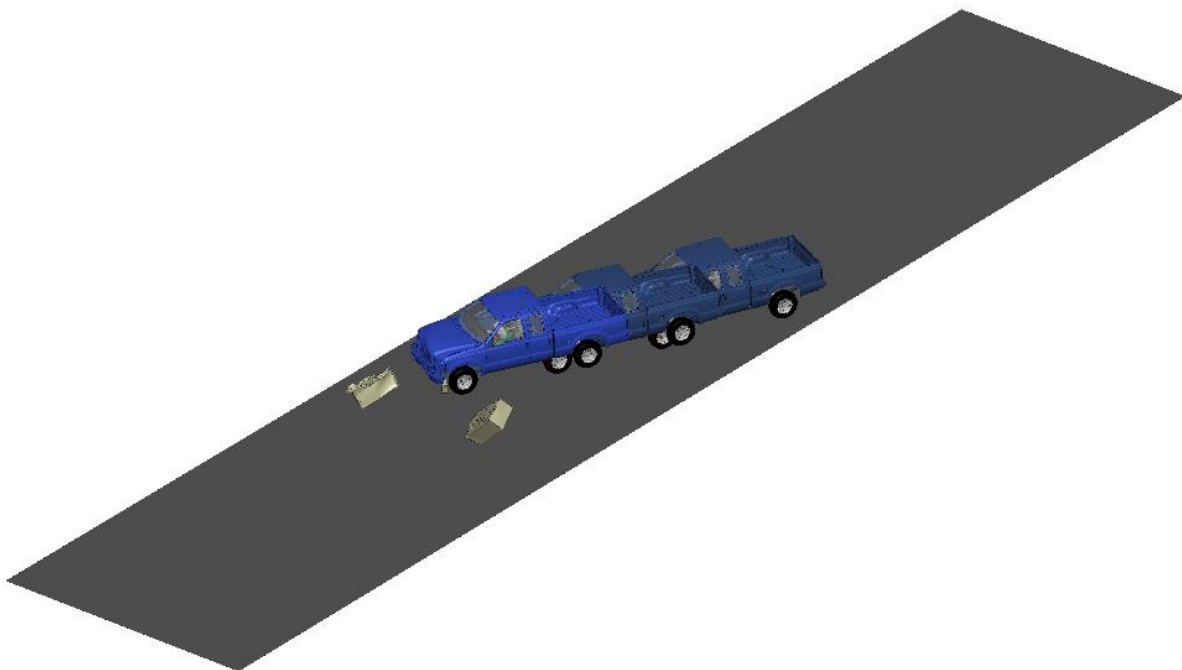
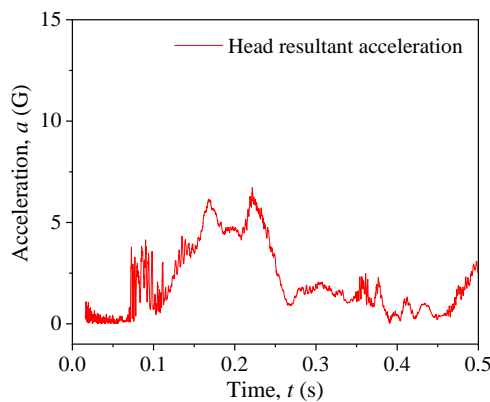
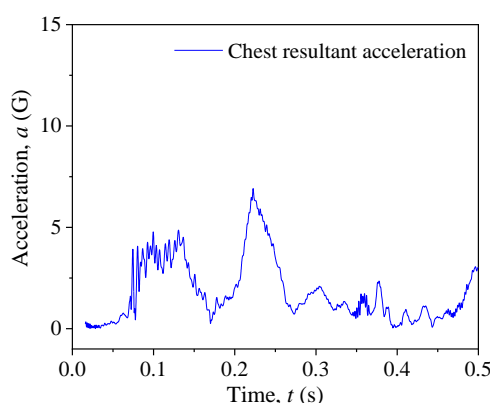
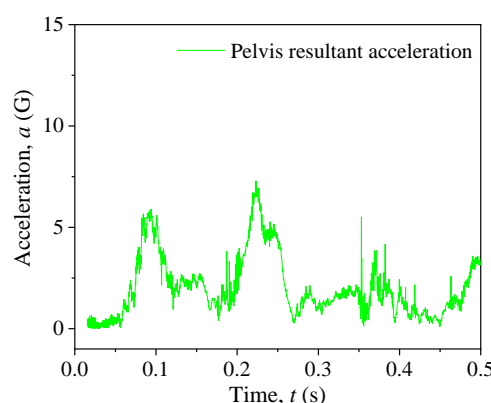


Figure 4.56 Vehicle trajectory during impact for Category 4 – Case 4.

Table 4.55 Vehicular responses, OIVs, and ORAs for Category 4 – Case 4.

Parameter	OIV (m/s)		ORA (G)		Vehicular Response	
	Longitudinal	Lateral	Longitudinal	Lateral	Roll angle	Pitch angle
Simulation Result	2.81	0.19	4.10	3.54	1.22°	0.57°
MASH Limit	12.2	12.2	20.49	20.49	75°	75°
Pass/Fail	Pass	Pass	Pass	Pass	Pass	Pass

Table 4.56 Dummy responses and injury parameters for Category 4 – Case 4.

Dummy head acceleration		Head impact criteria			
	Head injury parameter	Value	Threshold	Pass/Fail	
	HIC <sub>15</sub>	1.27	700	Pass	
	$p(\text{HIC}_{15})$	0 %	31%	Pass	
Dummy chest acceleration		Dummy pelvis acceleration			
					

The simulation results of Category 4 – Case 4 showed that the upper body of the mailbox unit impacted first was detached from the pedestal upon impact and was severely crushed by the vehicle before the upper body of the second unit was knocked off the pedestal. The upper body of the first unit was pushed forward in the vehicle's travel direction and the upper body of the second unit was pushed to the drive side of the vehicle due to rotation. The damage on the vehicle was a shallow V-shape dent on the front. The trajectory of the mailbox showed no possibility of hitting the windshield of vehicle and thus no possibility of penetrating the occupant compartment. The vehicle's roll and pitch angles, as well as the OIVs and ORAs in both longitudinal and lateral directions, were all within the MASH allowed limits. During impact, the dummy's head moved forward but did not touch the deployed airbag. The maximum head acceleration was approximately 6 G and the HIC<sub>15</sub> value was calculated to be 1.27, far below the threshold value of 700 and indicating no possibility of skull injury. The above analysis indicated that there was no potential occupant injury for this impact case.

#### 4.4.5 Category 4 – Case 5

In this case, a 2006 Ford F250 crashed into a dual-unit Type IV cluster mailbox on a flat road at 31 mph (50 km/h) and with 25° impact angle at the mid-point. Figure 4.57 shows the full simulation model before impact and the deformed vehicle model after impact. Figure 4.58 shows

the overlapping contour plot of vehicle trajectory for this case. The vehicle's roll and pitch angles, OIVs, and ORAs were calculated and summarized in Table 4.57. Table 4.58 gives the acceleration histories of the crash test dummy on the head, chest, and pelvis. The HIC<sub>15</sub> and the probability of skull injury were also calculated for this case, as given in Table 4.58.

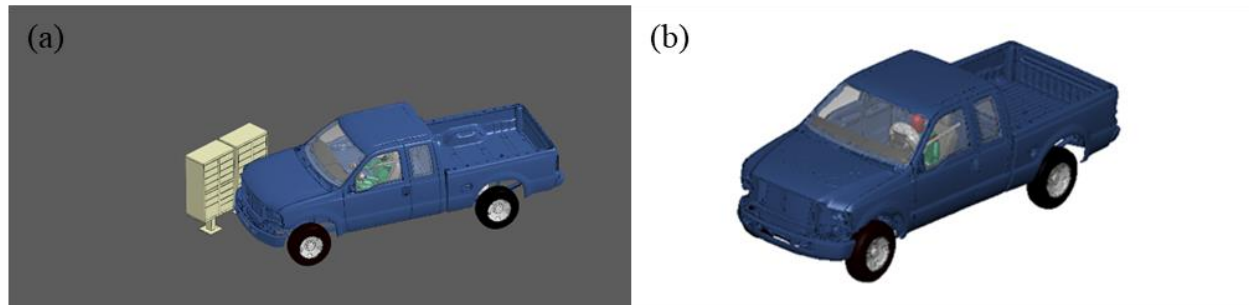


Figure 4.57 The full simulation model (a) and deformed vehicle model after impact (b) for Category 4 – Case 5.

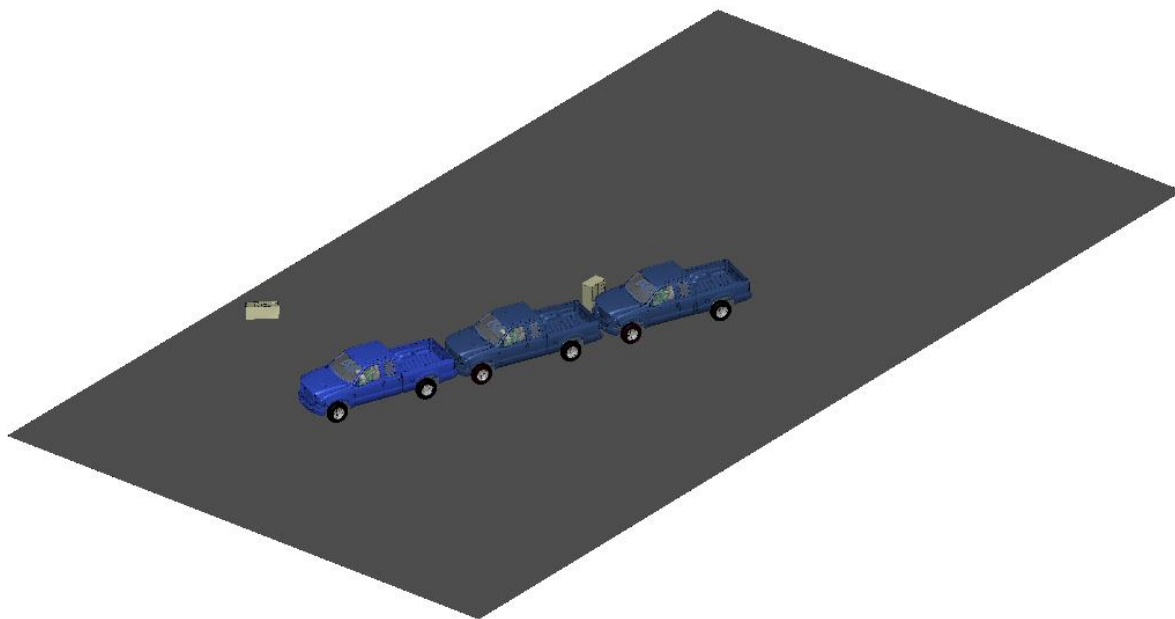


Figure 4.58 Vehicle trajectory during impact for Category 4 – Case 5.

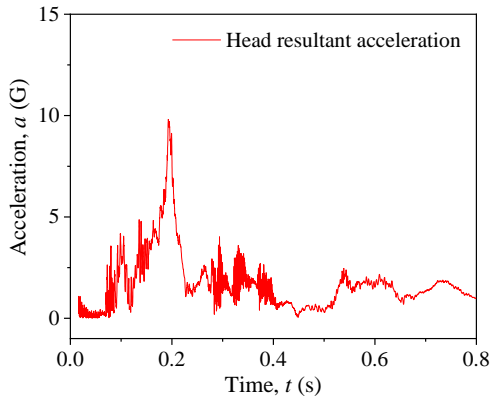
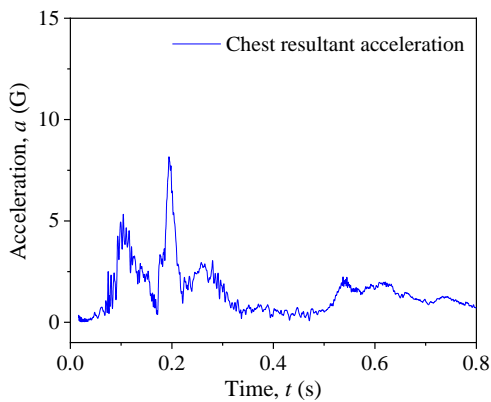
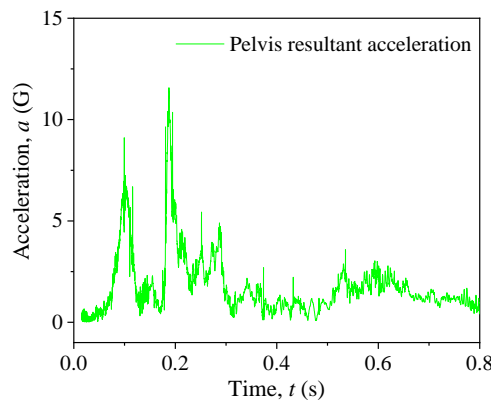
Table 4.57 Vehicular responses, OIVs, and ORAs for Category 4 – Case 5.

Parameter	OIV (m/s)		ORA (G)		Vehicular Response	
	Longitudinal	Lateral	Longitudinal	Lateral	Roll angle	Pitch angle
Simulation Result	1.74	0.46	1.44	0.96	1.17°	0.66°
MASH Limit	12.2	12.2	20.49	20.49	75°	75°
Pass/Fail	Pass	Pass	Pass	Pass	Pass	Pass

The simulation results of Category 4 – Case 5 showed that the mailbox unit impacted first remained almost intact except for slight contacts with the vehicle. The upper body of the second mailbox was detached from the pedestal and was pushed to the front-right of the vehicle's travel direction. The vehicle did not exhibit visible damage. The trajectory of the mailbox showed no possibility of

hitting the windshield of vehicle and thus no possibility of penetrating the occupant compartment. The vehicle's roll and pitch angles, as well as the OIVs and ORAs in both longitudinal and lateral directions, were all within the MASH allowed limits. During impact, the dummy's head moved forward but did not touch the deployed airbag. The  $HIC_{15}$  value was calculated to be 2.89, far below the threshold value of 700 and indicating no possibility of skull injury. The above analysis indicated that there was no potential occupant injury for this impact case.

Table 4.58 Dummy responses and injury parameters for Category 4 – Case 5.

Dummy head acceleration		Head impact criteria			
		Head injury parameter	Value	Threshold	Pass/Fail
		$HIC_{15}$	2.89	700	Pass
		$p(HIC_{15})$	0 %	31%	Pass
Dummy chest acceleration		Dummy pelvis acceleration			
					

#### 4.4.6 Category 4 – Case 6

In this case, a 2006 Ford F250 crashed into a single-unit Type IV cluster mailbox on a road behind the curb at 31 mph (50 km/h) and with 25° impact angle. Figure 4.59 shows the full simulation model before impact and the deformed vehicle model after impact. Figure 4.60 shows the overlapping contour plot of vehicle trajectory for this case. The vehicle's roll and pitch angles, OIVs, and ORAs were calculated and summarized in Table 4.59. Table 4.60 gives the acceleration histories of the crash test dummy on the head, chest, and pelvis. The  $HIC_{15}$  and the probability of skull injury were also calculated for this case, as given in Table 4.60.

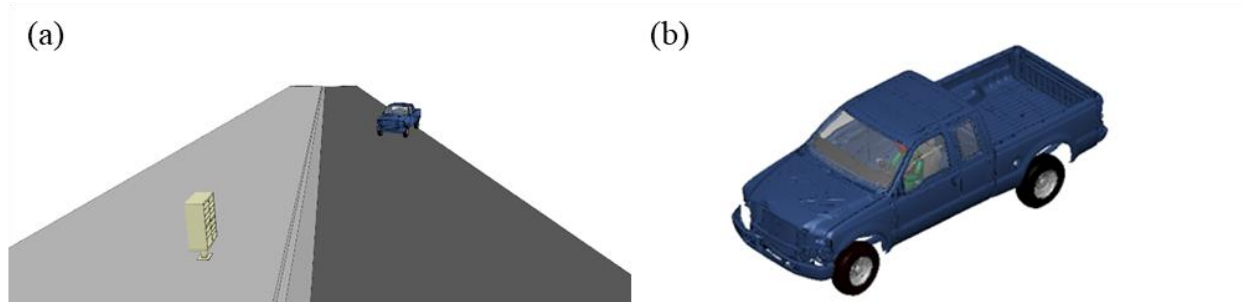


Figure 4.59 The full simulation model (a) and deformed vehicle model after impact (b) for Category 4 – Case 6.

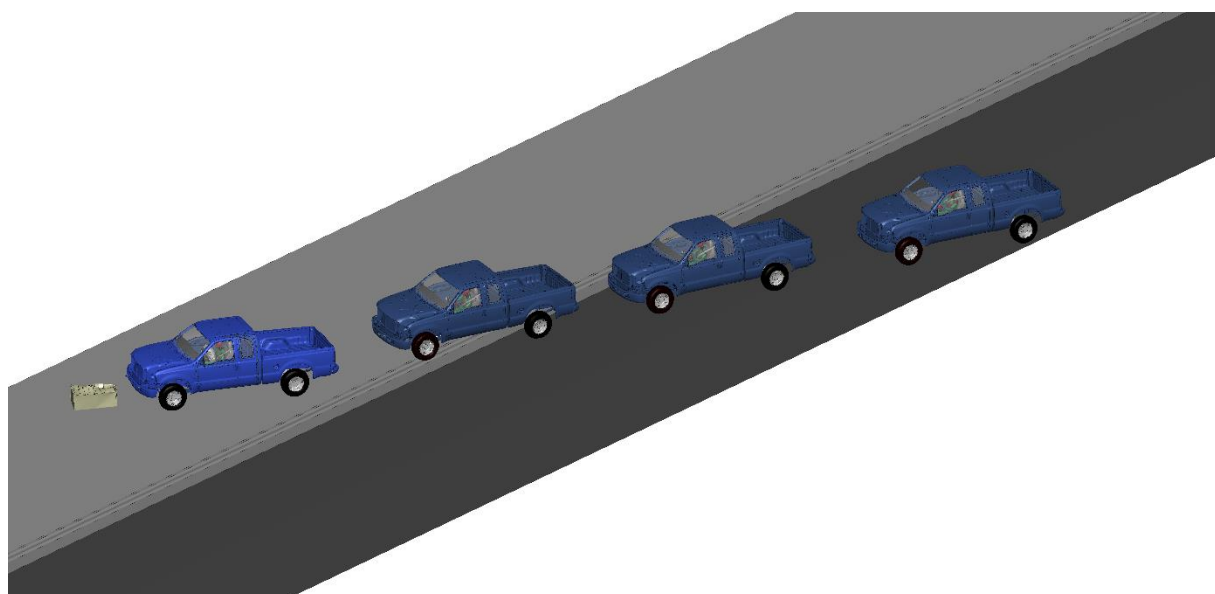


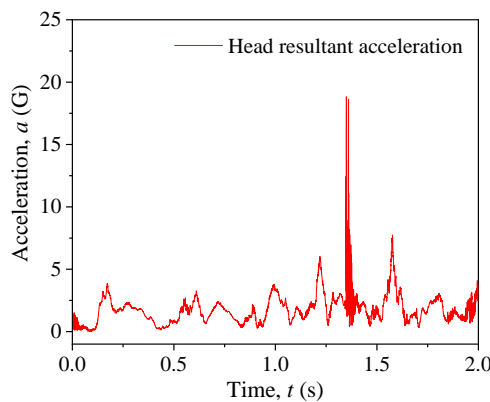
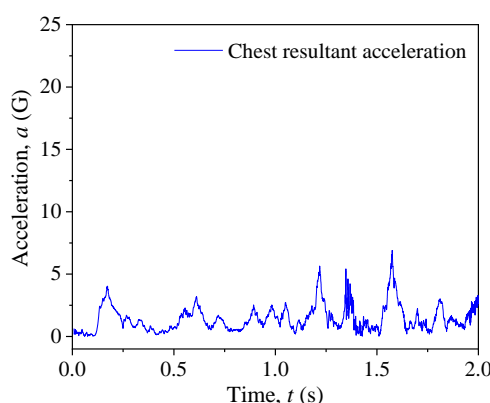
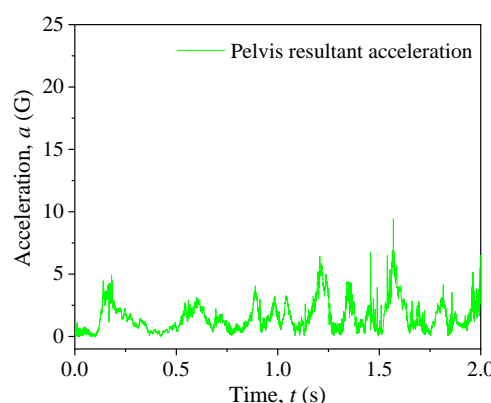
Figure 4.60 Vehicle trajectory during impact for Category 4 – Case 6.

Table 4.59 Vehicular responses, OIVs, and ORAs for Category 4 – Case 6.

Parameter	OIV (m/s)		ORA (G)		Vehicular Response	
	Longitudinal	Lateral	Longitudinal	Lateral	Roll angle	Pitch angle
Simulation Result	1.09	0.30	4.10	3.16	6.13°	2.52°
MASH Limit	12.2	12.2	20.49	20.49	75°	75°
Pass/Fail	Pass	Pass	Pass	Pass	Pass	Pass

The simulation results of Category 4 – Case 6 showed that the upper body of the mailbox was detached from the pedestal upon impact and was pushed forward in the vehicle's travel direction. There was no visible damage on the vehicle and there was no possibility for the mailbox to penetrate the occupant compartment. The vehicle's roll and pitch angles, as well as the OIVs and ORAs in both longitudinal and lateral directions, were all within the MASH allowed limits. During impact, the dummy's head moved forward but did not touch the deployed airbag. The HIC<sub>15</sub> value was calculated to be 1.53, which was far below the threshold value of 700 and indicating no possibility of skull injury. The above analysis indicated that there was no potential occupant injury for this impact case.

Table 4.60 Dummy responses and injury parameters for Category 4 – Case 6.

Dummy head acceleration		Head impact criteria			
	Head injury parameter	Value	Threshold	Pass/Fail	
	HIC <sub>15</sub>	1.53	700	Pass	
	$p(\text{HIC}_{15})$	0 %	31%	Pass	
Dummy chest acceleration		Dummy pelvis acceleration			
					

#### 4.4.7 Category 4 – Case 7

In this case, a 2006 Ford F250 crashed into a dual-unit Type IV cluster mailbox on a road behind the curb at 31 mph (50 km/h) and with 25° impact angle at the corner. Figure 4.61 shows the full simulation model before impact and the deformed vehicle model after impact. Figure 4.62 shows the overlapping contour plot of vehicle trajectory for this case. The vehicle's roll and pitch angles, OIVs, and ORAs were calculated and summarized in Table 4.61. Table 4.62 gives the acceleration histories of the crash test dummy on the head, chest, and pelvis. The HIC<sub>15</sub> and the probability of skull injury were also calculated for this case, as given in Table 4.62.

The simulation results of Category 4 – Case 7 showed that the upper bodies of both mailbox units were detached from the pedestals upon impacts and pushed forward in the vehicle's travel direction. The pedestals were then stuck under the vehicle's chassis and were detached from the ground bases. The damage to the vehicle was minimal and there was no possibility for the mailbox units to penetrate the occupant compartment. The vehicle's roll and pitch angles, as well as the OIVs and ORAs in both longitudinal and lateral directions, were all within the MASH allowed limits. During impact, the dummy's head moved forward but did not touch the deployed airbag. The HIC<sub>15</sub> value was calculated to be 2.51, far below the threshold value of 700 and indicating no possibility of skull injury. The above analysis indicated that there was no potential occupant injury

for this impact case.

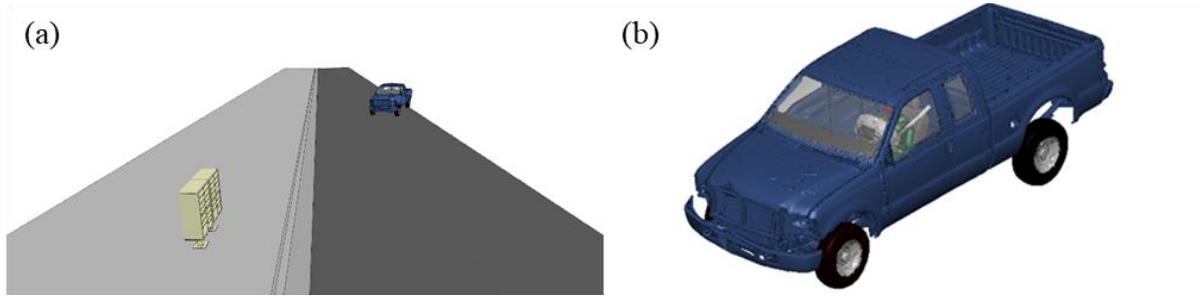


Figure 4.61 The full simulation model (a) and deformed vehicle model after impact (b) for Category 4 – Case 7.

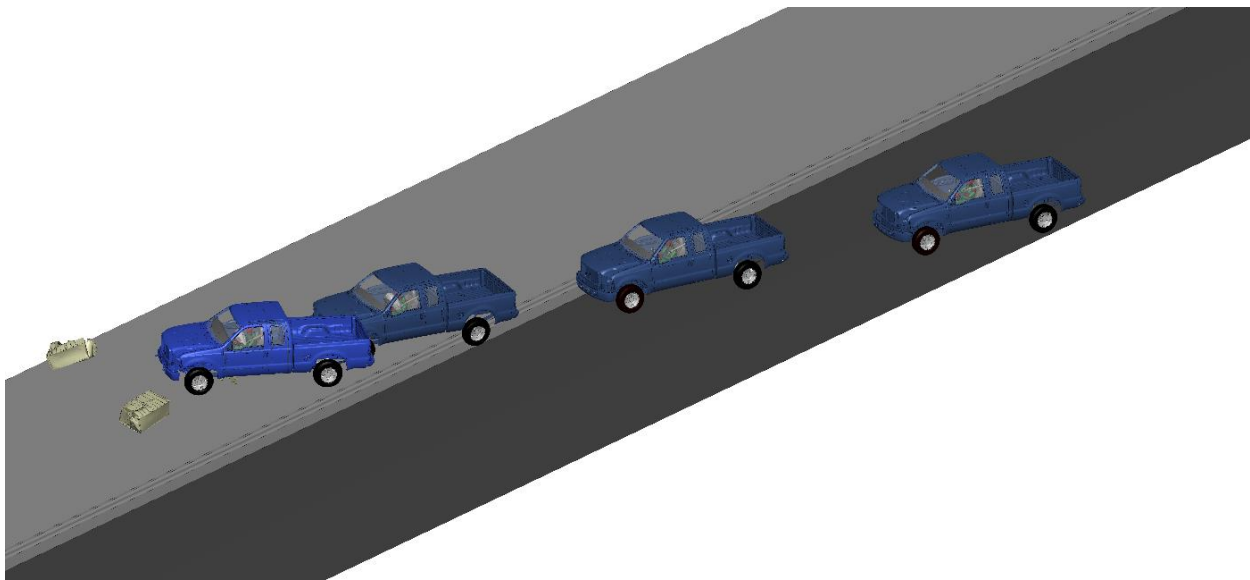


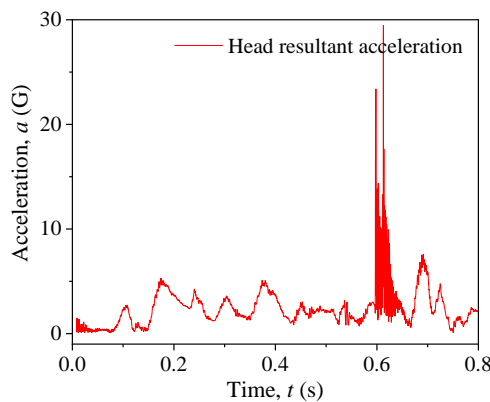
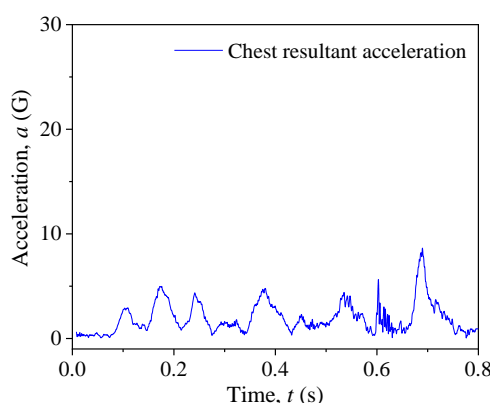
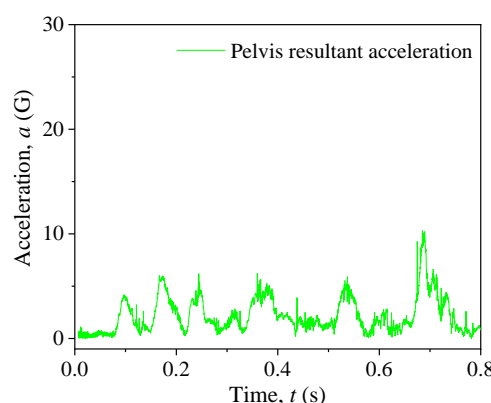
Figure 4.62 Vehicle trajectory during impact for Category 4 – Case 7.

Table 4.61 Vehicular responses, OIVs, and ORAs for Category 4 – Case 7.

Parameter	OIV (m/s)		ORA (G)		Vehicular Response	
	Longitudinal	Lateral	Longitudinal	Lateral	Roll angle	Pitch angle
Simulation Result	2.67	0.48	3.24	3.73	6.31°	2.53°
MASH Limit	12.2	12.2	20.49	20.49	75°	75°
Pass/Fail	Pass	Pass	Pass	Pass	Pass	Pass



Table 4.62 Dummy responses and injury parameters for Category 4 – Case 7.

Dummy head acceleration	Head impact criteria			
	Head injury parameter	Value	Threshold	Pass/Fail
	HIC <sub>15</sub>	2.51	700	Pass
	$p(\text{HIC}_{15})$	0 %	31%	Pass
Dummy chest acceleration	Dummy pelvis acceleration			
				

#### 4.4.8 Category 4 – Case 8

In this case, a 2006 Ford F250 crashed into a dual-unit Type IV cluster mailbox on a road behind the curb at 31 mph (50 km/h) and with 25° impact angle at the mid-point. Figure 4.63 shows the full simulation model before impact and the deformed vehicle model after impact. Figure 4.64 shows the overlapping contour plot of vehicle trajectory for this case. The vehicle's roll and pitch angles, OIVs, and ORAs were calculated and summarized in Table 4.63. Table 4.64 gives the acceleration histories of the crash test dummy on the head, chest, and pelvis. The HIC<sub>15</sub> and the probability of skull injury were also calculated for this case, as given in Table 4.64.

The simulation results of Category 4 – Case 8 showed that the mailbox unit impacted first was twisted due to slight contact with the vehicle and remained attached to the ground. The upper body of the second mailbox unit was detached from the pedestal and pushed forward in the vehicle's travel direction. The damage on the vehicle was minimal and localized on the front right corner. The trajectory of the mailbox showed that there was no possibility for it to hit the windshield of vehicle, eliminating the possibility of compartment intrusions. The vehicle's roll and pitch angles, as well as the OIVs and ORAs in both longitudinal and lateral directions, were all within the MASH allowed limits. During impact, the dummy's head moved forward and hit the deployed airbag. The HIC<sub>15</sub> value was calculated to be 5.04, far below the threshold value of 700 and

indicating no possibility of skull injury. The above analysis indicated that there was no potential occupant injury for this impact case.

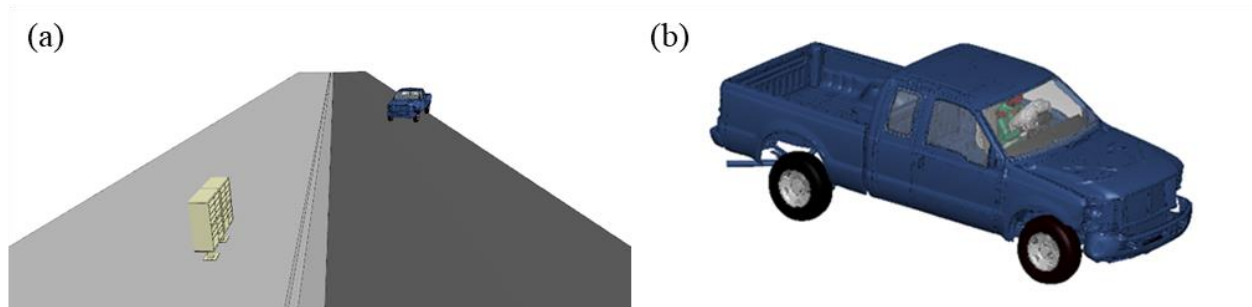


Figure 4.63 The full simulation model (a) and deformed vehicle model after impact (b) for Category 4 – Case 8.

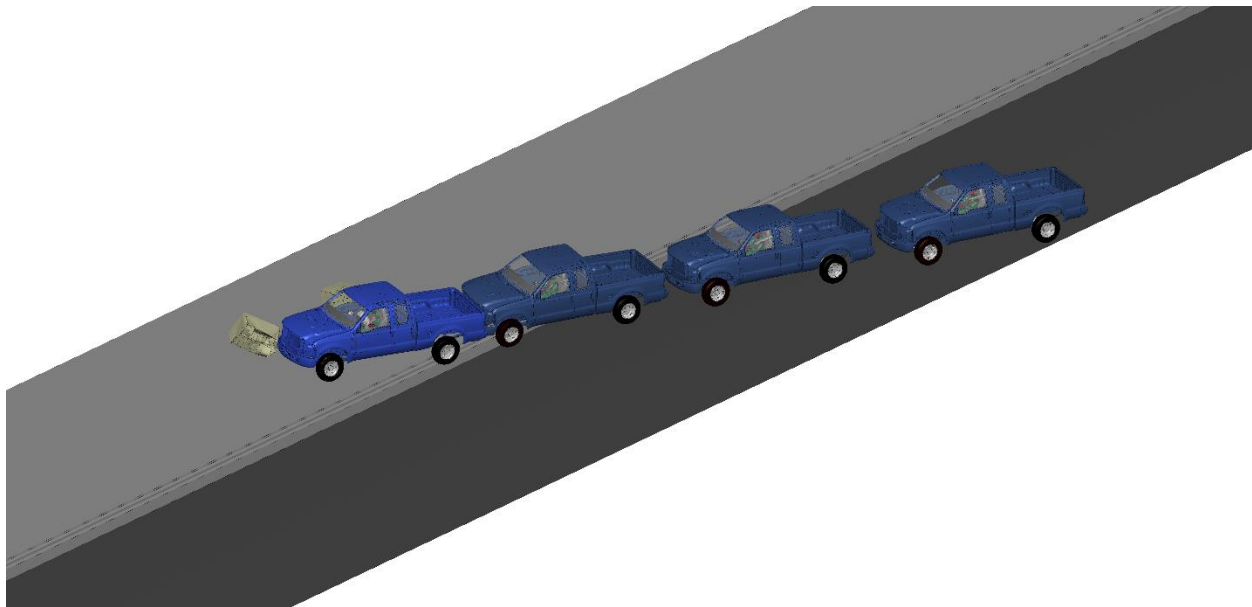
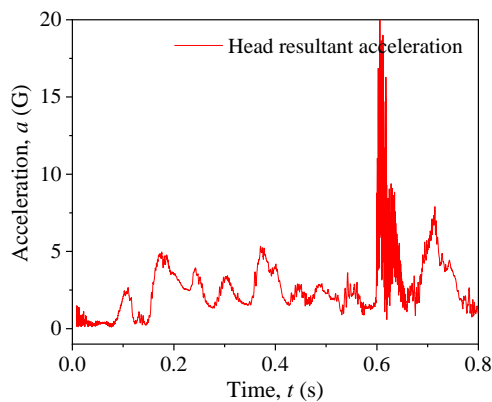
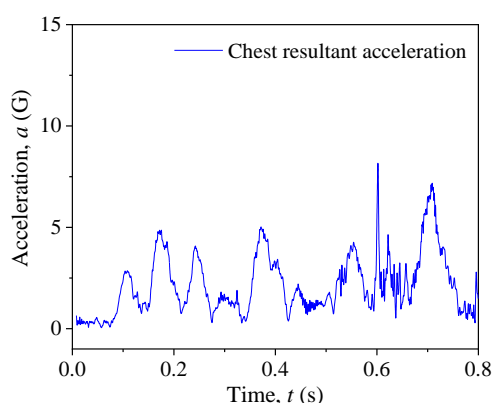
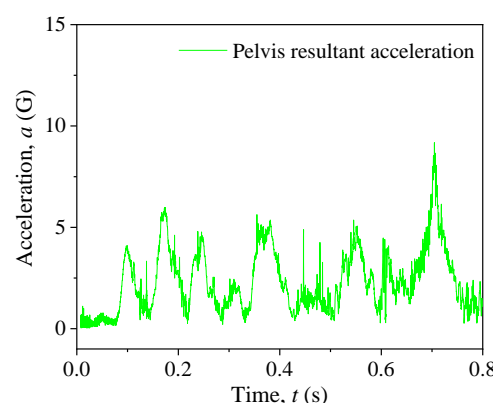


Figure 4.64 Vehicle trajectory during impact for Category 4 – Case 8.

Table 4.63 Vehicular responses, OIVs, and ORAs for Category 4 – Case 8.

Parameter	OIV (m/s)		ORA (G)		Vehicular Response	
	Longitudinal	Lateral	Longitudinal	Lateral	Roll angle	Pitch angle
Simulation Result	2.12	1.18	3.80	3.21	6.08°	2.92°
MASH Limit	12.2	12.2	20.49	20.49	75°	75°
Pass/Fail	Pass	Pass	Pass	Pass	Pass	Pass

Table 4.64 Dummy responses and injury parameters for Category 4 – Case 8.

Dummy head acceleration	Head impact criteria			
	Head injury parameter	Value	Threshold	Pass/Fail
	$HIC_{15}$	5.04	700	Pass
	$p(HIC_{15})$	0 %	31%	Pass
Dummy chest acceleration	Dummy pelvis acceleration			
				

## 5. Simulation Results and Analysis of the Bus Shelter

Four crash simulations were performed to evaluate the bus shelter at MASH TL-2 conditions. The simulation results were analyzed on occupant responses and potential injuries. The occupant risk was evaluated using MASH criteria on OIVs, ORAs, and roll and pitch angles of the test vehicles. The time histories of accelerations measured on the crash dummy (i.e., on head, chest, and pelvis) were also examined. The probability of skull injury was assessed based on the head injury criteria ( $HIC_{15}$ ). Vehicle trajectories during crash events were obtained and presented in overlapping contour plots to provide a comprehensive understanding of the impact responses. The trajectories of debris from the broken polycarbonate windshield were tracked and the maximum distance of the debris was determined for evaluating the potential risk for pedestrians. It should be noted that since there were no pedestrian models used in the crash simulations of this study, the risks of pedestrian injuries under direct vehicle impact could not be evaluated and thus not included in this study. Additionally, the injury severity of pedestrians hit by polycarbonate debris could not be determined and not included in this study.

In the crash simulations of the bus shelter, two MASH compliant vehicles, a 1100C small passenger car (i.e., a 2010 Toyota Yaris) and a 2270P pickup truck (i.e., a 2006 Ford F250), were used to crash into a Brasco Slimline SL-510-OF bus shelter on a flat road at an impact speed of 44 mph (71 km/h). The four simulation cases are summarized as follows.

- Case 1: The bus shelter impacted by a 2010 Toyota Yaris at  $0^\circ$ ;
- Case 2: The bus shelter impacted by a 2010 Toyota Yaris at  $25^\circ$ ;
- Case 3: The bus shelter impacted by a 2006 Ford F250 at  $0^\circ$ ; and
- Case 4: The bus shelter impacted by a 2006 Ford F250 at  $0^\circ$ .

### 5.1 Case 1: The bus shelter impacted by a 2010 Toyota Yaris at $0^\circ$

In this case, a 2010 Toyota Yaris crashed into the bus shelter at 44 mph (71 km/h) and with  $0^\circ$  impact angle. Figure 5.1 shows the full simulation model before impact and the deformed vehicle model after impact. Figure 5.2 shows the overlapping contour plot of vehicle trajectory for this case. Figure 5.3 shows the detailed simulation results on the interactions between the vehicle and the bus shelter. The vehicle's roll and pitch angles, OIVs, and ORAs were calculated and summarized in Table 5.1. Table 5.2 gives the acceleration histories of the crash test dummy on the head, chest, and pelvis. The  $HIC_{15}$  and the probability of skull injury were also calculated for this case, as given in Table 5.2.

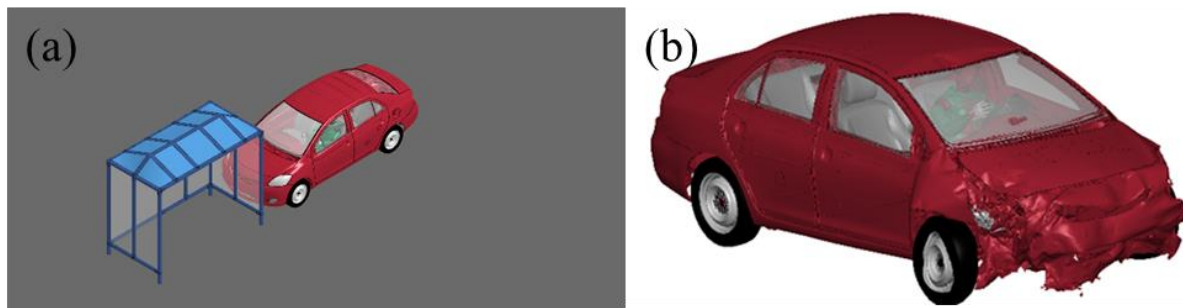


Figure 5.1 The full simulation model (a) and deformed vehicle model after impact (b) for Case 1.

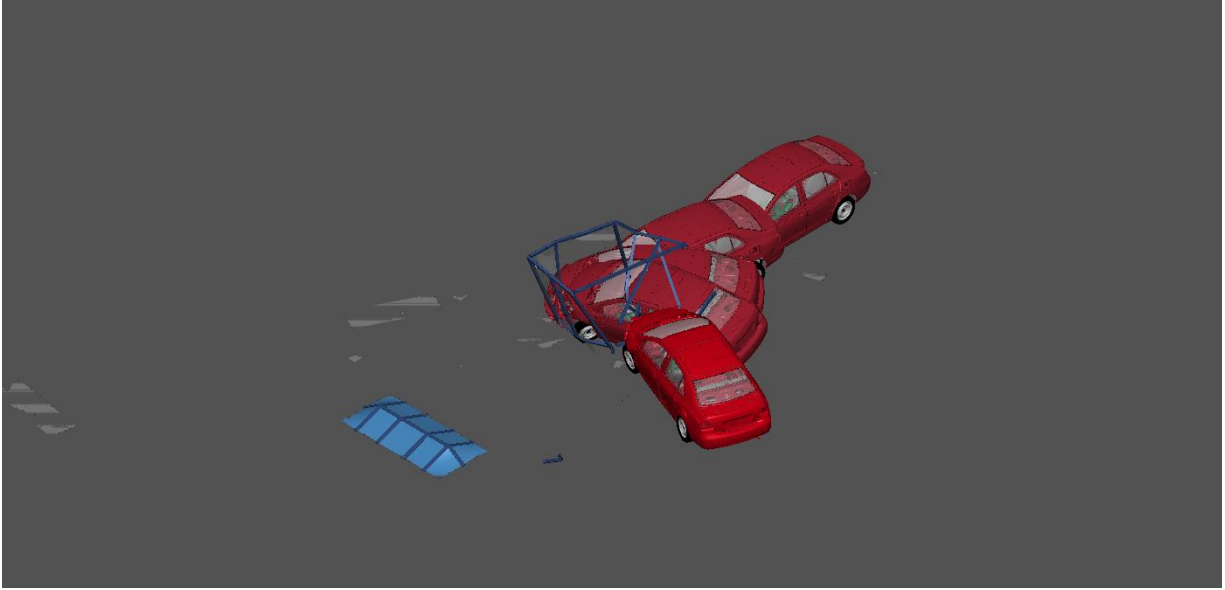


Figure 5.2 Vehicle trajectory during impact for Case 1.

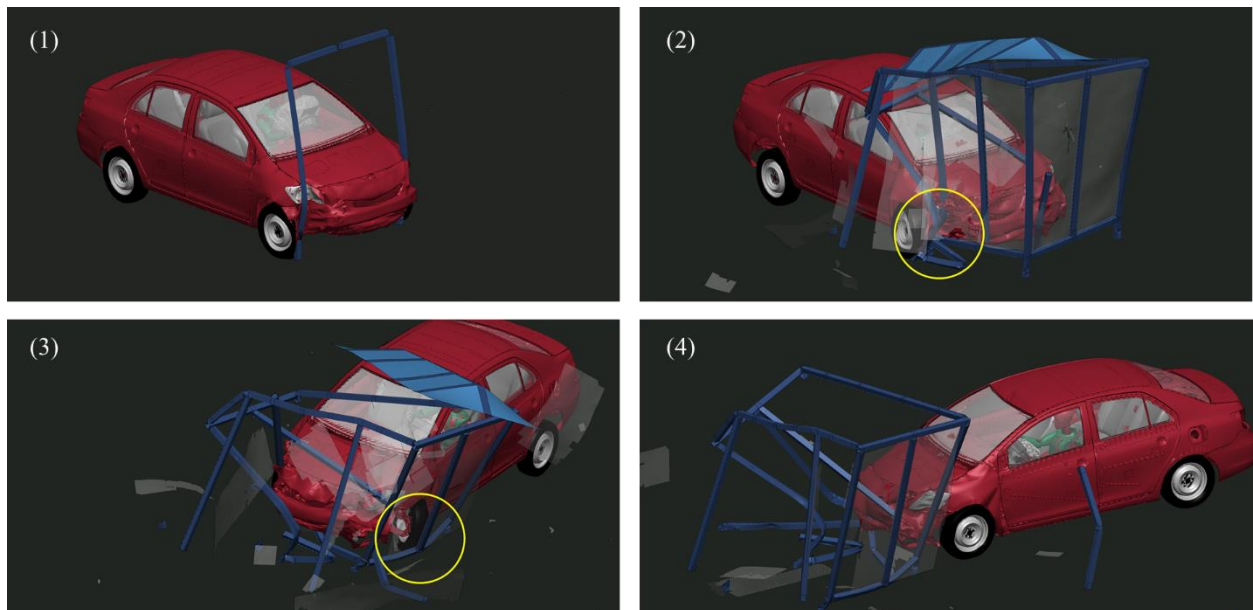


Figure 5.3 Crash simulation details for Case 1.

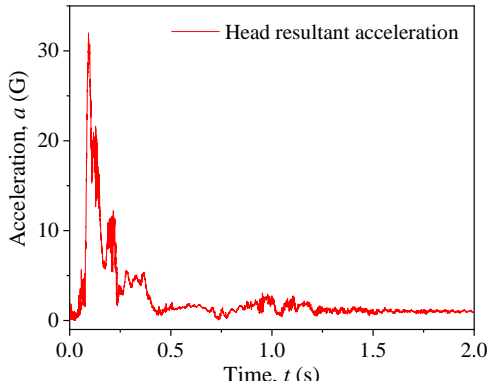
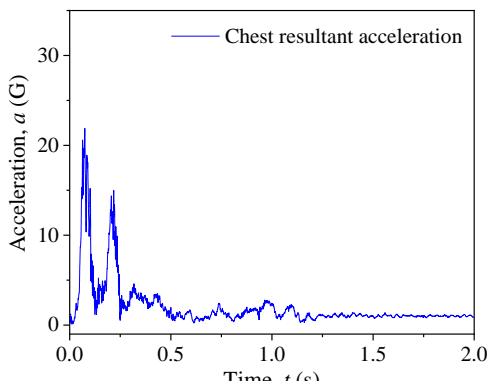
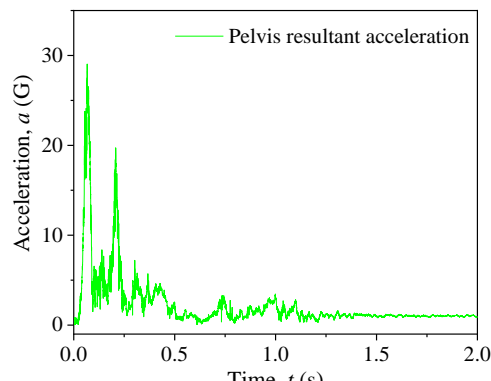
The simulation results of Case 1 showed that the middle column of the bus shelter on the impact side yielded immediately upon impact and the two front tires of the vehicle engaged with the two side columns (see Figure 5.3 (1), other components were hidden for better view). As the vehicle continued crashing into the bus shelter, it caused the entire bus shelter tilted forward in the vehicle's travel direction, leading to the failure of the cubical clip joints that held the roof to the frame. Due to engagement with the columns fastened to the ground, the vehicle yawed with the collapse of the bus shelter. After the joints connecting the roof and the bus shelter frame failed, the roof fell to the ground with a forward movement due to momentum (see Figure 5.3 (3)). The simulation results showed no penetration of the bus shelter frames of other components into the

occupant compartment. The vehicle's roll and pitch angles, as well as the OIVs and ORAs in both longitudinal and lateral directions, were all within the MASH allowed limits.

Table 5.1 Vehicular response, OIVs, and ORAs for Case 1.

Parameter	OIV (m/s)		ORA (G)		Vehicular Response	
	Longitudinal	Lateral	Longitudinal	Lateral	Roll angle	Pitch angle
Simulation Result	7.16	0.29	12.56	3.15	11.47°	10.89°
MASH Limit	12.2	12.2	20.49	20.49	75°	75°
Pass/Fail	Pass	Pass	Pass	Pass	Pass	Pass

Table 5.2 Dummy responses and injury parameters for Case 1.

Dummy head acceleration	Head impact criteria			
	Head injury parameter	Value	Threshold	Pass/Fail
	HIC <sub>15</sub>	67.33	700	Pass
	<i>p</i> (HIC <sub>15</sub> )	0.06%	31%	Pass
Dummy chest acceleration	Dummy pelvis acceleration			
				

For occupant response, the head acceleration of the crash test dummy was relatively high upon impacting the side columns of the bus shelter. Figure 5.4 shows the crash test dummy responses during the impact of Case 1. It can be seen that the dummy's head bent forward and fully contacted the deployed airbag. The peak head acceleration was approximately 32 G and the HIC<sub>15</sub> value was calculated to be 67.33, which was below the threshold value of 700 and indicated no possibility of skull injury. These results indicated no potential occupant injury for this impact case.





Figure 5.4 Crash test dummy response for Case 1.

Figure 5.5 shows the plan view of the after-impact scenario of Case 1. The maximum trajectory distance of the polycarbonate debris after impact was measured to be 110.6 ft (33.7 m). Most of the debris, including the collapsed frame and the bus shelter roof, were found around the bus shelter. The roof displaced 19.9 ft (6.07 m) measured from the furthest point on the roof to the center of the original bus shelter. Given the severity of bus shelter damage, pedestrians inside the bus shelter are highly likely to get severe injury and there is a large possibility of getting hit directly by the striking vehicle.

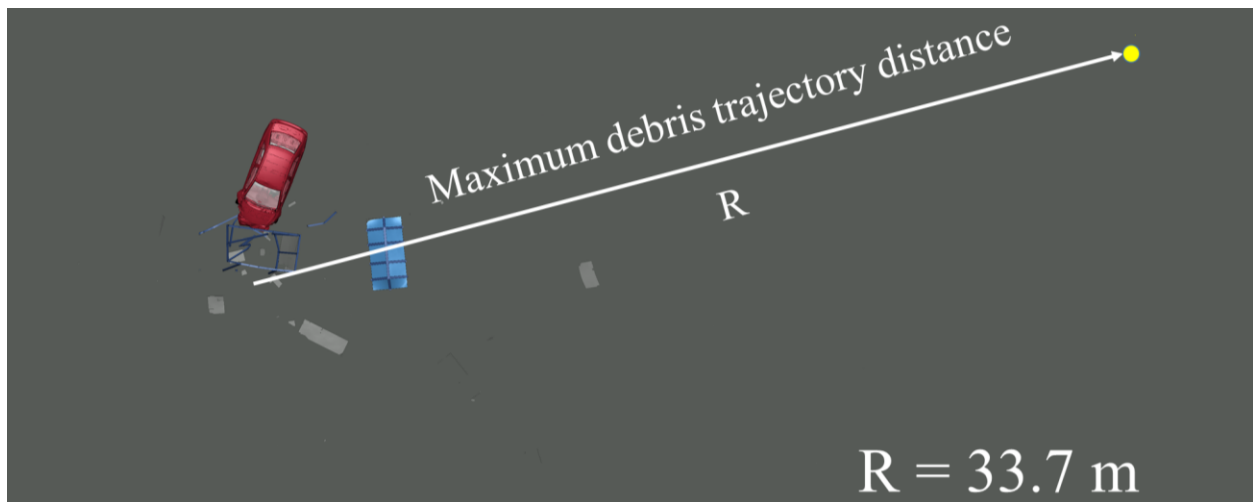


Figure 5.5 The maximum debris trajectory distance for Case 1.

## 5.2 Case 2: The bus shelter impacted by a 2010 Toyota Yaris at 25°

In this case, a 2010 Toyota Yaris crashed into the bus shelter at 44 mph (71 km/h) and with 25° impact angle. Figure 5.6 shows the full simulation model before impact and the deformed vehicle model after impact. Figure 5.7 shows the overlapping contour plot of vehicle trajectory for this case. Figure 5.8 shows the detailed simulation results on the interactions between the vehicle and the bus shelter. The vehicle's roll and pitch angles, OIVs, and ORAs were calculated and summarized in Table 5.3. Table 5.4 gives the acceleration histories of the crash test dummy on the head, chest, and pelvis. The  $HIC_{15}$  and the probability of skull injury were also calculated for this case, as given in Table 5.4.

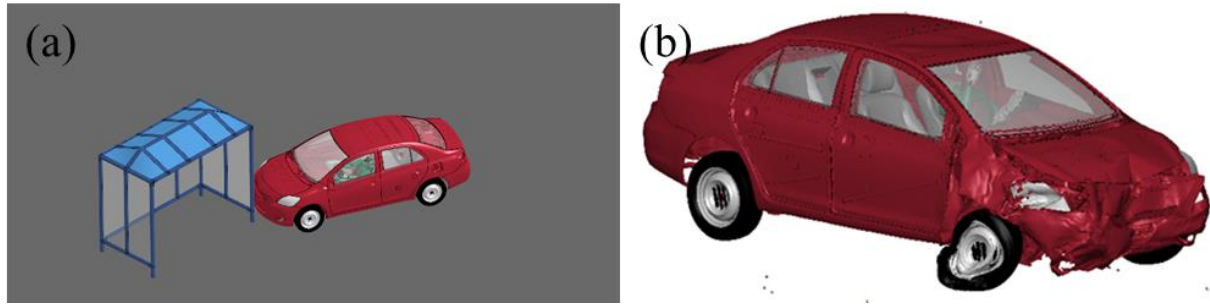


Figure 5.6 The full simulation model (a) and deformed vehicle model after impact (b) for Case 2.

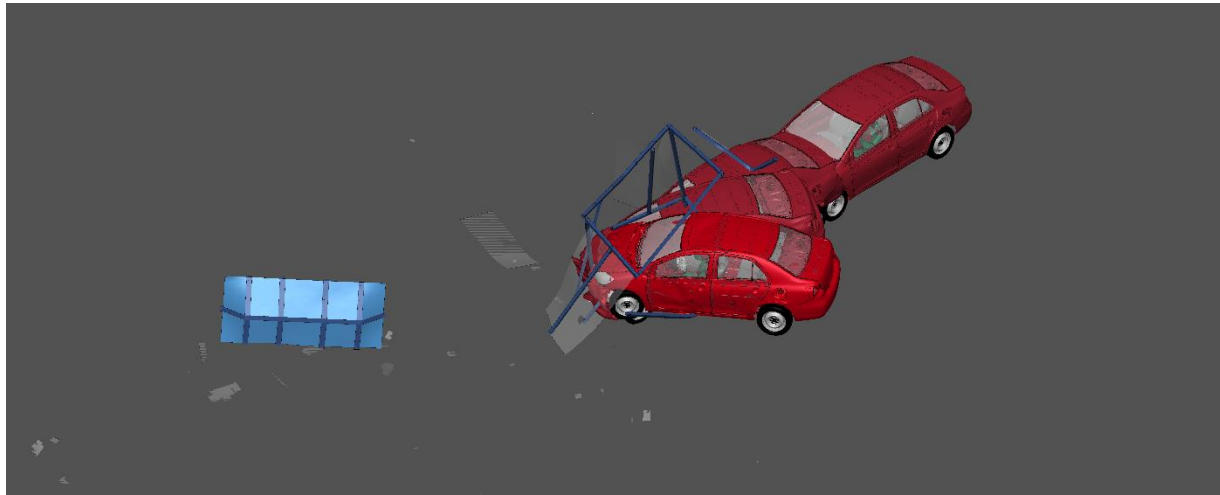


Figure 5.7 Vehicle trajectory during impact for Case 2.

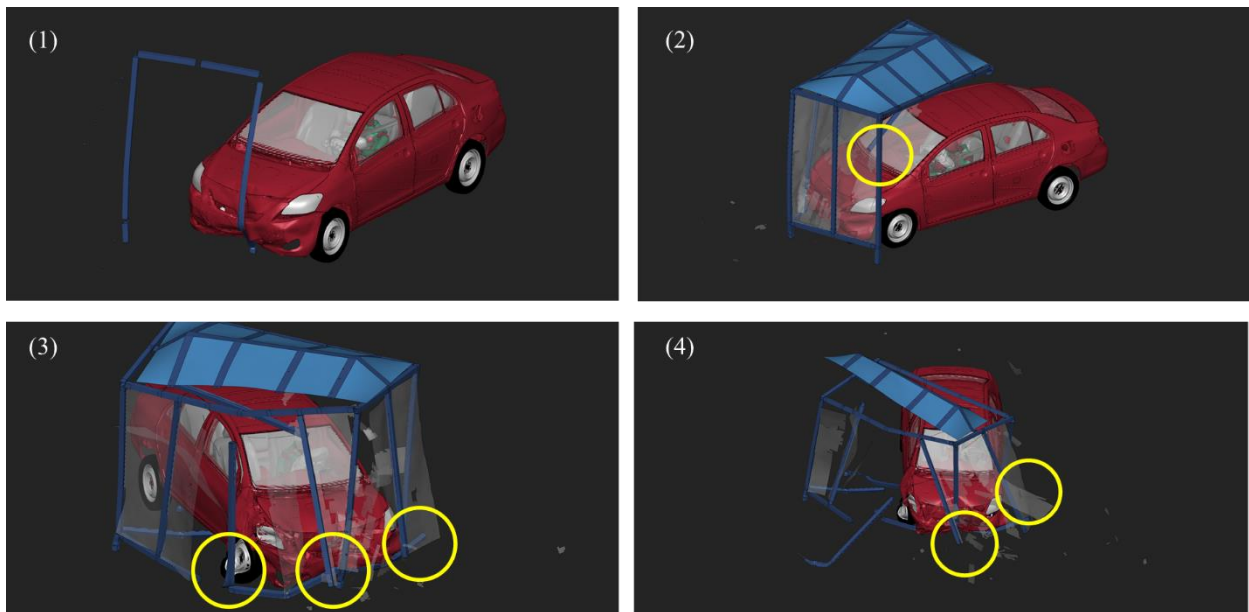


Figure 5.8 Crash simulation details for Case 2.



The simulation results of Case 2 showed that the corner column of the bus shelter impacted first yielded quickly due to severe bending. This corner column blocked the vehicle and crushed into the hood until the upper connection joint failed. The broken column hit and slid over the windshield without intruding into the occupant compartment. The vehicle continued moving forward towards the diagonal corner and was eventually stopped by the bus shelter frame. After the bus shelter frame lost structural integrity and the connection joints between the roof and frame failed, the roof fell off to the ground and moved forward in the vehicle's travel direction. The simulation results showed no penetration of the bus shelter frames of other components into the vehicle's occupant compartment. The vehicle's roll and pitch angles, as well as the OIVs and ORAs in both longitudinal and lateral directions, were all within the MASH allowed limits

Table 5.3 Vehicular responses, OIVs, and ORAs for Case 2.

Parameter	OIV (m/s)		ORA (G)		Vehicular Response	
	Longitudinal	Lateral	Longitudinal	Lateral	Roll angle	Pitch angle
Simulation Result	9.41	0.33	13.52	6.90	8.03°	12.67°
MASH Limit	12.2	12.2	20.49	20.49	75°	75°
Pass/Fail	Pass	Pass	Pass	Pass	Pass	Pass

Table 5.4 Dummy responses and injury parameters for Case 2.

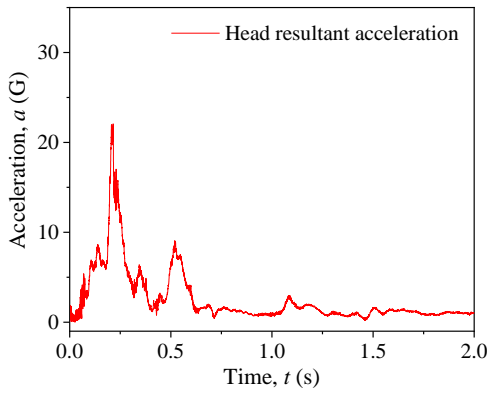
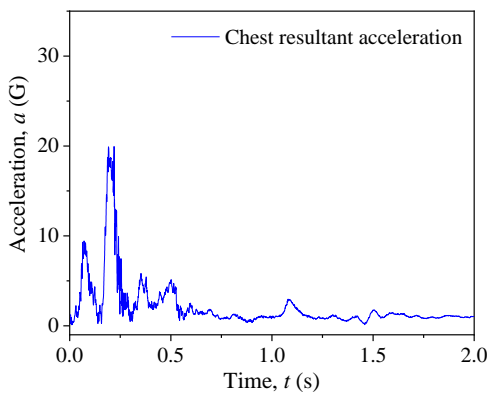
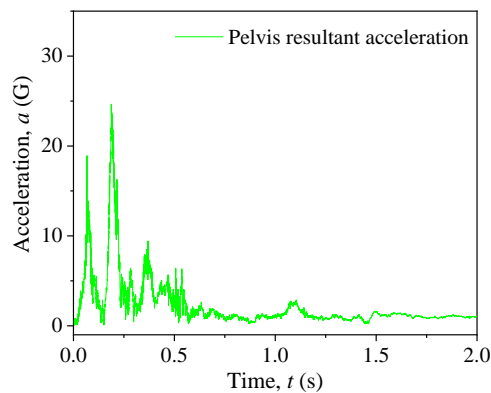
Dummy head acceleration		Head impact criteria			
		Head injury parameter	Value	Threshold	Pass/Fail
		HIC <sub>15</sub>	28.26	700	Pass
		$p(\text{HIC}_{15})$	0 %	31%	Pass
Dummy chest acceleration		Dummy pelvis acceleration			
					

Figure 5.9 shows the crash test dummy responses during the impact of Case 2. Upon impacting

the first corner column of the bus shelter, the vehicle's airbag started deploying while the dummy head moved forward. The dummy head did not reach the airbag when it was fully deployed; it hit the airbag when the vehicle hit the second corner column that was diagonal of the first corner column. The peak head acceleration was approximately 22 G and the  $HIC_{15}$  value was calculated to be 28.26, which was below the threshold value of 700 and indicated no possibility of skull injury. These results indicated no potential occupant injury for this impact case.

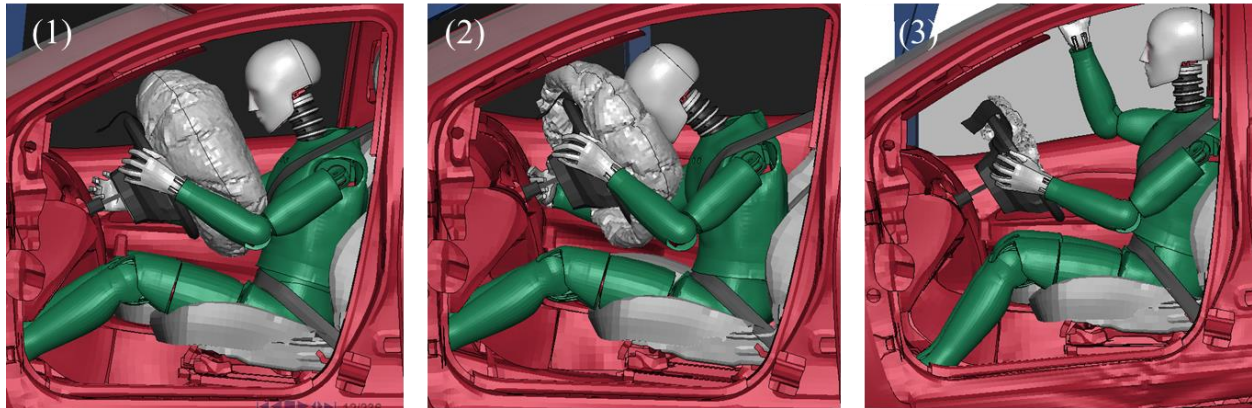


Figure 5.9 Crash test dummy response for Case 2

Figure 5.10 shows the plan view of the after-impact scenario of Case 2. The maximum trajectory distance of the polycarbonate debris after impact was measured to be 40.7 ft (12.4 m). It should be noted that the large polycarbonate debris at the bottom-right corner in Figure 5.10 slid to this point from its landing location, which was near the bus shelter and used to calculate its trajectory distance to the bus shelter. The bus shelter roof displaced 25.2 ft (7.67 m) from the furthest point on the roof to the center of the original bus shelter. Given the severity of bus shelter damage, pedestrians inside the bus shelter are highly likely to get severe injury and there is a large possibility of getting hit directly by the striking vehicle.

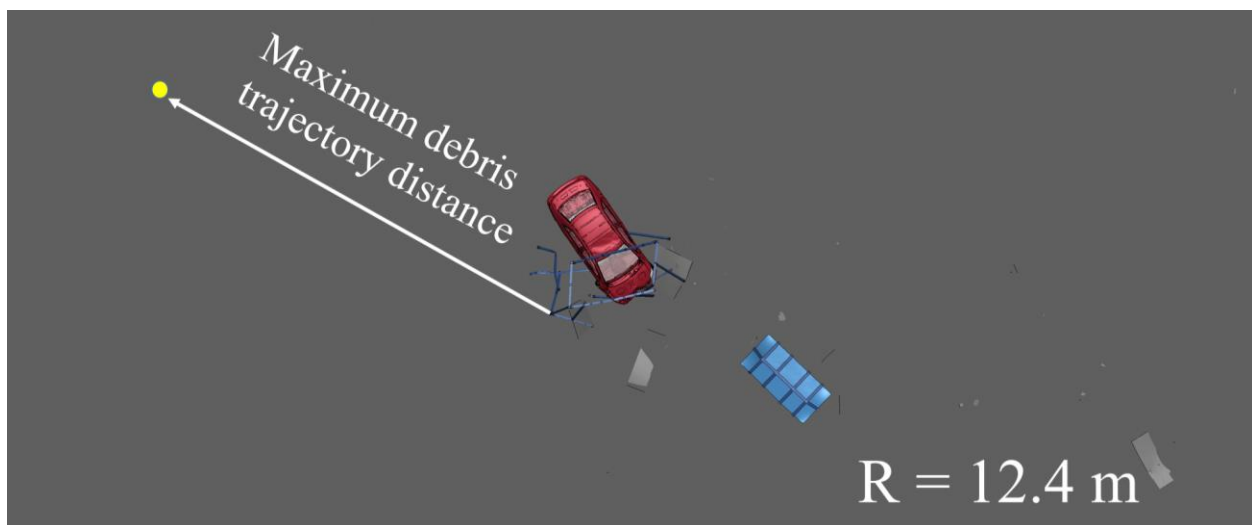


Figure 5.10 The maximum debris trajectory distance for Case 2.

### 5.3 Case 3: The bus shelter impacted by a 2006 Ford F250 at 0°

In this case, a 2006 Ford F250 crashed into the bus shelter at 44 mph (71 km/h) and with 0° impact angle. Figure 5.11 shows the full simulation model before impact and the deformed vehicle model after impact. Figure 5.12 shows the overlapping contour plot of vehicle trajectory for this case. Figure 5.13 shows the detailed simulation results on the interactions between the vehicle and the bus shelter. The vehicle's roll and pitch angles, OIVs, and ORAs were calculated and summarized in Table 5.5. Table 5.6 gives the acceleration histories of the crash test dummy on the head, chest, and pelvis. The HIC<sub>15</sub> and the probability of skull injury were also calculated for this case, as given in Table 5.6.

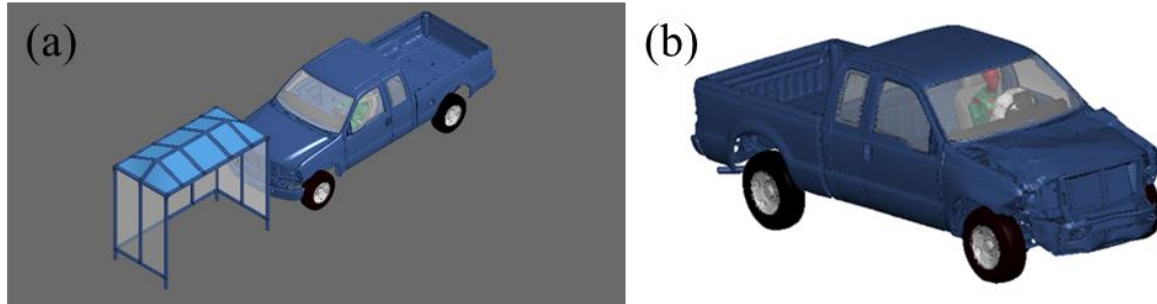


Figure 5. 11 The full simulation model (a) and deformed vehicle model after impact (b) for Case 3.

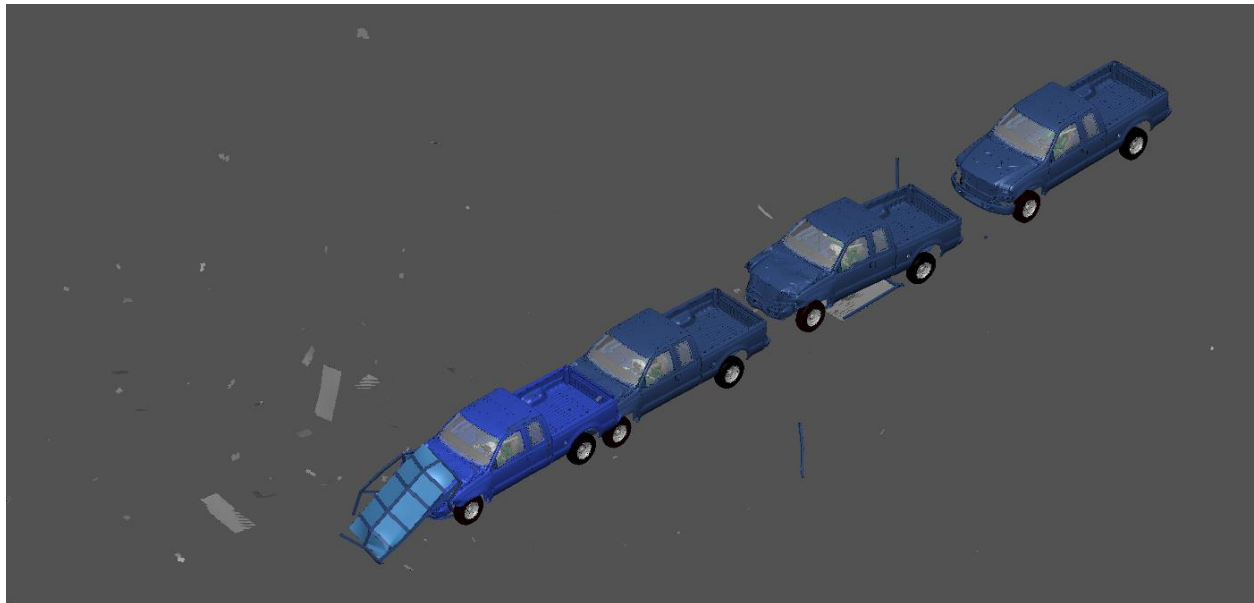
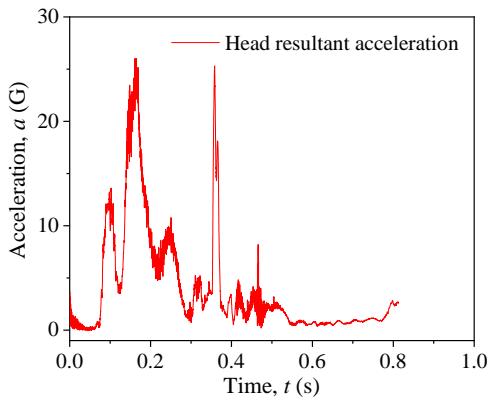
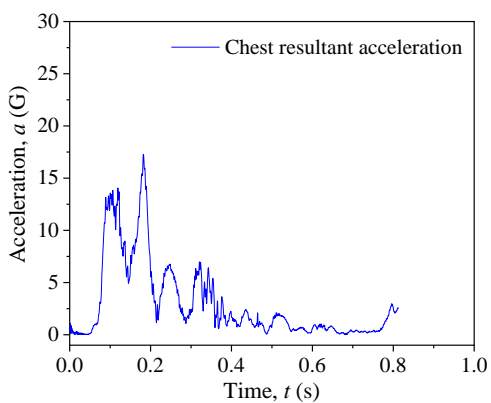
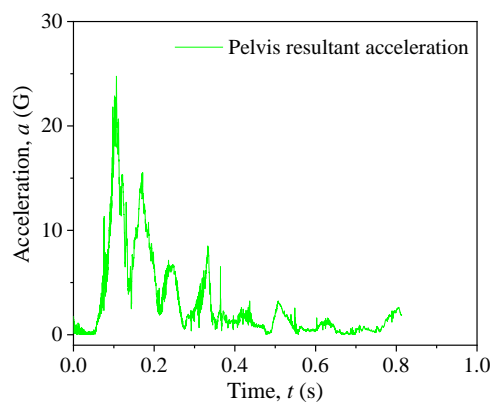


Figure 5.12 Vehicle trajectory during impact for Case 3.

Table 5.5 Vehicular responses, OIVs, and ORAs for Case 3.

Parameter	OIV (m/s)		ORA (G)		Vehicular Response	
	Longitudinal	Lateral	Longitudinal	Lateral	Roll angle	Pitch angle
Simulation Result	5.67	0.26	5.52	2.14	5.73°	4.33°
MASH Limit	12.2	12.2	20.49	20.49	75°	75°
Pass/Fail	Pass	Pass	Pass	Pass	Pass	Pass

Table 5.6 Dummy responses and injury parameters for Case 3.

Dummy head acceleration	Head impact criteria			
	Head injury parameter	Value	Threshold	Pass/Fail
	$HIC_{15}$	38.67	700	Pass
	$p(HIC_{15})$	0%	31%	Pass
Dummy chest acceleration	Dummy pelvis acceleration			
				

The simulation results of Case 3 showed that the middle column of the bus shelter on the impact side yielded immediately upon impact and the two side columns engaged with the vehicle and yielded (see Figure 5.13 (1), other components were hidden for better view). As the vehicle continued crashing into the bus shelter, the entire bus shelter was pushed forward in the vehicle's travel direction after losing connections with the ground base. Some of the connection joints for the roof failed, but the roof was not fully detached from the frame. Part of the frame and the roof were pushed to the front of the vehicle with no penetration into the occupant compartment. The vehicle's roll and pitch angles, as well as the OIVs and ORAs in both longitudinal and lateral directions, were all within the MASH allowed limits.

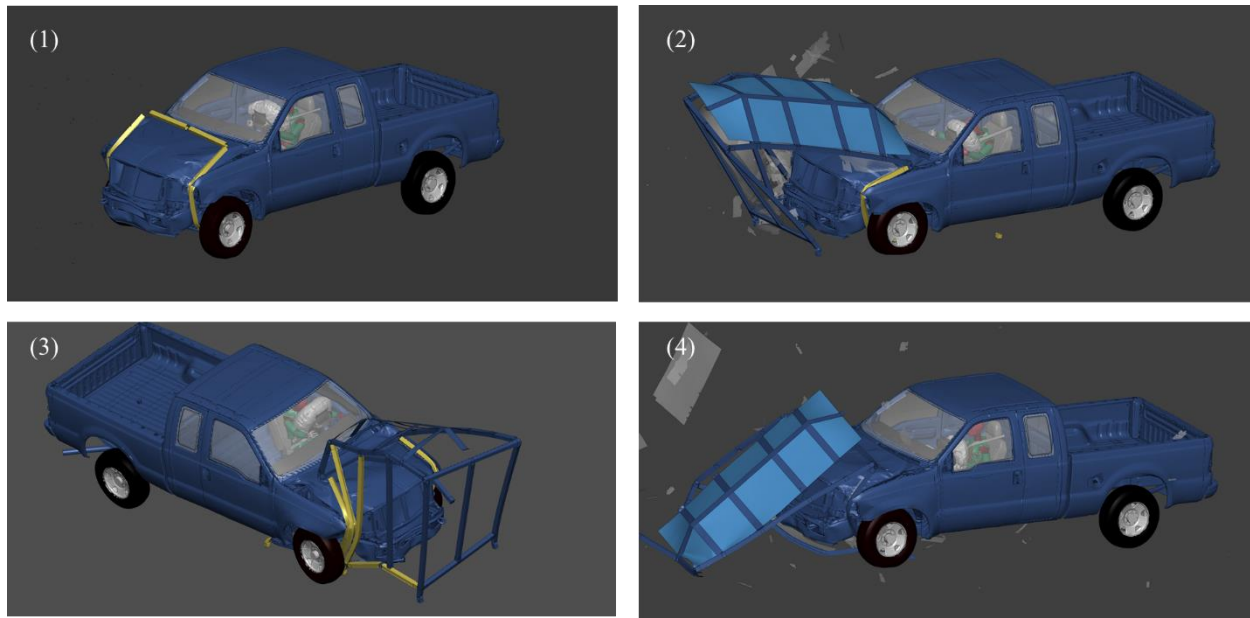


Figure 5.13 Crash simulation details for Case 3.

Figure 5.14 shows the crash test dummy responses during the impact of Case 3. Upon impacting the bus shelter, the vehicle's airbag started deploying while the dummy head moved forward. The dummy head hit the airbag shortly after the airbag reached full deployment. The peak head acceleration was approximately 26 G and the HIC<sub>15</sub> value was calculated to be 38.67, which was below the threshold value of 700 and indicated no possibility of skull injury. These results indicated no potential occupant injury for this impact case.

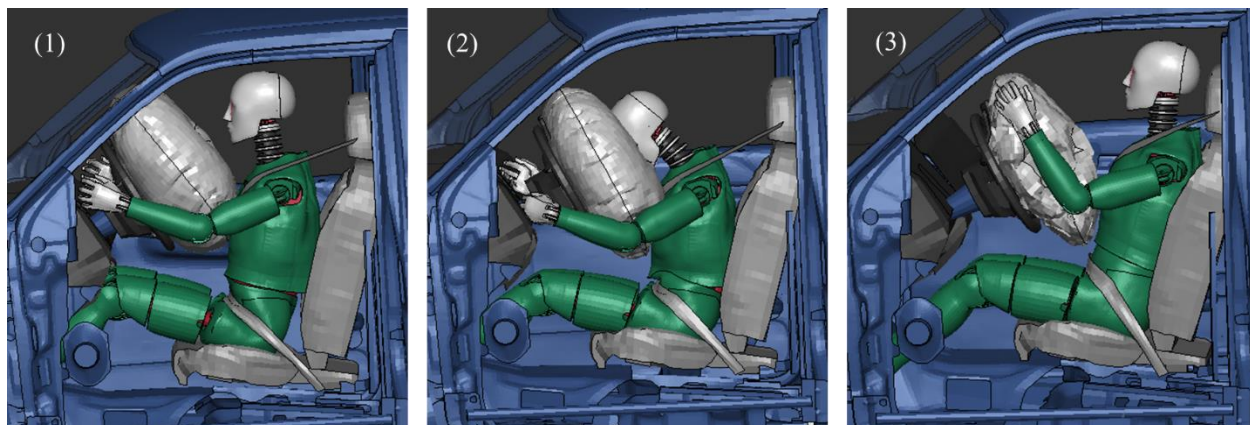


Figure 5.14 Crash test dummy response for Case 3.

Figure 5.15 shows the plan view of the after-impact scenario of Case 3. The maximum trajectory distance of the polycarbonate debris after impact was measured to be 123.7 ft (37.7 m). The bus shelter roof and partial frame were pushed and carried by the vehicle. At the instant shown in Figure 5.15, the vehicle still had a velocity of 25 mph (40 km/h) and bus shelter roof was approximately 56.4 ft (17.2 m) from the center of the original bus shelter. Given the severity of bus shelter damage, pedestrians inside the bus shelter are highly likely to get severe injury due to



direct impact by the striking vehicle.

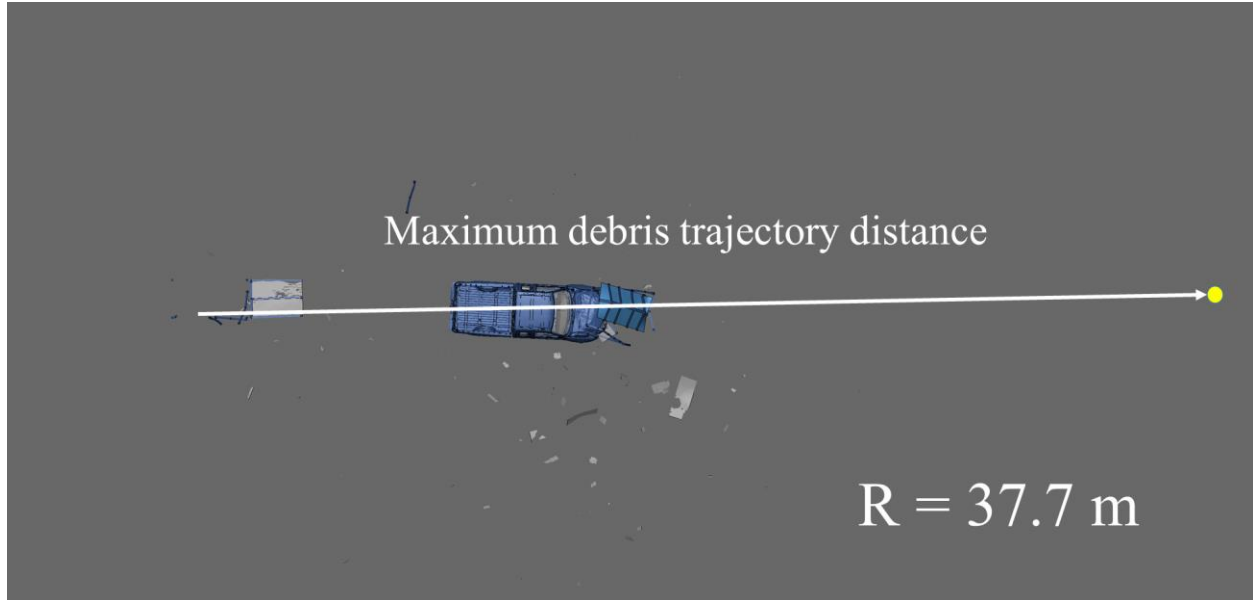


Figure 5.15 The maximum debris trajectory distance for Case 3.

#### 5.4 Case 4: The bus shelter impacted by a 2006 Ford F250 at 25°

In this case, a 2006 Ford F250 crashed into the bus shelter at 44 mph (71 km/h) and with 25° impact angle. Figure 5.16 shows the full simulation model before impact and the deformed vehicle model after impact. Figure 5.17 shows the overlapping contour plot of vehicle trajectory for this case. Figure 5.18 shows the detailed simulation results on the interactions between the vehicle and the bus shelter. The vehicle's roll and pitch angles, OIVs, and ORAs were calculated and summarized in Table 5.7. Table 5.8 gives the acceleration histories of the crash test dummy on the head, chest, and pelvis. The HIC<sub>15</sub> and the probability of skull injury were also calculated for this case, as given in Table 5.8.

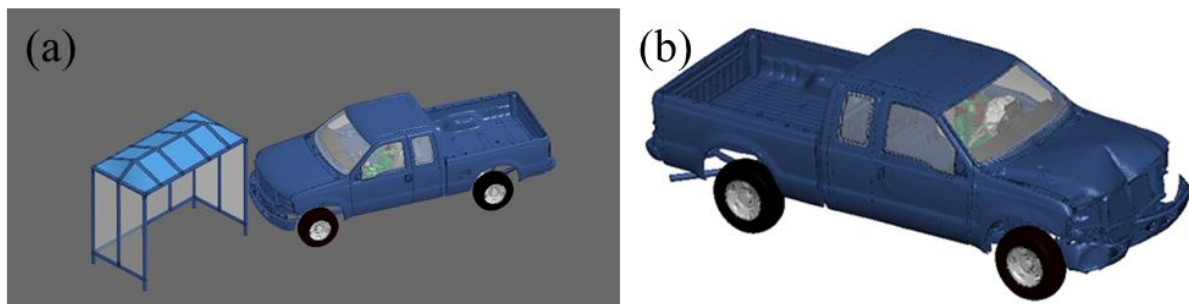


Figure 5.16 The full simulation model (a) and deformed vehicle model after impact (b) for Case 4.

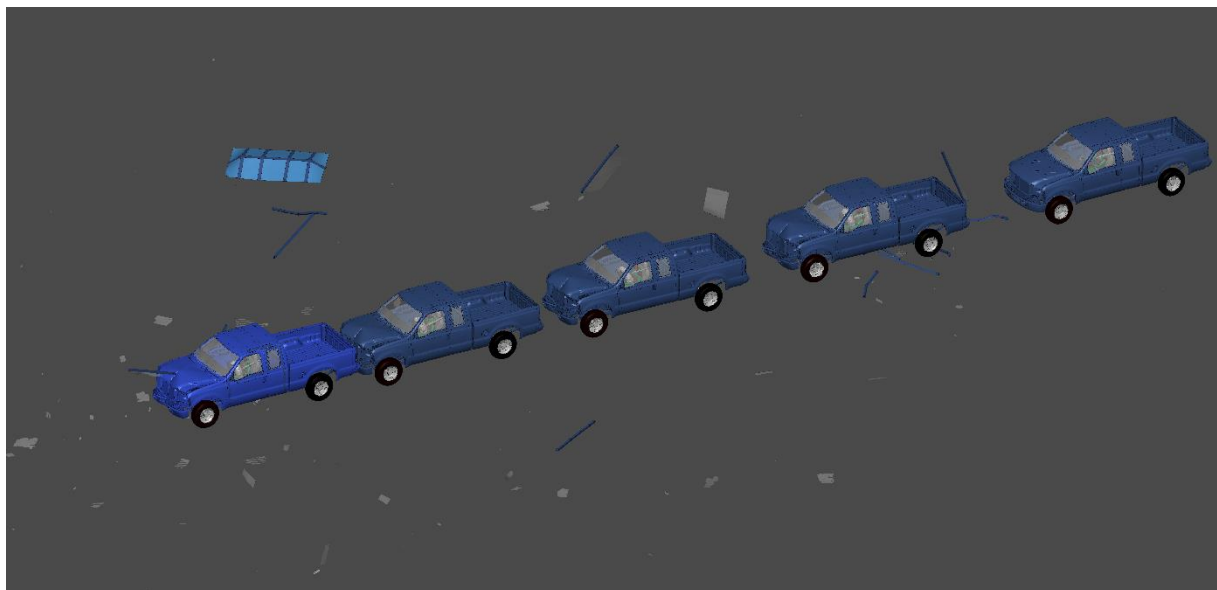


Figure 5.17 Vehicle trajectory during impact for Case 4.

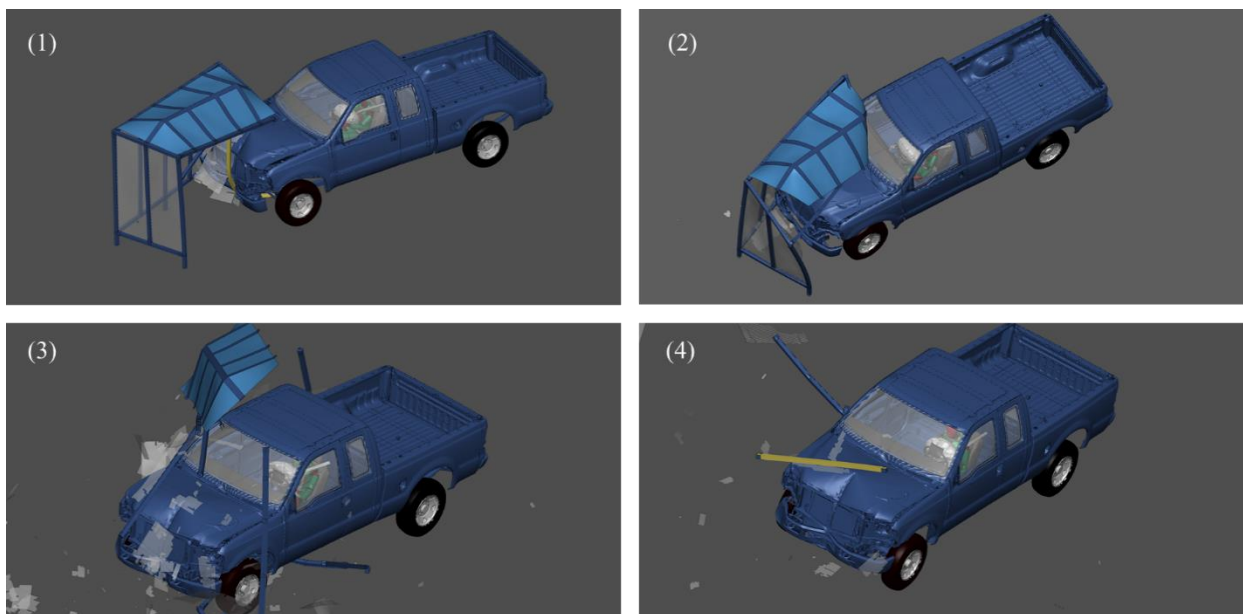
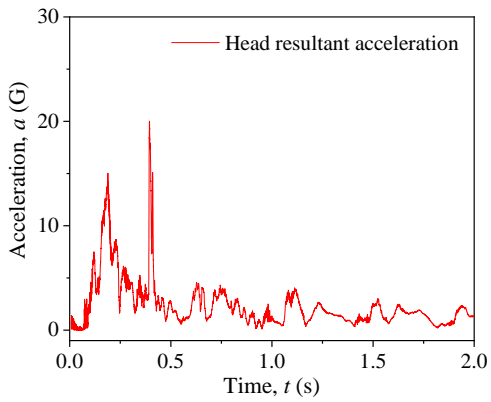
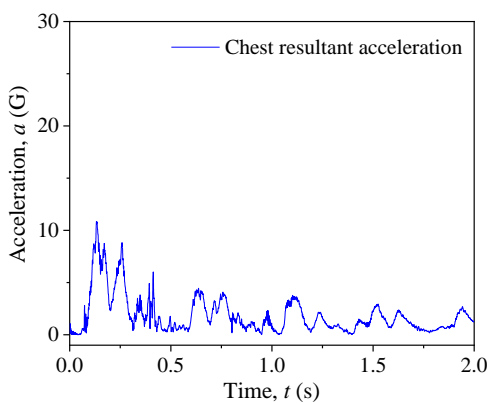
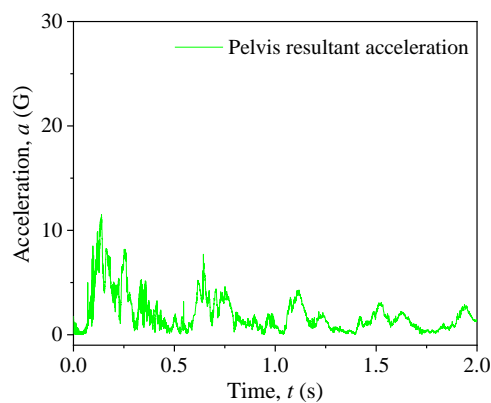


Figure 5.18 Crash simulation details for Case 4.

Table 5.7 Vehicular responses, OIVs, and ORAs for Case 4.

Parameter	OIV (m/s)		ORA (G)		Vehicular Response	
	Longitudinal	Lateral	Longitudinal	Lateral	Roll angle	Pitch angle
Simulation Result	5.28	0.45	2.53	3.00	3.92°	2.06°
MASH Limit	12.2	12.2	20.49	20.49	75°	75°
Pass/Fail	Pass	Pass	Pass	Pass	Pass	Pass

Table 5.8 Dummy responses and injury parameters for Case 4.

Dummy head acceleration	Head impact criteria			
	Head injury parameter	Value	Threshold	Pass/Fail
	$HIC_{15}$	11.93	700	Pass
	$p(HIC_{15})$	0 %	31%	Pass
Dummy chest acceleration	Dummy pelvis acceleration			
				

The simulation results of Case 4 showed that the bus shelter quickly lost structural integrity upon impact and dismembered completely after the vehicle reached the bus shelter corner that was diagonal of the one being impacted first. In this case, the damage of the vehicle was a V-shaped dent at the front and no components of the bus shelter penetrated the occupant compartment. The vehicle's roll and pitch angles, as well as the OIVs and ORAs in both longitudinal and lateral directions, were all within the MASH allowed limits.

Figure 5.19 shows the crash test dummy responses during the impact of Case 4. Upon impacting the bus shelter, the vehicle's airbag started deploying while the dummy head moved forward. The dummy head hit the airbag shortly after the airbag reached full deployment. The peak head acceleration was approximately 20 G and the  $HIC_{15}$  value was calculated to be 11.93, which was below the threshold value of 700 and indicated no possibility of skull injury. These results indicated no potential occupant injury for this impact case.



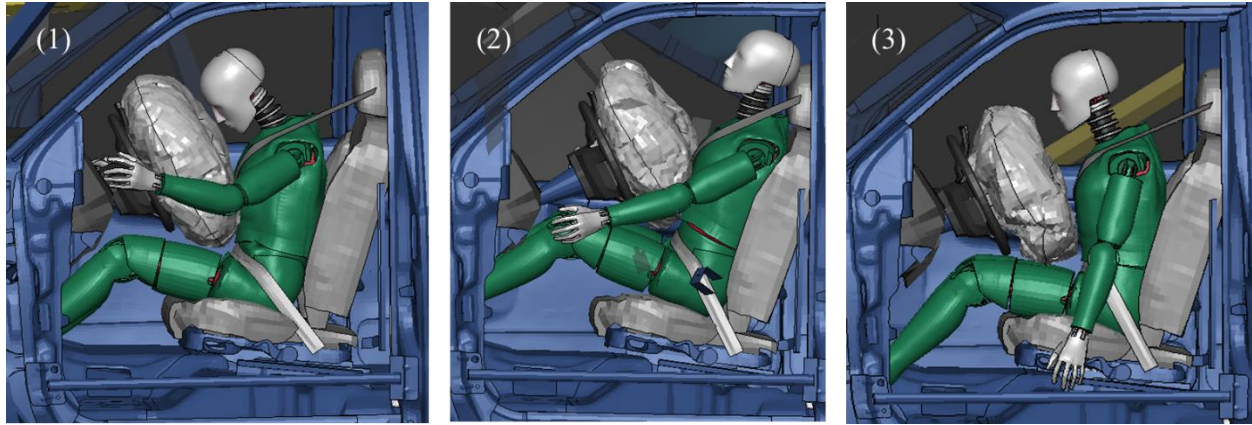


Figure 5.19 Crash test dummy response for Case 4.

Figure 5.20 shows the plan view of the after-impact scenario of Case 4. The maximum trajectory distance of the polycarbonate debris after impact was measured to be 173.9 ft (53.0 m). The bus shelter roof was knocked off to the right side of the vehicle's travel path and landed at approximately 69.2 ft (21.1 m) from the center of the original bus shelter. Given the severity of bus shelter damage, pedestrians inside the bus shelter are highly likely to get severe injury due to direct impact by the striking vehicle.

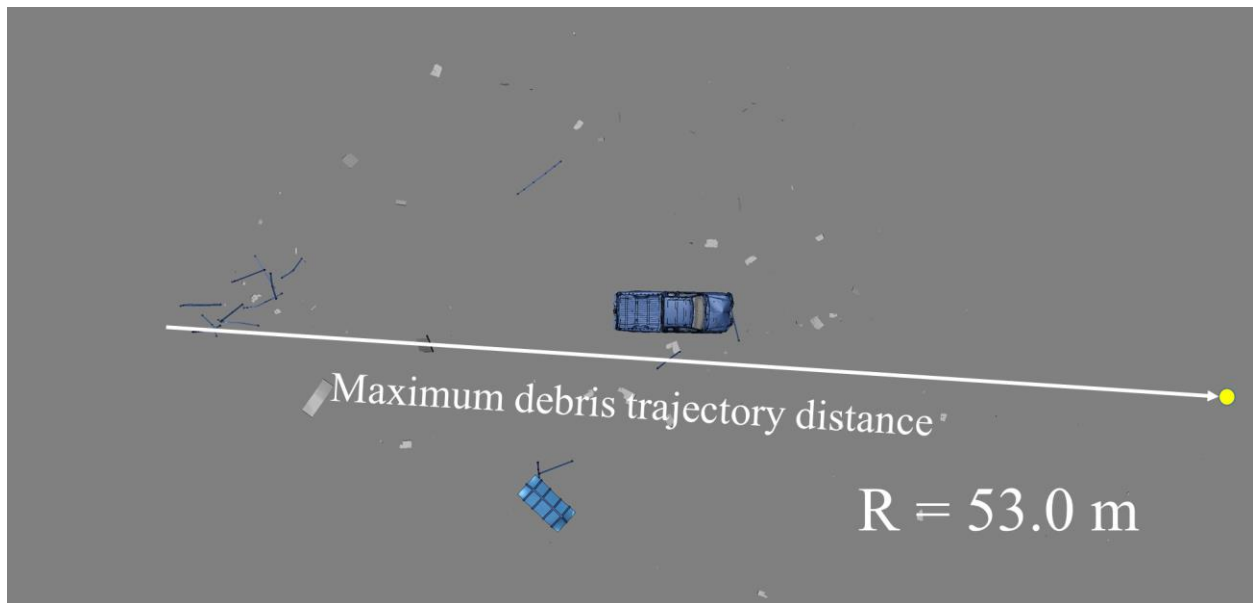


Figure 5.20 The maximum debris trajectory distance for Case 4.

## 6. Findings and Conclusions

In this project, two types of roadside utilities, a bus shelter and cluster mailboxes, were evaluated on occupant safety under vehicular crashes. Nonlinear finite element modeling and simulations were utilized as the main research tools in this study. Two commonly used cluster mailboxes, Type I and Type IV, were chosen and evaluated under vehicular impacts of two MASH-compliant vehicles, a 2010 Toyota Yaris small passenger car (1100C) and a 2006 Ford F250 pickup truck (2270P), at an impact speed of 31 mph (50 km/h) and at 0° and 25° impact angles. The cluster mailboxes were evaluated in two configurations, single- and dual-unit, and with two road conditions, on a flat road and behind a curb. For bus shelter evaluation, the 1100C and 2270P vehicles were used with an impact speed of 44 mph (71 km/h) and 0° and 25° impact angles. In all the crash simulations, a Hybrid III 50<sup>th</sup> percentile crash test dummy was used to obtain the time histories of dummy accelerations on the head, chest, and pelvis. Vehicular responses such as roll and pitch angles, occupant impact velocities (OIVs), and occupant ride-down accelerations (ORAs), and head injury criterion (HIC<sub>15</sub>) were determined and compared to the limit values specified by MASH. For bus shelter crash simulations, the trajectory distances of bus shelter debris and roof were measured to determine the potential risk for pedestrians inside and adjacent to the bus shelter. The simulation results provided insights in occupant risk assessment for roadside utilizes under vehicular crashes. Some of the major research findings are summarized as follows.

- For single-unit cluster mailboxes, the major failure was the separation of upper unit from the pedestal. The upper units had severe damages on the front and caused minimal damage on the vehicle's front. There was no penetration of mailbox components into the vehicle's occupant compartment. The vehicle's roll and pitch angles, as well as the OIVs and ORAs in both longitudinal and lateral directions, were all within the MASH allowed limits. The HIC<sub>15</sub> values calculated using dummy's head accelerations were all below the threshold value and thus indicated no possibility of skull injury. For single-unit cluster mailboxes, including both Type I and Type IV, no potential occupant injury was found in these impact cases.
- For dual-unit cluster mailboxes, the major failure was also the separation of upper units from the pedestals. For 25° impacts at the mid-point, the mailbox unit impacted first remained almost intact and the second unit failed similar to the case of the single-unit mailbox. For 0° impacts and 25° impacts at the corner, the damage to the vehicles was more severe than the single-unit cases due to the increased mass of the dual units. In all the dual-unit impact cases, there was no penetration of mailbox components into the vehicle's occupant compartment. The vehicle's roll and pitch angles, as well as the OIVs and ORAs in both longitudinal and lateral directions, were all within the MASH allowed limits. The HIC<sub>15</sub> values calculated using dummy's head accelerations were all below the threshold value and thus indicated no possibility of skull injury. For dual-unit cluster mailboxes, including both Type I and Type IV, no potential occupant injury was found in these impact cases.
- Under impact of the 1100C vehicle, the bus shelter lost structural integrity and the roof fell off for both 0° and 25° impacts. In both cases, the 1100C vehicle crushed into the bus shelter and was stopped by the frames that were still attached to the ground base. Although

the bus shelter failed, there was no penetration of bus shelter frames into the vehicle's occupant compartment. The vehicle's roll and pitch angles, as well as the OIVs and ORAs in both longitudinal and lateral directions, were all within the MASH allowed limits. The HIC<sub>15</sub> values calculated using dummy's head accelerations were all below the threshold value and thus indicated no possibility of skull injury. In both cases, no potential occupant injury was found in these impact cases. The bus shelter roof landed at 19.9 ft (6.07 m) and 25.2 ft (7.67 m) in the 0° and 25° impact cases, respectively, measured horizontally from the furthest point on the roof to the original center of the bus shelter. The debris of the polycarbonate windscreen landed as far as 110.6 ft (33.7 m) as in the 0° impact case. These results indicated that there is a potential of injury to adjacent pedestrians caused by the bus shelter roof and polycarbonate debris. Given the severity of bus shelter damage, pedestrians inside the bus shelter are highly likely to get severe injury and there is a large possibility of getting hit directly by the 1100C vehicle.

- Under impact of the 2270P vehicle, the bus shelter lost structural integrity quickly and was completely dismembered for both 0° and 25° impacts. In both cases, the 2270P vehicle crushed into and continued through the bus shelter and destroyed the frame. Although the bus shelter failed, there was no penetration of bus shelter frames into the vehicle's occupant compartment. The vehicle's roll and pitch angles, as well as the OIVs and ORAs in both longitudinal and lateral directions, were all within the MASH allowed limits. The HIC<sub>15</sub> values calculated using dummy's head accelerations were all below the threshold value and thus indicated no possibility of skull injury. In both cases, no potential occupant injury was found in these impact cases. The bus shelter roof landed at 69.2 ft (21.1 m) in the 25° impact case, measured horizontally from the furthest point on the roof to the original center of the bus shelter. In the case of 0° impact, the bus shelter roof stuck on the vehicle's front and was carried forward by the vehicle. The debris of the polycarbonate windscreen landed as far as 173.9 ft (53.0 m) as in the 25° impact case. These results indicated that there is a potential of injury to adjacent pedestrians caused by the bus shelter roof and polycarbonate debris. Given the severity of bus shelter damage, pedestrians inside the bus shelter are highly likely to get severe injury due to direct impact by the 2270P vehicle.

In summary, the simulation results showed that there was no potential occupant injury in vehicular crashes into both single- and dual-unit Type I and Type IV mailboxes under MASH TL-1 conditions. In vehicular crashes into the bus shelter under MASH TL-2 conditions, the simulation results indicated no potential occupant injury; however, there was a high likelihood of injury to adjacent pedestrians caused by the falling roof and windscreen debris. Furthermore, pedestrians inside the bus shelter were highly likely to get severe injury by the striking vehicles.

## 7. References

- [1]. AASHTO, M. (2009). Manual for assessing safety hardware (MASH). Washington, DC.
- [2]. AASHTO, M. (2016). Manual for assessing safety hardware (MASH) Second Edition. Washington, DC.
- [3]. Asadinia, N., Khalkhali, A., & Saranjam, M. J. (2018). Sensitivity analysis and optimization for occupant safety in automotive frontal crash test. *Latin American Journal of Solids and Structures*, 15(7).
- [4]. Austin, R. A. (2012). Lower Extremity Injuries and Intrusion in Frontal Crashes (No. DOT HS 811 578). National Center for Statistics and Analysis.
- [5]. Bligh, R. P., & Menges, W. L. (2010). NCHRP Report 350 Crash Testing and Evaluation of the S-Square Mailbox System (No. FHWA/TX-10/0-5210-7). Texas Transportation Institute.
- [6]. Bligh, R. P., Menges, W. L., & Sanders, S. K. (2001). Testing and Evaluation of Molded Plastic Mailboxes (No. FHWA/TX-01/1792-6,). Texas Transportation Institute, Texas A & M University System.
- [7]. Brasco International, Inc. (2011) Standard Wall Connection Detail. Retrieved from <http://www.brasco.com>
- [8]. Brasco International, Inc. (2012) Aluminum Hip Style Transit Shelter. Retrieved from <http://www.brasco.com>
- [9]. Brasco International, Inc. (2012) Standard Anchor Shoe Detail. Retrieved from <http://www.brasco.com>
- [10]. Brasco International, Inc. (2015). Brasco 2015 Product Catalog: Bike Bus BRT. Retrieved from <http://www.brasco.com>
- [11]. Campise, W. L., & Ross, H. E. (1984). Test and evaluation of neighborhood mailbox (No. FHWA/TX-84/52+ 343-2). Texas Transportation Institute, Texas A & M University System.
- [12]. Deng, X., Potula, S., Grewal, H., Solanki, K. N., Tschopp, M. A., & Horstemeyer, M. F. (2013). Finite element analysis of occupant head injuries: Parametric effects of the side curtain airbag deployment interaction with a dummy head in a side impact crash. *Accident Analysis & Prevention*, 55, 232-241.
- [13]. Faller, R. K., Magdaleno, J. A., Post, E. R., Warlick, B. A., & Wendling, W. H. (1988). FULL-SCALE VEHICLE CRASH TESTS ON NEBRASKA RURAL MAILBOX DESIGNS. *Transportation Research Record*, (1198).
- [14]. Florence Corporation (2012). Vital Cluster Box Unit – Type I. Retrieved from <https://www.florencemailboxes.com/sites/default/files/2017-02/1570-8.pdf>
- [15]. Florence Corporation (2012). Vital Cluster Box Unit – Type IV. Retrieved from <https://www.florencemailboxes.com/sites/default/files/2017-02/1570-13.pdf>

- [16]. Florence Corporation (2017). Cluster box units & accessories. Retrieved from <https://www.florencemailboxes.com/cluster-box-units>
- [17]. Hertz, E. (1993). A note on the head injury criterion (HIC) as a predictor of the risk of skull fracture. In *Proceedings: Association for the Advancement of automotive medicine annual conference* (Vol. 37, pp. 303-312). Association for the Advancement of Automotive Medicine.
- [18]. Keon, T. (2016). Alternative approaches to occupant response evaluation in frontal impact crash testing. *SAE International journal of transportation safety*, 4(1), 202-217.
- [19]. Kirkpatrick, S. W., MacNeill, R., & Bocchieri, R. T. (2003). Development of an LS-DYNA occupant model for use in crash analyses of roadside safety features. In *Transportation Research Board 82nd Annual Meeting*, Washington, DC, Jan (pp. 12-16).
- [20]. Linder, A., & Svensson, M. Y. (2019). Road safety: the average male as a norm in vehicle occupant crash safety assessment. *Interdisciplinary Science Reviews*, 44(2), 140-153.
- [21]. Mailbox (N/A) The 1570 Series Cluster Box Units [Online image] Retrieved from <http://mailboxdirects.com/1570-series-cluster-box-units>
- [22]. Manoogian, S., Duma, S. M., & Moorcroft, D. M. (2007). Pregnant occupant injury risk using computer simulations with NCAP vehicle crash test data. In *Proc. 20th ESV Conf.*, paper (No. 07-0168).
- [23]. Marzougui, D., Kan, C. D., & Bedewi, N. E. (1997). Development and validation of an NCAP simulation using LS-DYNA3D.
- [24]. Mike Myers (2018) Police are looking for driver and passenger who were involved in hit-and-run collision [Online Image] Herald News. Retrieved from [https://www.fontanaheraldnews.com/news/police-are-looking-for-driver-and-passenger-who-were-involved/article\\_9ed351c8-22f3-11e8-9243-bfce38019dd7.html](https://www.fontanaheraldnews.com/news/police-are-looking-for-driver-and-passenger-who-were-involved/article_9ed351c8-22f3-11e8-9243-bfce38019dd7.html)
- [25]. NCAC (2008). Technical Summary – NCAC 2008-T-003: Development & Validation of a Finite Element Model for the 2006 Ford F250 Pickup Truck. Retrieved from <http://www.ncac.gwu.edu/research/pubs/NCAC-2008-T-003.pdf>
- [26]. NCAC (2011). Technical Summary - Development & Validation of a Finite Element Model for the 2010 Toyota Yaris Passenger Sedan. Retrieved from <https://media.ccsa.gmu.edu/cache/NCAC-2011-T-001.pdf>
- [27]. NCAC (2012). Technical Summary - Extended Validation of the Finite Element Model for the 2010 Toyota Yaris Passenger Sedan. Retrieved from <https://media.ccsa.gmu.edu/cache/NCAC-2012-W-005.pdf>
- [28]. NCDOT (2013). North Carolina Department of Transportation Product Evaluation Program Bus Shelter Structural Adequacy Document. Raleigh, NC
- [29]. NCDOT (2017). North Carolina Department of Transportation Bus Shelter & Bus Stop Guidelines. Raleigh, NC
- [30]. Noureddine, A., Eskandarian, A., & Digges, K. (2002). Computer modeling and validation of a hybrid III dummy for crashworthiness simulation. *Mathematical and computer modelling*, 35(7-8), 885-893.

- [31]. Paulsen, G. W., Faller, R. K., & Reid, J. D. (1996). Design and testing of a breakaway base for a cluster box unit and a neighborhood delivery and collection unit. Midwest Roadside Safety Facility, University of Nebraska-Lincoln.
- [32]. Pearlman, M. D., & Viano, D. (1996). Automobile crash simulation with the first pregnant crash test dummy. *American journal of obstetrics and gynecology*, 175(4), 977-981.
- [33]. Reichert, R., Park, C. K., & Morgan, R. (2014). Development of Integrated Vehicle - Occupant Model for Crashworthiness Safety Analysis.". NHTSA report, Washington DC.
- [34]. Ressi, F., Sinz, W., Geisler, C., Öztürk, A., D'Addetta, G. A., & Freienstein, H. (2019). Estimating Preliminary Occupant Injury Risk Distributions For Highly Automated Vehicles With Respect To Future Seat Configurations And Load Directions.
- [35]. Ross Jr, H. E., & Walker, K. C. (1980). Crash Tests of Rural Mailbox Installations. *Work*, 3254, 6.
- [36]. Ross Jr, H. E., Sicking, D. L., Zimmer, R. A., & Michie, J. D. (1993). Recommended procedures for the safety performance evaluation of highway features (No. 350).
- [37]. Ross, H. E., Bullard, L., & Alberson, D. (1993). Mailbox Bracket Crash Tests (No. TTI-7-1945,).
- [38]. Ross, H. E., Miller, J. W., & Sicking, D. (1980). Test and Evaluation of Rural Mailbox Supports. Texas Transportation Institute, Texas A & M University.
- [39]. Sheikh, N. M., Bligh, R. P., Menges, W. L., & Haug, R. R. (2006). Crash Testing and Evaluation of the Shur-Tite® Multiple-Mailbox Mount (No. FHWA/TX-06/0-5210-2). Report No. FHWA/TX-06/0-5210-2. TTI, College Station, TX, 2006. Google Scholar.
- [40]. Shi, X., Cao, L., Reed, M. P., Rupp, J. D., & Hu, J. (2015). Effects of obesity on occupant responses in frontal crashes: a simulation analysis using human body models. *Computer methods in biomechanics and biomedical engineering*, 18(12), 1280-1292.
- [41]. Silvestri Dobrovolny, C., Bligh, R. P., Obinna, J., McDaniel, M., & Odell, W. (2019). Manual for assessing safety hardware crash testing and evaluation of multiple mailbox supports for use with locking architectural mailboxes. *Transportation research record*, 2673(7), 684-695.
- [42]. Silvestri Dobrovolny, C., White, K. M., & Haegelin, G. (2013). Mailbox Hazard and Risk Assessment. Report No. 405160-31. Texas Transportation Institute
- [43]. Spinelli, D. M., & Adelmann, T. (1999). Crash Simulation and Occupant Safety Analysis Using the Finite Element Method (No. 1999-01-3056). SAE Technical Paper.
- [44]. Tahan, F., Marzougui, D., Zaouk, A., Bedewi, N., Eskandarian, A., & Meczowski, L. (2005). Safety performance evaluation of secure mailboxes using finite element simulations and crash testing. *International Journal of Crashworthiness*, 10(4), 341-349.
- [45]. Takeo, U., Yasuhito, T., & Toshikazu, N. (2012). Applications of occupant safety simulation using MADYMO, vol 58, No. 165. Komatsu Tehnical Report.
- [46]. Teng, T. L., Chang, F. A., Liu, Y. S., & Peng, C. P. (2008). Analysis of dynamic response of vehicle occupant in frontal crash using multibody dynamics method. *Mathematical and Computer Modelling*, 48(11-12), 1724-1736.

- [47]. Untaroiu, C. D., Shin, J., & Lu, Y. C. (2013). Assessment of a dummy model in crash simulations using rating methods. *International Journal of Automotive Technology*, 14(3), 395-405.
- [48]. Vogel, J. C., Faller, R. K., Reid, J. D., & Sicking, D. L. (1998). A Review of Breakaway Supports for Small Signs and Mailbox Installations (No. TRP-03-68-98).
- [49]. Wang, S., Liu, D., & Cai, Z. (2018). Numerical analysis of occupant head injuries in impacts with dump truck panel. *Applied bionics and biomechanics*, 2018.
- [50]. Xu, T., Sheng, X., Zhang, T., Liu, H., Liang, X., & Ding, A. (2018). Development and validation of dummies and human models used in crash test. *Applied bionics and biomechanics*, 2018.
- [51]. Zhao, J., Katagiri, M., Lee, S., Hu, J. (2018) GHBMC M50-O Occupant Response in A Frontal Crash of Automated Vehicle. Paper presented at the meeting of 7th International Symposium: Human Modeling and Simulation in Automotive Engineering. Berlin, Germany.